ORIENTING IN 3D SPACE: BEHAVIORAL AND NEUROPHYSIOLOGICAL STUDIES IN BIG BROWN BATS

By

Ninad B. Kothari

A dissertation submitted to Johns Hopkins University in conformity with the requirements for the degree of Doctor of Philosophy

Baltimore, Maryland
December 2017

Abstract

In their natural environment, animals engage in a wide range of behavioral tasks that require them to orient to stimuli in three-dimensional space, such as navigating around obstacles, reaching for objects and escaping from predators. Echolocating bats, for example, have evolved a high-resolution 3D acoustic orienting system that allows them to localize and track small moving targets in azimuth, elevation and range. The bat's active control over the features of its echolocation signals contributes directly to the information represented in its sonar receiver, and its adaptive adjustments in sonar signal design provide a window into the acoustic features that are important for different behavioral tasks. When bats inspect sonar objects and require accurate 3D localization of targets, they produce sonar sound groups (SSGs), which are clusters of sonar calls produced at short intervals and flanked by long interval calls. SSGs are hypothesized to enhance the bat's range resolution, but this hypothesis has not been directly tested. We first, in Chapter 2, provide a comprehensive comparison of SSG production of bats flying in the field and in the lab under different environmental conditions. Further, in Chapter 3, we devise an experiment to specifically compare SSG production under conditions when target motion is predictable and unpredictable, with the latter mimicking natural conditions where bats chase erratically moving prey. Data from both of these studies are consistent with the hypothesis that SSGs improve the bat's spatio-temporal resolution of target range, and provide a behavioral foundation for the analysis and interpretation of neural recording data in chapters 4 and 6.

The complex orienting behaviors exhibited by animals can be understood as a feedback loop between sensing and action. A primary brain structure involved in sensorimotor integration is the midbrain superior colliculus (SC). The SC is a widely studied brain region and has been

implicated in species-specific orienting behaviors. However, most studies of the SC have investigated its functional organization using synthetic 2D (azimuth and elevation) stimuli in restrained animals, leaving gaps in our knowledge of how 3D space (azimuth, elevation and distance) is represented in the CNS. In contrast, the representation of stimulus distance in the auditory systems of bats has been widely studied. Almost all of these studies have been conducted in passively listening bats, thus severing the loop between sensing and action and leaving gaps in our knowledge regarding how target distance is represented in the auditory system of actively echolocating bats. In chapters 4, 5 and 6, we attempt to fill gaps in our knowledge by recording from the SC of free flying echolocating bats engaged in a naturalistic navigation task where bats produce SSGs. In chapter 4, we provide a framework to compute time-of-arrival and direction of the instantaneous echo stimuli received at the bats ears. In chapters 5 and 6, we provide an algorithm to classify neural activity in the SC as sensory, sensorimotor and premotor and then compute spatial receptive fields of SC neurons. Our results show that neurons in the SC of the free-flying echolocating bat respond selectively to stimulus azimuth, elevation and range. Importantly, we find that SC neuron response profiles are modulated by the bat's behavioral state, indicated by the production of SSG.

Broadly, we use both behavior and electrophysiology to understand the action-perception loop that supports spatial orientation by echolocation. We believe that the results and methodological advances presented here will open doors to further studies of sensorimotor integration in freely behaving animals.

Advisor: Dr. Cynthia Moss

Internal Committee: Drs. Peter Holland, Shreesh Mysore and Susan Courtney.

External Committee: Drs. Veit Stuphorn, Mounya Elhilali and Noah Cowan

Dedication

To my family

In loving memory of

Dr. Chintan Oza

Acknowledgements

MENTORS

I am thankful to Cindy (Dr. Moss) for her support, guidance, encouragement and the extraordinary amount of freedom and trust she conferred on me. I have learnt many things from Cindy and a few of them (of the many) I hope to always keep with me are, hard work and dedication to ones work, always appreciating the good qualities in people, always and immediately responding to emails (as she says – it only takes a few seconds), sharing data and information with others and, the art of working efficiently. I deeply share Cindy's constant endeavor to understand the neural correlates of complex behaviors when animals are freely moving (and flying!) and engaged in naturalistic tasks. Everyone deserves a second chance, and for that, I must thank Cindy for giving me a second chance, when she accepted me in her lab after I spent one year in Dr. Butt's lab at UMCP. For that matter, I also thank, Dan (Dr. Butt), for giving me my first break in the completely new field (for me) of neuroscience.

I am not sure how, I can ever thank Shreesh enough. In the completely new environment at JHU, I found in Shreesh both a mentor and a friend. I will always be indebted to him for time he has spent with me discussing spatial receptive fields and life. I have an immense amount of respect for him and I am extremely excited to join his lab as a post doc.

I would like to sincerely thank my entire thesis and proposal committee - Drs. Peter Holland, Veit Stuphorn, Shreesh Mysore, Mounya Elhilali, Susan Courtney, Noah Cowan, Jonathan Flombaum and of course, Cindy – for taking out time from their busy schedules to read my infinitely long thesis.

I have learnt a lot from all the amazing mentors that I have had the good fortune of working and interacting with, and, I believe, the best way to thank them is to carry these principles forward.

LAB MEMBERS

In my five (5+) years in the lab, I have made some life-long friendships that I will always carry forward with me. My graduate life would have been very dull without these amazing people.

My trajectory in the Batlab would have been very different had it not been for Mel (Dr. Wohlgemuth, as he likes to be addressed in public. Rightfully too!). He has been my mentor as well; I learnt all of my wet lab and surgery skills from him. It is surprising at how fun science can be, when you find a collaborator and friend, like Mel (hopefully, he also learnt a thing or two from me). I will always cherish the 'lunch, coffee and walk times' that Mel, Ben and I used to squeeze into our daily schedules (but, we can continue, as I am not going far). The more time you spend with Ben, the more you appreciate him. In the short period of time that Mohit and I overlapped in the lab, we became quite close friends. Mohit actually suggested and pushed me to record from flying bats (it actually worked!). In the past two years, I have had the good fortune of collaborating with Jinhong, whom I have come to respect as a very passionate and meticulous scientist (when are we going to make a video of a bat dancing to the Zootopia song!). And, how can I forget Wei Xian, she is the person, who, behind the scenes, keeps the Batlab machinery so well oiled (Thanks a ton, Wei!). I would also like to thank the many Batlab members that I have had the good fortune of working and interacting with - Silvio, Wu-Jung, Aaron, Michaela, Angie,

Brittney, Iven, Susanne, Chen, Dallas and Anand. I also want to thank my office mate, first for getting down on his knees and scrubbing our office floor and second, for all the great conversations we have had about science and life. I wish them all the best for their future success and look forward to their scientific contributions.

FRIENDS

I made lifelong friendships during my PhD years, but I cannot forget the evergreen friendships from the past that gave me the support and strength to carry on for all these years. The undying spirit of Ashutosh Tandon (Ashu) would be enough to make me want to continue with my PhD no matter how difficult and impossible it seemed. The wise and always unbiased advice from Saurabh Gupta would always be the checkpoint for my decisions. Sandeep Pandya and his wife Mamta have always been an inspiration for me. Their unflinching dedication towards their child has given me the confidence that no matter what the odds, there is always a way to overcome all difficulties. I would also like to thanks Sudipto Ghosh and Aditya Mutalik. They (and their families) have been part of our support system in the US.

FAMILY

Education, and even research, begins first at home and only later on in school or university; this is a maxim common in India, and, is very true in my case. Both of my parents have made tremendous sacrifices for empowering, my brother (Nishad) and me, with education and *philosophy of life* and values of dedication and passion towards ones work. They gave me the freedom to learn and explore, ask questions and also the confidence and ability to search for answers. I remember, as a 4 year old, my mother would take me to the local park (kamati baug)

and I would spend the entire day, catching insects, searching for frogs and lizards and playing with other kids. This was the beginning of my love for animals and biology. Later, I remember my dad, who was a very busy doctor (and still is), staying up late in the night to prepare custom illustrated dictionaries for books that he read to us on weekends. If I can achieve even 10% of this for my son (Neev), I will be overjoyed. Even today, so late in their lives, they are still our inspiration and guiding light. Thank you, Mom and Dad!

My younger brother, Nishad, and I share a very strong bond with each other (once again, I thank my parents for this). It is sometimes embarrassing for me to admit, but, has been a constant source of encouragement and he has given me a lot of courage to take the path of science and research. His extreme dedication to his work/research and students has always been an inspiration to me. Despite the tremendous distances that have often separated us, we talk frequently over the phone and discuss each other's work and life. I will always hold dear to me and cherish this relationship and friendship.

I have always considered myself extremely fortunate to have a great family and friends, but I consider myself most fortunate for the second family, I am now also an integral part of – my wife's side of the family. It would have been almost impossible for me to take the step of leaving a well-paying job for a career in science. My thesis would have been indefinitely delayed had it not been for my mother-in-law who stayed with us for 6 months to take care of our son and the whole house, which gave me the freedom to work very long hours on this thesis and research. I would also like to thank Charu, who is more like my sister than sister-in-law. She is the bright light keeping the whole family together. She has been our support system taking care of all of our personal and financial affairs saving us many trips back to India.

Finally, I would like to thank Aru, my wife and partner; none of this would have been possible without her. All of my successes are because of her constant encouragement, understanding and sacrifice. We have gone through many hardships, times when we were separated for years, personal crises, but, in the end, our love endured. In 2011, Aru gave me the freedom, and decided to accompany me on our most crazy adventure, a PhD and a life in science. It has been a rewarding ride, crazy at times, but our constant support for each other has made it all worth it. I remember the numerous times when I would keep her awake late in the night, just to discuss some ideas about experiments or my algorithm for classification of neurons in the colliculus; for all the patience that she has had and for all the lost sleep, I thank her. Lastly, I want to thank Aru for sharing with me, the most wonderful gift of all, our son, Neev. I am not religious, but, if reincarnation can somehow be true, I would always ask for the same partner.

Although this thesis is considered as a milestone and achievement for me, I could not have reached this junction in my life without the support and guidance of my mentors, friends and family who have constantly enriched my life and brought the best out of me.

Contents

LIST OF TABLES

LIST OF FIGURES

ABBREVIATIONS

nLM	nucleus lentiformis mesencephalic
AOS	accessory optic system
LGN	Lateral Geniculate Nucleus
TB	Trapezoid body
On	Olivary nuclei
VnLL	Ventral nucleus of the lateral lemniscus
DnLL	Dorsal nucleus of the lateral lemniscus
SC	Superior colliculus
SCs	Superficial layers of the SC
SCi	Intermediate layers of the SC
SCd	Deep layers of the SC
SCid	Intermediate and deep layers of the SC
IC	Inferior colliculus
ICX	External nucleus of the IC
OT	Optic Tectum
SZ	Stratus zonale
SGS	Stratum griseum
SO	Stratum Opticum
SGP	Stratum griseum profundum
FEF	Frontal Eye Fields
MT	Middle Temporal Area
PBN	Parabigeminal nucleus
pPBN	Peri- Parabigeminal nucleus
OTn	Nucleus of the Optic Tract
PTn	Pretectal nucleus
PTc	Pretectal complex
pPTn	Posterior pretectal nucleus
DLG	dorsal lateral geniculate
VLG	Ventral lateral geniculate
IP	Inferior Pulvinar
LP	lateral posterior nucleus of the thalamus
Pul	Pulvinar
PPC	posterior parietal cortex
AEV	Anterior ectocylvian visual area
SV	Suprasylvian fringe
HRP	Horseradish peroxidase
SP	Substance P
PV	Parvalbumin
SST	Somaostatin
SSG	Sonar sound groups

"You have control over doing your respective duty, but no control or claim over the result. Fear of failure, from being emotionally attached to the fruit of work, is the greatest impediment to success because it robs efficiency by constantly disturbing the equanimity of mind."

— Ramananda Prasad

The Bhagavad Gita

Page intentionally left blank

Hobbes : I suppose research is out of the question.

Calvin : Oh, like I'm going to learn about bats and then write a report?! Give me a break!

- Bill Watterson
Calvin & Hobbes*

1

Introduction

Consider an activity that many of us engage in on a regular basis, driving. For most experienced drivers, out on the road, with the radio blaring, one's mind may become lost in other thoughts, and the task of driving relies heavily on overlearned skills, as if it is a pre-programmed motor activity: automaticity (Charlton and Starkey, 2011). Driving, however, is a complex task. It requires the integration of multi-modal sensory information, which guide motor commands for steering and orienting to different stimuli. A driver is constantly bombarded with stimuli (see Figure. 1.1) and is required to pay attention to the rear view mirror, occasionally orienting the eyes to watch each side view mirror, not to mention the constant vigilance on the front of the road. The task does not end here: the driver's peripheral vision must be on high alert for pedestrians who might walk onto the road while looking at their cell phones. An interesting thing to note here is that each target of a driver's gaze is a stimulus in three- dimensional (3D) space. Images in each mirror, the road, vehicles in front and behind, are all located at different directions and distances with respect to the driver's head.

*I borrowed this quote from Kaushik's thesis but also found it online.

How does the brain represent the natural 3D world and what are the behaviors humans, and animals in general, use to enhance and sharpen these representations in real-world tasks? These questions form the main theme of this thesis.

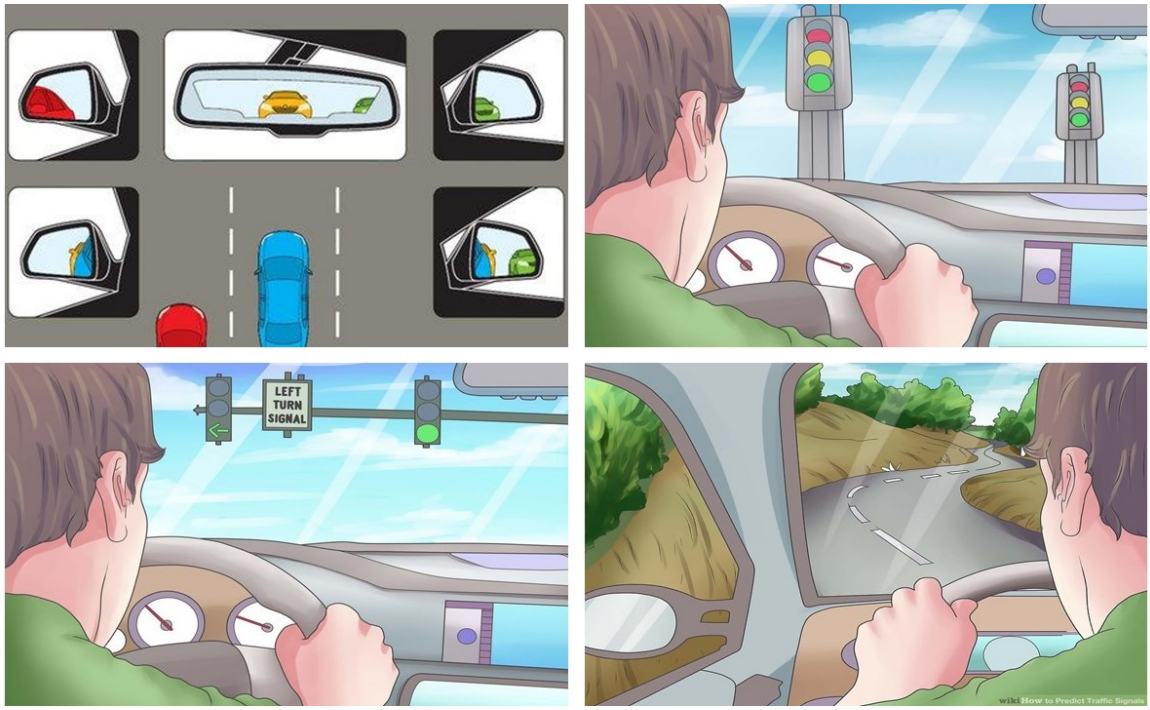

Figure 1.1. Orienting in 3D space while driving

Images from www.caranddriver.com and www.wikihow.com

The next few sections first explain orienting behaviors and then give a brief introduction to the problem of orienting in 3D space, with separate discussions of orienting in 2D space and orienting in depth. Following this is an introduction to the superior colliculus (SC), a midbrain nucleus, which is regarded as the hub of species-specific sensorimotor integration and which plays an important role in representing, as well as generating, orienting movements. This section is followed by an introduction to echolocating bats and their adaptive sonar behaviors. Finally, this

chapter will be concluded with a brief overview of the organization of following chapters to highlight how different ideas are connected throughout the thesis.

1.1 Orienting in 3D space

The physical world is three-dimensional (3D). From insects to birds, fish to reptiles, rodents to primates, including humans, most animals orient to and interact with stimuli in 3D space. The species-specific repertoire of orienting behaviors is defined as motor actions, which enable an animal to direct sensor organs to stimuli of interest, through eye, head, body and arm (reaching) movements (Schiller and Stryker, 1972; Roucoux et al., 1980a; Munoz et al., 1991; Cowie and Robinson, 1994; Pare et al., 1994; Stuphorn et al., 2000; Gandhi and Katnani, 2011), as well as pinnae movements in animals with movable ears (Henkel and Edwards, 1978; Stein and Clamann, 1981; Valentine et al., 2002). In echolocating bats, the active production of sonar vocalizations, which enables bats to gather information from the environment, is also an orienting movement (Valentine et al., 2002).

Despite the importance of orienting in 3D space, most of our knowledge about these behaviors comes largely from decades of research in restrained animals, generally studied either with 2D stimuli (azimuth and elevation) or stimuli at different depths. Very few studies have used freely behaving animals engaged in a natural task of 3D orienting (Gawryszewski et al., 1987; Van Horn et al., 2013; Finlayson et al., 2015). Thus, considering our current knowledge about orienting behaviors, I will discuss orienting in 3D space in two parts, 1) Orienting to stimuli in 2D space (azimuth and elevation) and 2) Orienting in depth. However, I would like to stress that considering the problem of *'understanding the neural underpinnings of orienting in 3D space'* as two separate

phenomena - orienting in 2D space and orienting in depth - takes away from the important fact that these behaviors are the behavioral outcome of an inseparable integration and feedback between incoming multimodal sensory information and motor movements and should be studied as a whole, not in isolation.

1.1.1 Orienting in 2D space

1.1.1.1 Representation of azimuth and elevation in the brain

Light falling on photoreceptors in the retina is essentially transforming the 3D external environment into a 2D projection. From here information in retinotopic coordinates is relayed to the central visual system (lateral geniculate nucleus (LGN), early visual cortices and the superior colliculus) where retinotopy is roughly maintained (Golomb and Kanwisher, 2012; Sereno and Huang, 2014). Thus, estimating of the 2D (azimuth and elevation) coordinates of an object in the visual world happens via a space code. In other words, the brain has a topographic map having a direct functional transformation of the retinotopy in the retina. For example, the early visual cortices are arranged as a log polar map of the retinal image (Horton and Hoyt, 1991; Engel et al., 1997). Unlike vision, auditory stimuli received by an animal with binaural hearing is not organized in spatial coordinates at the auditory receptor level, but rather it has a tonotopic organization. Most mammals and birds, and even some insects, use inter-aural level differences (ILD) to compute the location of a sound source in two dimensions (azimuth and elevation) (Pollack, 2000; Grothe et al., 2010; Wohlgemuth et al., 2016b). In addition, sounds that arise from locations other than the midline, arrive at different times at each ear, causing a timing difference detectable by the auditory system if the delay is large, especially in animals that have large heads. This inter-

aural time difference (ITD) can also be used to localize sounds in two dimensions (Knudsen and Konishi, 1978; Fuzessery et al., 1990; Popper, 1994; Knudsen and Brainard, 1995; Grothe, 2003; Pollak et al., 2003; Schnupp and Carr, 2009; Grothe et al., 2010; Wohlgemuth et al., 2016b). Furthermore, spectral cues, in the form of pinnae, head and body transfer functions are also important for the estimation of sound source elevation (Popper, 1994; Slee and Young, 2010; Wohlgemuth et al., 2016b).

Auditory information travels from the cochlea to the cochlear nucleus as a monaural stream, beyond which it gets mixed to form binaural and monaural stream and gets relayed to the trapezoidal body (TB), Olivary nuclei (On), Ventral and Dorsal nuclei of the Lateral Lemniscus (VnLL and DnLL, respectively) and finally gets relayed to the external nucleus of the inferior colliculus (ICX) and superior colliculus (SC) as a topographic map of 2D space (Popper, 1994; Cohen and Knudsen, 1999; Hyde and Knudsen, 2000).

1.1.1.2 Motor movements for orienting in azimuth and elevation

For viewing stimuli, which do not require large changes in the visual angle, many animals with movable eyes make eye movements, called saccades, to scan the environment. In animals with eyes in the front of the head, saccades are conjugate eye movements, in which both eyes move in the same direction, and by approximately equal amounts, to a visual stimulus (Wurtz and Albano, 1980; Sparks and Hartwich-Young, 1989; Stein and Meredith, 1993; Gandhi and Katnani, 2011). In the case of large angles between visual stimuli, eye movements may be accompanied by head and body movements. Because saccadic eye movements and head movements are often mapped in coordinates of 2D visual space, azimuth and elevation, I refer to them, here, as movements for orienting in 2D space (Dean et al., 1986; du Lac and Knudsen,

1990; Gandhi and Katnani, 2011). However, in following sections, I also discuss eye, head and body movements for orienting in depth.

1.1.2 The third dimension: depth

To understand how animals represent and orient to stimuli in depth, it is important to emphasize that the representation of stimuli at different depths, as well as motor movements to interact with them, require the integration of both sensation and motor action. The accurate perception of depth is difficult, if not impossible, to achieve without motor movements (Cornilleau-Pérès and Gielen, 1996; Kral, 2003). For example, conjugate eye movements (saccades) to a location in 3D space need to be accompanied by vergence eye movements as well as lens accommodation to get accurate depth information (Green et al., 1980; Chaturvedi and Gisbergen, 1998; DeAngelis, 2000; Cumming and DeAngelis, 2001; Van Horn et al., 2013). Thus, in this section I will not segregate the representation of depth from orienting to depth. Although, estimation of stimulus location in 3D follows some common principles across animal species, many species have developed specializations for solving this problem. Below, I give examples from different animals and demonstrate why sensation is inseparable from motor action, for depth perception.

1.1.2.1 Visual animals with movable eyes: Vergence eye movements

Most visual animals, including primates and humans, can move their eyes in their orbits and display a repertoire of eye movements (Land, 1999). Many animals, especially those that have

a large separation between their eyes use disjunctive eye movements (vergence eye movements) to bring visual stimuli at different depths into their central field of vision (area centralis or fovea) (Stryker and Blakemore, 1972; Zuidam and Collewijn, 1979; Green et al., 1980; Cumming and DeAngelis, 2001). Another related eye movement required for orienting in depth is lens accommodation movements of the ciliary muscles. Accommodation occurs when animals, including adult and infant humans as well as primates, orient to objects at different depths. Lens accommodation can occur due to blurring of images on the retina or due to binocular disparity changes due to vergence movements (Haynes et al., 1965; Banks, 1980; Sawa and Ohtsuka, 1994; Gamlin and Yoon, 2000). This raises the question of whether the saccadic and vergence systems share neural circuitry or they are independent of each other? A similar question regarding the lens accommodation system also arises. These issues will be discussed in detail in section 1.2.4.

1.1.2.2 Head bobbing, peering and optic flow

Let us now consider two different classes of animals, insects and avians. Both insects and birds have very disparate visual, auditory and motor systems. Both classes of animals, however, routinely demonstrate complex behaviors like tracking targets, behaviors for mate selection, interacting with conspecifics, planning movements to stalk and capture targets, defending territory and navigating space (Land and Collett, 1974; Srinivasan et al., 1999, 2000; Troje and Frost, 2000; Wessberg et al., 2000; Nordström and O'Carroll, 2009). These behaviors require a representation of egocentric 3D space and species in each class have evolved some common and as specialized behaviors for representing and orienting to objects in 3D space.

Most insects and birds have small-sized heads, thus limiting or eliminating the use of binocular disparity as a strategy to solve the problem of depth perception (Kirschfeld, 1976; Köck

et al., 1993; Kral, 2003). Additionally, non-predatory birds have eyes that are located at relatively lateral positions thus decreasing the area of binocular overlap, meaning that binocular vision is limited or completely non-existent (Kral, 2003) due to which, it is unlikely that the species of each of this class use the same mechanisms as humans and primates, like binocular disparity, to solve the problem of depth perception (Kirschfeld, 1976; Srinivasan et al., 1999; Kral, 2003). To overcome the disadvantage of having small heads, fixed focus eyes and/or peripherally located eyes, both insects and birds have evolved head and body movement behaviors to use motion parallax to aid in localizing targets in the depth dimension. Mantids and locusts, for example, exhibit head movements before making jumps or before attacking prey (Kral 2003). These self-generated sideways head movements, known as "peering" behavior, induces motion parallax which has been shown to aid these insects in the estimation of depth. In separate studies, Wallace (1959), Sobel (1990) and Poteser and Kral (1995), moved targets along or against the head motion of the insect, thus manipulating the amount of motion parallax induced. In cases when the relative motion of the target was in the same or opposite direction of the peering head movements, the animal either jumped too far or too short, respectively (Wallace 1959, Sobel 1990, Poteser and Kral, 1995).

Another example of head and body movement has been documented in many avian species. One such example is the 'head bobbing' behavior of pigeons (Troje and Frost, 2000; Necker, 2007). The head-bobbing consists of a thrust phase and a hold phase, which is thought to be under visual control. It is hypothesized that head-bobbing engages an optokinetic loop, which serves to stabilize retinal motion and is thought to serve a comparable function as saccades in

mammals (Troje and Frost, 2000; Kral, 2003). While flying, pigeons also exhibit head-bobbing behavior at the time of landing and take-off (Davies and Green, 1994; Necker, 2007).

Another important cue for depth processing that has been identified and studied extensively in insects and birds is optic flow. When an animal moves in 3D space, different stationary objects and background patterns create distinctive patterns of optic flow over large areas of the retina, which can be measured and used to generate the perception of self-motion as well as to estimate depth (Frost and Wylie, 2000; Srinivasan and Zhang, 2004). In a set of classic experiments, Srinavasan and colleagues trained honey bees to fly through a tunnel lined with asymmetric grating patterns on opposite walls which created a differential optic flow illusion of artificial depths. Using this paradigm they demonstrated that honey bees adjust their distance from the walls to attempt to match the optic flow on the two walls to estimate their relative distance from objects in the environment (Srinivasan, 1996, Srinivasan, 2011, Srinivasan 2000). It was recently shown that flying budgerigars also behave in a similar manner and balance optic flow across their eyes (Bhagavatula, 2011). It has been demonstrated that neurons in the nucleus lentiformis mesencephali (nLM) and the accessory optic system (AOS) in the pre-tectal nucleus of the bird, contain six different populations of neurons which decompose the entire optic flow into six dimensions of rotation and translation movements (Wylie et al., 1998; Frost and Wylie, 2000; Xiao and Frost, 2013). Recently, Frost and colleagues, found neurons in the pre-tectum area of the mid-brain, which fire when the animal is subjected to motion parallax stimuli (Xiao and Frost, 2013).

1.1.2.3 Temporal patterning of echolocation calls in bat: A strategy for increasing depth resolution

Echolocating bats demonstrate extraordinary depth estimation, which is required for obstacle avoidance, landing and prey capture (Griffin, 1958). It has been shown that bats can estimate target depth using the delay between the vocal production time and echo arrival time (Simmons, 1971, 1973a). The bat's active sense of echolocation allows it to adaptively modulate sonar call parameters to extract task relevant information from the environment (Griffin, 1958; Simmons et al., 1979; Moss and Surlykke, 2001, 2010; Schnitzler and Kalko, 2001). Once such adaptive behavior is the temporal patterning of sonar calls. For example, bats produce clusters of sounds at very short and regular pulse intervals (i.e. higher pulse repetition rate), flanked by sonar sounds, which are emitted at longer pulse intervals. These clusters of sonar sounds have been termed sonar sound groups (SSGs) and such adaptive sonar behavior has been reported in both laboratory and field studies, when bats encounter complex environments which require greater spatio-temporal resolution (Surlykke and Moss, 2000; Moss and Surlykke, 2001; Moss et al., 2006; Petrites et al., 2009; Aytekin et al., 2010; Kothari et al., 2014; Sändig et al., 2014; Falk et al., 2015).

It has been hypothesized that SSGs help bats to sharpen the resolution of target depth (Moss and Surlykke, 2001, 2010; Moss et al., 2006; Kothari et al., 2014). For example, in a laboratory study, Moss et al (2006) reported that big brown bats increase the production of SSGs when they capture insects in the vicinity of vegetation clutter, and similarly, Falk et al (2014) found that this species produced more SSGs as they foraged in an artificial forest, compared to an open room. Petrites et al. (2009) reported that bats increase the production of SSGs when

navigating in a highly cluttered environment. A related finding, reported by Sändig et al. (2014), showed that bats engaged in a wire-avoidance task increased the production of SSGs with increasing task difficulty. In a more recent study, Wheeler et al showed that bats flying in increased density of clutter, created through a maze of chains, produce more SSGs, and with more number of calls in each SSG, with increased proximity to clutter (Wheeler et al., 2016).

These studies have led to the hypothesis that the bat's production of SSGs improves its spatio-temporal resolution of sonar objects (targets or obstacles), especially in the depth dimension (Moss and Surlykke, 2001; Moss et al., 2006; Kothari et al., 2014) and thus, similar to peering and head bobbing behavior in insects and birds, SSGs are an adaptive strategy for orienting in depth.

1.1.3 Section summary

In this section, I have introduced the problem of orienting in 3D space, an important behavior exhibited by animals interacting in the natural world. I then gave a brief summary of how 2D space is represented in the brain, followed by movements for orienting in 2D space. Finally, I described how different animals solve the problem of orienting in depth and why orienting in depth is an integration of sensory acquisition and motor movements. One of the most intriguing questions of neuroscience is the problem of sensorimotor integration - how sensory information, across different modalities is integrated in the brain, to generate orienting behaviors for interacting with stimuli in the physical world. This problem is surprisingly complex and requires various computations before it can generate the appropriate motor behavior.

Gross anatomical projections in the brain, neurophysiological and clinical studies, all point to the midbrain superior colliculus as a major hub for sensorimotor integration and orienting behaviors. In the following section, I will give a brief introduction to the superior colliculus and review our current knowledge regarding the role of the SC in orienting behaviors and its role in an attention network.

1.2 The Superior Colliculus

One of the most thoroughly studied sub-cortical brain regions in the vertebrate brain is the mammalian superior colliculus (SC) or its avian homologue, the optic tectum (OT). Much of the knowledge about the SC/OT comes from comparative studies across different vertebrate species (Hartline et al., 1978; Wurtz and Albano, 1980; Sparks, 1988; Sparks and Mays, 1990; Stein and Meredith, 1993; Knudsen and Brainard, 1995; Valentine et al., 2002; Krauzlis et al., 2013). Over the years the scientific opinion about the role and function of the SC has changed considerably and it is only in past two decades that the SC is considered as an important hub for sensorimotor integration and a center for orienting of attention.

The SC receives, species-specific multimodal sensory input, in which the external 2D space (azimuth and elevation) is topographically organized over the SC laminae, with maps from different sensory modalities in register with each other. In the sections below I will first give a brief timeline of how views of the SC in the scientific community have changed over the past 150 years. This is followed by a brief discussion of the role of SC in orienting in 2D space. In that section, I will briefly outline the functional anatomy of the SC and connectivity of the SC with

different brain regions. Finally, I describe the current evidence supporting the role of the SC in orienting in 3D space.

1.2.1 A brief time line

One of the earliest documented studies of the midbrain SC was performed by Adamuk in the 1860's using microstimulation ((Wurtz and Albano, 1980; Knudsen, 2011), demonstrating its role in oculomotor control. However, over the subsequent few decades, a series of lesion experiments in the SC of monkeys (Knoll, 1869, Bechterew, 1884, Ferrier and Turner, 1901, Levinsohn, 1909) yielded no significant effects in pupil size, pupillary light reaction or saccadic behavior were observed. Additionally, most observable deficits vanished after 2-3 days of lesioning. These results cast a strong doubt on the previously claimed role of the SC in visuo-motor function.

However, in an excellent review paper in the early 1920's, Wilson (Wilson, 1921) re-examined the previous lesion studies and found large gaps in the extent of lesions and data interpretations, calling into question the claims denying the SC a place in the oculomotor system hierarchy. This classic paper also describes several clinical cases in which external symptoms like lack of pupil dilation, absence of pupillary light reflex, abnormality in eye movement were attributed to tumors in and around the SC region.

Despite mounting clinical evidence that indicated a role of the SC in eye movements, along with anatomical evidence that demonstrated SC connectivity with sensory cortical regions and motor sub-cortical regions, all of which pointed towards a more general role of the SC in species specific orienting (Wilson, 1921; Barris et al., 1935; Crosby and Henderson, 1948), it was not until the early 1970s that research interest in the superior colliculus peaked again with the seminal

work of Robinson, Wurtz and Goldberg (Goldberg and Wurtz, 1972a, 1972b; Robinson, 1972).. More recent work in barn owls, primates and mice has indicated a much larger role of the SC in the attention network, especially for stimulus selection (McPeek and Keller, 2004; Lovejoy and Krauzlis, 2010; Mysore and Knudsen, 2011; Krauzlis et al., 2013; Duan et al., 2015). Thus, after more than a century, the 'lost glory' of the SC has been restored, and it is regarded, today, as a hub for sensation, spatial attention, and orienting.

1.2.2 Functional organization, anatomy and connectivity

A conserved anatomical feature of the SC/OT, across species, is its laminar structure (Wurtz and Albano, 1980; Knudsen, 1982; Stein and Meredith, 1993; May, 2006), which has been coarsely divided into three main divisions (see Figure. 1.2). Figure. 1.2 also displays the general view of how information flows through the SC for sensorimotor integration, with multimodal sensory information arriving in the superficial and intermediate layers, which finally drive the premotor commands in the deeper layers. Owing to similarities in the oculomotor systems in primates and humans, much of the literature between 1970 and 2005 was focused on primates, but a significant amount of research also focused on cats and barn owls. More recently, due to the increasing availability of genetic and molecular techniques in mice, mice are now increasingly being used to elucidate brain mechanisms of attention (Erlich et al., 2011; Bezdudnaya and Castro-Alamancos, 2014; Duan et al., 2015), as well as to study perceptual decision making, a realm of studies which was previously restricted only to primates (Carandini and Churchland, 2013).

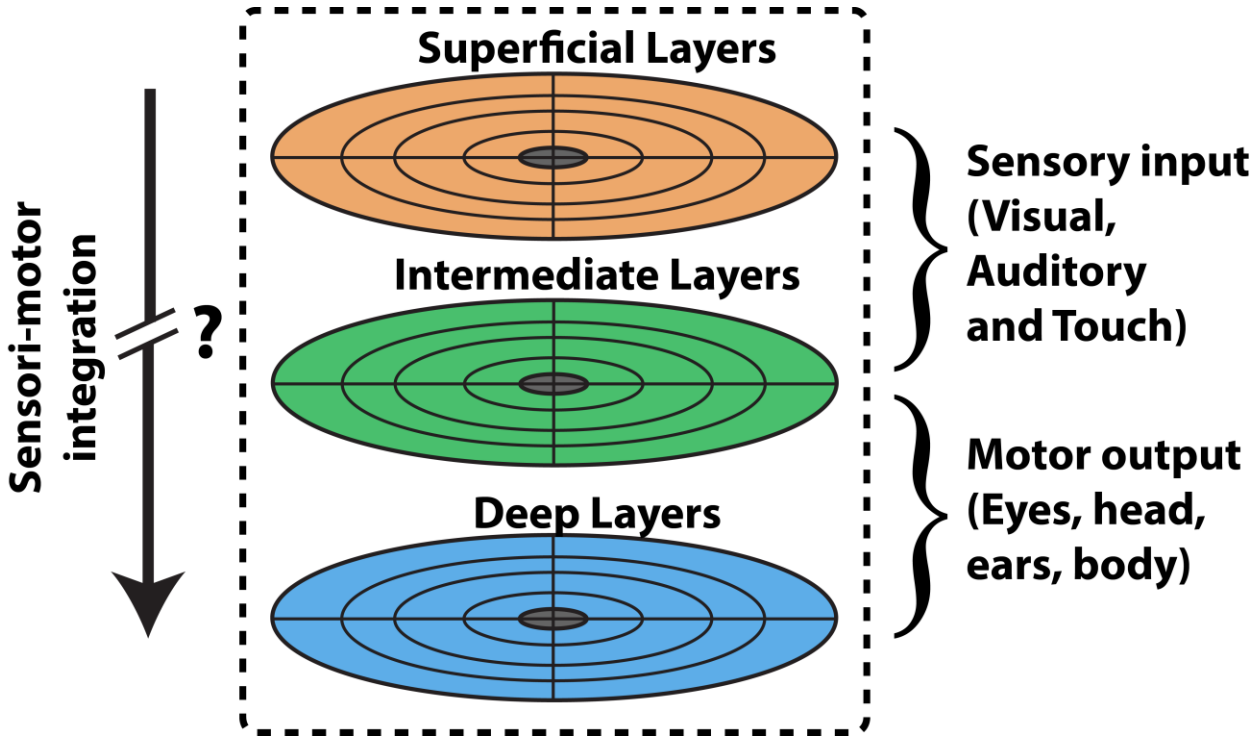

Figure 1.2 SC laminae and coarse functional anatomy.

In the descriptions below, I will start each subsection with a description of the representation and current knowledge in primates and then further, in subsequent paragraphs, highlight the major differences between primates and mice or bats. I would like to add that there is a vast species diversity of echolocating bats, and the functional anatomy and connectivity data for the SC of no single species is complete. Another important point to note is that the size of laminae, the internal and external connectivity, variations in sensory inputs, as well as premotor signals originating from SC laminae, are all strongly species-specific and are influenced by the ecological niche the animal inhabits as well as the relative contributions of different sensory modalities to the animal's behavior.

1.2.2.1 Superficial Layers

1.2.2.1.1 Sub-layers

Following the general SC anatomy of most mammals, the superficial layer (SL) in primates is further segregated into 3 sub-laminae called the stratum zonale (SZ), stratum graseum superficiale (SGS) and stratum opticum (SO) (Wurtz and Albano, 1980). Similar organization is found in several mammals for which vision is the dominant sensory modality, such as cats (Kanaseki and Sprague, 1974), tree shrews (Graham Casagrande 1980) and hamsters (Mooney et al., 1984). In primates, as well as cats, the SGS is further sub-divided into the upper and lower layers, uSGS and lSGS, respectively (May, 2006). As in primates and cats, where the SGS has been further divided into uSGS and lSGS (Wurtz and Albano, 1980; May, 2006), a similar laminar structure had been proposed for mice and rats (Hofbauer and Dräger, 1985; Edwards et al., 1986; May, 2006). In a recent study, however, a slightly different laminar structure has been proposed (Byun et al., 2016). Byun and colleagues used a systematic approach to investigate gene expression within four molecular families: transcription factors, cell adhesion molecules, neuropeptides, and calcium binding proteins. Their analysis revealed 12 molecules with distinct expression patterns in mouse sSC which further revealed 10 different SCs neuronal types. Based on the characteristic positions of these molecules in the SCs of adult mice they propose 4 laminae 1) layer 1, which is the combination of the previously defined SZ and uSGS and is identified by the presence of substance P (SP), 2) layer 2 is the SGSl and is identified by the presence of somatostatic (SST) and parvalbumin (PV) neurons, 3) layer 3 sits just below the boundary dividing the SGS and SO and is identified by the presence of transcription factor Brn3b. Brn3b transcription factor has been shown to control the development of RGCs in the mammalian retina

and its deletion can lead to axon defects in the eye and brain, defects in central projections that differentially compromise a variety of visually driven behaviors (Badea et al., 2009). 4) Layer 4 is defined by the lower boundary of SO. Unfortunately, we do not yet know how these relate to the different SCs cell types that have been previously identified based on cell morphology, axonal and dendrite projections and sizes in different species (May, 2006; Byun et al., 2016). Of particular interest to this thesis is the fact that in many species of echolocating bats, such as the *E. fuscus,* which primarily use sonar as the primary sensory input for navigation and foraging (Griffin, 1958), the SZ is completely absent , and the SGS and SO, which receive retinal input are just approximately 50-60 µm deep. In addition, in the mustached bat, *Pteronotus parnellii* the layers are less than 60 µm deep and indistinguishable (Cotter, 1985; Covey et al., 1987).

1.2.2.1.2 Connectivity

In all species investigated so far, the superficial layers of the SC primarily receive visual input (Wurtz and Albano, 1980; May, 2006). Only recently, Hoffmann and colleagues (Hoffmann et al., 2016), recorded responses of neurons in the SC of an echolocating bat, *Phyllostomus discolor,* to visual stimuli. They confirm that, similar to other mammals, the SC of this species of echolocating bat contains cells in superficial layers that only respond to visual stimulation. Not surprisingly, visual responses have also been found in the superficial SC layers of species known to be highly reliant on long range vision for navigation and foraging – for instance, the Egyptian fruit bat (which produces echolocation calls using tongue clicks), and the flying fox (which does not echolocate (Pettigrew, 1986; Rosa and Schmid, 1994; Thiele et al., 1996; Pettigrew et al., 2008) .

Although, the afferents and efferents, of the superficial layers follow a common framework across species, there is species-specific diversity of visual inputs and outputs. Figure. 1.3a and 3b, by showing an example of the retinal and striate cortex inputs to the primate SC, demonstrates the common structural pattern observed across most mammals (Huerta and Harting, 1984a, 1984b). The superficial layers contain a retinotopic map of the contralateral visual hemifield so that central visual regions are represented rostrally, peripheral regions caudally, upper visual regions medially, and lower regions laterally.

Afferent connections: Retinotectal projections: As previously mentioned, a common theme in discussions of the SC is conserved structure and connectivity, accompanied by species specific variations indicated in the density, laterality and connectivity, to and from the SC, across species. And these differences mainly reflect how reliant a particular species is on a particular sensory modality as well as how its peripheral sensory organs are arranged. This is particularly evident when one compares the retinal afferents to the superficial layers of the SC across species with frontal eyes, like monkeys and cats, and animals that have eyes located more laterally, like mice and rats, and finally bats, which rely predominantly on echolocation for spatial orientation.

In primates the retinotectal afferents are restricted to the superficial part of SGS, often known as upper SGS or SGSu (Lund, 1972; Bunt et al., 1975; Wurtz and Albano, 1980). This is also the case for most other mammals, including cats (Lund, 1972). It must be noted, however, that in primates (and possibly in humans) the retinocollicular projections differ from those of other mammals, mainly due to the presence of the high acuity region of the fovea (Hubel et al., 1975; Wurtz and Albano, 1980). As shown in Figure. 1.3, the contralateral retina projects to the entire rostro-caudal extent of SGSu lamina of the colliculus. The central visual field, within 10^{o} of the

foveal region, occupies more than 30% of the rostro-caudal extent of the colliculus, but surprisingly the projections from the retina representing this part of the visual field are less dense and patchy. The ipsilateral retina also makes a very small but patchy projection to the rostral part of the SGS layer (Hubel et al., 1975; Pollack and Hickey, 1979; Wurtz and Albano, 1980; May, 2006 but also see Lund, 1972; Huerta and Harting, 1984b for a slighty different view on ipsilateral projections to the rostral pole of the primate SC). A similar organization is seen in the cat, which also has a foveal region – area centralis (Graybiel, 1975). Thus, extra-foveal but binocular region of the visual field (Figure. 1.3 – contralateral in pink and ipsilateral in cyan) projects to the central part of the SGSu where contralateral and ipsilateral projection form alternate bands. A similar pattern is also seen in cats (Lund, 1972; May, 2006). The retinal projections from the monocular visual field project only to the contralateral caudal pole of the SGSu (Cynader and Berman, 1972; Lund, 1972; Bunt et al., 1975; Hubel et al., 1975; Pollack and Hickey, 1979; Wurtz and Albano, 1980; Huerta and Harting, 1984a, 1984b; Stein and Meredith, 1993; May, 2006).

Mice and rats, animals which are not predatory in nature, have more laterally placed eyes; the visual field with binocular overlap is minimal and most of the visual field is monocular. This is directly reflected in the pattern of retinal projections to the SC. It has been demonstrated that the binocular field of vision for mice is approximately 20^{o} (Dräger and Hubel, 1975; Drager and Hubel, 1976; Scholl et al., 2013; Sterratt et al., 2013) for each visual hemifield. In accordance with such a limited visual overlap it has been shown that almost all of the crossed retinal ganglion cells project topographically to the contralateral SC, whereas only about 3-5% of RGCs project to the ipsilateral superficial SC (Lund, 1965; Lund et al., 1980; Linden and Perry, 1983; Salinas-Navarro et al., 2009; Hong et al., 2011) . This is in contrast to monkeys and cats where a small proportion

of crossed RGCs projected to the SC (Linden and Perry, 1983). Also, the ipsilaterally projecting RGCs originate from the ventrotemporal crescent area of the retina (Hong et al., 2011). Although, rats and mice lack a fovea, a numerous reports have identified locations in the retina with increased cell densities (Hong et al., 2011). These locations might account for the slight, but anisotropic, magnification of the representation of central visual field on the SC (Dräger and Hubel, 1975; Drager and Hubel, 1976). Additionally, there is a segregation of retinal projections to the SC laminae, most contralateral projections are to the superficial SGS, while the ipsilateral connections are to the deeper SGS and SO.

In echolocating bats, some of which are less reliant on vision than echolocation, for example, *Eptesicus fuscus, Myotis lucifugus* and the *Artibeus jamaicensis*, the optic nerve fibers completely project to the contralateral SC (Cotter, 1985). On the other hand, *Pteropus giganteus*, a flying fox which is a non-echolocating bat species and the echolocating bat, *Rousettus aegyptiacus*, which have highly developed vision, have a retinocollicular projection which follows the more primate like pattern, where the temporal hemiretina projects ipsilaterally, while the nasal hemiretina projects contralaterally (Cotter and Pierson Pentney, 1979; Cotter, 1981; Pettigrew, 1986; Thiele et al., 1991).

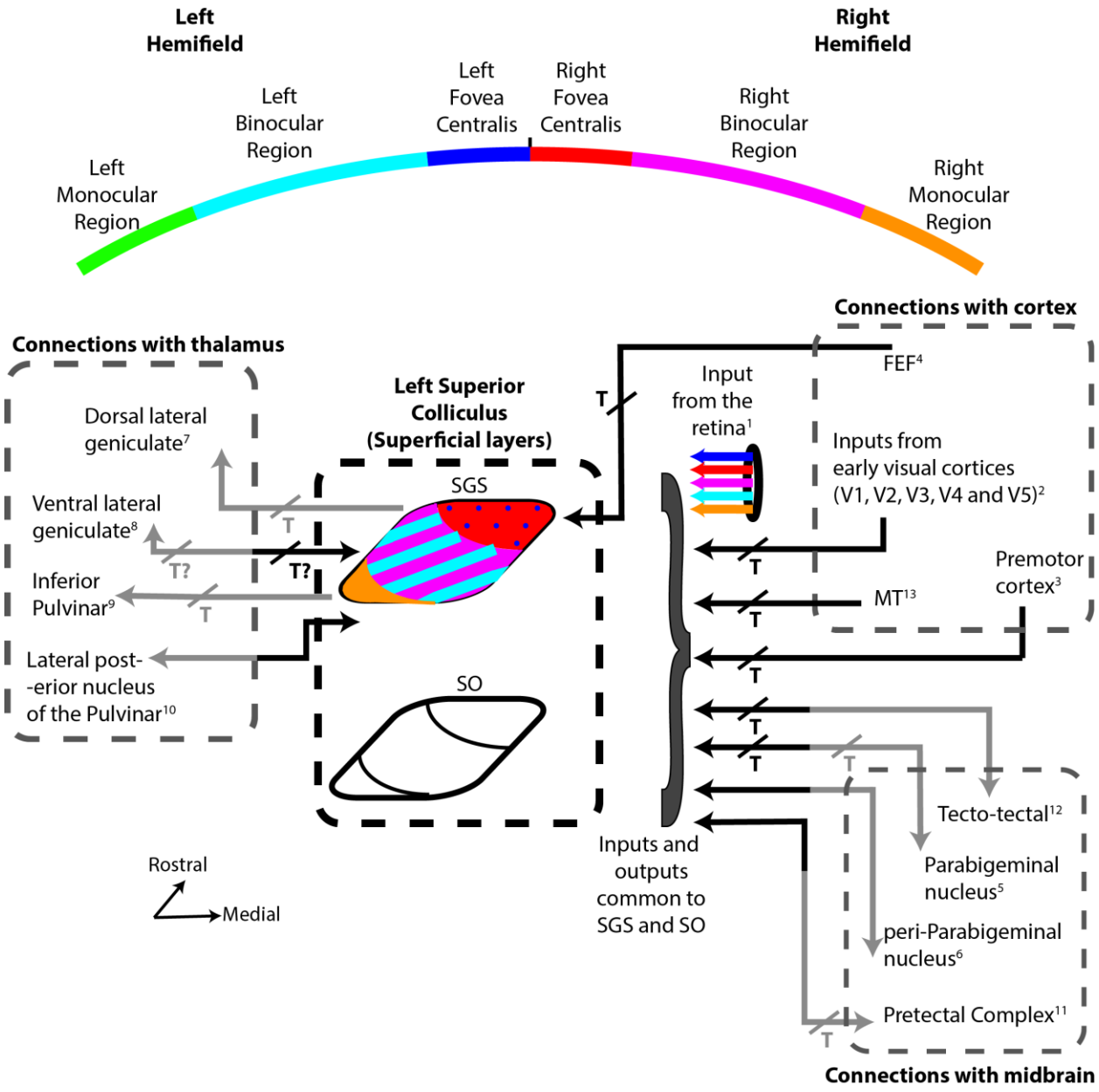

Figure 1.3 Afferent and efferent connections of the superficial layers of the SC.

Afferent connections: Corticotectal projections: The second major input to the superficial layers of the SC is from layer 5 of the striate cortex (Lund, 1972, 1975; Langer and Lund, 1974; Wurtz and Albano, 1980; Huerta and Harting, 1984b; Stein and Meredith, 1993; May, 2006).

Interestingly, the corticotectal afferents are topographically arranged and closely follow the distribution pattern of the retinotectal afferents, to form retinotopic map of the 2D visual field across the superficial SC laminae. In other words, the area of the visual cortex receiving afferents from one region of the retina, projects to the area of the SC receiving inputs from the same region of the retina. In primates, the topographically matched afferents from the primary visual cortex (Brodman area 17 or V1), secondary visual cortex (Brodmann area 18 or V2) and the associative visual cortex (Brodmann area 19 or V3, V4 and V5) have nerve endings throughout the SGS (Lund, 1972; May, 2006) and SO. The associative cortex also projects to SGI (Lui et al., 1995). The Frontal Eye Fields (Brodmann area 8 or FEF), which also contains a retinotopic map of the visual field (Sommer and Wurtz, 2000), also projects in a topographically arranged manner to SGS and SO (Künzle et al., 1976). In macaques and owl monkeys, the midtemporal area (MT) also projects to SGS and SO layers (Fries, 1984, 1985). Further, using retrograde HRP labeling, surprisingly, it was found that even the smallest amount of injection in the superficial layers caused labeling in the premotor cortex (Brodmann area 6) along with other areas mentioned above (Fries, 1984, 1985). Further, these projections from the premotor cortex seem to be topographically organized where the rostral SC receives inputs from the presumed hand representation while the more caudal parts, encoding the peripheral visual field, receive premotor inputs from the presumed arm and trunk representation areas. One hypothesis explaining inputs from the premotor areas to the SC is that these projections mainly send corollary discharge information regarding impending movements (Fries, 1985). In cats, as should also be the case in primates, using postembedding immunocytochemistry, the cortical and retinal inputs to the SC have been found to be glutamergic (Mize and Butler, 1996).

Mice, rats and most rodents follow the same pattern of connectivity from the cortex to the SCs as in primates (Linden and Perry, 1983; May, 2006). A notable exception is in rats, where area part of V2 (Brodmann area 18b) does not project to the superficial layers (Harvey and Worthington, 1990). In the insectivorous echolocating bat *E. fuscus* a projection from the ipsilateral visual cortex to the SCs has been demonstrated (Zhang et al., 1987).

Afferent and efferent connections to the parabigeminal and pretectal complex: The *SCs* (primarily the SGS) receives dense connections from the parabigeminal nucleus and the pre-tectal complex as well as sends dense connections to both these regions (May, 2006). The parabigeminal nucleus (PBN) is considered as a satellite nucleus to the SC and sends multiple streams of connections to the SCs layers (Graybiel, 1978). The PBN sends bilateral cholinergic projections to the SCs where the crossed projections appeared only in the foveal (rostral) regions of the superficial layers whereas the uncrossed projections were topographically arranged across the rostro-caudal extent (Baizer et al., 1991). A lot more is known about the connectivity between the PBN and SC in cats as well about the visual properties of PBN cells (Kawamura et al., 1974; Graybiel, 1978; Edwards et al., 1979a; May, 2006). Located below the PBN is yet another nucleus called the peri-PBN (pPBN) and it has been shown also to be reciprocally connected with the SGS (May, 2006). The avian homologues of the PBN and pPBN are two nuclei called the Ipc and the Imc. In cats and primates it is now accepted that the SC has reciprocal but ipsilateral connectivity with the pretectal complex (PTc), mainly with its nuclei, nucleus of the Optic Tract (OTn) and the posterior pretectal nucleus (pPTn) (Graybiel, 1978; Wurtz and Albano, 1980; May, 2006). Further it is believed, mainly from data in cats, that the projection from the SCs to PTc is topographical, mainly because the region of PTc, upon which stimulation produces lens accommodation, comes

from the rostral pole of the SGS and SO. In mice and rats, in addition to the above connections, the olivary pretectal nucleus (OPt) also appears to project to the SCs. It terminates exclusively in uSGI of the rostral pole of the SC (Taylor et al., 1986).

Efferent and afferent connections with the Thalamus: The superficial layers mainly project to 3 main visual thalamic nuclei. The dorsal lateral geniculate (DLG), the ventral lateral geniculate (VLG) and the inferior pulvinar (IP). In both squirrel monkeys and macaques, ipsilateral projections to the DLG arise from the upper lamina of SGS (uSGS) and have been noted to not originate from the SO (Harting et al., 1978, 1991a; Wilson et al., 1995). Another point to note is that in macaques the parabigeminal nucleus also projects heavily to the DLG (Harting et al., 1991b). In an excellent comparative study across 19 species it was shown that the SGS-DLG connectivity is topographic (Harting et al., 1991a). In the greater bush baby, galago crassicaudatus, it has been shown that in the DLG, the retinal, tectal and parabigeminal converge on DLG neurons (Feig and Harting, 1994) however, cortical afferents do not converge on these cells. Similar to the DLG, the uSGS also sends ipsilateral visual afferents to the VLG. In many species like cats, squirrels and tree shrews it has been shown that multiple subdivisions (including the retinorecepient division) of the pregeniculate nucleus (the homologue of VLG in primates) send topographic projections back to the SGS (May, 2006). However, in macaques, there is only one study which has demonstrated reciprocal connectivity between the VLG and the SGS, where the all subdivisions of the VLG excluding the retinorecepient subdivision send back projections back to the SGS, and it is not known whether these are topographically arranged (Livingston and Mustari, 2000). In primates the deeper layers of the SGS (lSGS) provide a dense ipsilateral and

topographically arranged projection to the inferior pulvinar (IP) (Huerta and Harting, 1983, 1984b; May, 2006).

Mice and rats have similar connectivity with the thalamus as in primates. Some of the notable exceptions are mentioned below. Apart from the above mentioned connections, the inter-geniculate leaflet, which is sandwiched between the DLG and the VLG, is reciprocally connected with the SO (and partially SGI) in rats and hamsters. The inter-geniculate leaflet and even the VLG has been implicated in the control of circadian rhythms (Taylor et al., 1986; Morin et al., 2003; May, 2006). In contrast to primates, where only the inferior pulvinar receives major projections from the SCs, in rats and hamsters, the entire pulvinar as well as the lateral posterior nucleus of the thalamus (LP) receives input from the SO (Taylor et al., 1986). Additionally, these inputs have been shown to be not topographically organized in rats and hamsters, which is further contrary to what is found in primates and cats (Perry, 1980; Mooney et al., 1984; May, 2006).

Tectotectal connectivity: I have devoted a separate section, following the discussion of intermediate and deep layers, to discuss how the two colliculli talk to each other. Also, see individual Figures 3, 4.

1.2.2.2 Intermediate and deep layers

Although intermediate and deep layers of the SC (*SCid*) are often considered as separate from each other, many researchers often combine them as their functional and cellular architecture is quite intermingled (Wurtz and Albano, 1980; May, 2006). I will do the same here.

1.2.2.2.1 Sub-layers

The *SCid* is further segregated into 4 sub-laminae called the stratum griseum intermediate (SGI), stratum album intermediate (SAI), stratum griseum profundum (SGP) and stratum album profundum (SAP). Such similar organization is found in several mammals where vision is the dominant sensory modality like primates (Wurtz and Albano, 1980), cats (Kanaseki and Sprague, 1974) and tree shrews (Graham Casagrande 1980).

1.2.2.2.2 Connectivity

The intermediate and deep layers of the SC, in a species specific manner, receive multimodal inputs from different sensory areas demonstrating that the sensory modality which can provide the animal with information regarding stimuli of interest or stimuli which can be threatening, are routed to the SC and end up as afferents to the intermediate and deep layers (See, Figure. 1.2). After selection of the stimuli of interest, the intermediate and deep layers of the SC send out efferents to primary motor centers which can control orienting movements of the eyes, ears, head, arms and body, again, in a species specific manner.

In the next section, I will mainly focus on a comparative study of SC connectivity in primates, mice/rats and bats. Here, I will first outline the connectivity patterns observed in primates and later highlight the major differences observed in mice/rats and echolocating bats. Moreover, as the connectivity of the SCid with other brain areas is extensive and diverse compared to the quite simplistic connectivity of the superficial layers, I have created a table (Table 1) which lists brain areas which send afferent and efferent connections to the SCid. Table 1 also has columns for comparing the connectivity between primates, rats/mice and bats. Here, I acknowledge Doreen Valentine, one of Dr. Moss' graduate students, as the idea of this

comparison table has been borrowed from her thesis. The connections with the SCid have been organized into seven groups, based on their source of projection, 1) cortex, 2) Diencephalon, 3) Pretectum, 4) Midbrain, 5) Pons and Medulla, 6) Cerebellum and 7) Cervical spinal cord. Subcortical connectivity data for primates is still incomplete and so in Table 1, I have marked with asterisks (*), in the column for primates, where data has been supplied from tracing and anatomical studies in cats. Further, as most connections to the intermediate and deep layers are to or from both layers and difficult to segregate, I will only differentiate the connections which specifically arise from either of these layers when solid data exists for the above mentioned species. Finally, I will mention species specific specializations that exist, for example infrared space maps in snakes and electrosensory maps in electric fish.

Afferents from the cortex. Table 1.1 shows in detail the afferent connections from various cortical areas in primates. In short, topographical and ipsilateral visual input to SCid comes from the striate cortex (Area 17) but not from Brodmann areas 18 and 19. Auditory cortex (Brodmann area 22) also projects to the SCid. Almost the entire posterior parietal cortex (PPC), with dense inputs from the posterior bank of the intraparietal fissure, projects to the SCid. Efferent connections are also observed from the Inferotemporal cortex (IT, Brodmann areas, 20 and 21). Interestingly the only somatosensory inputs to the SC in primates come from the secondary somatosensory cortex, S2 (Brodamnn area 2). Further, the premotor cortex (Area 6), motor cortex (Area 4) as well as the insular cortex (Area 14) also project to SCid. In primates most of the cortical afferents are ipsilateral and glutamergic (Lund, 1972; Kawamura et al., 1974; Künzle et al., 1976; Tigges et al., 1979; Wurtz and Albano, 1980; Harting et al., 1980; Fries, 1984, 1985, Huerta and Harting, 1984a,

1984b; Lui et al., 1995; May, 2006). The visual, auditory and somatosensory cortical projections to the SC are topographically arranged and each sensory modality specific map has been shown to be in register with the sensory map of visual space (Stein and Meredith, 1993). I will discuss this in more detail in a separate section below.

Subcortical afferents. In cats, Edwards et al have described over 40 areas which project to the SCid (Edwards et al., 1979b). Similarly in the echolocating bat, *Pteronotus parnellii*, *Covey* et al have demonstrated, using anterograde and retrograde tracing via WGA-HRP a similar number of subcortical structures projecting to the SCid (Covey et al., 1987). Here, I am not listing all of these structures but they are listed in Table 1.1.

Efferents from the intermediate and deep layers: The efferents from the intermediate and deep layers of the SC are as complex as its afferents. The efferent connections from the SC are organized into 2 groups based on whether the projections are uncrossed (ipsilateral) or crossed (contralateral). The Ipsilateral connections are further divided into ascending and descending connections. The contralateral ascending fibers form the predorsal bundle. The ipsilateral descending fibers form the tectobulbar (tectopontine) bundle. Figure. 1.4 is a schematic diagram which lists all the efferent connections based on the above mentioned organization.

	Monkey[1]	Rat/mouse[2]	Bat[3]
Cortex			
Visual areas			
Prestriate cortex (Area 18)	-	+	-
Prestriate cortex (Area 19)	+	+	-
Ectosylvian gyrus	+		
Middle suprasylvian gyrus (Area 7)	+		
Posterior suprasylvian gyrus (Area 21)	+		
Anterior ectocylvian visual area (AEV)	+		
Intraparietal sulcus	+		
Inferotemporal cortex (area 20a, 20b)	+		
Frontal eye fields	+	+	
Auditory areas			
Primary auditory cortex	-	+	+?
Secondary auditory cortex	+	+	+?
Suprasylvian fringe (SF)	+		
Somatosensory areas			
Primary somatosensory cortex	-	+	
Anterior ectosylvian sulcus (SIV)	+		
Ventral bank of rostral sprasylvian sulcus	+		
Rostral lateral sprasylvian cortex (SV)	+?		
Motor areas			
Premotor cortex (Area 6)	+	+	
Secondary eye fields (SEF) (Part of Area 6)	+		
Primary motor cortex (Area 4)	+	+	
Other cortical areas			
Prefrontal cortex	+	+	
Cingulate cortex	+?	+	
Diencephalon			
Ventral LGN (Pregeniculate nucleus)	+	+**	-
Zona incerta	+	+	+
Hypothalamus	+	+	+
Reticular nucleus of the thalamus	+		
Pulvinar	+	+**	
Pretectum			
Nucleus of the Posterior Commissure	+	+	+
Anterior pretectal nucleus	+	+	
Posterior pretectal nucleus	+	+	
Nucleus of the Optic Tract	+	+	+

Table 1-1 Afferents to the intermediate and deep layers of the SC.

Table 1.1 (continued)

	Monkey[1]	Rat/mouse[2]	Bat[3]
Midbrain			
Parabigeminal nucleus	+	+	
Lateral parabrachial nucleus	+		
Inferior Colliculus: central nucleus (ICC)			+
Inferior Colliculus: external nucleus (ICX)	+	+	+
Inferior Colliculus: pericentral nucleus (ICP)	+	+	+
Nucleus of the brachium of the Inferior Colliculus	+*		
Peri-parabigeminal area	+*	+	+
Parabrachial nucleus	+*		
Nucleus of the sagulum	+*	-	
Cunneiform nucleus	+*		
Fields of Forel	+*		
Midbrain tegmentum	+	+	+
Substantia nigra (pars reticularis)	+	+	+
Paralemniscal area	+	+	+
Periaqueductal gray	+*	+	
Contralateral SC (via Commisussural pathway)	+	+	+
Brainstem			
Dorsal nucleus of the lateral lemniscus (DNLL)	-	+	+
Ventral nucleus of the lateral lemniscus (VNLL)	+		-
Anterolateral periolicary nucleus (ALPO)	+		+
Dorsomedial periolicary nucleus (DMPO)	+		+
Nuclei of the trapezoid body	+*		-
Sensory trigeminal complex	+	+	+
Locus coeruleus	+*		
Raphe dorsalis	+*	+	
Gigantocellularis Nucleus	+*		
Paragigantocellularis lateralis Nucleus	+*		
caudal pontine reticular nucleus	+*	+	
oral pontine reticular nucleus	+*	+	
Perihypoglossal nuclei	+*		+
Cuneate nucleus	+*		
Gracile nucleus	+*		
Other CNS			
Cerebellum	+	+	+
Lateral cervical nucleus	+*	+	+
Retina	+?	+	

Table 1.1 continued. Afferents to the intermediate and deep layers of the SC.

[1] (Wilson and Toyne, 1970; Lund, 1972; Tigges and Tigges, 1981; Huerta and Harting, 1984b; Lui et al., 1995; May, 2006)

[2] (Domesick, 1969; Harting et al., 1973, 1991b; Dräger and Hubel, 1975; Drager and Hubel, 1976; Perry, 1980; Huerta and Harting, 1984b; Beninato and Spencer, 1986; Neafsey et al., 1986; Taylor et al., 1986; Stuesse and Newman, 1990; Harvey and Worthington, 1990; Vertes et al., 1999; Helms et al., 2004; May, 2006; Ghitani et al., 2014)

[3] (Cotter, 1981, 1985; Covey et al., 1987; Kobler et al., 1987; Zhang et al., 1987; Casseday et al., 1989; Covey and Casseday, 1995)

+ indicates verified presence of afferents

- indicates verified absence of afferents

A blank box indicates lack of data

* data from studies in cats

** data from studies in tree shrews

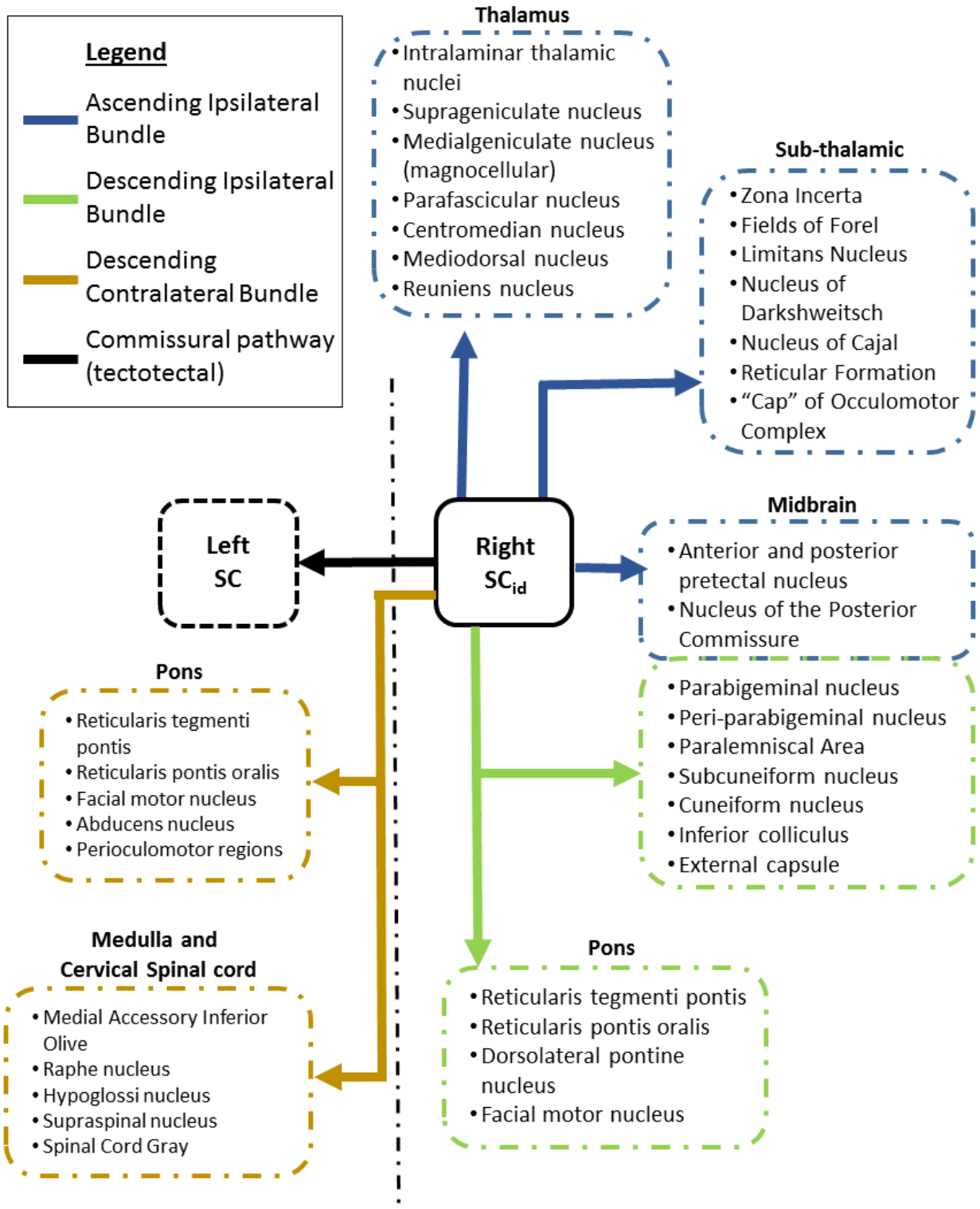

Figure 1.4 Efferent connections from the intermediate and deep layers.

Data for this figure is from (Wurtz and Albano, 1980; Stein and Meredith, 1993; May, 2006)

1.2.2.3 Tectotectal connections

The colliculi communicate with each other by sending efferent connections via the commissural pathway (see Figure. 1.4). Except for rabbits, most vertebrates (also fish), show strong connections between the two colliculi (Nagata et al., 1980; May, 2006). There are, however, distinct species specific differences which reflect the behavioral repertoire of the animal. Tectotectal neurons have been observed across mainly the SO, SGI and SGP, with scattered neurons in the SGS. The main target of the projections are to a mirror symmetric regions in the SGI but overall the connections are observed to be diffuse with targets also present in the SO and SGS (May, 2006). In cats and rats the rostral half of the SC sends tectotectal projections (Yamasaki et al., 1984; Olivier et al., 1998), while in primates the entire colliculus, except the caudal pole, sends tectotectal connections (Olivier et al., 1998; May, 2006). Oliver et al (1998) have hypothesized that this difference reflects the differences in the oculomotor range between species.

Further, it is important to note that nearly half of the tectotectal connections are inhibitory (GABAergic), while the other half are excitatory (glutamergic). Both populations show similar distributions (Appell and Behan, 1990; Olivier et al., 2000), although, this is debated (Takahashi et al., 2010). Although, the exact functional role of the tectotectal projections is not yet known, there are several hypotheses. Takahashi et al (2010) have mapped in detail the tectotectal projections in cats. Their studies indicate that glutamergic SC neurons have mirror symmetric connectivity. Whereas GABAergic neurons had asymmetric connectivity, where the medial SC projected to the lateral regions of the opposite SC while the lateral regions projected medially. They hypothesize that this pattern of inhibitory connectivity plays a role in conjugate

upward and downward vertical saccades. Hafed et al (2008) and Goffart et al (2012) hypothesize that a balance of activity between the two deep SC plays a role in visual fixation.

1.2.3 Role of the SC in orienting in 2D space

It seems that the SC/OT evolved as a site where the internal representation of visual sensory input could be used to select the stimulus of interest and subsequently control behavior by enabling the animal to orient its gaze towards objects of interest and away from objects that might pose a threat (Stein and Meredith, 1993; May, 2006). It would, however, be extremely uneconomical if the representation of space for different sensory modalities would be routed to specialized brain regions for the purpose of orienting behaviors. Further, such a design of the brain would require another difficult engineering problem to be solved: how to integrate the dispersed sensory representations and generate a single command for orienting the gaze of the animal? One economical and logical solution is to integrate all sensory modality specific representations of sensory space in a single brain region. This is what we find in the superior colliculus across species and independent of the dominant modality used by the animal to navigate and capture prey (Stein and Meredith, 1993).

1.2.3.1 Topography: Sensory maps in the SC

From the information regarding the patterns of afferent connections received by the SC from different sensory modalities, it is amply clear that most projections to the SC laminae are topographically arranged. The presence of topographic, sensory modality-specific maps across

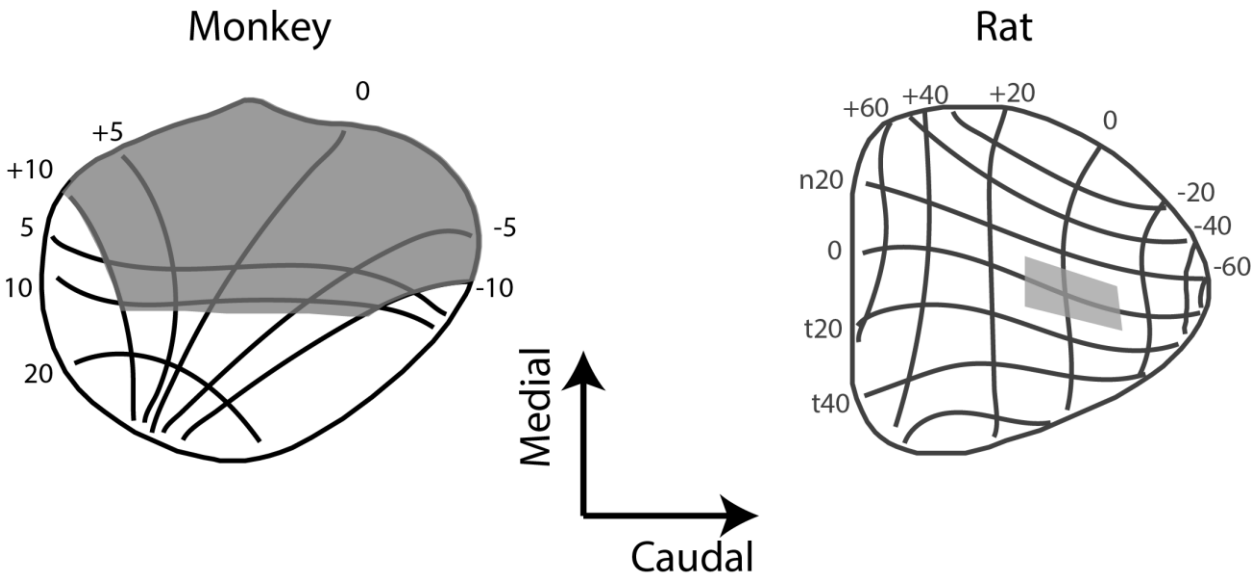

Figure 1.5. Topography of 2D visual space on the superficial SC in the rat and monkey. Figure adapted from (Stein and Meredith, 1993)

the SC laminae has been the topic of considerable research across species (Wurtz and Albano, 1980; Sparks, 1988; Stein and Meredith, 1993; May, 2006). Along with connectivity information, topography of sensory space has been studied using electrophysiological recordings of SC neurons. In one of the first classic experiments exploring the detailed organization of the primate SC, Cynader and Berman, demonstrated an orderly map of visual space in anesthetized primates (Cynader and Berman, 1972). To generalize, in animals where the dominant sense is vision, the superficial layers are organized in retinotopic coordinates and all other visual inputs, from the cortex as well as inputs from subcortical visual centers, follow the same pattern of retinotopy. Azimuth and elevation of 2D projection of visual space is mapped along the rostro-caudal and medial-lateral dimensions across the SC laminae, respectively. For example, in animals with front facing eyes, like humans and primates, the central visual field of view is mapped on to the rostral pole of the SC, while peripheral visual space is mapped caudally (Cynader and Berman, 1972;

Schiller et al., 1974). Figure. 1.5, shows the organization of the field of view of primates and rats across the superficial layers of the SC.

Since then, following the lead from connectivity studies which indicate that auditory and somatosensory information is also routed to the SC, many studies have shown the presence of a topographical arrangement of auditory and somatosensory space along the intermediate and deep SC laminae (Dräger and Hubel, 1975; Drager and Hubel, 1976; Stein et al., 1976; Middlebrooks and Knudsen, 1984a; Wong, 1984; Valentine and Moss, 1997). It is very interesting to note, that although the superficial layers of the SC respond mainly to visual stimuli, in more ventral layers, cells with visual, auditory and somatosensory responses are intermingled (Wurtz and Albano, 1980; Sparks, 1988; Stein and Meredith, 1993; May, 2006). Here, the question arises whether the different sensory maps are aligned with each other? And, is one sensory map the master?

1.2.3.1.1 The curious case of echolocating bats

Before attempting to answer the question of the master map of the midbrain SC, it is important to discuss the case of topographically space maps in echolocating bats. Despite multiple studies which aimed to search for topography of auditory space in the SC of echolocating bats that use frequency modulated (FM) sonar signals, except for a limited and coarse representation of azimuthal acoustic space in the deep layers of the SC of the little brown bat (Wong, 1984), and the big brown bat (Valentine and Moss, 1997) no study has found strong topography of sensory space (in this case auditory space) in the SC of echolocating FM bats (Jen et al., 1984; Poussin and Schlegel, 1984a). Although Valentine and Moss found a hint of a

topographic organization, all that could be said was that neurons selective to sounds emitted from a centrally placed speaker were located more anteriorly as compared to neurons selective to more peripheral sounds (Valentine and Moss, 1997). A recent study, however, has shown for the first time topography of visual space in the superficial SC and also an aligned map and highly topographic map of auditory space in the deeper layers of the SC in the echolocating bat, *Phyllostomus discolor* (Hoffmann et al., 2016). One explanation for this discrepancy in topography of auditory space, also mentioned in the study by Hoffmann and colleagues (Hoffmann et al., 2016), can be attributed to the fact that *P. discolor* is an omnivorous bat species which relies mainly on fruit, nectar and pollen, which is why it has a much greater reliance on vision and olfaction as compared to other echolocation. The other insectivorous bats species which only have a limited topography of auditory space are mostly aerial hunters and mostly rely on echolocation for navigation and hunting. It has been well documented that alignment of auditory and somatosensory maps with that of the visual map strongly depends upon the development of the visual space map (Knudsen and Brainard, 1991; Stein and Meredith, 1993; Meredith and Stein, 1996; Wallace et al., 2004). This is suggestive that in insectivorous echolocating bat species with poorly developed vision the auditory map does not develop a well-defined topographical representation due to the absence of the guidance from an overlying map of visual space (Hoffmann et al., 2016).

1.2.3.1.2 Alignment of sensory maps: Is there a unified sensory map?

In one of the first demonstrations of an alignment between topographical sensory maps across sensory modalities, Stein and colleagues, showed in anesthetized cats, the alignment of

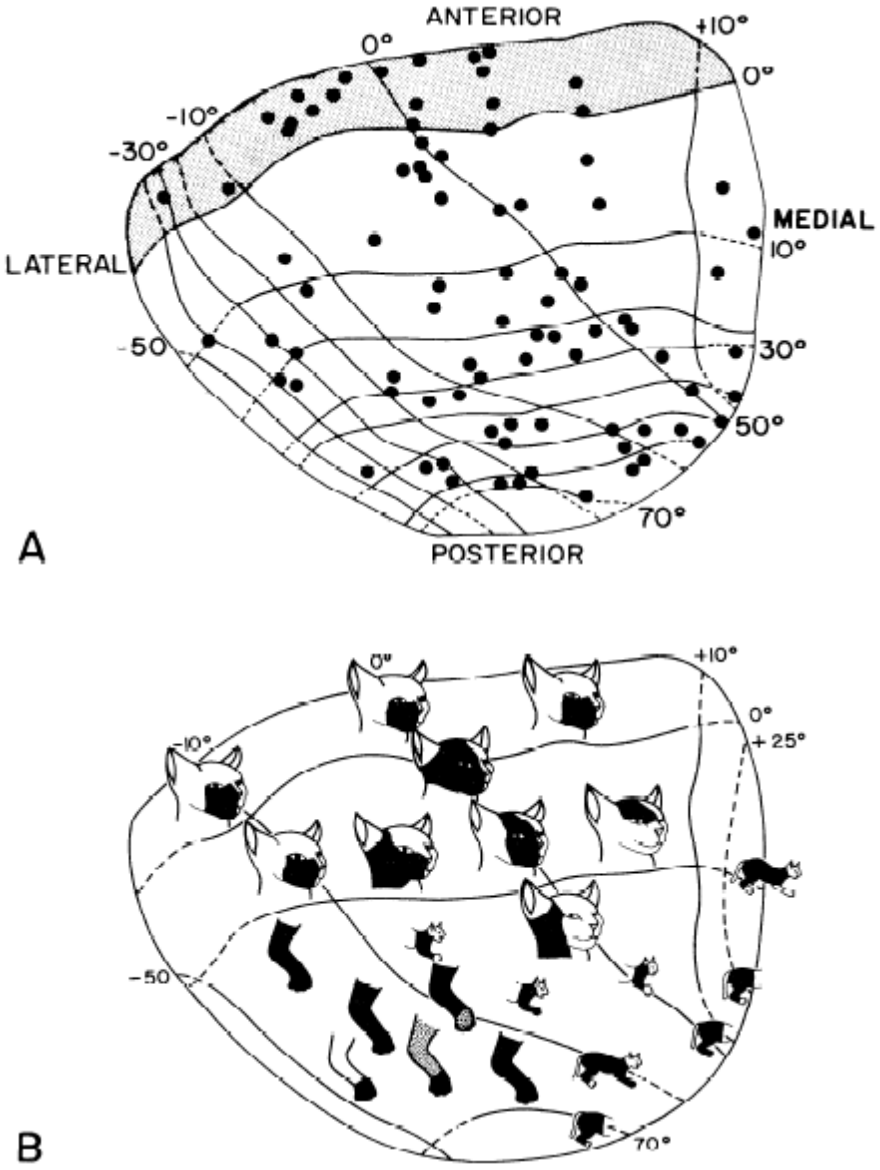

Figure 1.6. Alignment of somatosensory and visual space maps in the cat. Figure adapted from (Stein et al., 1976)

visual and somatosensory maps (Stein et al., 1976). They found a disproportionately large trigeminal representation, basically representing the face and whiskers, occupying almost the entire rostral half of the SC (Figure. 1.6). This matches well with the representation of the visual space in cats which have frontally placed eyes and have a large binocular overlap region (Sterling and Wickelgren, 1969; Lund, 1972; Huerta and Harting, 1984b). In about the same period, Drager

and Hubel, demonstrated in the anesthetized mouse, a topographical alignment of visual, somatosensory and auditory receptive fields. In mice, the whisker system is (vibrissae) forms an integral part of the sensory input to the animal. Drager and Hubel found, similar to the cat, that neurons responding to tactile stimulation of whiskers fired vigorously only when the receptive fields of visual neurons, found in the same electrode penetration, had visual receptive fields which were crossed by whiskers. Stimulation in parts of the body which were more caudal did not evoke any firing. In other words the parts of the vibrissae which were visible to the eyes were represented in the same topographic location on the SC laminae. Similar results were obtained for cells which fired in response to auditory stimuli (Drager and Hubel, 1975, 1976; Dräger and Hubel, 1975). Since these initial studies, there have been many demonstrations of the alignment of sensory maps; in barn owls (Knudsen, 1982; Knudsen and Brainard, 1995), guinea pigs (King and Palmer, 1983), hamsters (Chalupa and Rhoades, 1977), iguanas (Gaither and Stein, 1979; Stein and Gaither, 1981), mice (Dräger and Hubel, 1975; Drager and Hubel, 1976), cats (Stein et al., 1976) and bats (Hoffmann et al., 2016).

In most of these animals, representation of auditory and somatosensory space were shown to be in alignment with the map of visual space. This implies is that the coordinates of auditory and somatosensory space have been transformed into retinal coordinates (Sparks, 1988). However, there are logical considerations which go against this hypothesis.

Most of the above-cited studies were performed under highly artificial conditions, where an animal is anesthetized or head restrained, without freely moving ears, eyes, neck, head or body. Such experimental paradigms are based on the assumption that the aligned sensory maps are static (Sparks, 1988). In reality, the sensory periphery of animals has many degrees of

freedom. Many animals, for example monkeys and humans, can move their eyes independent of their heads and body. Similarly, many animals, for example cats and bats, can move pinnae independent of their heads and body. The hypothesis that sensory maps are aligned to a map of visual space or the assumption that the alignment of sensory maps creates a modality independent map of sensory space hits a road block here. In the case where eyes and pinnae can move, which will create a misalignment of sensory space across modalities, it is important to consider other possibilities. One possibility is that sensory maps are dynamic; every time the eyes or ears move, the maps of the other sensory modalities shift to maintain alignment and sustain a unified modality independent map of sensory space (Jay and Sparks, 1984) (Jay and Sparks, 1984). Another possibility is that the sensory maps are not alignment but rather serve to provide a transformation required to orient an animal's gaze to a stimulus of interest (i.e. motor map or orienting movements present in the deep layers of the SC) (Schiller and Koerner, 1971; Sparks, 1986). These possibilities are discussed below following the discussion of motor maps in the SC.

1.2.3.2 Topography: The motor map

1.2.3.2.1 A map of eye-movements:

As early as 1870, it was demonstrated that electrically stimulating in the SC can elicit eye movements (Adamuk, 1870). However, only a century later, the landmark detailed electrical stimulation experiments by Robinson showed for the first time that there existed a topographic map of eye movements in the deeper layers of the monkey SC (Robinson, 1972). Figure. 1.7a shows the saccadic eye movement map in macaques left superior colliculus. Each arrow shows the direction and amplitude of the saccade. The panel on the right (Figure. 1.7b) is the same map

plotted as contours of equal amplitudes. This motor map in primates was confirmed by Schiller and Stryker where they did combined microstimulation and recordings (Schiller and Stryker, 1972). It is important to note that in the case of primates the locus of the stimulation site has a topographical encoding of the direction and amplitude of the saccade. And, within limits, this is independent of the position of the eyes in the orbits (Sparks and Hartwich-Young, 1989). Further, there is a strong correspondence between the motor map of saccades in the deep layers and the map of visual space in the superficial layers (Robinson, 1972; Schiller and Stryker, 1972).

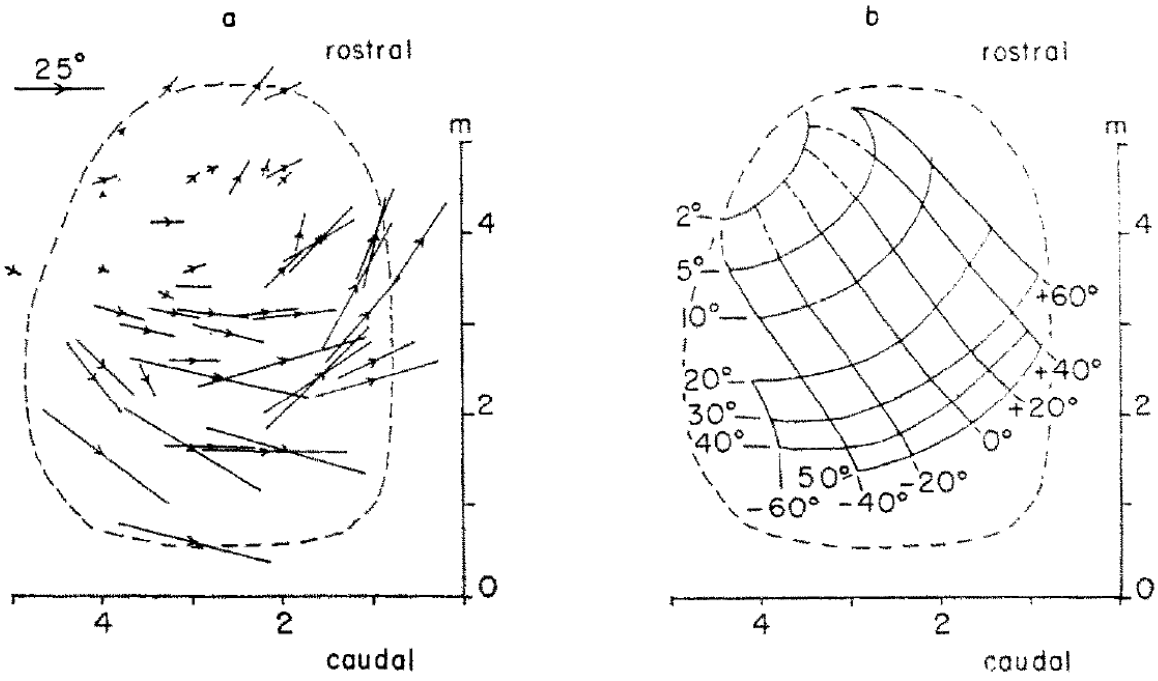

Figure 1.7. Topographical map of saccadic eye movements elicited by micro-stimulation in the SC of primates. Figure adapted from (Robinson, 1972)

1.2.3.2.2 A map of combined eye and head movements:

It is interesting to note that when similar experiments were carried out in head-fixed cats, a topographic map of eye-movements aligned with the map of the overlying map of visual space

was not found. The direction and amplitude of the saccades evoked strongly depended on the initial eye position of the eyes in the orbit (Guitton et al., 1980; Roucoux et al., 1980b; McIlwain, 1986, 1990). One explanation for this discrepancy between primates and cats has been proposed states that mechanical constraints limit the maximum deviation of eyes in cats to 25 degrees. If the head is kept fixed then it would not be possible to cover the entire visual space, which is encoded in the superficial layers, just with eye movements. Thus, in cats, orienting movements have to be considered as combined eye-head movement to shift the gaze of the animal to a stimuli of interest (McIlwain, 1990). Implications of these results will be discussed in a later section – A map of gaze error and goals. This hypothesis has been confirmed in cats by multiple studies using electrical stimulation in head-free cats (Guitton et al., 1980; Roucoux et al., 1980a; Munoz and Guitton, 1991; Pare et al., 1994). Similar results were later reported in rhesus monkeys by Freedman and colleagues, where they also showed that instead of the SC sending separate commands for controlling eye and head movements separately, the locus of stimulation on the topographic map in the SC along with the current position of the eyes in the orbits decided the amount by which the eyes and the head would move to shift the gaze of the animal to the desired location in 2D sensory space (Freedman et al., 1996; Freedman and Sparks, 1997; Gandhi and Katnani, 2011). A topographic map of head movements has also been reported in barn owls (du Lac and Knudsen, 1990; Masino and Knudsen, 1990, 1993).

1.2.3.2.3 Map of pinna and vibrissae movements:

Similar to how movements of the eyes and head can orient the gaze of an animal to the desired location in the visual field, movements of the pinnae can orient the acoustic gaze towards

a salient auditory stimulus. Stimulation experiments in cats, rats and also echolocating bats has demonstrated an orderly map of pinna (cats, rats and bats) and vibrissae movements (cats and rats) (Syka and Radil-Weiss, 1971; Stein and Clamann, 1981; McHaffie and Stein, 1982; Valentine et al., 2002).

1.2.3.2.4 Map of motor movements and vocalizations in echolocating bats

Schuller and Radtke-Schuller (1990) reported that microstimulation in deep layers of the SC, elicited vocal orienting responses (sonar vocalizations) in the horseshoe bat (*Rhinolopus rouxi*). Valentine et al (2002) conducted one of the first systematic studies to understand the coordinated vocal-motor, head and pinna orienting movements elicited by microstimulating in the SC of echolocating bats. They reported a topographic map of coordinated orienting movements (echolocation calls, head and pinna movements) where the direction of evoked behaviors held a relationship with the site of stimulation.

1.2.3.3 A map of gaze error representing goals in 2D sensory space

In this section we come back to the very interesting and pressing question of how are all the topographic sensory maps related to each other and also what is their relation to the motor map? Another related question that comes up is how the different motor maps are related to each other? As previously mentioned, using head-restrained/anesthetized animals, many studies have highlighted the alignment of visual, auditory and somatosensory maps (Drager and Hubel, 1975, 1976; Dräger and Hubel, 1975; Stein et al., 1976; Chalupa and Rhoades, 1977; Gaither and Stein, 1979; Stein and Gaither, 1981; King and Palmer, 1983; Meredith et al., 1992; Knudsen and

Brainard, 1995; Wallace et al., 1998; Hoffmann et al., 2016). Although this hints at the suggestion that the auditory and somatosensory afferent coordinates are transformed into retinal coordinates there is an apparent caveat to this assumption. In animals with movable eyes, the auditory and somatosensory position information represented with the in-register map will be now representing misaligned coordinates with the motor system (Pöppel, 1973; Jay and Sparks, 1984). A similar situation arises in animals that have movable pinnae; do the auditory and visual topographic maps still remain in register? As previously mentioned, one hypothesis to explain the apparent mismatch between sensory maps when eyes, pinnae or the body moves w.r.t. to each other is that the maps topographically represent the amount of combined movement of the eyes, head and body required to orient the animal towards the target of interest. There have been some extremely clever and seminal studies confirming this hypothesis (Jay and Sparks, 1984, 1987; Sparks et al., 1987).

In a delayed saccade task, Jay and Sparks, trained Rhesus monkeys to look to either visual or auditory targets in a completely darkened room. A speaker with a LED on a track allowed targets to be presented at most locations on an imaginary sphere surrounding the animal. The animals had to fixate at any one of three fixation lights along the horizontal meridian. At the beginning of each trial, one of the three fixation lights was randomly activated. After a variable interval, an auditory (broad-band noise burst) or visual target was presented and the animal was required to look to the target location in order to receive a liquid reward (Jay and Sparks, 1984, 1987; Sparks et al., 1987). For every sound-sensitive cell encountered in the SC, the position of the eyes in the orbit had a distinct effect upon the response to an auditory stimulus. The results showed that the auditory receptive fields shifted with the position of the eyes in the orbits.

However, when the receptive fields were plotted as a function of the movement required to look to the target, the data obtained with the different fixation positions are closely aligned. Thus, the sensory receptive fields of auditory neurons is not determined solely by the position of the auditory stimulus in space, but depends upon motor error, the position of the eyes in the orbit relative to target position. This was an excellent demonstration that the map of auditory space found in the monkey SC is not a static representation. With each movement of the eyes in the orbit, the population of neurons responsive to an auditory stimulus in a particular spatial location changes to a new site within the SC, a site representing the new motor error signal.

1.2.3.4 The superior colliculus and attention

Almost inseparable and complementary to the role of the SC in orienting an animal to a stimuli is its role in attention. Studies elucidating this aspect of SC functionality have been developing along with the studies exploring the sensorimotor functions of the SC. Before describing the current knowledge about the role of the SC in attention, it is important to discuss why the motor function of the SC and its role in attention are closely related. Most studies exploring the motor functions of the SC used anesthetized or head restrained animals, with a single artificial stimuli which had no behavioral significance to the animal. The real world, however, consists of multiple simultaneous stimuli competing for the attention of an animal. In such a complex environment, orienting towards a stimulus can be broken into many functional steps, each of which has to be resolved for the final behavioral outcome of an overt or covert orienting response. The fundamental components of attention have been described in detail in many excellent review papers (Desimone and Duncan, 1995; Miller and Cohen, 2001; Fecteau

and Munoz, 2006; Knudsen, 2007a, 2011; Mysore and Knudsen, 2011; Krauzlis et al., 2013). In brief, selecting a stimulus of interest from an array of competing stimuli to decide which piece of information gains access to working memory for further evaluation, first requires the representation of external world information to be represented in relevant coordinates in the brain. These representations have been referred to as the salience or priority map (Desimone and Duncan, 1995; Fecteau and Munoz, 2006; Knudsen, 2007a; Mysore and Knudsen, 2011; Krauzlis et al., 2013). To select the piece of information, from amongst of all the competing stimuli, which is most relevant to the current behavioral context or for survival, requires the brain to have the ability to select between these competitive stimuli. Further, the problem of deciding the most salient stimulus requires top down influence from knowledge about the internal state (current behavioral context), information from working memory, past knowledge (this might include long term memory) as well bottom up information about more intrinsic aspects of the physical stimulus like loom, contrast, intensity etc, to bias the priority maps and make the final decision of the motor output. Figure. 1.8 shows a schematic of showing the connectivity and flow of information within the network formed by the fundamental components of attention.

1.2.3.4.1 The Superior Colliculus as a node for stimulus selection

In the early 1970's, seminal work done by Wurtz and colleagues, gave one of the first demonstrations that the activity of SC neurons was enhanced when the animal attended to a stimulus in the receptive field (RF) of the cell being recorded as compared to when the animal did not attend to the RF stimulus (Goldberg and Wurtz, 1972b). Subsequent studies established that the SC contained a topographic map of salient stimuli, often referred to as a stimulus priority

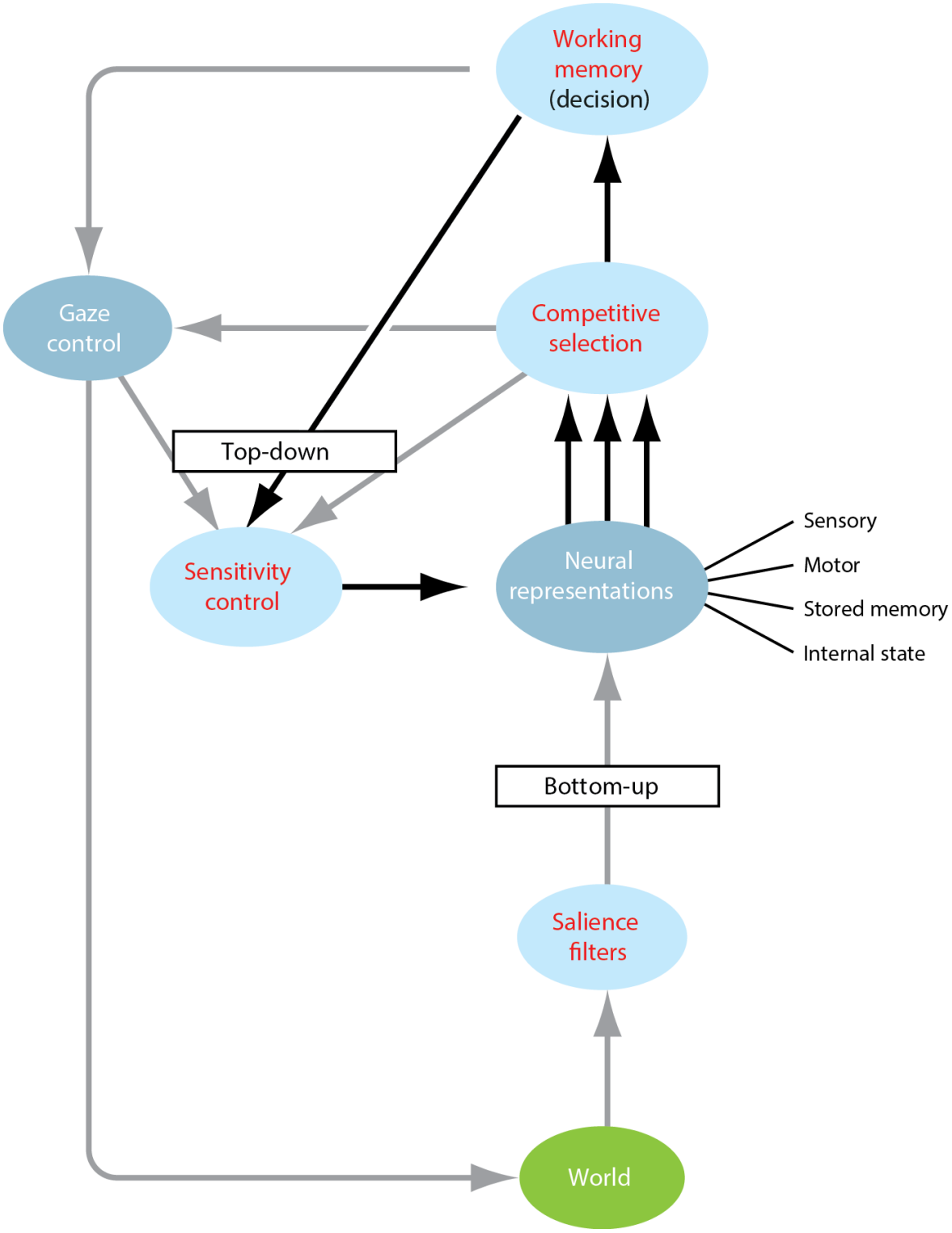

Figure 1.8. Fundamental components of attention. Figure adapted from (Knudsen, 2007b)

map, encoded in motor error coordinates (Wurtz and Mohler, 1976; Kustov and Robinson, 1996; Basso and Wurtz, 1998; Horwitz and Newsome, 1999; Carello and Krauzlis, 2004; Müller et al., 2005; Knudsen, 2011). The presence of salience maps in other brain regions has also been established, Frontal Eye Field (FEF or forebrain gaze fields of birds) (Knudsen et al., 1995; Bruce et al., 2004; Thompson and Bichot, 2004; Wardak et al., 2006), Lateral Intraparietal area (LIP) (Gottlieb et al., 1998) and also the pulvinar (Robinson and Petersen, 1992; Zhou et al., 2016).

The establishment of a stimulus priority map requires the resolution of conflict between multiple stimuli. Many models of target selection propose that competitive interactions between different stimuli is one way of resolving this conflict (Wolfe, 1994; Itti and Koch, 2001). The presence of a salience map in the SC does not necessarily imply a causal role in the process. McPeek and Keller were one of the first to demonstrate that the SC plays a causal role in target selection. They used a visual search task in which the monkey was trained to saccade to an odd-ball stimulus. Trials were randomly interspersed with single stimuli trials to check for impairment without stimulus competition. This task checked for an entirely bottom up effect of overt attention. In certain blocks of trials certain loci of the SCid were reversibly inactivated with Lidocane or Muscimol. In inactivation trials and in the presence of competing stimuli, the monkeys were unable to select the odd-ball stimulus, when it was present in the inactivated region. When the odd-ball was located out of the inactivated region or in the case of single stimuli trials, there was no degradation in the performance (McPeek and Keller, 2004). In the same year, Carello and Krauzlis, using a sub-threshold current microstimulation experiment, demonstrated that stimulating the SCid at specific loci could bias the stimulus competition towards the stimulated location in an overt orienting task (Carello and Krauzlis, 2004; Krauzlis et al., 2004).

Further, using extracellular recordings and reversible inactivation studies, it has now been demonstrated that the SC also plays a causal role in target selection and control of covert attention (Ignashchenkova et al., 2004; Lovejoy and Krauzlis, 2010).

Despite the demonstration that the SC is involved in target selection for both overt and covert orienting, the mechanisms of this process were elucidated only recently in a series of classic experiments in the optic tectum (OT) of barn owls (Mysore et al., 2010, 2011, Mysore and Knudsen, 2011, 2012, 2014). As previously described, the OT contains a topographic map of aligned visual and somatosensory maps, as well as a motor map of head movements, similar to mammals (Knudsen and Konishi, 1978; Knudsen, 1982; du Lac and Knudsen, 1990; Knudsen and Brainard, 1995). Using pairs of visual and/or auditory, competing and spatially distinct stimuli, it was demonstrated that when one of the competing stimuli was the strongest, it globally suppressed the representation of all remaining stimuli. Interestingly, this global inhibition, differed from the classical suppressive surround which tapers with distance. This suppression which mediates the competitive interactions between stimuli was found to be divisive as it was independent of the spatial distance between the two competing stimuli (Mysore et al., 2010). In a similar experimental setup, also in head-fixed owls, it was demonstrated that as a precursor of generating a map of salience, neurons in the owl OT signaled, in a binary fashion, a topographic discrimination signal to signal the strongest stimulus. A most important finding of this work was the demonstration that these signals were generated flexibly and indicated, in a binary fashion, the “relative strengths” of the competing stimuli, which is an important requirement in the natural environment (Mysore et al., 2011). The above two results demonstrated the stimulus interactions for bottom up stimuli. In a subsequent experiment, top down effects, by

microstimulation in the auditory gaze fields (AGF) of owls (Knudsen and Cohen, 1995; Winkowski and Knudsen, 2006) further demonstrated that top down influences from the AGF, onto the SC priority map, biases the competition in favor of the microstimulated location to enhance the quality of signaling of the highest priority stimulus (Mysore and Knudsen, 2014). Using circuit modeling as well as, anatomy, it was demonstrated that the SC, along with the two OT satellite nuclei (Ipc and Imc) contains sufficient and necessary circuit components for achieving selection from a spatial map of stimulus priority (Mysore and Knudsen, 2012; Goddard et al., 2014).

1.2.4 Role of SC in 3D orienting

Thus far, I have provided background to show that the midbrain SC/OT plays a major role in the creating a 2D map of sensory space that is aligned across sensory modalities into ego centric coordinates of output motor movements of the eyes, head and body. Further, it has also been demonstrated that the SC plays a causal role in selecting the most salient target in 2D space, based on bottom up sensory information which is relayed directly to the SC from the sensory periphery and top-down modulation information relayed from the cortex. A point that has not been stressed so far, however, but is crucial for the focus of this thesis, is that most experiments in the mammalian SC or the non-mammalian OT have used only 2D stimuli (i.e. stimuli which spans only the azimuth and elevation dimensions) to understand the role of the SC in orienting. These limitations of past experiments have limited our knowledge about the role of the SC in orienting in the third dimension, depth. In this section, I aim to provide, from the limited existing data, evidence, that supports the hypothesis that *the SC plays a role in orienting in 3D space*.

1.2.4.1 Indirect evidence

Let us consider visual animals with movable eyes as a starting point. As mentioned previously, animals orient to objects at different locations in 2D space using saccades, while they make vergence movements to orient to objects at different depths. For such animals, the above hypothesis poses an important question – whether the systems for saccadic eye movements and vergence eye movements are independent of each other or do these systems share common brain hardware as well as a common movement code. Owing to the difference in the dynamics between saccadic and vergence eye movements, much of the early work studied these systems separately and supported the dichotomy suggested by Hering in 1868 (Westheimer, 1954; Rashbass and Westheimer, 1961; Yarbus, 1967). However, later studies, using real targets in three dimensions, provided evidence that saccadic and vergence movements were executed simultaneously, with similar velocity vectors, and that there was a dynamic interaction between the two movements where saccades were generally slowed down by simultaneous vergence (Steinman et al., 1990; Collewijn et al., 1995; Chaturvedi and Gisbergen, 1998). This debate of dichotomy is still not settled and for an in depth review see (Cullen and Van Horn, 2011).

Indirect evidence also comes from the observation that many visual cells in the SCs are tuned to binocular disparity (Berman et al., 1975; Bacon et al., 1998; Mimeault et al., 2004). It must be noted, however, that binocular disparity sensitivity is not a sufficient condition for depth perception (Cumming and DeAngelis, 2001). Further, the lateral intraparietal (LIP) area in monkeys, which contributes to visual depth processing (Gnadt and Mays, 1995), has been shown to send target depth signals to the SC and frontal eye fields (FEF). Efferent anatomical projections

from the SC to premotor nuclei also supports the role of the SC in orienting in 3D space (May, 2006; Cullen and Van Horn, 2011).

1.2.4.2 Direct evidence of the role of the SC in orienting in 3D space: primate studies

It has also been shown that stimulating intermediate layers in the caudal portion of the SC during combined saccade and vergence movements can eliminate or interrupt the vergence component (Chaturvedi and Gisbergen, 1998; Chaturvedi and van Gisbergen, 1999; Chaturvedi and Van Gisbergen, 2000b; Van Horn et al., 2013). However, Walton and Mays (Walton and Mays, 2003) looked for topographic organization of depth tuning in the SC of monkeys and reported that although most cells show modulation of activity (mainly suppression) during combined vergence and saccadic movements, there is no clear topography for depth tuning in the monkey SC. These results indicate that although the SC encodes depth information (in terms of vergence and accommodation motor commands), there is no evidence for a topographical arrangement of depth-tuned neurons in the SC. Further evidence comes from considering the near response, when an animal shifts its gaze from a far target to a neat target. The near response comprises of vergence eye movements, pupillary constriction as well as control of accommodation (Leigh and Zee, 1983)

1.2.4.3 Direct evidence of the role of the SC in orienting in 3D space: echolocating bats

By estimating the delay between a sonar vocalization and returning echo, bats compute the range/distance to an object (Simmons, 1973), and indeed echolocating bats are champions of 3D spatial navigation (Griffin, 1958; Ulanovsky and Moss, 2008). A population of neurons in

the echolocating bat show facilitated and echo-delay tuned responses to pulse-echo pairs, and it has been hypothesized that echo-delay tuned neurons provide the neural basis of distance measurement in bat sonar (Hartridge, 1945; Simmons, 1973b). So far, evidence for range tuning in the bat auditory system has been gathered primarily by presenting pairs of sounds to passively listening (anesthetized or awake and head restrained) bats. The first sound mimics the bat's own vocalization and the second delayed and attenuated sound simulates the echo from an object in the environment. By varying the delay between the pulse and the echo, objects at different ranges can be encoded. Pulse-Echo delay facilitated neurons show greater firing rate for specific delays of echoes (range). Echo delay tuned neurons in bats have been characterized in the midbrain (Dear and Suga, 1995; Valentine and Moss, 1997), thalamus (Yan and Suga, 1996) and the auditory cortex (Suga and Horikawa, 1986; Dear et al., 1993b).

Microstimulation experiments in the deep layers of SC in head restrained bats revealed that the SC plays a role in echolocation call production. Additionally, pinna and head movements were also elicited using micro-stimulation (Valentine et al., 2002). Additionally, the latency of premotor multiunit activity in the deep layers of the SC of bats trained to track a swinging target were found to be correlated with the duration of sonar vocalizations (Sinha and Moss, 2007). The duration of sonar vocalizations has been shown to correspond to target range as bats adaptively control call duration to avoid overlap of calls with incoming echoes (Schnitzler and Kalko, 2001; Aytekin et al., 2010). With this in mind, evidence that the SC plays a role in eliciting sonar vocalizations as well as the correlation of vocal premotor activity with pulse duration is strong evidence favoring the role of the SC in 3D orienting in echolocating bats and in mammals in general.

1.2.4.4 Section summary

Up until now, I have discussed the role of the superior colliculus in creating a representation of egocentric and aligned multimodal sensory space, which is used to select the most salient stimuli and then generate motor commands for orienting. As most of the past research focused on orienting in 2D space, we have limited knowledge about the role of the SC in orienting in 3D. To further our understanding of the role of the SC in representing 3D space and encoding 3D orientation movements, the study of an animal that relies heavily on distance information to guide spatial orientation is important. To this end, in the next section I will describe the adaptive echolocation behavior of bats and provide arguments to justify the use of echolocating bats to answer the question regarding the role of the SC in orienting in 3D space.

1.3 Echolocation and adaptive sonar behavior of bats

Out of the more than 1300 species of bats in the world, more than 700 use echolocation for spatial navigation and foraging (Wilson D. E. and Reeder D. M., 2005; Maltby et al., 2009; Fenton and Simmons, 2015). A series of experiments by Griffin and colleagues, spanning more than a decade since 1930, elucidated that bats use a sophisticated implementation of SONAR (Griffin, 1958). In brief, echolocating bats produce ultrasonic sounds, that reflect off objects in the surrounding environment, and listen to the returning echoes to generate, over a series of calls, an acoustic image of the 3D environment around them (Moss and Surlykke, 2001, 2010; Ulanovsky and Moss, 2008; Lewicki et al., 2014). In this brief introduction I will describe the echolocation call structure of bats. The time and frequency trade-offs influencing the call design

and call timing, and I will focus mainly on the adaptive echolocation behavior of bats which has been shown to assist bats in orienting in 3D space.

1.3.1 Bat echolocation signals

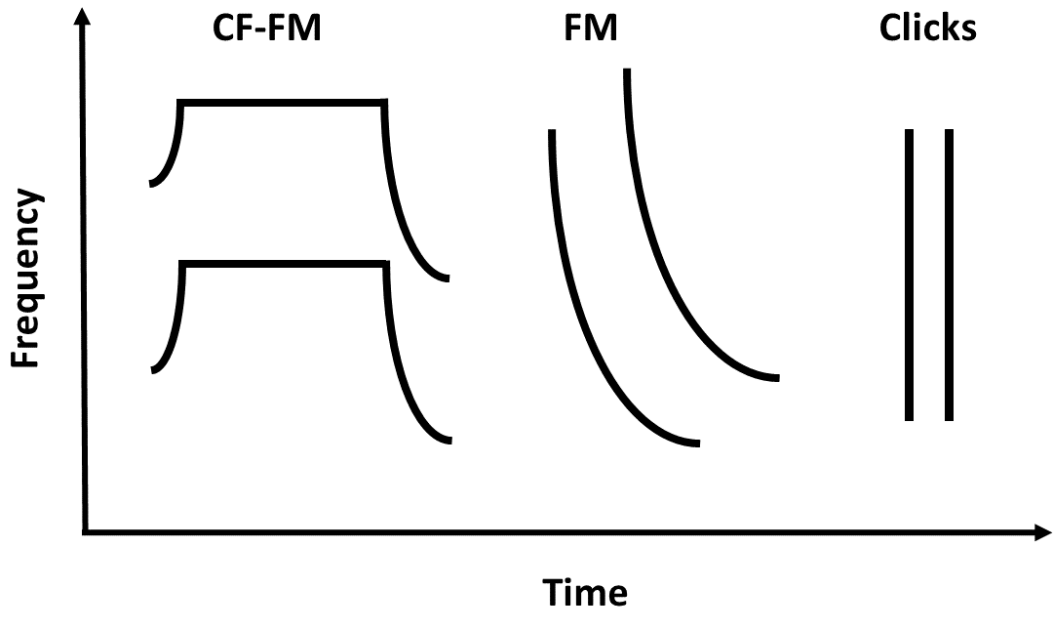

Figure 1.9. A schematic of the three major classes of bat echolocation calls.

Bats display a wide variety of echolocation calls as well as varied call intensities. Bats have adapted their echolocation call structure and parameters to suit their needs for foraging and navigation (Neuweiler, 1990; Schnitzler and Kalko, 2001; Surlykke and Kalko, 2008; Surlykke et al., 2009a; Jakobsen et al., 2013b). Figure. 1.9 shows a time-frequency schematic of the 3 major classes of echolocation calls. Bats produce these echolocation calls either through their open mouths, noses or clicking of their tongues. Bats which predominantly produce constant frequency (CF) calls flanked on one or both sides with frequency modulated (FM) sweeps are

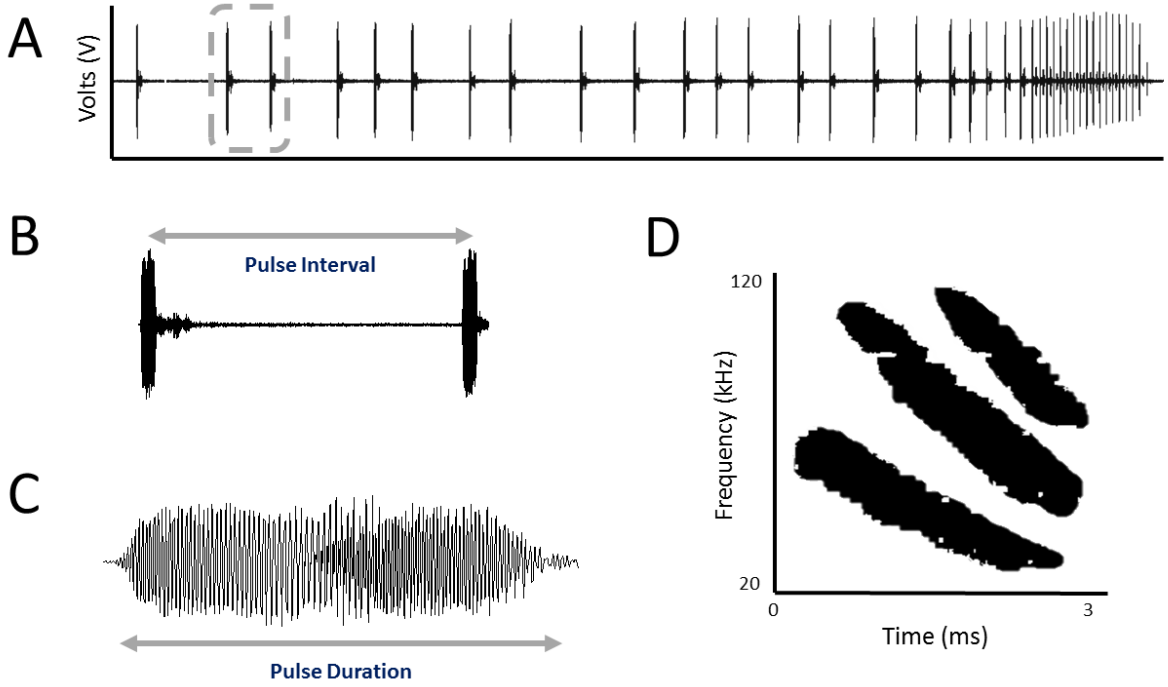

Figure 1.10. Timing and echolocation call structure of Eptesicus fuscus.

classified as CF-FM bats. In contrast, bats that predominantly produce FM sweeps are classified as FM bats. The third category of echolocation calls, produced by a single species of bats, *Rousettus aegyptiacus*, are tongue clicks (Popper and Fay, 1995; Schnitzler and Kalko, 2001; Thomas et al., 2004; Jones and Holderied, 2007; Maltby et al., 2009). *Eptesicus fuscus*, also known as the big brown bat, which is the species of bats used in all studies in this thesis produces short duration FM sweeps. Figure. 1.10 displays a series of vocalizations produced by an *E. fuscus*¸ while tracking an approaching target while resting on a platform and also displays the call structure in more detail in Figure XB and C and a spectrogram in XD. The important echolocation call parameters like pulse duration, pulse interval and frequency bandwidth, that bats adaptively modulate to get task-relevant information from their environment are also highlighted in Figure. 1.10. The tradeoffs between these parameters are described in below.

1.3.2 Adaptive echolocation behavior of bats for orienting in 3D space

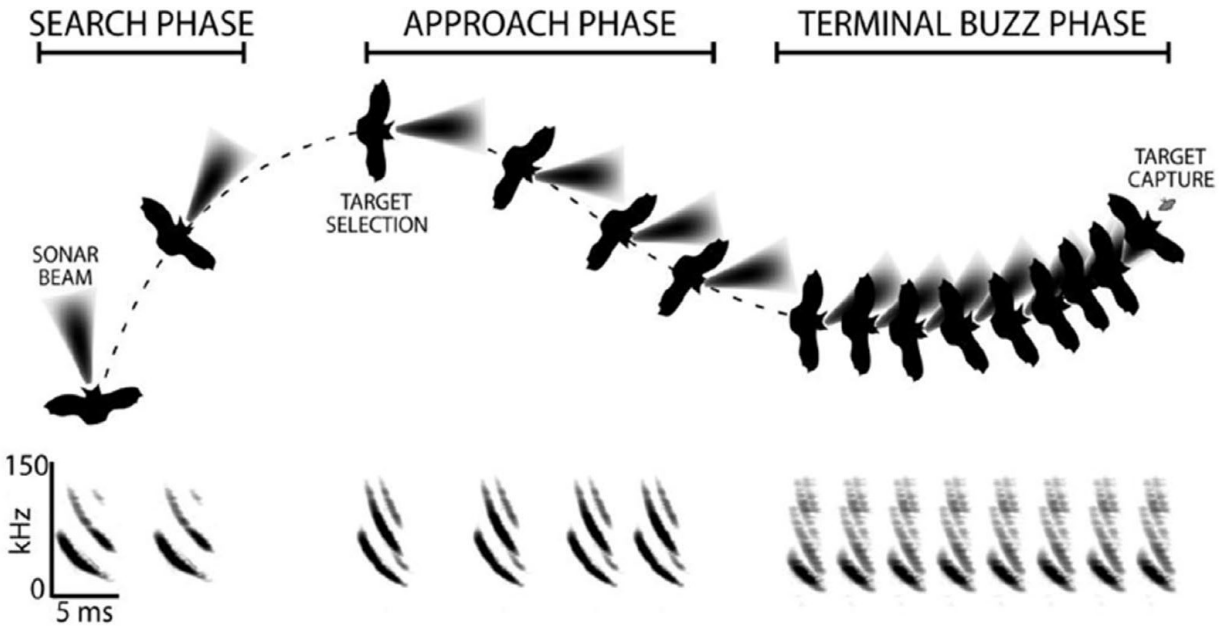

Figure 1.11. Typical adaptive echolocation behavior of insect eating bats during foraging. Figure adapted from (Moss and Surlykke, 2010)

For foraging and navigating the three dimensional aerial world, bats need to detect prey for food and also detect and discriminate between different objects in the environment to develop an acoustic image of their surroundings. Figure. 1.11 displays a cartoon of typical foraging behavior of a bat in the field. The foraging behavior of bats has been divided into three phases known as the *search phase*, *approach phase and the terminal buzz phase* (Griffin, 1958; Simmons et al., 1979; Moss and Surlykke, 2001; Schnitzler and Kalko, 2001). Figure. 1.11 shows spectrograms of typical search, approach and buzz sonar calls. The following three trends are important to note in this typical sequence of behaviors and will be explained in more detail below, mainly focusing on the adaptive echolocation behavior of the *Eptesicus fuscus*.

1) **Search phase > Approach phase > Buzz phase: Decrease in pulse duration.**

2) **Search phase < Approach phase < Buzz phase: Increase in pulse repetition rate.**

3) **Search phase < Approach phase < Buzz phase: Bandwidth increase.**

In short, bats emit narrow bandwidth, long duration calls at a low pulse repetition rate during the search phase. They emit broadband and comparatively short duration calls at a comparatively higher pulse repetition rate. While in the buzz phase they produce extremely short duration (sub-millisecond) calls at very high pulse repetition rates (more than 150 calls per second). It should be noted that pulse repetition rate is the inverse of pulse interval between consecutive calls. Below, I describe the physical constraints and tradeoffs due to which bats modulate pulse duration, pulse interval, pulse bandwidth to extract the required information in complex environments.

1.3.2.1 The problem of signal processing: Modulating Pulse Interval and pulse duration

Consider the situation where an obstacle or target are in close proximity, say distance *d* from the bat. Emitting a long signal, a signal which is longer than $2*d/c_{sound}$, (where c_{sound} is the speed of sound in air), will cause the echo to return to the bats ears while the bat is still in the process of vocalizing, thus, causing a loss of information. The conditions when interfering signals (either the bats own call or an echo from an obstacle) precede the target echo, such situations are referred to as *forward masking*. Further, a similar situation arises when a target is located in close proximity to background environmental clutter. Here, if the emitted sound is of a longer duration, then there will be an overlap between the returning echoes of the target and clutter, again causing a problem of signal loss. Such situations where interfering signals arrive after the target echo are called *backward masking*. In either of the above situations, bats reduce the

duration of the emitted sounds to avoid the interfering of signals (Moss and Surlykke, 2001; Schnitzler and Kalko, 2001; Surlykke et al., 2009b).

A third situation arises when the bat forages or navigates in clutter and produces echolocation calls at a high pulse repetition rate (i.e. at short pulse intervals). Each call causes a stream of echoes to arrive at the bats ears. If the pulse repetition rate is high enough, the echo streams from consequent calls can overlap, again causing a masking of signal and loss of information. In such situations, it has been observed that bats adjust the call rate to avoid overlap between echo streams (Moss and Surlykke, 2001; Schnitzler and Kalko, 2001; Surlykke et al., 2009b; Kothari et al., 2014). Here it is important to note that a higher pulse repetition rate is required to increase the information flow when a bat is about to capture its target (as shown in the buzz phase in Figure. 1.11).

1.3.2.2 Signal detection v/s localization

During the early part of foraging, the search phase, the problem of detecting the prey is paramount. Most aerial foraging bats have been known to produce long, narrow bandwidth sonar sounds, often called quasi-CF calls (QCF) during the search phase. More direct evidence of this is obtained from bats which emit CF-FM calls. The longer CF part concentrates most energy in this very narrow acoustic band and which causes glints to form in the returning echo especially when it reflects from a fluttering insect. The probability of receiving a reflected glint increases with longer duration of the CF call. It is also hypothesized that emitting QCF/CF calls increases the probability of target echo detection as it activates the neuronal filters in the auditory pathway for a longer duration. On the other hand, shorter broad band signals increase the localization

accuracy (Kober and Schnitzler, 1990; Neuweiler, 1990; Moss and Zagaeski, 1994; Kalko, 1995; Moss and Schnitzler, 1995).

These above-mentioned adaptations are clearly observable in the schematic in Figure. 1.11. In the early search phase, the bat produces longer duration shallow FM signals to increase the prey detection probability. In the approach phase, once the target is detected, the bat increases the pulse repetition rate, produces more broadband signals of shorter duration. While in the buzz phase the bat produces extremely short duration signals, to avoid the masking problem between the overlap of its own call and the returning echo.

1.3.2.3 Sonar sound groups

As described in Figure. 1.11 as well as in a previous section, bats reduce the interval between sonar calls as the distance to prey decreases, and interspersed in foraging call sequences are sonar sound groups (SSGs). SSGs are a clustering of sonar sounds, where the bat emits a group of sonar sounds at very short but with regular pulse intervals (i.e. higher pulse repetition rate), flanked by sonar sounds which are emitted at longer pulse intervals. The production of SSGs is an adaptive sonar behavior that has been reported in both laboratory and field studies of bat echolocation, in free-flying animals (Surlykke and Moss, 2000; Moss and Surlykke, 2001; Moss et al., 2006; Petrites et al., 2009; Kothari et al., 2014; Sändig et al., 2014; Falk et al., 2015) and those tracking moving prey from a stationary position (Aytekin et al., 2010; Kothari et al., 2014). Past studies have shown that bats temporally cluster sonar sounds to produce SSGs when they are engaged in complex tasks and has led to the hypothesis that the bat's production of SSGs

improves its spatio-temporal resolution of sonar objects (targets or obstacles) in the environment (Moss and Surlykke, 2001; Moss et al., 2006; Kothari et al., 2014).

1.3.3 Conclusion: Open questions

In the introduction, I started by motivating the importance of orienting in 3D space. Animals exhibit, species specific, adaptive movements for improving spatial resolution for orienting in depth like vergence eye movements in primates and humans, head bobbing behavior in birds and peering behavior in insects. As described in the previous section, bats produce sonar sound groups (SSGs) which have been hypothesized to facilitate the sharpening of spatio-temporal resolution.

These diverse behaviors that bats exhibit for orienting in 3D space require feedback between sensing and action, which are enabled through diverse sensorimotor networks in the central nervous system. As mentioned in previous sections of this introduction, a major hub for sensorimotor integration is the midbrain superior colliculus (SC) and although there is a large body of work demonstrating that the SC creates multimodal topographic maps of sensory and motor movements for orienting in 2D space, there is, however, very limited evidence, mainly from studies in primates and echolocating bats, supporting a greater role of the SC in orienting in 3D space.

Question: Does temporal patterning of sonar sounds (SSGs) increase the spatio-temporal resolution of 3D space in echolocating bats engaged in goal oriented tasks?

- **Chapter 2:** Prior work has examined SSGs in various behavior contexts; however, a comprehensive analysis of previous results has not been undertaken. In chapter 2, we provide a comprehensive comparison of data from field and lab experiments, to provide evidence, for the hypothesis that under challenging conditions bats increase the production of SSGs as it improves the spatio-temporal resolution of target range.
- **Chapter 3:** Here, we ask whether temporal patterning of sonar calls (SSGs) are used by the bat in tracking unpredictably moving targets; a situation often faced by bats in the wild when they pursue erratically moving prey, especially eared prey, which have evolved evasive maneuvers to avoid getting captured by echolocating bats. We provide evidence that bats actively modulate the pattern of their vocalizations at times when there is greater unpredictability in target motion, supporting the hypothesis that the production of sonar sound groups is a strategy actively used by echolocating bats to improve the spatio-temporal localization or targets in 3D space.

The results and hypothesis from these behavioral experiments (chapter 2 and 3) form the foundation for the neurophysiology experiments presented in remaining chapters.

Question: How do you quantify the bats acoustic stimulus space as it flies?

- **Chapter 4:** To investigate the representation of 3D space in the brain of a free flying bat, we first need a way to reconstruct the auditory information a bat would receive at its ears as it flies through its environment. Here, we provide a framework for reconstructing the instantaneous 3D auditory stimulus space experienced by the bat. The methodological advances presented in this chapter enable us to further examine

the representation of 3D space in the SC of free flying echolocating bats. This framework also opens the door to further studies of neural mechanisms of 3D orienting behaviors in freely behaving animals engaged in naturalistic tasks.

Questions: Does the SC of free-flying echolocating bats represent 3D auditory space in free flying echolocating bats? Does the production of SSGs cause the sharpening of receptive fields in the SC of free-flying echolocating bats?

- **Chapter 5:** Here, we attempt to bridge the gaps in our current knowledge of the SC by conducting neural recordings from the SC of a freely flying echolocating bats Our results provide the first evidence demonstrating depth tuning and 3D spatial response profiles of SC neurons in free flying echolocating bats engaged in a naturalistic task. Our results also provide strong evidence that the mammalian SC is a structure involved in representing 3D egocentric sensory space and encoding species specific orienting movements to objects in 3D space.

  More importantly, there is not neurophysiological evidence supporting the hypothesis regarding the sharpening of spatio-temporal representation facilitated by the production of SSGs. In chapter 5 we provide the first evidence that the spatial receptive field are sharpened in the range dimension when bats produce sonar sound groups. Further, despite decades of work studying range tuning in bats, almost all studies have been conducted in passively listening bats, using pairs of sounds mimicking the pulse and echo. Our results provide the first evidence of range tuning in the brain of an actively echolocating bat engaged in a naturalistic task.

Question: How can extracellular neural activity recorded in a freely behaving animal engaged in a natural task be classified into sensory, sensorimotor and vocal-premotor activity?

- **Chapter 6:** Traditionally, most studies in the SC using awake behaving animals have used animals, mainly primates, which are head restrained, and perform tasks using artificial stimuli. The control offered in these experiments has been crucial for the tremendous amount of knowledge generated, which has elucidated the role of the SC as a hub for sensorimotor integration and attention. In such experiments, because of the strictly controlled 'trial-based' structure of the behavior, sensory, sensorimotor and premotor cells can be identified by separating the sensory and motor behaviors in time. This allows the experimenter to solve the problem of assigning neural activity to independent behavioral/sensory events. This is also true in the case of a passively listening bat, as it is straightforward to identify and characterize sensory activity.

  In the natural environment, when an animal interacts with natural stimuli, it performs a cascade of orienting behaviors which are associated with sequences of sensory and motor events. In such situations, assigning neural activity, reliably, to sensory or motor events is a challenging problem. In this chapter, I will describe an approach (algorithm) that I developed which allows us classify neurons recorded during free flight as sensory, sensorimotor and vocal premotor.

"Much of human behavior can be explained by watching the wild beasts around us. They are constantly teaching us things about ourselves and the way of the universe …."

— Suzy Kassem

Rise Up and Salute the Sun: The Writings of Suzy Kassem

2

Timing matters: Sonar call groups facilitate target localization in bats

2.1 Introduction

How do animals process, organize and retrieve information from a rich and complex environment? Furthermore, how is this information integrated with motor programs to support perceptually-guided behaviors? The active sensing system of the echolocating bat presents an opportunity to address these questions. The bat produces ultrasonic signals and uses information carried by echoes to detect, localize and discriminate objects in the environment. It is well established that echolocating bats adapt the duration, spectrum, directional aim and timing of sonar signals in response to information extracted from echoes (Griffin, 1958; Jen and McCarty, 1978; Petrites et al., 2009; Moss and Surlykke, 2010). Past research has considered the functional importance of adaptive control of bat sonar call parameters (pulse duration, interval, spectrum and beam aim) in the context of behavioral tasks, such as prey capture and obstacle avoidance, and the environment in which the bat operates, e.g. open space, forest edge, or within dense

vegetation (Griffin et al., 1960; Kalko and Schnitzler, 1989, 1993; Simmons et al., 1979; Surlykke and Moss, 2000; Siemers and Schnitzler, 2004; Moss et al., 2006; Jones and Holderied, 2007). Layered on the adaptive changes in sonar signal parameters is the temporal patterning of calls, but the functional importance of this behavior is not well understood. Here, we compare the global temporal patterning of sonar vocalizations in different situations from both field and laboratory studies of the big brown bat, *Eptesicus fuscus,* with the goal of advancing our understanding of the environmental and task conditions that influence the bat's control over the timing and grouping of calls.

When the big brown bat is hunting and searching for prey in an open habitat, long, shallow FM (frequency modulated) signals facilitate target detection by concentrating sound energy in a narrow frequency band over an extended period of time. During target approach and interception, the bat emits broadband vocalizations that support target localization in azimuth, elevation and range, as each frequency band in the echo provides a time marker for its arrival at the bat's ears (Moss, and Schnitzler, 1995; Surlykke and Moss, 2000). In addition, the FM bat actively adjusts the duration of signals to avoid overlap of sonar emissions and echoes, and modifies sonar call intervals to receive echoes from one sonar emission before producing the next (Kalko, 1995; Wilson and Moss, 2004; Surlykke et al., 2009).

The bat's adjustments of sonar signal repetition rate and duration are tied to target range; however, echolocation call parameters also depend on the bat's azimuth and elevation relative to a selected prey item, and most importantly, its plan of attack. If a bat approaches an insect, flies past it and returns to intercept it, the temporal patterning of the bat's signals are distinctly different from those produced by the bat if it flies directly to attack the prey (Moss and Surlykke,

2001; Moss et al., 2006). Thus, the temporal patterning of the bat's echolocation signals provide explicit data on its adaptive motor commands to actively probe objects in the auditory scene.

In more challenging behavioral contexts, the bat produces clustered groups of vocalizations, previously termed sonar ”strobe groups,” because three or more signals within such a group typically have relatively stable pulse intervals (5% tolerance), and are flanked by calls with larger intervals (Moss et al., 2006). Here we refer to these call groups as “sonar sound groups,” to include the production of two, as well as three or more calls emitted in clusters, surrounded by longer pulse intervals (1.2 times the mean interval within the call cluster). For call pairs, or doublets, it is not relevant to consider the stability of call intervals, and hence the term “strobe” would not apply. Petrites et al (2009) and Hiryu et al (2010) have defined ‘strobe groups’ slightly differently. However, the basic concept of a group of sounds with near constant pulse intervals, surrounded by calls with larger intervals remains the same.

A previous study of the vocal behavior of echolocating bats flying in environments with acoustic clutter reported that big brown bats produce pairs of vocalizations, or sound doublets, flanked by calls with longer intervals (Hiryu et al., 2010). Furthermore, these pairs of vocalizations showed specific and reliable differences between the frequency content of individual calls. The big brown bat altered the frequency of the second vocalization in the doublet with respect to the first, and it was hypothesized that such spectral adjustments permit the disambiguation of echo cascades from the first and second vocalization in the pair. The change in frequency across vocalizations in a sonar sound doublet suggests that the bat combines echo information from the

first and second calls to represent a complex environment. In this way, the bat may be integrating echo information over a sequence of acoustic snapshots (see Moss and Surlykke, 2001).

Other studies of bats foraging in the laboratory have highlighted the temporal patterning of sonar calls produced by bats. Moss and Surlykke (2001) and Moss et al. (2006) reported that the prevalence of sonar sound groups was greater when the big brown bat foraged close to background clutter than in the open room. They observed that bats tended to produce sonar sound groups when selecting a target, changing the direction of the flight path, or when the bats were in close proximity to obstacles. These observations led to the hypothesis that sonar sound groups have immediate consequences for the bat's perception of space and are used in planning a flight trajectory that requires a more detailed and updated estimate of target localization (Moss and Surlykke, 2001; Moss et al., 2006). These ideas demand more a complete investigation, and in this article, we further consider the echolocating bat's temporal control of sonar calls to represent the environment in a variety of habitats and behavioral contexts.

Here we compare echolocation behaviors in several distinct studies of the big brown bat (*E. fuscus*) from both the field and the laboratory, and under different environmental and task conditions. We re-examine data from our previously published studies (Surlykke and Moss, 2000; Moss and Surlykke, 2001; Moss et al., 2006; Ghose and Moss, 2006; Ghose et al., 2009; Surlykke et al., 2009a), along with newly collected data. Our focus is on the bat's temporal control over sonar call production, and we consider a variety of factors that may contribute to the timing of bat sonar calls, including wing beat, background clutter, target motion, and bat flight trajectory. We hypothesize that for more demanding spatio-temporal localization tasks, the echolocating

bat actively adjusts the timing of calls to increase the reliability and/or resolution of spatial and temporal information acquired from echoes.

2.2 Methods

Audio recordings were taken from echolocating big brown bats, behaving in the lab and the field, and the focus here is on the timing of sonar call production. Microphone and data acquisition systems were specific to the field and lab studies and are detailed below. Previously, Moss and Surlykke (2001) and Moss et al., (2006) defined sonar sound groups as clusters of three or more vocalizations which occur with a near constant PI (within 5% error with respect to the mean PI of the sound group), and are flanked by calls with a larger PI at both ends (at least 1.2 times larger). We refer to the property of sound groups flanked by calls with larger PI at both ends as meeting an Island Criterion (see Figure. 2.1c and 2.1d). The terminology Island Criterion refers to the temporal isolation of sonar sound groups within the ongoing stream of sonar vocalizations. Additionally, we term the near constant PI within a sound group as meeting a Stability Criterion (see Figure. 2.1d). Since the Stability Criterion cannot be defined for sonar call doublets which are pairs of sonar sounds produced with a short PI compared with surrounding calls, are characterized solely by the Island Criterion (see Figure. 2.1c). The Island Criterion was used in the current study, to characterize a broader scope of temporal call patterning, and we collectively refer to clustered signals as **Sonar Sound Groups.** Hence, sonar sound groups with three or more clustered sonar sounds satisfy both the Island Criterion and the Stability Criterion, whereas the sonar sound doublets only satisfy the Island Criterion.

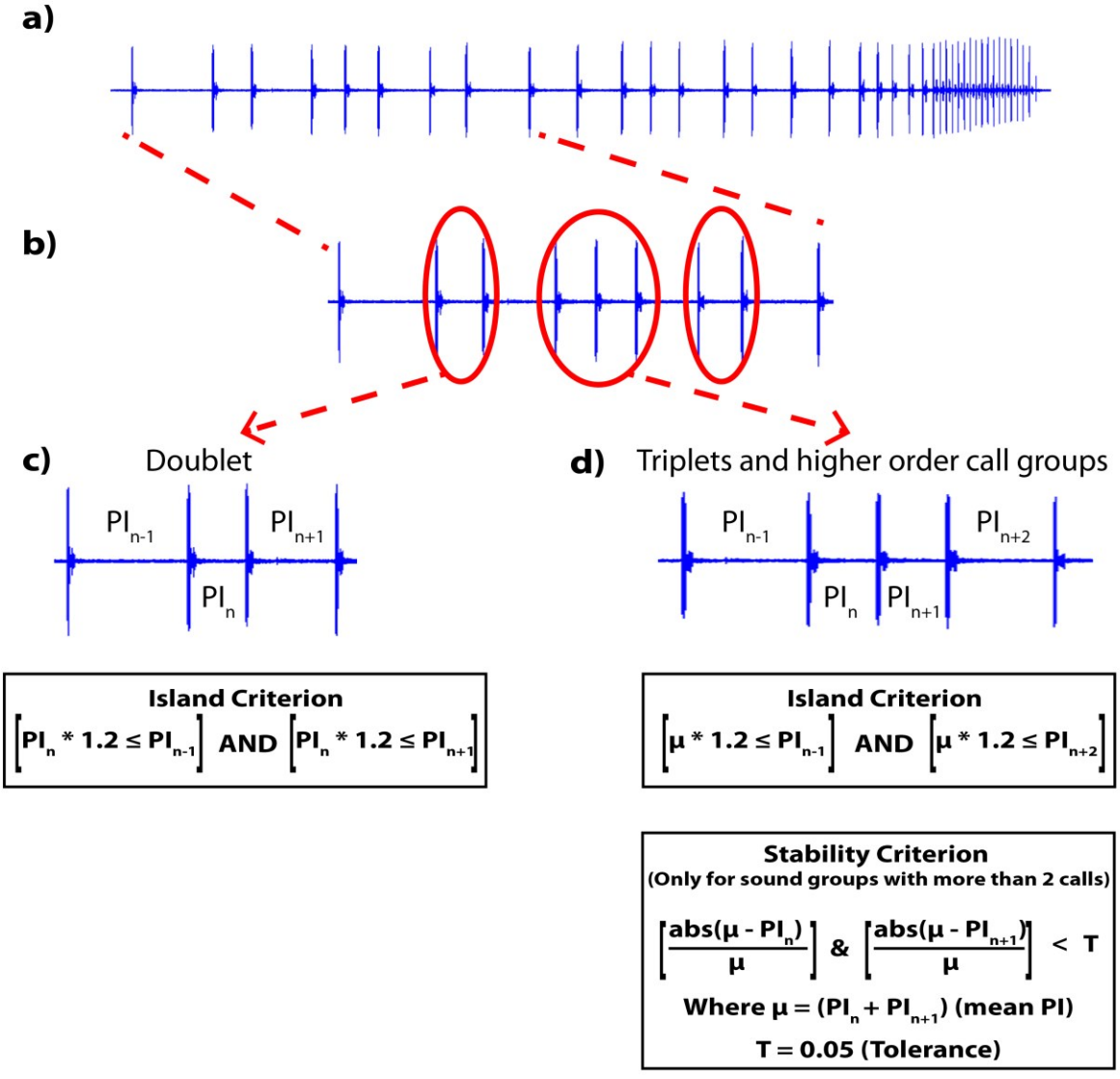

Island Criterion

$$\left[PI_n * 1.2 \leq PI_{n-1}\right] \text{ AND } \left[PI_n * 1.2 \leq PI_{n+1}\right]$$

Island Criterion

$$\left[\mu * 1.2 \leq PI_{n-1}\right] \text{ AND } \left[\mu * 1.2 \leq PI_{n+2}\right]$$

Stability Criterion
(Only for sound groups with more than 2 calls)

$$\left[\frac{abs(\mu - PI_n)}{\mu}\right] \;\&\; \left[\frac{abs(\mu - PI_{n+1})}{\mu}\right] < T$$

Where $\mu = (PI_n + PI_{n+1})$ (mean PI)

T = 0.05 (Tolerance)

Figure 2.1. Sonar sound groups. a) A sonar call sound stream from a bat tracking a tethered meal worm following the Simple Motion (SM) trajectory. **b)** Doublets and Triplet sound groups. **c)** A doublet is identified by the PI of the calls at either end of the doublet being at least 1.2 times larger than the PI of the doublet (Island Criterion). **d)** Higher order sonar sound groups are identified by a stable PI within the call group (Stability Criterion). The stable PI is indicated here as the mean (μ) and the PI is considered stable if all the PIs within the group are within a tolerance of +/- 5% (T) of the mean PI. Also, the PI of the calls at either end should be at least 1.2 times the mean PI of the calls in the sound group (Island Criterion). Here the example given is of a triplet sound group.

2.2.1 I. Field Recordings.

Field recordings of *E. fuscus* were taken at two different sites (Figure. 2.2; sites A and B). Recordings at site A were carried out in the months of August and September of 1999, when bats were commuting from a roost in Rockville, MD, U.S.A. The bats emerged from their roost which was a small opening in the roof of a town house. The opening faced a group of trees, and a hand held ultrasound microphone was used to record the vocalizations as the bats flew out (Figure. 2.2a). Further details of the methods and the site of the 1999 field recordings are reported in Surlykke and Moss, 2000. Recordings were made at Site B in the month of May, 2013. Site B was located at Lake Artemesia, MD and can be briefly described as a rectangular open space (approximately 15 m x 30 m) flanked by a baseball field and a deserted road on either end of its longer dimension and a thicket of trees and a small creek on opposites sides of its narrower dimension (Figure. 2.2b). The setup at Site B consisted of 9 G.R.A.S. ¼" microphones placed in a cross-shaped array, 6 on a horizontal line and 2 above and 1 below the center microphone forming a 4 microphone vertical line. The horizontal microphones were placed from left to right at 0 m, 1.36 m, 2.70 m, 3.60 m, 4.50 m and 6.11 m and the vertical microphones (with the 4th microphone at 3.60 m as center) were placed 2.85 m and 1.15 m above and 0.57 m below the horizontal line. The amplified (Avisoft power modules) sounds were digitized, Avisoft USGH 1216 at 300 kHz sampling rate and stored on a laptop computer. We recorded 4 seconds files, 2 seconds pre-trigger and 2 seconds post-trigger. Triggering occurred when a feeding buzz was heard on a D240x Peterson bat detector. The microphones were calibrated before and after each recording session with a GRAS 42 AB sound calibrator.

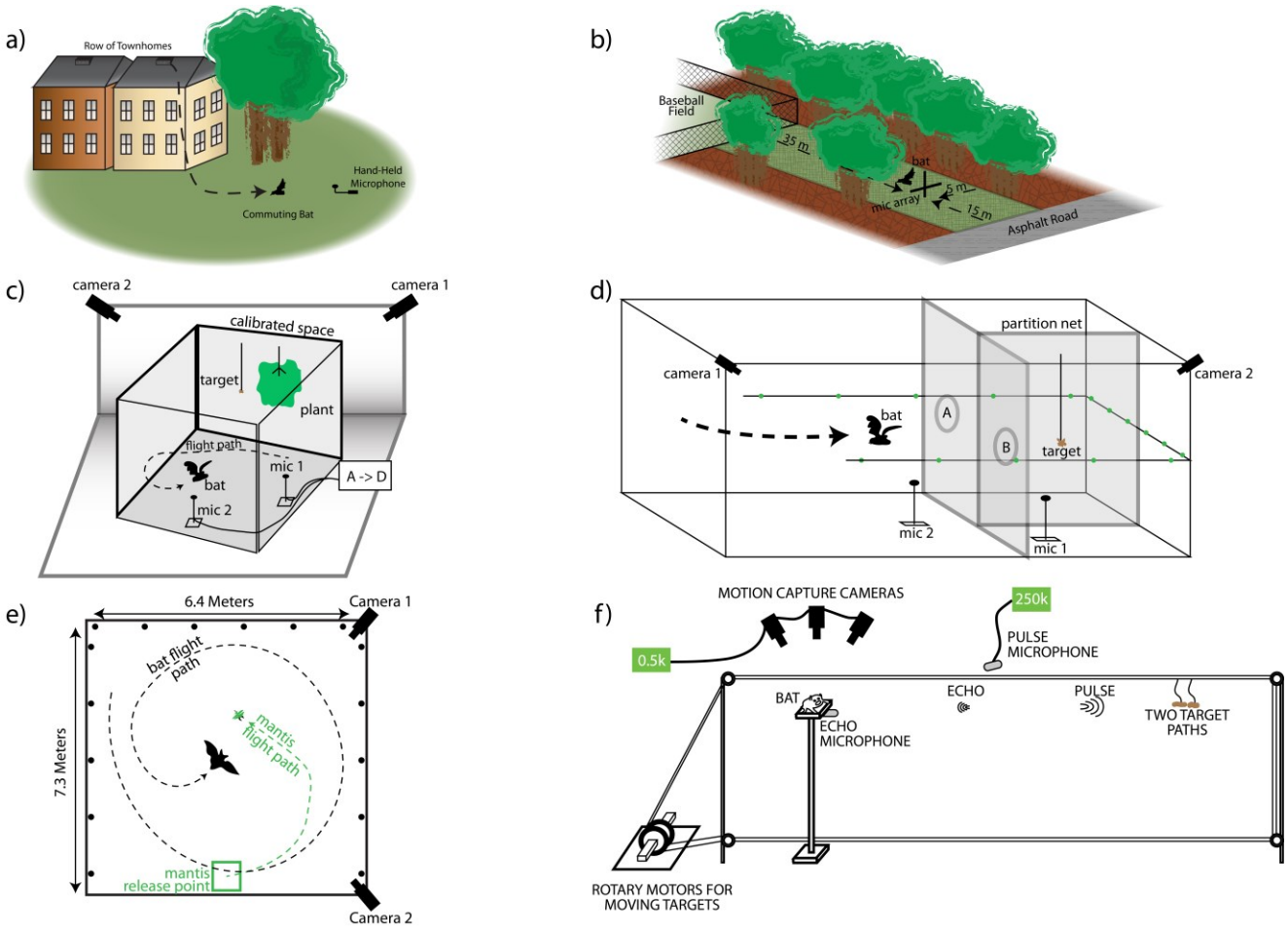
a)
Row of Townhomes
Hand-Held Microphone
Commuting Bat
b)
Baseball Field
35 m
bat
5 m
mic array
15 m
Asphalt Road
c)
camera 2
camera 1
calibrated space
target
plant
flight path
bat
mic 1
mic 2
A -> D
d)
partition net
camera 1
camera 2
bat
A
B
target
mic 2
mic 1
e)
6.4 Meters
Camera 1
bat flight path
mantis flight path
7.3 Meters
mantis release point
Camera 2
f)
MOTION CAPTURE CAMERAS
250k
PULSE MICROPHONE
0.5k
BAT
ECHO MICROPHONE
ECHO
PULSE
TWO TARGET PATHS
ROTARY MOTORS FOR MOVING TARGETS

Figure 2.2. Field and laboratory experimental setups. a) Schematic of the Rockville, MD field site. Bats were exiting from behind a slatted vent near the roof on the side of a town home. This town home was at the end of a row of town homes that opened up onto a small field with a few trees. The bats' vocalizations were recorded as they flew out of the house and onto the field. **b)** Layout of the Lake Artemesia, MD field site. The recording site was a narrow corridor of grass between trees, bounded at one end by a baseball field and at the other by a paved road. The bats were recorded with a microphone array placed at the road-end of the corridor. **c)** Laboratory setup for catching tethered mealworms in the presence of clutter. The clutter was a fern-like artificial plant hung from the ceiling, and mealworms were tethered to the ceiling at varying distances from the plant. Two cameras in the corners of the room capture 3D flight trajectory data, while microphones on the floor recorded sonar vocalizations. **d)** Top-down view of the laboratory setup for the flying mantis experiment. The mantis was released from a platform, and the bat was released by the researcher elsewhere in the room. Two cameras recorded the 3D flight path, while microphones on the floor and walls (round marks) recorded the sonar vocalizations, and beam shape, respectively. **e)** Experimental setup for the net-hole experiment. The room was portioned as shown into three sections. The mealworm was hung in one of the two smaller sections on the right end of the room, and the bat flew through either hole 'A' or hole 'B' do catch the mealworm. Behavioral measurements as described above (i.e. flight path, vocalizations, beam shape) were collected. **f)** Schematic of the setup for the platform tracking experiment. A bat is trained to sit on a platform and track a tethered mealworm that is moved in the range axis with a computer controlled set of rotary stepper motors. The bats' vocalizations and returning echoes are recorded by ultra-sonic microphones in front and underneath the bat, respectively. Motion capture cameras collect ear and head movement data.

2.2.2 Recordings from free flying *E. fuscus* in the laboratory.

Here we describe three different experiments, in which flying bats captured stationary (tethered mealworm) and moving insect (free-flying praying mantises) targets in a closed laboratory flight room, and in some studies in the presence of obstacles. The data presented here have been analyzed to examine and compare the bat's production of sonar sound groups under a variety of conditions. In all of these laboratory studies, bats flew freely in a large flight room, with walls and ceiling lined with acoustic foam (Sonex 1), and a carpeted floor. Two high speed Kodak MotionCorders (240 frames/sec) or Photron video cameras (250 frames/sec) recorded the bat's flight behavior under IR illumination, and the stereo video data were used to reconstruct the bat's 3D flight path within a calibrated volume in the room (Figure. 2.2c, 2.2d and 2.2e). The bat's echolocation signals were recorded with two Ultrasound Advice microphones positioned on the floor and digitized with an IoTech 512 Wavebook at a sample rate of 240 kHz/channel. Only the data three seconds prior to the time when the bat captured or hit the tethered mealworm was analyzed and presented here.

2.2.2.1 Bats taking tethered insects in the laboratory under different clutter conditions:

Bats were trained to take mealworms from a tether in an open (uncluttered) flight room. Clutter was introduced by an artificial houseplant, resembling a fern, approximately 80 cm in diameter and 50 cm high, hanging from the ceiling at the same elevation as the tethered mealworm. Trials were run with the tethered insects presented in an open room and at different distances from the vegetation, ranging from 10 cm to 40 cm. The setup is shown in Figure. 2.2c. For more details, refer to Moss et al., 2006.

2.2.2.2 Obstacle avoidance task and prey capture in the laboratory:

A mist net was used to divide the flight room into two partitions. One side of the room was further subdivided with a mist net to create two sub-compartments. A tethered mealworm was hung randomly in either of the two sub-compartments, and bats were trained to search for the tethered mealworm, and then fly through an opening in the mist net to collect its food reward in the sub-compartment where it was presented (as shown in Figure. 2.2d). This task forced the bat to find the food reward behind the mist net and negotiate the obstacle (opening in the net) to collect the reward, hence requiring goal-oriented behavior in a complex environment (For further details, see Surlykke et al., 2009a).

2.2.2.3 Pursuit and capture of free-flying insects in the laboratory:

Bats were trained to capture a freely flying praying mantis. Figure. 2.2e shows the experimental setup with an example bat and mantis trajectory. The bat was released from different locations in each trial while the mantis was released from the same location. The hearing of the praying mantis was impaired by applying Vaseline to its midline ear (Triblehorn et al., 2008), and therefore the insect continued to fly when the bat produced ultrasonic signals which would otherwise trigger a dive response by the mantis. This experiment enabled us to study the sonar call production behavior of bats in an insect-tracking task. For more details, refer to Ghose et al., (2009) and Ghose and Moss, (2006).

2.2.3 Lab recordings of E. fuscus tracking a target while resting on a platform.

Big brown bats (*E. fuscus*) were trained to sit on a platform and track a moving food reward (mealworm – Figure. 2.2f). The food reward was tethered and suspended from a

rectangular loop of fishing line with pulleys on 3 corners, and a rotary servo motor (Aerotech BMS60 brushless, slot less rotary servo motor attached to an Ensemble MP10 motor controller) on the fourth corner that drove the fishing line in either direction (see Figure. 2.2f). The rotary stepper motor was programmed via a computer interface through Matlab (2012a), controlling the velocity, acceleration, deceleration, and the distance the food reward traveled. This method engaged the bat in naturalistic sonar tracking behavior, while also allowing the experimenter precise control over the target motion with respect to the bat, which is not possible in free flight studies. This setup moved the target along the range axis on a straight line towards the bat. Because the bats were resting on the platform, the timing of calls would be coordinated with respiration but not influenced by wing beat (Wong and Waters, 2001; Wilson, W.W., and Moss, 2004; Koblitz et al., 2010). Bat sonar vocalizations were collected using two Ultrasound Advice UM3 microphones (M1 and M2 in Figure. 2.2f) and were digitized using a National Instruments A/D PCI card interfaced with Matlab (2012a). Two high speed infrared Phantom Miro cameras and 3 infrared Vicon Motion tracking cameras were used to track the head and pinnae movements of the bats. The Aerotech Servo motors, audio capture, high speed video and Vicon motion tracking cameras were all synchronized using the a single TTL trigger pulse generated via the Matlab-National Instruments A/D interface. Data analysis from the high speed video and Vicon motion tracking systems is not presented here.

Initial stages of this task involved clicker training to condition the bat to associate a sound with the delivery of a food reward; the experimenter then slowly moved the food reward by hand while the bat used echolocation to track its position. Once the bat learned to track the food reward using echolocation, the insect was hung from the fishing line and initially moved small

distances with the rotary stepper motor system. As the bat learned the task, the total target distance was increased to 2.5 meters. During training, a single type of target motion was used: The target started at a distance of 2.5 meters, accelerated at a rate of 7 m/s^2, traveled a distance of approximately 2 meters with constant velocity of 4 m/s (mimicking the approximate flight velocity of a bat during the approach phase (Hayward and Davis, 1964) and then decelerated at a rate of 5 m/s^2. We refer to this motion as Simple Motion (SM). The end of the trial was marked when the tethered mealworm reached the bat. The bat would generally take the mealworm in the mouth and in the event it missed, the bat was then rewarded by hand. Additionally, catch trials were introduced, where the mealworm was stopped before it reached the bat to make sure that the bats were not just echolocating at random. Most trained bats would stop echolocating as soon as the mealworm stopped. The movement of the target with respect to the stationary bat is shown in Figure. 2.3a. Figure. 2.3b shows an example sonar recording of a bat tracking a mealworm. Sonar call spectrograms of an approach call (marked red) and a feeding buzz call (marked by green) are also shown. As previously demonstrated by Aytekin et al., 2010, well-trained bats actively adapt sonar PI according to the distance of the target (see Figure. 2.3c). Once the bat became skilled at the SM tracking task, two novel types of target motion were introduced to the bat. We refer to these target motions as Complex Motions 1 & 2 (CM1 and CM2, respectively). In the novel complex motion trajectories, the target first moved towards the bat, after which it oscillated back and forth before finally reaching the bat. The target displacement relative to the stationary bat is shown in Figure. 2.3a (Complex 1 – red, Complex 2 – black). The different parameters of the Simple Motion and two Complex Motions are shown in Table 2.1.

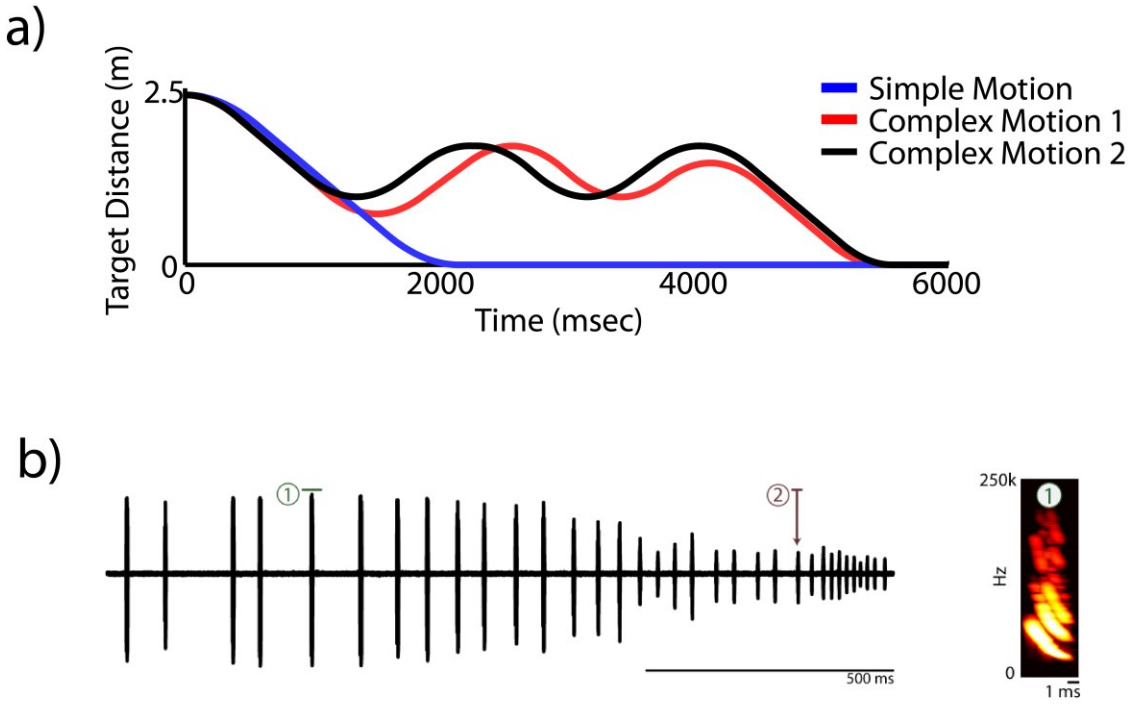
a)
Target Distance (m)
2.5
0
0
2000
4000
6000
Time (msec)
Simple Motion
Complex Motion 1
Complex Motion 2
b)
①
②
500 ms
250k
Hz
0
1 ms
1 ms
c)
Pulse Duration
Pulse Interval
Pulse Duration (msec)
Pulse Interval (msec)
8
6
4
2
0
180
120
60
0
0
30
60
90
120
150
180
Target Distance to Bat (cm)

Figure 2.3. Platform experiment. a) Distance versus time for each type of target motion of the tethered mealworm. The blue line represents simple motion in only one direction, while the red and black lines are the more complicated, back-and-forth motions. **b)** Left, example oscillogram of a sequence of vocalizations produced by a bat tracking a tethered mealworm in the setup shown in (a) moving in the simple motion trajectory. Right, spectrograms of the pulses highlighted by the red and green boxes on the left demonstrating the stereotyped changes in duration and frequency that are correlated with target distance. **c)** Quantification of changes in pulse duration and pulse interval as a bat tracks a moving target on the setup shown in (a).

Trial Type	Forward Velocity	Backward Velocity	Acceleration	Deceleration	Total Motion Time
Simple Motion	4 m/s	NA	7 m/s^2	5 m/s^2	1.8 sec (approx.)
Complex Motion 1	4 m/s	3.5 m/s	10 m/s^2	10 m/s^2	5.3 sec (approx.)
Complex Motion 2	4 m/s	3.5 m/s	10 m/s^2	10 m/s^2	5.5 sec (approx.)

Table 2-1 Motion parameters for each type of target motion a bat was presented with for the platform tracking experiment.

The main focus of this experiment was to test the hypothesis that the big brown bat actively produces clustered sound groups to resolve spatial location when target trajectory is uncertain. In order to introduce target motion uncertainty, trial types (CM1, CM2 and SM) were randomized. Within the random presentation of trajectory types, a sequence of CM (1 or 2) followed by two or three SM trials, was presented. All analysis was performed on entire trials of the sequence of CM and SM trials.

2.2.4 Analysis methods

Recorded sonar vocalizations were analyzed using custom written Matlab routines. Examples of a doublet and triplet sound groups are shown in Figure. 2.1 and the criteria to identify sonar sound groups is illustrated. Individual details of the analysis for each experiment are given below.

2.2.4.1 Flight trajectory analysis:

In the field at site B, the 3D position of free-flying bats was computed based on arrival time differences at the nine microphones in the array using cross-correlation and then computing the position based on the sound emission times and triangulating (Surlykke et al., 2009b). The 3D position of the bat in the laboratory was calculated by using a calibrated region of overlap from the two high speed video recordings (Moss et al., 2006).

2.2.4.2 2. Analysis of sonar signals produced by bats:

The emitted sounds were analyzed using custom Matlab software to relate sound features, i.e. pulse timing, duration, and interval, to the bat's 3D position and distance to targets

and obstacles. For more details of the sonar vocalization analysis in bat flight experiments, please refer to (Moss et al., 2006; Ghose and Moss, 2006; Ghose et al., 2009; Surlykke et al., 2009a).

2.3 Results

2.3.1 Temporal control of echolocation signals produced by bats in the field

Comparing bat echolocation patterns in the field and lab allows one to evaluate natural and artificial constraints on behavior. Here we report on the natural sonar behavior of big brown bats in the field as they i) commuted from a roost (Site A) or ii) foraged (Site B). Vocalizations recorded in the late evening when bats emerged from their roost were classified as "commuting sonar calls." After bats flew out of their roost, they flew mainly in one direction and showed no circling around the roost area. No feeding buzzes were recorded in this setting, indicating that bats were not foraging immediately after flying out of their roost. Big brown bats are generally known to fly to foraging sites away from their roosts, where they find a high density of prey. The roosting sites are often found in locations, which are safe for the bats and their young, such as man-made structures, caves, mines as well as tree cavities (Brigham and Fenton, 1986; Agosta, 2002). Vocalizations recorded at foraging sites were classified as "foraging sonar calls." The bat's flight and acoustic behavior during foraging was distinct from that observed in commuting animals. Foraging bats typically circled in a restricted area, following a relatively stereotyped trajectory, in contrast to the commuting trajectories which were straight in one direction. Many recordings at site B contained terminal buzzes, indicating that the bats were actively hunting. Figure. 2.4a shows a typical trajectory of a bat while it was foraging at site B. Figure. 2.4b shows

the corresponding sonar pulse interval (PI) plot. Each marked point (in blue) on the PI plot and the 3D trajectory in Figure. 2.4a and Figure. 2.4b shows a sonar vocalization. Sonar sound groups are marked in red (doublets) and black (sound groups with several sonar calls) solid circles on each plot. The first 3 black solid circles in Figure. 2.4b (and corresponding 4 black solid circles Figure. 2.4a) indicate a sound group, which consists of four calls in a series. Similarly the first and second red solid circles are doublets (and the corresponding red solid circles in Figure. 2.4a are the doublet vocalizations). The sonar sound groups with two calls (red) and four calls (black) have been marked in different colors for illustration purposes. Figure. 2.4c shows the PI plots of sound recordings at Site A when the bats were flying out of their roosts and commuting. Sonar sound groups were rarely observed in commuting bats (see one exception marked by black squares) and no feeding buzzes were recorded at site A. Figure. 2.4d compares the mean number of sonar sound groups recorded when the bats were commuting and foraging (mean of 4.5 +/- 1.5 sonar sound groups when the bats were foraging). All of the recordings at site B were approximately 4.2 seconds. The recordings at site A were shorter and of variable length as the bats flew straight out and did not circle around the roosting site.

2.3.2 Flying bats produce sonar sound groups under different conditions in the lab.

Here we compare the timing of calls produced by big brown bats across several conditions in the laboratory. Figure. 2.4e shows the mean number of sound groups produced by the bat in the final three seconds of flight before a successful or failed attempt to capture the target (tethered mealworm or a flying praying mantis), in the open room, in the presence of clutter (plant) or with obstacles (nets) in the environment. Successful attempts are the trials in which

the bat took the mealworm off the tether or captured the free-flying (deafened) mantis. Failed attempts are trials

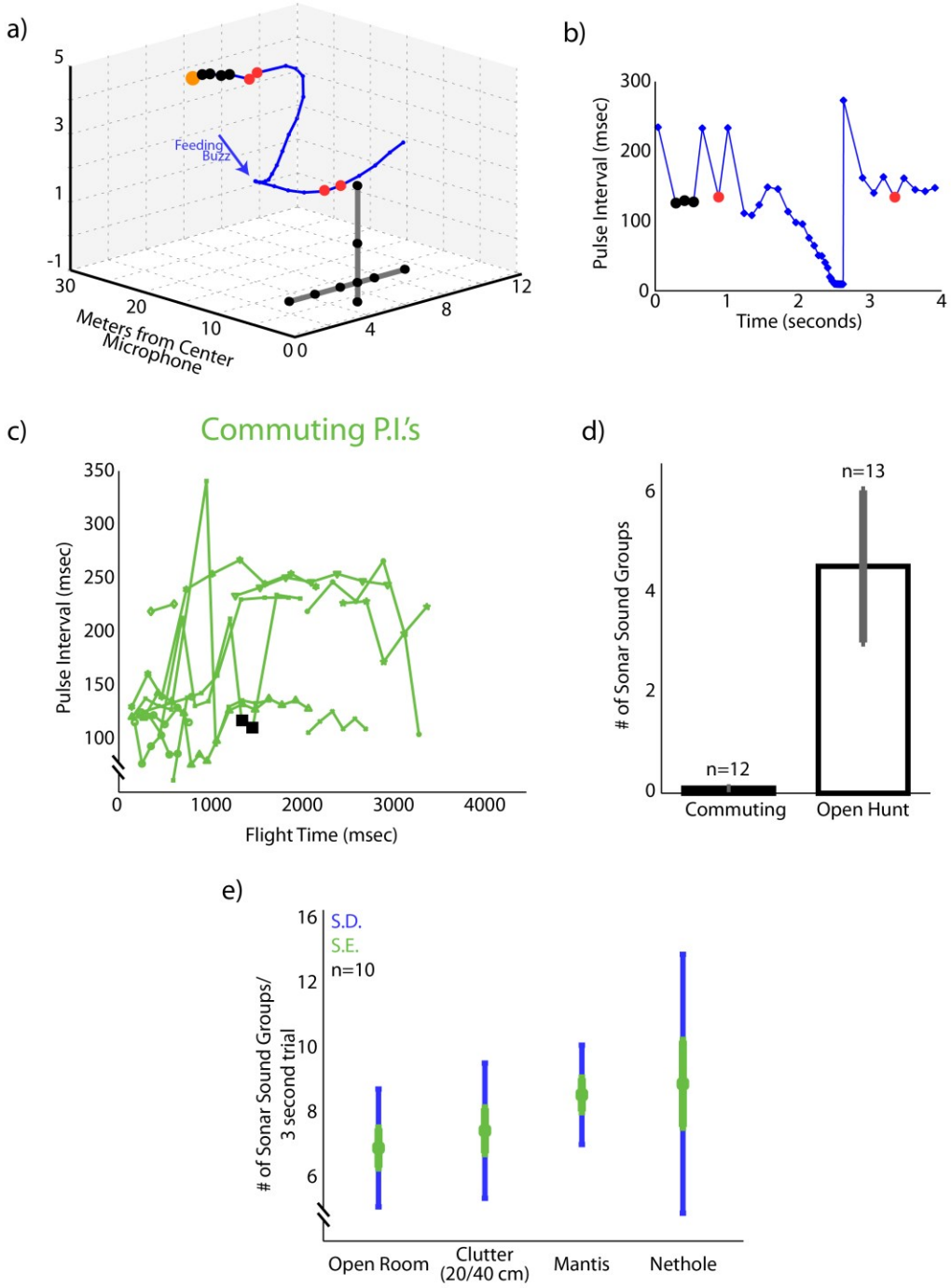

Figure 2.4. Sonar sound groups under varying conditions. a) One trial plotted in 3D from the Lake Artemesia field site. The bat's flight path is shown in blue, and timing of the vocalizations with blue dots. Black dots highlight vocalizations in a 4 call sound group, calls marked in red are 2-call sound groups. The microphone array is shown in black. **b)** Time versus pulse interval for the trial shown in (a). As in (a), P.I.'s marked with black are quartets, and those with red dots are doublets. **c)** Time versus pulse interval for the recordings of commuting bats at Rockville, MD. Only one sequence of vocalizations (shown in red) qualified as a sound group by our definition. The low (around 120 ms) and high (around 240 ms) PIs correspond to emitting a call per wing beat or only for every second wingbeat respectively. Sometimes the bats skipped two wingbeats and PI became even longer, around 350 ms. **d)** Number of sound groups uttered per trial for the commuting bats at Rockville, MD; and the hunting bats of Lake Artemesia, MD. **e)** Average number of sound groups per trial in the four laboratory flight experiments (clutter, nethole, mantis, open room). Green errorbars denote the standard error, blue the standard deviation.

in which the bat produced the terminal buzz and hit the insect but either dropped it or failed to take it off the tether. The mean number of sonar sound groups per trial (three seconds of data prior to the time of capture of the target) increased with an increase in complexity of the environment and the task. In the open room task, bats produced an average of 7.38 +/- 2.13 sonar sound groups per trial. When clutter in the form of an artificial plant was introduced to the environment, the average number of sonar sound groups increased to 8.0 +/- 2.44 sonar sound groups per trial. In the task where the bats tracked and captured a freely flying praying mantis, the mean number of sonar sound groups was, 9.3 +/- 1.8 sonar sound groups per trial. And finally, in the dual task of obstacle avoidance (net hole) and prey capture, the mean number of sonar sound groups was 9.70 +/- 4.69 sonar sound groups per trial. All numbers reported here are per trial.

2.3.2.1 Bat tracking an erratically moving target while resting on a platform.

Field, net, plant and free-flight insect capture experiments all show that bats produce sonar call groups under conditions of clutter or dynamic target trajectory. Here we extend this work to explicitly test the hypothesis that bats actively control the timing of calls and produce an increased number of sonar call groups under conditions of target trajectory uncertainty.

2.3.2.2 Increase in sound group doublets and triplets with increase in uncertainty in target position

Box plots showing the number of sonar sound groups produced by bats tracking a target in the CM and SM trial sequences are displayed in Figures 5a and 5b for two bats, Bat A and Bat

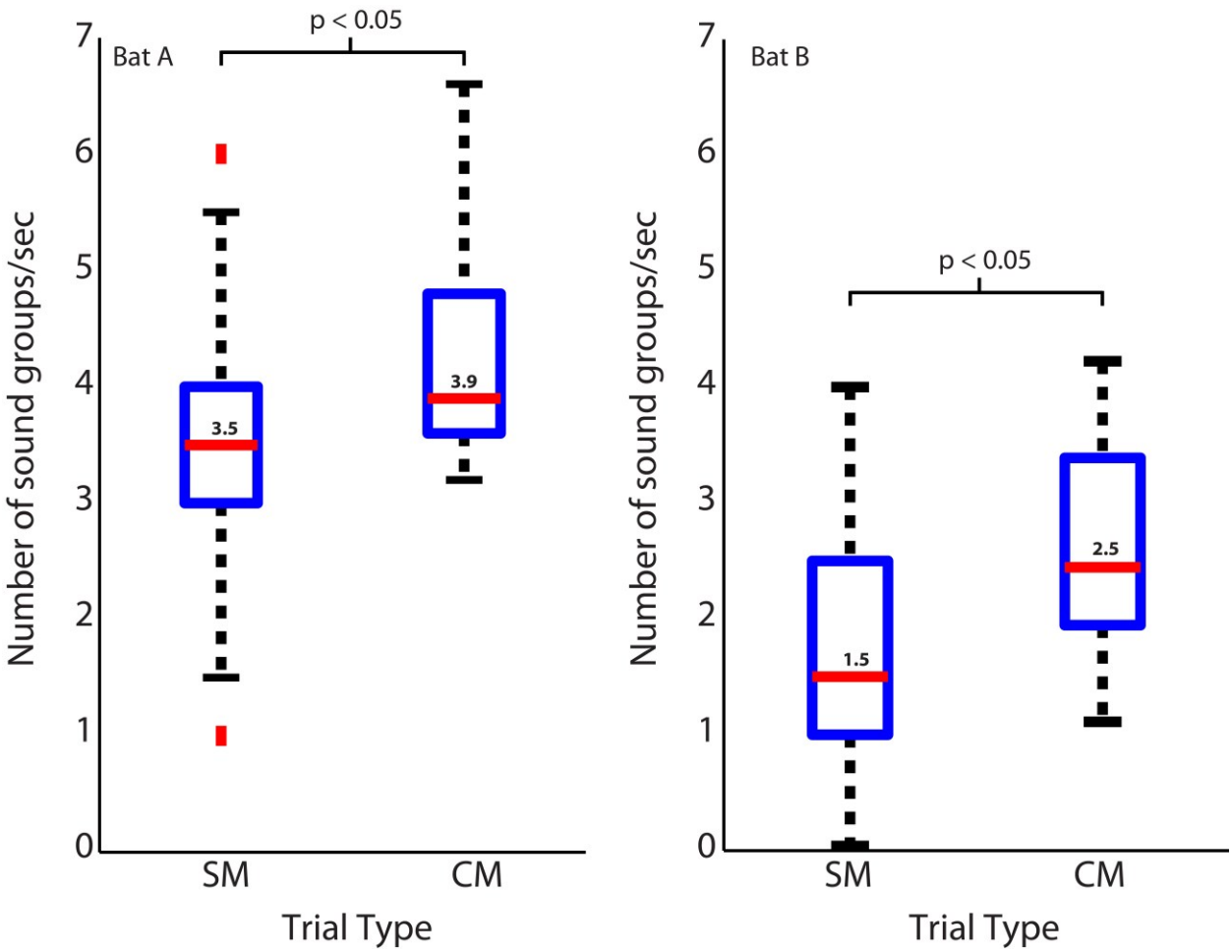

Figure 2.5. Sound groups during simple and complex target motions. a) Bat A sound group usage for simple and complex target motion trials. Blue box represents the middle 50% of the data, red bar is the median, green bar is the mean. Black bars detail the range of the data, and red dots are outliers. **b)** Same as in (a), but for Bat B.

B, respectively. Both bats showed a significant decrease in the number of sonar sound groups in the sequence of SM trials, as the predictability of the target position increased in repeated SM trials, as compared to randomly introduced CM trials. The median number of sonar sound groups produced per unit time (seconds) for Bat A was 3.9 for the CM trials, which was significantly greater than the median of 3.5 for the SM trials ($p < 0.05$ Mann-Whitney U test). The median of

the number of sonar sound groups produced per unit time (seconds) for Bat B was 2.5 in the CM trials, which was significantly greater than the median of 1.5 in the SM trials ($p < 0.05$ Mann-Whitney U test). Moreover, in instances when several SM trials were presented in sequence, the number of sonar sound groups produced by the bat decreased as trial-to-trial target trajectories became more predictable (data not shown). Box plots show the spread of the data.

2.3.2.3 Comparison of call group parameters across different conditions

In addition to producing sonar calls, as presented in Figures 4 and 5, bats actively adjusted other sonar signal temporal parameters. Here we compare pulse intervals of sonar sound groups across different experimental conditions (Figure. 2.6a). As noted above, commuting bats do not produce sound groups and therefore no data from recordings at field site A is included here. The average sound group PI (Pulse Interval) for bats flying under conditions of clutter was 35.35 +/- s.e.m. of 7.21. Average sound group PI for bats performing in the net hole and mantis experiments was 25.10 +/-s.e.m. of 2.84 and 29.80 +/- s.e.m. of 6.98 respectively. When the bat captured tethered mealworms in the open room condition, the average sound group PI was 33.64 +/- s.e.m. of 6.17. When the bat tracked tethered meal worms from a resting position on a platform, the average sound group PI was 44.68 +/- s.e.m. of 0.51. In field site B, the average sound group PI was 118.17 +/- s.e.m. of 8.19. Many of these pairwise comparisons of PI in different environments were significantly different from one another (Table 2.3). To summarize, PI's of experiments in the large flight room were comparable, but significantly less than the mean PI of sonar sound groups produced by bats in the platform experiment, while bats hunting in the field produced sonar sound groups with the largest PI's. The net hole experiment in the large

flight room resulted in the shortest sonar sound group PI's, presumably because the room was partitioned into smaller quadrants for this experiment. Figure. 2.6b compares the mean number of sounds in sound groups across the different conditions. Table 2.2 summarizes the proportion of time the bat produced sonar sound groups with 2, 3, or more than 3 sonar calls (N=2, N=3 or N>3 respectively). Our data also indicates that on average bats produce sound groups with more calls (N>=3) in the field compared to the laboratory.

In one further set of analysis, we examined the bat's proportional use of sonar sound groups across laboratory tasks and field conditions. For this analysis, we compared the proportion of sonar pulses the bat's produced as part of sonar sound groups compared to the total number of sounds produced by the bat during each behavioral condition (Figure. 2.6c). This analysis shows that the experimental condition with the highest proportional use of sonar sound groups was in the task in which the bat tracked a target moving back and forth (Complex Motion trials) from the platform. All foraging flight experiments in the laboratory and the field showed very similar sonar sound group production.

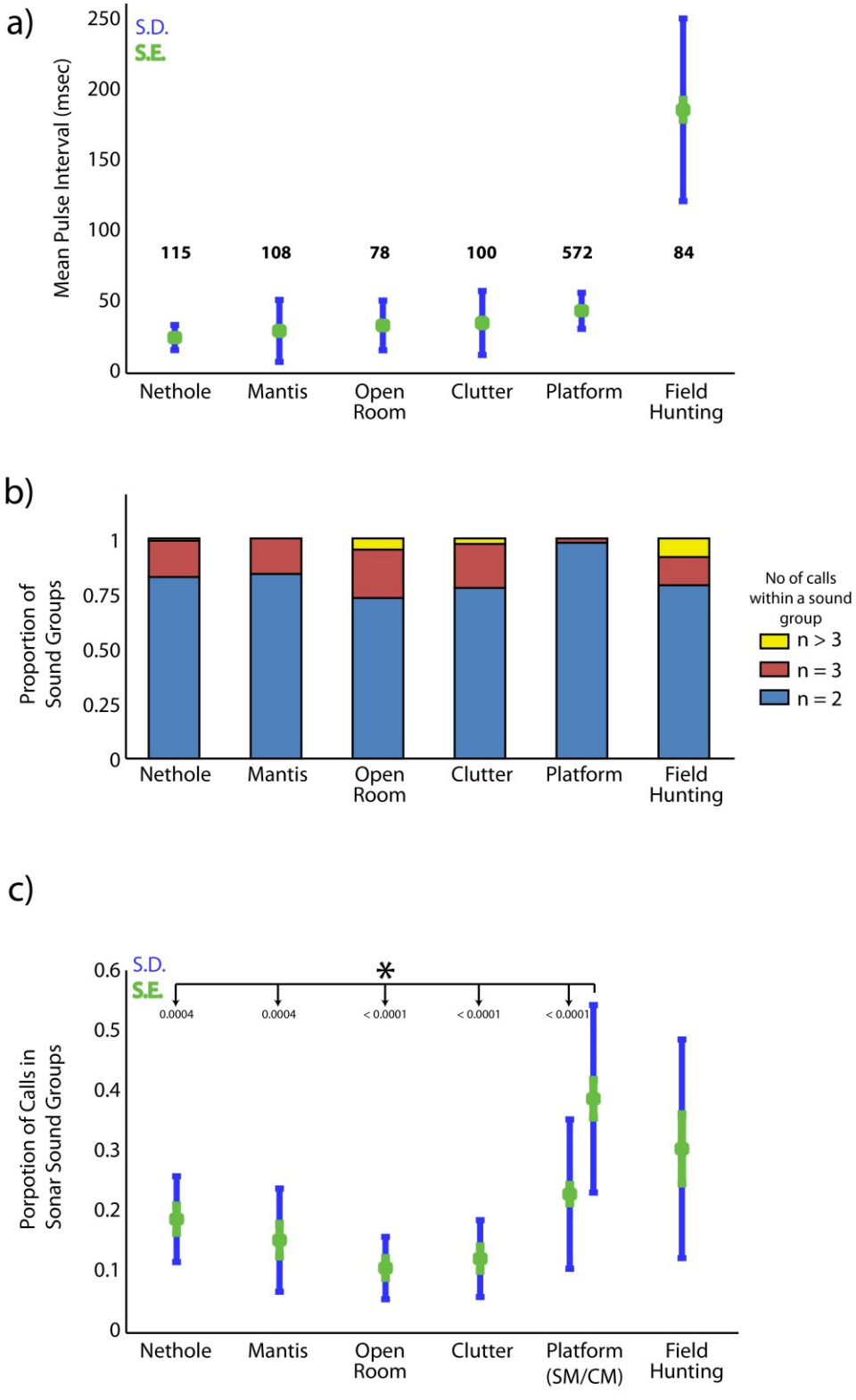
a)
S.D.
S.E.
Mean Pulse Interval (msec)
250
200
150
100
50
0
115
108
78
100
572
84
Nethole
Mantis
Open Room
Clutter
Platform
Field Hunting
b)
Proportion of Sound Groups
1
0.75
0.50
0.25
0
No of calls within a sound group
n > 3
n = 3
n = 2
c)
S.D.
S.E.
*
0.0004
0.0004
< 0.0001
< 0.0001
< 0.0001
Porpotion of Calls in Sonar Sound Groups
0.6
0.5
0.4
0.3
0.2
0.1
0
Platform (SM/CM)

Figure 2.6. Sound group parameters across conditions. a) Mean pulse interval time for sound groups in each experimental condition. Standard error in green, standard deviation in blue. The mean P.I. for bats hunting in the field is significantly greater than all other experiments. Refer to Table 2.3 for a pairwise comparison of the mean sonar sound group PI between conditions. **b)** Proportion of 2, 3, or 3+ call sound groups produced in each experimental condition. **c)** Proportion of sounds produced by the bats in sonar sound groups as compared to the total number of sounds produced under different behavioral conditions. Standard error in green, standard deviation in blue.

	Clutter	Net Hole	Mantis capture	Open space	Platform	Field - foraging
N=2	77.5	82.5	83.9	72.9	89.5	78.7
N=3	20	16.4	16.1	22	10.5	12.8
N>=4	2.5	1.1	0	5.1	0	8.5
Sample size (trials)	10	10	10	8	91	10

Table 2-2. Number of sounds, 2, 3 or more than 3, calls contained in sound groups for each experimental condition. Values in percentages. For example, 89.5% of sound groups for the platform experiment were sound groups with 2 calls (doublets).

	Field Hunting	Platform	Open Room	Mantis	Net Hole
Clutter	$< 10^{-10}$	< 0.00005	0.58	0.07	< 0.001
Net Hole	$< 10^{-10}$	< 0.00005	< 0.001	0.33	
Mantis	$< 10^{-10}$	< 0.00005	0.2		
Open Room	$< 10^{-10}$	< 0.00005			
Platform	$< 10^{-10}$				
Field Hunting					

Table 2-3. p-values for pairwise, two-tailed T-tests performed on the sonar sound group PI data reported in Figure. 2.6a. A Bonferroni correction was performed to account for multiple comparisons, resulting in a p-value threshold of 0.0033.

2.4 Discussion

By comparing the echolocating bat's temporal control of sonar vocalizations in both field and laboratory settings, it is evident that bats increase the production of sonar sound groups when faced with challenging tasks, e.g. tracking and capturing a target with an unpredictable trajectory or taking prey in the presence of clutter. We found that when bats are foraging in the field, they produce sonar sound group during the approach stages of insect capture, well before the terminal buzz, presumably because they require higher spatio-temporal localization accuracy to position an insect with a potentially erratic flight path. In contrast, when the bats are commuting from a roost to a foraging site, almost no sonar sound groups were recorded. These results parallel those found in the lab. When the bat is flying in an open flight room, comparatively few sonar sound groups are produced; but when the bat is catching tethered insects in the presence of acoustic clutter, there is an increase in the production of sonar sound groups. Furthermore, in the net hole experiment, where the bat had to shift its attention between an opening in the net and a more distant tethered insect, there was a large increase in the production of sonar sound groups. Lastly, we found that when the bat is tracking erratically moving prey items, either from a resting position on a platform or catching a flying insect on the wing, the prevalence of sonar sound groups increased significantly. Taken together, these results provide further evidence that bats actively produce sonar sound groups when faced with challenging spatial tasks.

It has been well documented that bats actively adjust a number of call parameters (sonar beam direction, frequency, intensity, duration and interval) as they perform echolocation tasks in diverse settings (Schnitzler and Kalko, 2001; Ghose and Moss, 2003; Aytekin et al., 2010; Moss

et al., 2006; Chiu et al., 2009; Mantani et al., 2012; Brinkløv et al., 2010; Jakobsen et al., 2013; Ratcliffe et al., 2013; Surlykke et al., 2009b; Surlykke and Kalko, 2008). The overarching goal of the current report is to re-examine the hypothesis that temporal patterning of sonar vocalizations is central to the bat's success at navigating and intercepting prey under complex laboratory and field conditions and to develop insight in to the perceptual consequences for the bat's production of sonar sound groups. In the sections below we attempt to shed light on some of the basic questions regarding sonar sound groups: 1) Do sonar sound groups have behavioral significance? 2) Under what circumstances do bats produce sound groups? 3) How does the bat adapt its sonar behavior to different environmental or clutter boundaries? 4) How might sonar sound groups perceptually sharpen spatio-temporal localization in bats? The answers to these questions will help us to advance our understanding of temporal processing in spatial perception by sonar in bats.

2.4.1 Do bats actively produce sound groups to enhance information carried by echo returns?

One of the first and very important questions one must ask when examining the temporal patterning of sonar signals is whether call clustering has functional significance for the animal. In this context, we emphasize that the definition of sonar sound groups is arbitrary and defined by the researcher (see Moss et al., 2006), and should be updated as we learn more about sonar behavior, to capture information that has behavioral relevance. Relevant to this point, we note that the average PI of sound groups in the field are much longer (115 ms) than in any condition

in the lab (25-37 ms), which suggests that the environmental conditions directly influence the intervals of sonar sound groups used for spatial perception.

The data we have presented here provides evidence that bats actively produce sonar sound groups under task conditions that require spatio-temporal accuracy in tracking and figure ground segregation. Figure. 2.4b shows that in the field when bats emerge from their roosts and are commuting to another site, they produce very few sonar sound groups. Feeding buzzes were never observed in this situation, indicating that the bats were not actively engaged in searching or tracking prey as they emerged from their roosts, and we infer that spatial localization requirements were low. In contrast, actively foraging bats produce a significantly greater number of sonar sound groups as they engage in goal-oriented tasks.

One way to test the functional importance of a behavior is to modify certain environmental parameters and then observe the animal's responses. The bat's echolocation behavior in the platform target tracking experiment reported here serves to illustrate how the bat actively produces sonar sound groups when it encounters uncertainty in the trajectory of the target (see Figure. 2.5). The complex target trajectories (CM trials) were designed to have multiple back and forth motion (Figure. 2.3a – red and black motion trajectories). A bat introduced to CM trials for the first time would experience uncertainty in the target's spatio-temporal position compared to the simple motion target trajectory on which the bat was initially trained. When the bat tracked the target moving with the CM trajectory it increased the number of sound groups produced per unit time (seconds) (Figure. 2.5) as compared to when the bat tracked the target with repeated SM trajectories. This experiment therefore provides direct evidence that changing the complexity and uncertainty of the moving target changes the bat's

echolocation behavior, indicating that temporal patterning of sonar vocalization is a strategy employed by the big brown bat to improve its spatio-temporal resolution of an uncertain target's position.

2.4.2 De-coupling sonar sound groups from wing beat strokes.

The production of sonar calls can be energetically expensive and hence coupling sonar calls with the upstroke of the wing beat cycle, and therefore coinciding with exhalation (Suthers et al., 1972) can help reduce the energy cost of sonar vocalizations (Speakman et al., 1989; Speakman and Racey, 1991). A previous study by Moss et al., 2006 examined the relation between sonar call production and wing beat. The results indicate that for sonar vocalizations of freely flying bats in the laboratory, calls with pulse intervals larger than 70 milliseconds were coupled to the upstroke of the wingbeat, but for PIs shorter than 70 ms, call timing occurred across different phases of the wingbeat cycle (see Moss et al., 2006, for more details). In this earlier study, however, analysis included only measurements of the peak and trough of the bat's wing beat cycle. Because the bat's wing beat can show asymmetries in the up/down stroke excursion, it is important to look more closely at the relation between sonar sound group production and wing beat.

Koblitz et al., 2010 examined emission times of sonar sound groups and their coupling with different phases of wing beat in the big brown bat. Their results indicate that the emission of sonar sound groups has a tri-modal distribution. The first call of the sound group occurs at the end of the down stroke, the center of the sound group occurs when the wings are horizontal and the last call of the sound group occurs at the end of the upstroke. In this study the bats were trained to fly across a room without any obstacles or acoustic clutter. In future research, it would

be interesting to analyze the relation between the sonar sound group emission patterns and wing beat when a bat is performing complex flight maneuvers.

In the experiment reported here in which bats tracked a moving target from a stationary position on a platform, sonar sound groups were prominent (Figure. 2.5). Obviously, wing beat is completely absent in bats echolocating from a platform; however, bats would be expected to coordinate their sonar call production with respiration to optimize on energy consumption. We have not measured the respiration of bats while they perform the tracking task on the platform, and this could be investigated in future experiments.

2.4.3 Spatially-guided behavior

The data presented in this report suggest that echolocating bats increase sonar sound group production in the context of spatially challenging behaviors. When a bat is flying in an open room in the laboratory, sonar sound group production is relatively low. When the bat is navigating through obstacles, however, sonar sound groups are produced as the bat inspects each opening in a net through which it can fly to gain access to a food reward. This comparison suggests that sound group production is not used solely in the context of hunting, but is also employed when the bat is negotiating obstacles. These laboratory results are consistent with data from field recordings. Furthermore, bats hunting in the field sometimes, but not always, produce sound groups just prior to the buzz phase, indicating that this call pattern may be important for target capture. By contrast, bats commuting in a familiar environment produce very few sound groups. This comparison offers another demonstration of how a bat increases sound group production during goal-directed behaviors, but not during routine commuting flight. Furthermore, considering that sonar sound group production increases under challenging

conditions (i.e. spatial navigation around obstacles, insect capture), we provide evidence that sonar sound groups are used actively by bats when they attempt to gather more detailed information about the location of objects in the environment. This idea is supported by the finding that bats used sonar sound groups most frequently when it tracked the complex motion of the target from a resting position on a platform. The complex motion tracking condition may capture some of the target uncertainty a bat encounters in the field as it pursues insects engaged in evasive maneuvers.

2.4.4 Temporal control over sonar calls varies with task and environmental complexity

In this article we have presented evidence of temporal clustering of sonar calls when bats are engaged in a variety of tasks, both in the lab and the field, when they are flying freely or tracking an unpredictably moving target from a stationary position on the platform. An important question that arises is whether bats vary the properties of sonar sound groups across different environmental conditions and task complexities. In this section we compare and further analyze the data presented in Figure. 2.6 to show that bats indeed modify sonar sound group parameters with environment and task conditions. Most noteworthy are the differences in the prevalence of sound group production, the number of sounds in a group, and the pulse interval of calls in a group, all of which appear to be related to the uncertainty of the target trajectory, figure-ground segregation, and the environment in which the bat echolocates.

2.4.4.1 Prevalence of sonar sound groups changes according to uncertainty of target trajectory.

Sonar call groups were produced by bats as they foraged in the field and the laboratory. Our interpretation of this result is that the bat increases sound group production to more accurately resolve the location of the insect from the clutter. This interpretation is further corroborated by the laboratory studies that placed different demands on the bat's spatial localization by sonar. Specifically, when a bat tracked a moving prey item from a resting position on a platform, its sonar sound group production increased when the target trajectory was unpredictable. When the insect moved towards the bat with a simple and already familiar velocity path, the bat produced very few sonar sound groups. In contrast, when the bat tracked an insect that moved back and forth with changing velocities and directions, sonar sound group production increased significantly (see Figure. 2.5a). This result suggests that the echolocating bat actively controls the timing of its calls to track an erratically moving target.

2.4.4.2 Sonar sound groups help bats separate figure and ground.

Eptesicus fuscus has been observed hunting near vegetation (Simmons et al., 2001). To be successful foragers, bats hunting in cluttered environments must be able to discriminate between acoustic clutter resulting from vegetation and their desired targets. Our results (Figure. 2.4) indicate that in the experiments when bats had to capture tethered mealworms placed near an artificial plant or in the experiment in which bats were required to localize an insect behind an opening in a mist net, the animals increased the rate of sonar sound group production.

2.4.4.3 Bats scale the PI of sonar sound groups according to the boundaries of their immediate environment.

Modulating PI can be an effective strategy to avoid mixing of calls and echoes from distant clutter, which may represent the effective boundary of the bat's active space. A survey of field site B indicates that a bat following a stereotypical flight trajectory would on average be at a distance from the boundaries (thicket of trees) that is approximately four times the distance from boundaries (walls, ceiling and floor) in the laboratory. The average PI (Figure. 2.6a) of all the sonar sound group recordings from field site B is about 185 ms +/- 27.03. This scales well with the boundaries of the foraging site. In the laboratory study of the bat resting on the platform and tracking an erratically moving target, the distance of the bat from the far wall was 5 meters. To allow sufficient time for an entire echo stream to arrive from objects distributed along a range axis of 5 m, a bat would wait 30 ms before producing its next call in the sound group, and the average PI would be maintained above 30 ms (Figure. 2.6a). A comparison of the sound group PI's when the bat is stationary on the platform and tracking a moving target to the sound group PI's produced by the bat when it is flying under different conditions in the laboratory offers strong evidence that bats adjust the PI of their sound groups to the boundaries of their immediate environment (Figure. 2.6a and Table 2.3). A closer examination of the average distance of the bat from the boundaries in each of these experiments (platform compared to the laboratory flight experiments) reveals that in the prey tracking experiment, the bat on the platform is approximately 5 meters from the wall, while in the laboratory flight experiments, the bat typically flies through the middle of the room with an average distance of less than 3 meters from the nearest wall (see Figure. 2.2 for schematics of each experimental flight room). From the

laboratory to the field, the boundaries of the environment increased by a factor of 4, which is approximately the same factor by which the PI is scaled. Our data suggests that the bat tends to cluster its calls when it is actively tracking an object of interest, and the PI of the sound group is adjusted by the bat according to the environment in which it operates.

A recent study by Hiryu et al., 2010 showed that under extreme clutter conditions in which the bat reduced its PI to below that set by the environmental boundary (also referred to as the "outer window;" see Wilson and Moss, 2004), it employs a different strategy to disambiguate echo streams between two calls within a sonar sound group. In their study, the bat shifted frequencies of calls within a sonar call doublet to enable assignment between calls and cascades of echoes in a highly cluttered environment. In most settings, bats adjust the pulse interval of sonar sound groups to avoid overlap of echo streams. However, under extreme clutter conditions, bats shift frequencies of calls within sound groups to disambiguate echo streams (Hiryu et al. 2010). Here we see that when bats do not adjust call group PI to the environmental boundaries, they adopt additional vocal strategies to support spatial perception by sonar.

2.4.4.4 The number of calls per sonar sound group depends on the task and environment.

Another observation that may contribute to our understanding of the functional importance of sonar call timing to spatial resolution of the environment is the number of sounds contained in groups (doublets, triplets or higher order sonar sound groups) we observed under different conditions. The two extremes are the platform, where we rarely observe sonar sound groups with three or more calls, and the field where we frequently observe sonar sound groups with more than four or five (see Figure. 2.6b). When bats flew in the laboratory flight room, we typically observed sound groups with two, three or four. As we have a comparatively few trials

for the flight conditions, we do not have enough statistical power to test significance (Figure. 2.6b). However, we hypothesize that the bat adapts the number of sonar sounds per sonar sound groups according to its immediate environment and its challenges. Future experiments with a greater number of recordings should be able to elucidate this further.

Data from many different studies demonstrate that sonar sound group production occurs at times when spatio-temporal localization demands are high. Bats increase the prevalence of sonar sound groups when they are tracking erratically moving prey, when trying to resolve target from clutter, and when navigating complex scenes. For each of these behavioral situations, the bats produced sonar sound groups at times when increased spatial resolution was paramount for success.

Here we consider why sonar sound group production may help the bat to localize and track an object. When a bat is tracking a moving insect, computing the distance and velocity of the insect involves computations of the insect's position with respect to the bat over longer temporal windows. The production of sonar call doublets may serve two purposes: 1), increase the echo return rate over a restricted time window, which may serve to increase the reliability of echo reception by the sonar receiver. 2) By keeping the pulse interval stable, as in the case of sonar sound groups, the bat receives echo updates with a regular periodicity, which may allow the bat to more easily assign different echo streams to the original sonar pulses. The same idea applies to a bat navigating a complex maze or when the environment is full of acoustic clutter and many objects are reflecting echoes. In all of these contexts, sampling information from the environment is simplified by stable temporal timing of sensory updates.

In conclusion, this study of the echolocating big brown bat in a number of different tasks and acoustic situations of varying in complexity, demonstrates that that this animal employs temporal control of its sonar calls to effectively probe its sensory world. In more simple acoustic environments, the bat monotonically tends to decrease pulse interval with respect to target distance. Conversely, when the bat is placed in a more dynamic and complex environment, it temporally organizes its sonar vocalizations into sound groups, which are structured to provide periodic updates about the sensory world. The increase in sonar sound group production is not limited to instances of hunting, since bats navigating obstacles also produce sound groups, which may aid in building a detailed representation of the environment. The results of this study motivate further experiments and models examining how the timing of sensory signals may shape perception.

All fixed set patterns are incapable of adaptability or pliability. The truth is outside of all fixed patterns.

— Bruce Lee

3

Adaptive sonar call timing supports target tracking in echolocating bats

3.1 INTRODUCTION

Echolocating bats navigate and capture prey by producing ultrasonic signals and listening to echo returns from objects in the environment (Griffin, 1958). Fundamental to echolocation is the bat's dynamic modification of sonar call parameters, such as pulse duration (PD), pulse intensity, pulse interval (PI) and spectral content in response to information carried by returning echoes (Griffin et al., 1960; Moss and Surlykke, 2010; Simmons, 1979). In their natural habitats, bats often pursue evasive and erratically moving insects in cluttered conditions, further complicating the task of localizing and intercepting prey (Kalko and Schnitzler, 1989; Schnitzler and Kalko, 2001). We hypothesize that the bat's adaptive adjustments in sonar signal design allow it to parse echoes from closely spaced objects and integrate information across sonar sequences to build a three dimensional acoustic scene (Lewicki et al., 2014; Moss and Surlykke, 2010).

Bats use differences in the timing, intensity and spectrum of echoes at the two ears to localize the direction of sonar targets in azimuth and elevation (Lawrence and Simmons, 1982; Shimozawa et al., 1974; Wohlgemuth et al., 2016a), and the time delay between calls and echoes is used to localize objects in distance (Hartridge, 1945; Simmons, 1973). Insectivorous bats reduce the interval between sonar calls as the distance to prey decreases (Kalko and Schnitzler, 1989; Moss and Surlykke, 2001; Simmons et al., 1979), and embedded in foraging call sequences are sonar sound groups (SSGs), which are defined as clusters of echolocation signals at short pulse intervals, flanked by signals at longer intervals. The production of SSGs is an adaptive sonar behavior that has been reported in both laboratory and field studies of bat echolocation, in free-flying animals (Falk et al., 2015; Kothari et al., 2014; Moss and Surlykke, 2001; Moss et al., 2006; Petrites et al., 2009; Sändig et al., 2014; Surlykke and Moss, 2000; Wheeler et al., 2016) and those tracking moving prey from a stationary position (Aytekin et al., 2010; Kothari et al., 2014). Past studies have shown that bats temporally cluster echolocation calls to produce SSGs when they are engaged in complex tasks that require high spatio-temporal resolution. For example, in a laboratory study, Moss et al (2006) reported that big brown bats increased the production of SSGs when they captured insects in the vicinity of vegetation clutter, and similarly, Falk et al (2014) found that this species produced more SSGs as they foraged in an artificial forest, compared to an open room. Petrites et al. (2009) also reported that bats increased the production of SSGs when navigating in a highly cluttered environment. A related finding, reported by Sändig et al. (2014), showed that bats engaged in a wire-avoidance task increased the production of SSGs with increasing task difficulty. In a recent study, Wheeler et al., (2016) reported that big brown bats not only increased both the number of SSGs, but also the number

of sonar vocalizations contained in each SSG as they encountered greater clutter along their flight path. These observations have led to the hypothesis that the bat's production of SSGs serves to improve its spatio-temporal resolution of objects (targets or obstacles) in the environment.

In the natural environment, bats frequently intercept free-flying, erratically moving prey (Roeder, 1962; Roeder, 1967), a task which requires enhanced spatio-temporal sonar resolution. Erratic insect flight trajectories create uncertainty about prey location, and it has been shown that bats tracking free-flying insect prey produce SSGs (Ghose et al., 2009; Triblehorn et al., 2008), but past studies have not directly studied the bat's sonar behavior under conditions where target motion predictability is systematically manipulated.

To rigorously investigate whether SSGs are used by bats to localize erratically moving targets, we designed an experiment that engages an animal in a naturalistic insect-tracking task, while also permitting precise control over the relative bat-target position and systematic manipulation of the predictability in target trajectory over successive trials (Aytekin et al., 2010; Kothari et al., 2014; Mao et al., 2016; Wohlgemuth et al., 2016b). We hypothesize that bats increase the production of SSGs as the unpredictability of the target's motion increases.

3.2 MATERIALS AND METHODS

3.2.1 Experimental Setup and animal training

Four big brown bats (*Eptesicus fuscus*) were trained to rest on a platform and track a moving prey item (mealworm). The experimental setup is described in detail in Kothari et al., 2014 and is presented briefly here. A tethered insect food reward was suspended from a rectangular loop of

fishing line, and its motion was controlled using a rotary servo motor (Aerotech BMS60 brushless, slotless rotary servo motor attached to an Ensemble MP10 motor controller), interfaced with custom Matlab software (2012a) that controlled the velocity, acceleration, deceleration, and distance the target traveled (Figure 3.1a). Experiments were carried out under low-level, long wavelength illumination that precluded the bat's use of vision (Hope and Bhatnagar, 1979). This method engaged the bat in naturalistic sonar tracking behavior, and it also allowed the experimenter precise control and repeatability over the relative motion between the bat and target, which is not possible in free-flight experiments.

Bat sonar vocalizations were recorded using two Ultrasound Advice UM3 microphones (see Pulse microphone and Echo microphone in Figure 3.1a) and were digitized using a National Instruments (NI) A/D PCIe card interfaced with Matlab (2012a). The triggering of the Aerotech Servo motors and the start of the microphone recording were synchronized using a single TTL pulse generated via the Matlab-NI interface. Details regarding the initial training paradigm are also described in Kothari et al., 2014.

Briefly, individual bats were trained on single target motion tracking, wherein the target started at a distance of 2.5 meters, accelerated at a rate of 7 m/s^2, traveled a distance of 2 meters with constant velocity of 4 m/s, mimicking the approximate flight velocity of a bat during the approach phase of insect capture (Hayward and Davis, 1964), and then decelerated at a rate of 5 m/s^2. The displacement and velocity with respect to the stationary bat are shown in Figure 3.1b (blue trace). We refer to this motion as Simple Motion (SM). When data collection began, bats encountered new target motion trajectories, detailed below.

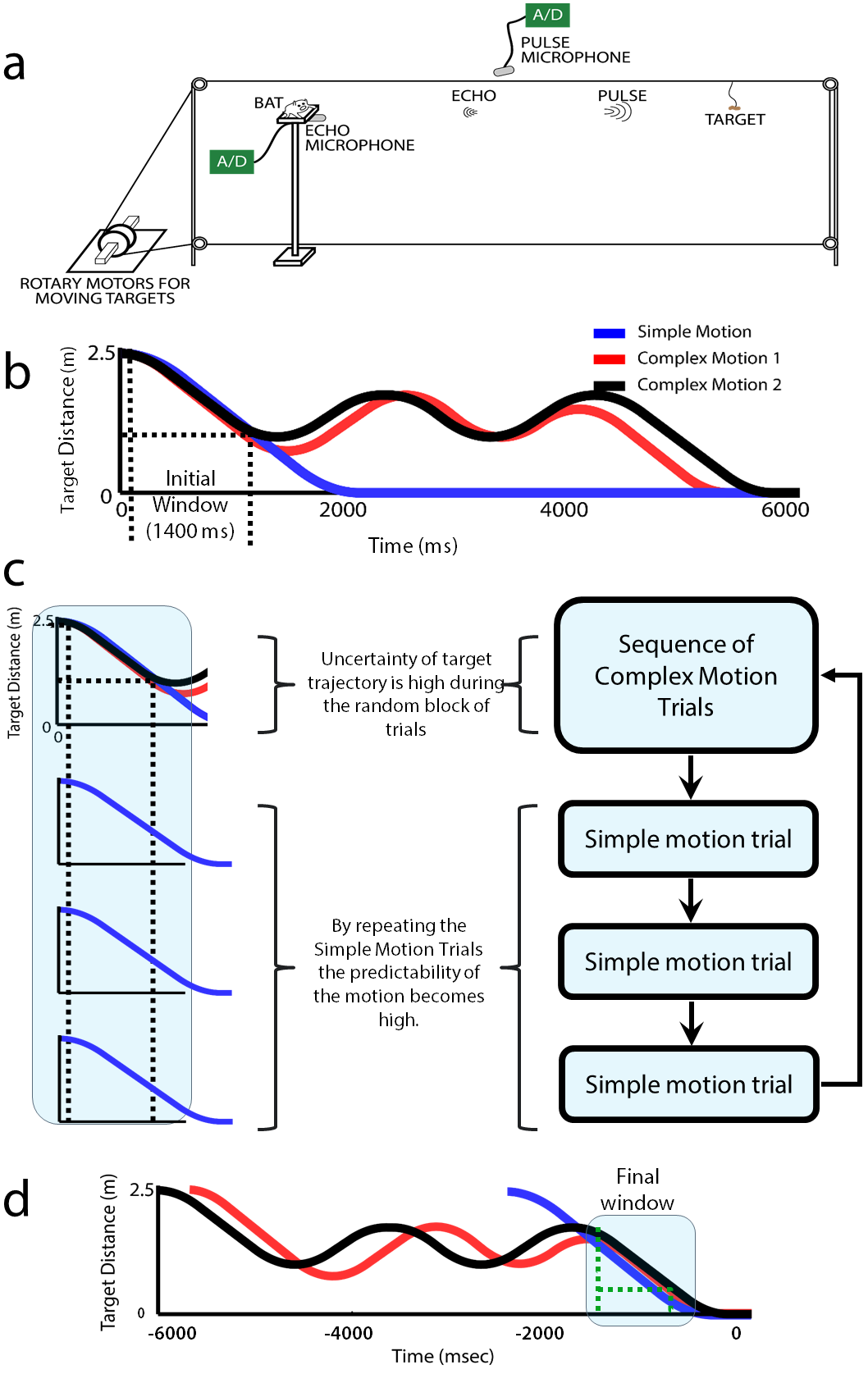
a
A/D
PULSE
MICROPHONE
BAT
ECHO
PULSE
TARGET
ECHO
MICROPHONE
A/D
ROTARY MOTORS FOR
MOVING TARGETS
b
Simple Motion
Complex Motion 1
Complex Motion 2
Target Distance (m)
2.5
0
Initial
Window
(1400 ms)
0
2000
4000
6000
Time (ms)
c
Target Distance (m)
2.5
0
0
Uncertainty of target
trajectory is high during
the random block of
trials
Sequence of
Complex Motion
Trials
Simple motion trial
Simple motion trial
Simple motion trial
By repeating the
Simple Motion Trials
the predictability of
the motion becomes
high.
d
Target Distance (m)
2.5
0
Final
window
-6000
-4000
-2000
0
Time (msec)

Figure 3-1. Experimental design. **a.** Bats are trained to rest on a platform and track an approaching target (shown at the far end) attached to a string. The string is connected with a motor via a pulley system. Microphones connected to A/D converters (shown in green) are used to collect sonar calls of the bat. **b.** The displacement of the target, with the x-axis denoting the time of each trial where zero indicating the start of the trial. The y-axis is the distance of the target from the bat, so, when the target starts it is at 2.5 meters from the bat. The SM, CM1 and CM2 target motions are shown in blue, red and black respectively. Each target motion has been slightly displaced to clearly display the overlap of the motions in the initial phase. **c.** Is a flowchart showing the progression of trials within each recording session. Following a presentation of a sequence of complex motions (CM1 or CM2) followed by a sequence of 3 simple motions (SM). **d.** To demonstrate that the final approach motions of the targets for each of the SM, CM1 and CM2 are identical, the motion sequences have been redrawn according to when the target reaches the bat. Here, x-axis is the trial time with zero indicating the time of arrival of the target at the bat. The y-axis is the target distance from the bat. Here again, the target motions have been displaced to clearly indicate the overlap of the final approach phase (indicated by the two green lines) of the target.

3.2.2 Experimental Design

Once the bat reliably tracked the tethered insect following the simple motion (SM) trajectory, two novel types of target motion trajectories were introduced to the bat on the day of the experiment. We refer to these target motion trajectories as Complex Motion 1 & 2 (CM1 and CM2, respectively). In the novel complex motion trajectories the target first moved towards the bat, after which it oscillated back and forth, before finally reaching the bat. The target displacement and velocities relative to the stationary bat are shown in Figure 3.1b (CM1 – red, CM2 – black). The simple and two complex motion trajectories were designed with the following criteria:

1) Initial target motion phase (Initial time window). The initial phase of target motion was comparable across motion trajectory conditions. This phase is marked by the two dashed black lines in Figure 3.1b. After the initial phase, the target motion paths diverged and followed pre-determined trajectories, with the target approaching the bats directly in the SM trials, while oscillating back and forth before arriving at the bat in the CM trials. By presenting the same initial trajectories across target motion conditions, the bat's echolocation behavior can be directly compared at the start of each trial for SM and CM trajectories.

In order to introduce target motion uncertainty, a sequence of CM trajectories were presented to the bat. This is indicated in Figure 3.1c as the first block in the trial flowchart. After the presentation of randomly presented CM trials, a sequence of SM trials was presented to the bat, as shown in Figure 3.1c. It should be noted that the SM was a target trajectory already presented repeatedly to the bat during the training phase, so, presenting a sequence of SM trials provides increased predictability of the target motion. This experimental paradigm allowed us to

record and analyze the behavioral changes in the bat's echolocation behavior while tracking a target with an unpredictable trajectory (repeated complex motion trials) and compare it with the behavior exhibited when it tracked a repeated and predictable target motions (serial presentation of SMs).

2) Final target motion phase (Final time window). Figure 3.1d shows the motion trajectories aligned with respect to when the target reached the bat. As can be seen from Figure 3.1d, the final motion phase for each of the target trajectories was also designed to be comparable across trials. This *target arrival window* is marked by the two dashed green lines in Figure 3.1d. By examining the target arrival window, we could analyze how the bat's sonar behavior changed as its familiarity with the complex trajectories (CM1 and CM2) increased over a period of days.

3.2.3 Analysis techniques.

The digitized sonar vocalizations were analyzed and identified using custom written Matlab (2012a) routines. Once the sonar calls were identified using the automatic routine, they were manually verified and corrected for errors. Manual verification included checking call spectrograms to identify instances where echoes overlapping with calls were erroneously identified as individual calls by the automated routine. Only call onsets were used for the analysis. Call parameters such as pulse interval (PI), pulse duration (PD) and pulse onset (PO) were computed from the identified and corrected calls. Measures of start and end call frequency, sweep rate and bandwidth were not computed, as the frequency response of microphones was not calibrated.

Sonar sound groups (SSGs) were identified according to the following criteria: Clusters of vocalizations flanked by calls with larger PI at the ends (a minimum of 1.15 times larger PI). When

three or more calls occurred within a SSG, a PI stability criterion was also applied: PI stability with 5% tolerance with respect to the mean PI of the SSG (Kothari et al., 2014; Moss et al., 2006). Figure 3.2 shows an example trial block (CM-SM1-SM2-SM3), with dashed black lines highlighting the initial time window (identical motion phase), the trace in blue is the raw audio trace of the bats vocalizations, and SSGs are identified with red brackets.

3.3 RESULTS

Four big brown bats (*Eptesicus fuscus*) tracked from a stationary position an insect prey reward, which was tethered from a fishing line and delivered via a pulley system to the bat, as shown in Figure 3.1a. Once the bats reliably tracked the food reward in the Simple Motion (SM) target trajectory condition, they were introduced to two novel Complex Motion (CM1 and CM2) target trajectories on the day of the experiment. Data was collected from Bats A and C, for 5 days, and from Bats B and D, for 6 days.

3.3.1 Bats increased production of sonar sound groups while tracking targets with unpredictable trajectories, but produced the same average number of calls:

Figure 3.2 shows an example trial block when a bat was presented with a sequence of CM1-SM1-SM2-SM3-CM1-CM2 target trajectories. Figure 3.2, top panel, shows the target motion trajectories. The distance of the target to the bat is plotted on the y-axis, and the trial time on the x-axis. The panels below show the timing of echolocation calls in a sequence of trials presented to the bat (sequentially from top to bottom). In Figure 3.2, the raw audio trace of the bat's sonar vocalizations

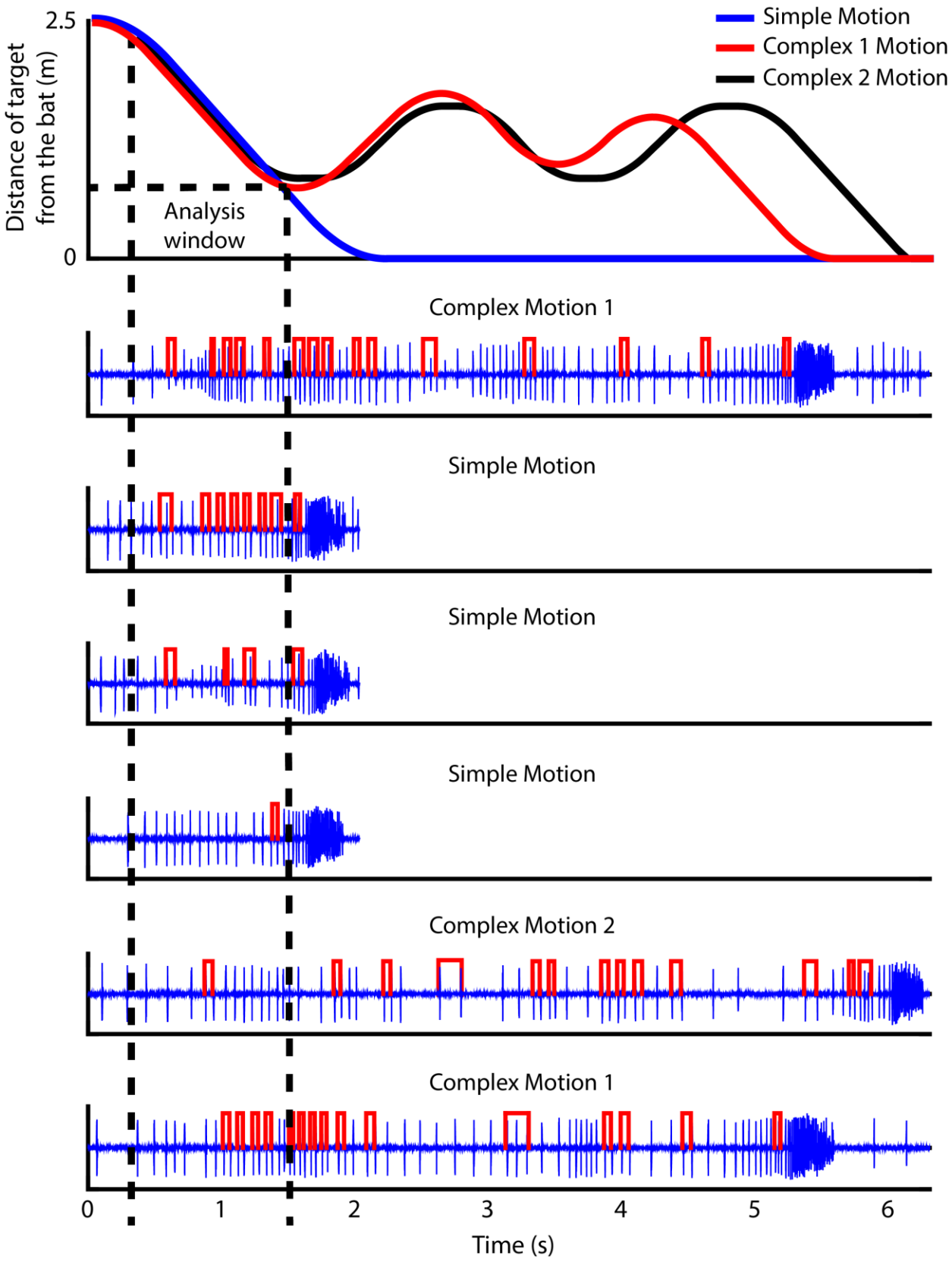
Simple Motion
Complex 1 Motion
Complex 2 Motion
Distance of target from the bat (m)
2.5
0
Analysis window
Complex Motion 1
Simple Motion
Simple Motion
Simple Motion
Complex Motion 2
Complex Motion 1
0
1
2
3
4
5
6
Time (s)

Figure 3-2 Example trial sequence. The top panel shows the target displacement for each motion (SM, CM1 and CM2) presented to the bat. X-axis is the time and y-axis is the distance of the target from the bat. The black dashed lines, extending throughout the figure indicate the initial window of analysis where the target motions for each motion trajectory are nearly identical. The panels below show an example trial sequence. The raw audio recording at the microphone is shown in blue, with SSGs indicated in red. The trial sequence in this example is CM1, SM, SM, SM, CM2 and CM1. It can be seen that as the predictability in target motion decreases (across the repeated SM motions), bats reduce the production of SSGs (red) within the initial window. The number of SSGs in the following CM2 trial are also reduced after which, in the following CM1 motion, the bat produces more SSGs due to increased target motion unpredictability.

is shown in blue and SSGs are bracketed in red. The analysis time window is indicated by the two dashed black lines, which extend vertically across all panels in the figure. Figure 3.2 illustrates a trend showing that the bat reduced the production of SSGs (within the initial target motion phase, indicated by two dashed black lines, see Materials and Methods) as the SM trajectory was presented consecutively to the bat. The data show that as the SM trajectory was repeated, and the predictability of the target's trajectory over trials increases, the bat reduced the number of SSGs (shown in red). Further, the bat showed reduced SSGs in the analysis window of the initial motion phase of the CM2 trial that followed a sequence of three SM trials, followed by an increase in SSGs on the subsequent CM1 trial.

To quantify changes in the production of SSGs across the CM-SM1-SM2-SM3 sequence, Figure 3.3, shows a comparison of the mean number of SSGs produced across all of the CM-SM1-SM2-SM3 sequences recorded. Mean and s.e.m. values for all bats are summarized in Table 1. A 1-way repeated measures ANOVA (MATLAB procedure *anova1*) compared number of SSGs, within the initial analysis window (indicated by the dashed black lines in Figure 3.2), across all CM-SM1-SM2-SM3 sequences. All four bats showed a main effect of trajectory condition on the number of SSGs. As the uncertainty in target position decreased over sequential presentation of SM trials, the mean number of SSGs decreased ($p<10^{-4}$), indicating that bats reduce the number of SSGs as the predictability in target trajectory increased from SM1 to SM3. Post-hoc comparisons were carried out between CM-SM1, CM-SM3 and SM1-SM3 using the Holm-Bonferroni method, confirming that the bats significantly reduced the number of SSGs between CM-SM3 and SM1-SM3 ($p<0.001$ for Bats A, B and C and $p<0.05$ for Bat D).

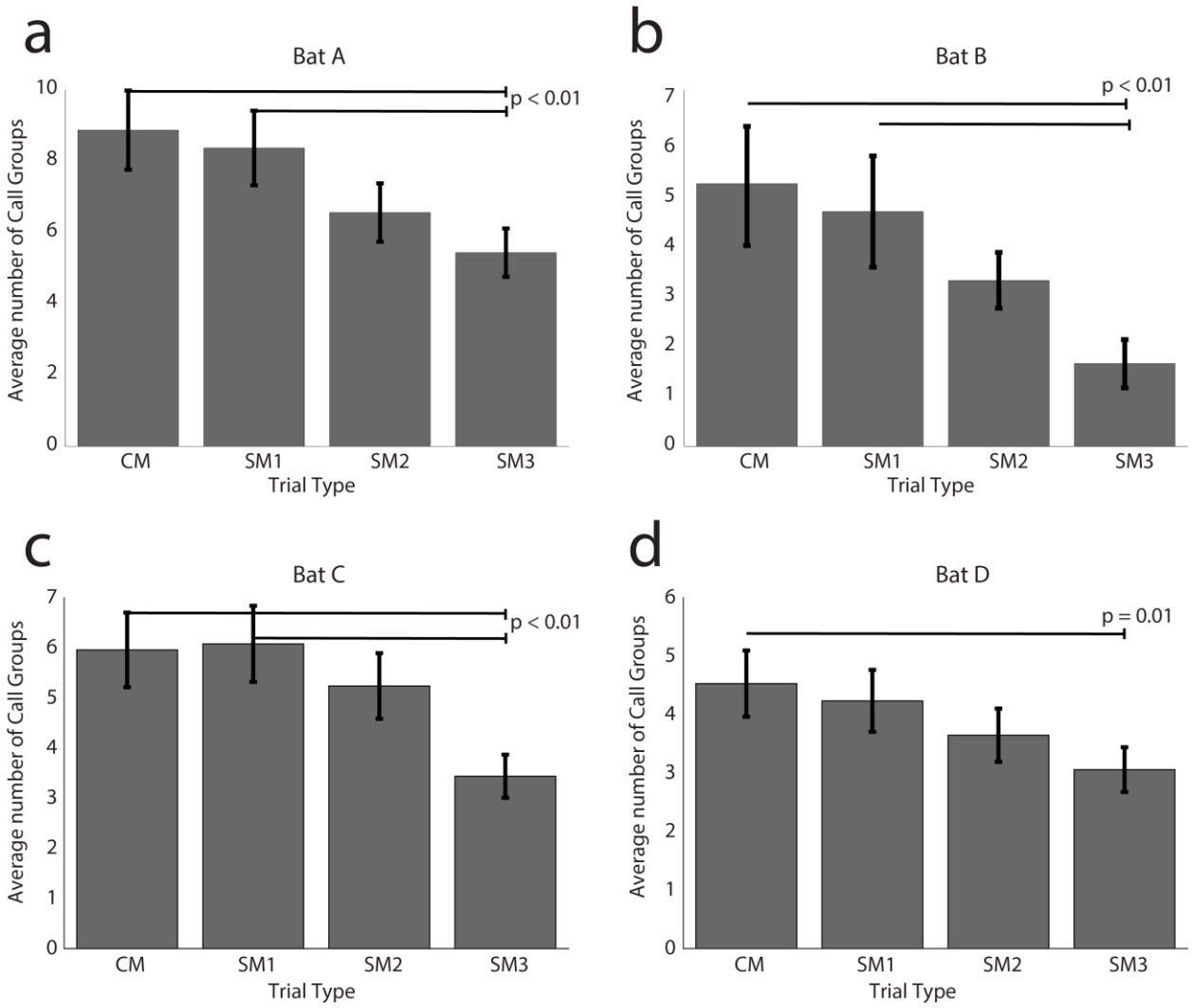

Figure 3-3 Bats reduce the production of SSGs as target motion becomes more predictable. **a, b, c** and **d** show the average number of SSGs produced by all four bats when presented with a unpredictable complex target motion (CM1 or CM2) followed by more predictable simple target motion (SM1, SM2 and SM3). The error bars indicate s.e.m.

Further, we investigated whether the bats produced more echolocation calls during the period of uncertainty in target motion (indicated by the dashed black lines in Figure 3.2). Figure 3.4a, b, c and d show the average (error bars are s.e.m.) number of sonar calls produced by all 4 bats in the sequentially presented CM-SM1-SM2-SM3 trials during the 'initial window' of the

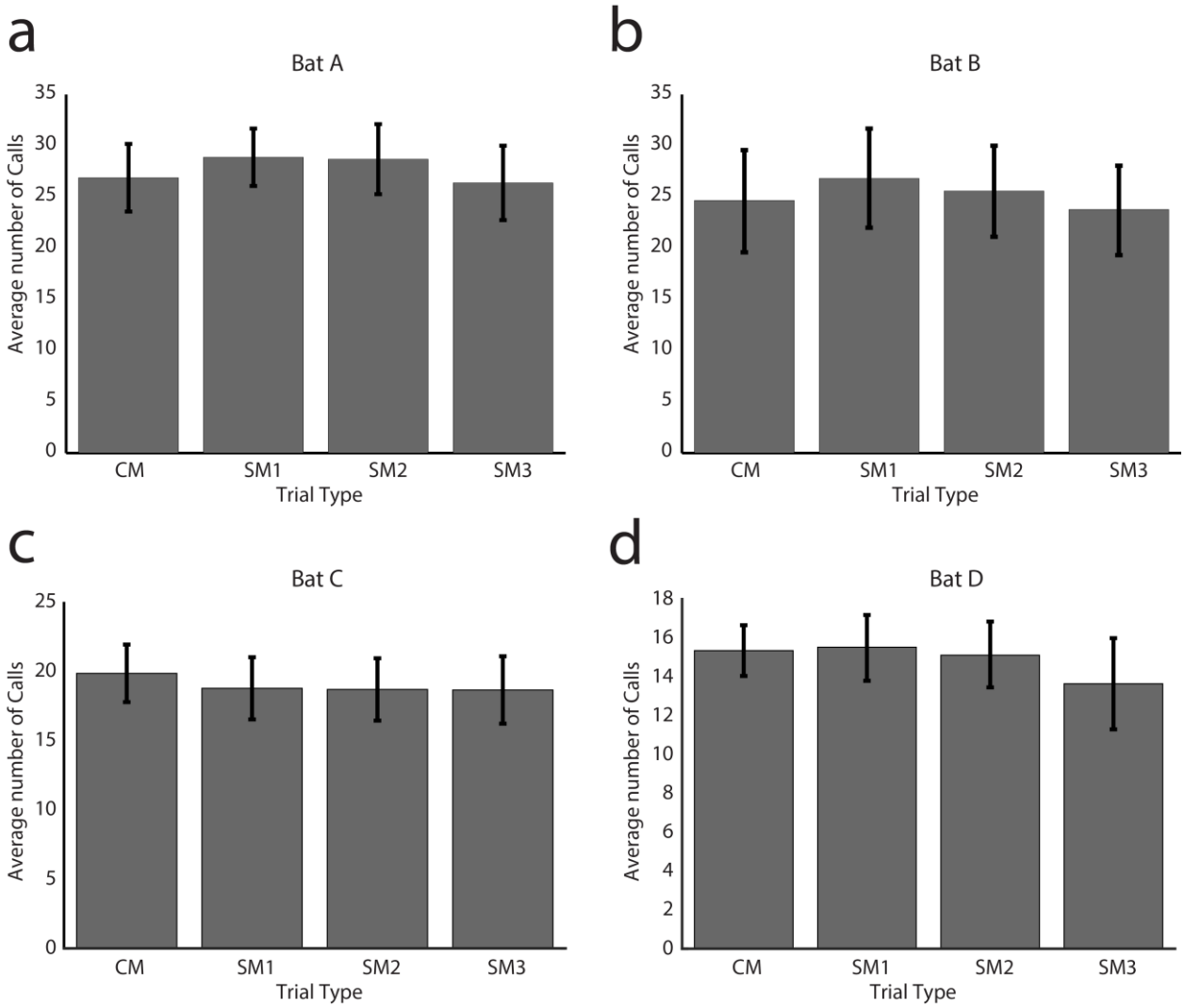

Figure 3-4 Bats produce the same number of calls in the initial window, irrespective of target motion unpredictability. **a, b, c** and **d** show the average number of sonar calls produced by all four bats within the *initial window* (see Figure 3.2 – black lines) when presented with unpredictable complex target motion (CM1 or CM2) followed by more predictable simple target motion (SM1, SM2 and SM3). The error bars indicate s.e.m.

target trajectory (indicated by dashed black lines, Figure 3.2). The average number of sonar calls produced during the initial time window **was not** statistically different across the sequentially presented trials (1-way repeated measures ANOVA, $p>0.1$). Thus, bats increase the production

of SSGs when target trajectory is unpredictable, but they do not change the average number of sonar calls produced.

Table 3-1 Reduction in sonar sound groups as predictability in target trajectory increases sequentially from CM-SM1-SM2-SM3.

	Mean number of sonar sound groups produced ± SEM			
	CM	**SM1**	**SM2**	**SM3**
Bat A	8.93±1.32	8.41±1.38	6.39±0.94	5.51±0.75
Bat B	5.44±1.15	4.78±1.03	2.78±0.97	1.778±0.59
Bat C	5.97±0.87	6.07±0.91	5.24±0.71	3.32±0.41
Bat D	4.59±0.68	4.27±0.72	3.61±0.48	3.02±0.39

3.3.2 As bats experienced repeated target motions, they reduced production of sonar sound groups.

Figure 3.1d shows the distance of the target from the bat on the y-axis, and the SM and CM target trajectories are aligned in the final approach of the food reward, with time 0 ms corresponding to when the target reached the bat. Figure 3.1d illustrates that the end trajectories of the complex motions (CM1 and CM2) are comparable to the SM, and this time window is marked by two dashed green vertical lines. We refer to this as the ***final time window***. In Figure 3.5 the SSG data analysis was restricted to the final time window, when the target trajectories of the CM motions were identical. All bats showed a reduction in the production of SSGs across days

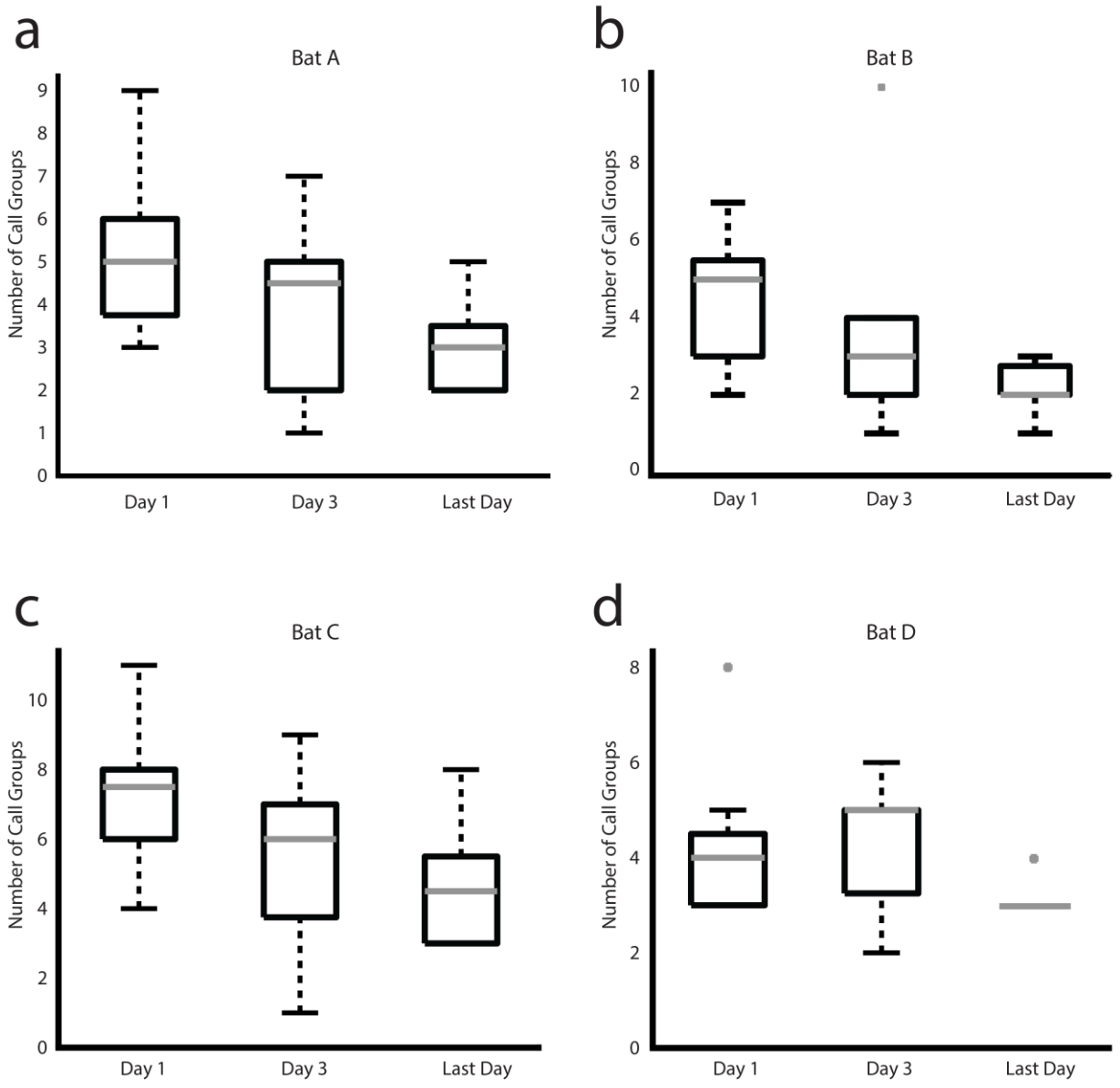

Figure 3-5 Bats produce less SSGs as familiarity with novel target trajectories increases. **a, b, c** and **d** show box plots of the number of SSGs produced by all four bats in the *final window* (see Figure 3.1d, indicated by two green lines) as their familiarity with the novel complex motions (CM1 and CM2) increases over a period of days.

(Figure 3.5), as the familiarity with the complex target trajectories increased. Figure 3.5 shows box plots of the sonar sound groups produced by the bat in the final time window for the CM1 and CM2 target trajectories, for the first day (when the two complex target trajectories were first introduced to the bats), an intermediate day (Day 3) and the last day of data collection (For bats A and C, last day was day 5 while for Bats B and D, last day was day 6).

Further, we investigated whether the bats produced fewer sonar calls during the 'final window' (Figure 3.1d, green lines) as the bats experienced the complex target motions, over a period of days. We calculated the total number of calls produced by bats during the final window and compared these over a period of days (Day 1, Day 3 and Last Day) and found **no significant** change in the total number of calls (1-way repeated measures ANOVA, $p>0.2$) although the bats reduce the production of SSGs over days.

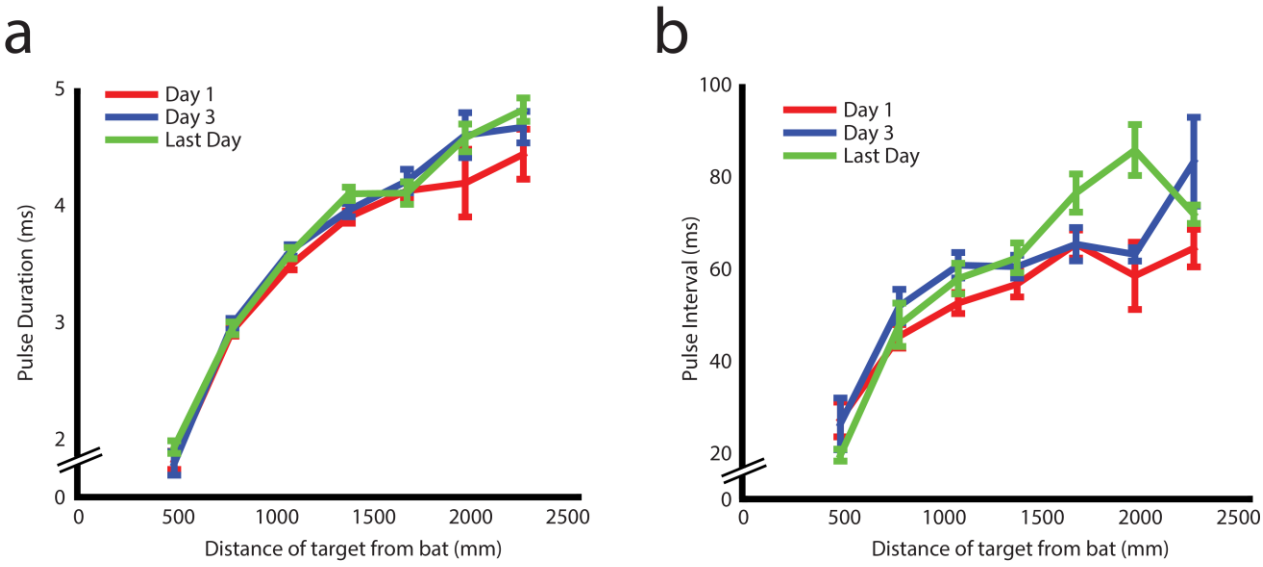

Figure 3-6 Comparison of PD and PI of sonar sound groups as bats learned a novel target trajectory. **a** and **b** show a comparison of pulse duration (PD) and pulse interval (PI) over a period days as their familiarity with the novel complex target motions (CM1 and CM2) increases.

3.3.3 Comparison of Pulse Duration and Interval of sonar sound groups across test days.

To investigate whether bats adapted pulse duration (PD) and/or pulse interval (PI) of calls over repeated presentations of complex target trajectories, we compared the PD and PI of calls within SSGs for complex motion (CM1 and CM2) trajectories across days. Figure 3.5a and 5b shows the mean and s.e.m. changes in PD and PI, respectively, with respect to target distance and across days (Day1, Day 3 and Last Day are plotted in red, blue and green respectively). Day 1 was the first day when the bats were introduced to complex motion and Last Day was the final day of data collection. For bats A and C, the last day was day 5 while for Bats B and D, the last day was day 6. To investigate if bats adapted the PD and PI of SSGs across days and target distance we performed a 2-way repeated measure ANOVA. 'Days' and 'target distance' were included as the two main variables of the ANOVA. There was a significant change in both PD and PI for target distance ($p < 0.001$) but no significant change was observed in these call parameters (PD and PI) across days ($p > 0.2$). No significant interaction effect was observed ($p > 0.4$).

3.4 DISCUSSION

When insectivorous bats pursue erratically moving prey, they must precisely track changing target position by processing information carried by sonar signals. Precise target localization is crucial for the bat's planning of subsequent motor behaviors, such as timing the production of sonar calls and the trajectory of flight. Bats dynamically adapt sonar call parameters to extract task relevant echo information from the environment and the temporal patterning of sonar calls

(sonar sound groups - SSGs) is an important component of the bat's adaptive vocal behavior. The production of SSGs has been recorded in echolocating bats in the field and in the laboratory (Aytekin et al., 2010; Falk et al., 2014; Hiryu et al., 2010; Kothari et al., 2014; Moss and Surlykke, 2001; Moss and Surlykke, 2010; Moss et al., 2006; Petrites et al., 2009; Sändig et al., 2014; Surlykke et al., 2009; Wheeler et al., 2016). Bats often track erratically moving prey, and in this study we show that bats increase the production of SSGs when target motion is unpredictable. Our results are consistent with the hypothesis that task demands for spatial localization accuracy evoke temporal clustering of echolocation calls.

3.4.1 Temporal patterning of sonar sounds may enhance localization of unpredictably moving targets.

Many insects have evolved erratic flight trajectories to evade predation by echolocating bats. Insects that hear ultrasound, for instance, exhibit evasive flight maneuvers in response to echolocation signals (Roeder, 1962; Roeder, 1967; Triblehorn and Yager, 2005). In the experiments presented here, we specifically manipulated the predictability of target trajectories presented to the bat. Our results show that bats significantly increase the production of SSGs when the predictability of target motion decreases (Figure 3.3), consistent with the hypothesis that SSGs are used by echolocating bats to increase spatio-temporal resolution when demands for sonar localization accuracy are high (Kothari et al., 2014; Moss et al., 2006; Petrites et al., 2009; Sändig et al., 2014). Further, it is important to state that the consecutive presentation of simple motion trials (SM1, 2 and 3, which have been repeatedly presented to the bat during training) might involve an anticipatory and predictive component of the bat's behavior. During

the presentation of SM1, 2 and 3, the anticipation of the next trial following a similar trajectory can be considered as a source of predictability, which influences the bat's echolocation behavior, i.e. a reduction in sonar sounds groups. This is further demonstrated in Figure 3.2 where the bat produces less number of SSGs during the initial phase for CM2 after which the bat again produces more SSGs for the next CM1, presumably because the target motion predictability decreases.

3.4.2 Bats reduce production of sonar sound groups as experience with a target trajectory increases.

On the first day of data collection, complex motion trajectories (CM1 and CM2) were novel to the bat. The CM and SM motion trajectories were designed to have nearly identical trajectories during their final approach (final window indicated by two dashed green lines– Figure 3.1d). Our results (Figure 3.5) demonstrate that as bats are exposed to the complex motion trajectories (both CM1 and CM2), over a period of days, they reduce the production of sonar sound groups during the more predictable and familiar trajectory in the final window, which is common across all motion conditions (CM1, CM2 and SM). This result demonstrates that the production of SSGs changes with target motion predictability.

Bats dynamically adjust pulse duration (PD) to avoid the overlap between incoming echoes and the outgoing sonar call. Additionally, bats can also adjust the pulse interval (PI) of sonar calls to avoid ambiguity of echo assignment over successive calls (Falk et al., 2015; Moss and Surlykke, 2001; Schnitzler and Kalko, 2001; Wilson, W.W., and Moss, 2004). In our study, only the predictability of target motion was manipulated across trials and days. Further, we found no significant change in either PD or PI as the predictability in the target motion increased (Figure

3.1c) across the CM-SM1-SM2-SM3 target trajectory presentations. Similarly, we also did not find any significant change in PD or PI across days, as the bats became more familiar with the novel complex motions (Figure 3.6).

3.4.3 SSGs: Created through control of temporal patterning or addition of calls?

Our results demonstrate that bats actively increase the production of SSGs as the target predictability decreases (Figure 3.3). Additionally, bats also decrease SSG production as they become increasingly familiar with complex target trajectories over a period of days (Figure 3.5). This raises the question whether bats increase the number of sonar calls to produce SSGs (call

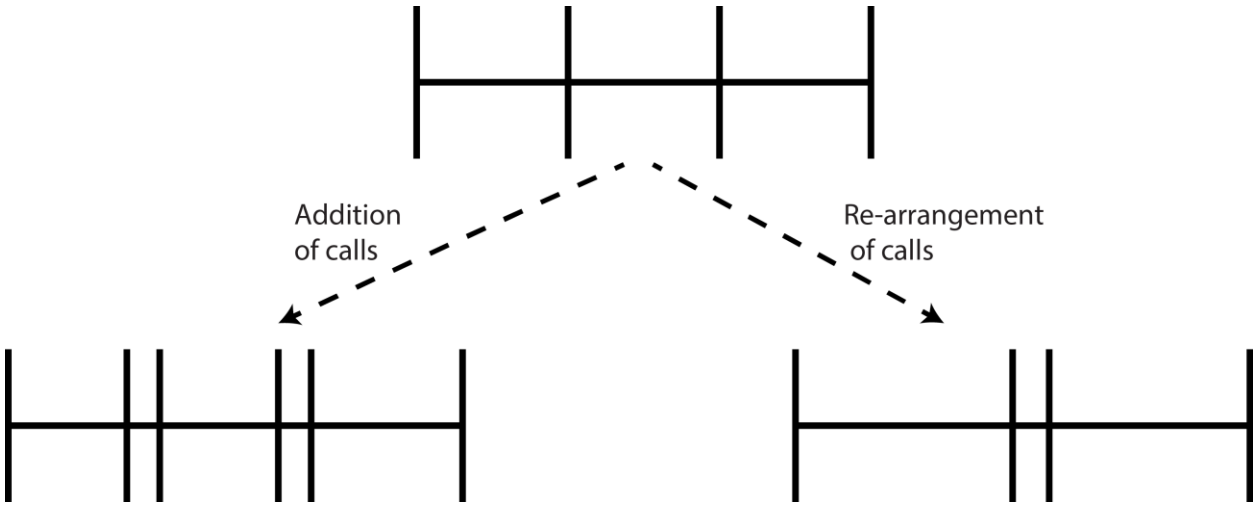

Figure 3-7 The call addition v/s temporal rearrangement strategies This figure demonstrates two ways in which bats can produce SSGs in the same time interval (shown in the top panel). The top panel shows a sequence of four calls produced by a bat. By producing two extra calls, a bat could produce SSGs by adding calls (left bottom panel), while SSGs could also be produced using the same number of calls by temporally rearranging the calls (bottom right panel).

addition), or temporally rearrange calls to produce SSGs while producing the same number of sonar calls (temporal patterning)? Both strategies are illustrated schematically in Figure 3.7:

1) Call Addition: By adding extra calls to a sonar call stream sonar sound groups could be produced.
2) Temporal Rearrangement: Here, the bat actively modifies the time of emission of the sonar calls so as to group them in clusters.

In context of the results of Figure 3.3.3, it could be argued that due to the increased unpredictability during the presentation of CM-SM1 target trajectories, bats produce more calls and coincidentally more SSGs are produced By this argument, the total number of sonar calls made should be greater in the case of CM and SM1 as compared to the SM3. Our data (Figure 3.4) do not support this interpretation as there is no statistically significant difference between the number of calls made by the bats during the initial phase of CM, SM1, SM2 or SM3.

The second strategy (temporal rearrangement) would be revealed if the bats actively control the temporally patterning of sonar calls to produce SSGs. In support of this strategy, all bats in this study produced the same number of calls (Figure 3.4) in the *initial time window* (indicated by the two black lines in Figure 3.2b), strongly supporting the Temporal Rearrangement strategy, and hence, that bats actively cluster their sonar calls to produce SSGs. The temporal rearrangement strategy implies that SSGs have behavioral significance and help the bat track a target when its trajectory is unpredictable. This strategy also implies sensorimotor planning, as information from previous calls is used to plan temporal patterning of subsequent sonar calls to extract relevant information from the environment (Koblitz et al., 2010; Moss and Surlykke, 2010; Ulanovsky and Moss, 2008).

3.4.4 Possible ethological basis for temporal patterning of sonar calls for intercepting eared insects.

In some insect species, the temporal pattern of ultrasonic vocalizations of attacking echolocating bats can provide cues to trigger evasive and unpredictable maneuvers, like diving and erratic trajectories (Corcoran et al., 2009; Ghose et al., 2009; Roeder, 1962; Roeder, 1967; Triblehorn and Yager, 2005). While foraging, bats gradually decrease pulse interval as the distance to the target decreases (Moss and Surlykke, 2001; Schnitzler and Kalko, 2001; Simmons et al., 1979; Surlykke and Moss, 2000). Triblehorn et al (2005, 2008) found that the bat's gradual decrease in pulse interval (as would be observed during normal foraging conditions) provides insects with more time to trigger evasive responses and escape capture. However, in cases where bats temporally pattern their sonar calls to create rapid changes in pulse intervals (sonar sound groups) the insects have less time to initiate evasive maneuvers and their escape rate decreased. Ghose et al (2009) also reported that bats produce sonar sound groups while tracking erratically moving insects. Does the production of SSGs benefit the echolocating bat as it forages for insect prey? Previous work suggests that temporal patterning of sonar calls provides bats with an element of surprise which increases the chances of successful insect capture (Ghose et al., 2009; Triblehorn and Yager, 2005; Triblehorn et al., 2008). Our data suggests that actively producing SSGs also helps bats to track an unpredictably moving target.

3.4.5 Implications for range tuning of neurons in the auditory system of echolocating bats.

Bats estimate target distance by measuring the time delay between sonar sound production and the reception of echoes. Neural representations of target range have been studied by presenting pairs of sounds (mimicking the bats own call and the returning echo) to passively listening bats and recording from auditory neurons, which show pulse-echo (P/E) delay facilitation and tuning for particular P/E delay pairs. Echo delay-tuned neurons have been characterized in the auditory cortex (Hagemann et al., 2010; O'Neill and Suga, 1982; Schuller et al., 1991; Suga and O'Neill, 1979), thalamus (Olsen and Suga, 1991; Yan and Suga, 1996) and mid-brain (Dear and Suga, 1995; Ehrlich et al., 1997; Portfors and Wenstrup, 1999; Valentine and Moss, 1997) of echolocating bats.

Delay tuning of neurons has been shown to be modulated by the temporal pattern and repetition rate of pulse-echo pairs (Bartenstein et al., 2014; Hechavarría et al., 2013; O'Neill and Suga, 1979). The delay tuning curves become sharper/narrower for shorter pulse intervals, thus implying there may be perceptual sharpening of range estimation. Our findings are consistent with the previous proposals of Moss et al (2001, 2006) and also Sändig et al (2014) that SSGs may serve to sharpen sonar range perception in bats operating under challenging conditions. However, to the best of our knowledge, only one prior study has demonstrated the dependence of echo delay tuning in the bat auditory midbrain on the stability of pulse intervals of P/E pairs, which mimic sonar sound groups (Ulanovsky and Moss, 2008, see Figure 3.2). We believe that a critical test of this would be to characterize echo delay tuning of neurons in the auditory system of an actively echolocating bat engaged in a naturalistic task.

In summary, our results demonstrate that echolocating big brown bats actively increase the production of sonar sound groups when target motion is unpredictable and fewer when the motion is more predictable, thus supporting the hypothesis that temporal patterning of sonar calls sharpens sonar resolution for tracking erratically moving targets. Further, our finding that bats produce sonar sound groups without increasing the total number of calls suggests that this adaptive sonar behavior involves sensorimotor planning.

"-Bumblebee bat, how do you see at night?

-I make a squeaky sound that bounces back from whatever it hits. I see by hearing."

— Darrin Lunde

Hello, Bumblebee Bat

4

Echo Model: Reconstructing the instantaneous acoustic stimulus space at the ears of the bat

The *echo model* is a physics based model which takes into account the instantaneous 3D position of the bat, 3D positions of the objects, the bats head direction vector, time of production of the sonar sound as well as the physical parameters of sound in air to compute the direction and time of arrival of echoes at the bat's ears.

4.1 Motivation: Understanding echo sensory space in a flying bat

Past studies of echo delay-tuned neurons have measured responses in bats passively listening to simulated pulse-echo pairs (P/E pairs) (O'Neill and Suga, 1982; Wong et al., 1992; Dear et al., 1993a; Tanaka and Wong, 1993; Chittajallu et al., 1995; Dear and Suga, 1995; Yan and Suga, 1996; Valentine and Moss, 1997). Experiments which involve, restraining an animal's behavior and using artificial stimuli (P/E pairs) to characterize a neurons response have greater

control over the stimulus design as well as unaccounted variables (like head and body movements) which might otherwise influence neural firing patterns.

It is now well accepted that neural activity is modulated with behavioral state (Posner and Petersen, 1989; Reynolds and Chelazzi, 2004; Petersen and Posner, 2012). A most dramatic effect is observed when neural responses are compared in anesthetized and awake animals (Niell and Stryker, 2008, 2010). Recent work in monkeys, rodents and even flies has demonstrated that the animal's behavioral state, and more specifically action, can significantly modulate neural responses to sensory stimuli (Niell and Stryker, 2010; Maimon, 2011; Keller et al., 2012; Fu et al., 2014).

The bat's adaptive and self-generated sonar vocalizations are an essential element of their natural behavior for completing the loop between sensing and action. The above mentioned limitations in past research drove us to characterize spatial tuning profiles of neurons in the SC in a free flying echolocating bat engaged in a naturalistic navigation task. To answer the question at hand, precise information regarding the 3D spatial location of echo sources as well as time of arrival of echoes at the bats ears is essential. One approach to solve this problem is to mount an ultrasonic microphone on the bats head (Hiryu et al., 2010). This solution is inadequate because a single microphone can only provide information regarding the time of arrival of echo stimuli and not be used to resolve the 3D location of echo sources. The solution to this problem is to add an array of ultrasonic microphones (at least 3 ultrasonic microphones are required to resolve echo sources in 3D – see Methods for explanation) in addition to the neural telemetry device. Due to size and weight considerations and also due to limitations of noise floor and sensitivity of microphones, this is also an infeasible solution with current technology.

Thus, due to limitations of current technology and models, to reconstruct the instantaneous echoscape that a bat would experience at its ears as it flies, we came up with a physics based model, which we refer to as the *echo model*. In the sections below, I outline the construction and validation of the echo model.

4.2 Echo model

As shown in **Error! Reference source not found.**, the '*echo model*' is a physics based odel which takes into account the instantaneous 3D position of the bat, 3D positions of the objects, the bats head direction vector, time of production of the sonar sound as well as the physical parameters of sound in air to compute the direction and time of arrival of echoes at the bat's ears. In the sections below, I outline the general theory and construction of the echo model in detail.

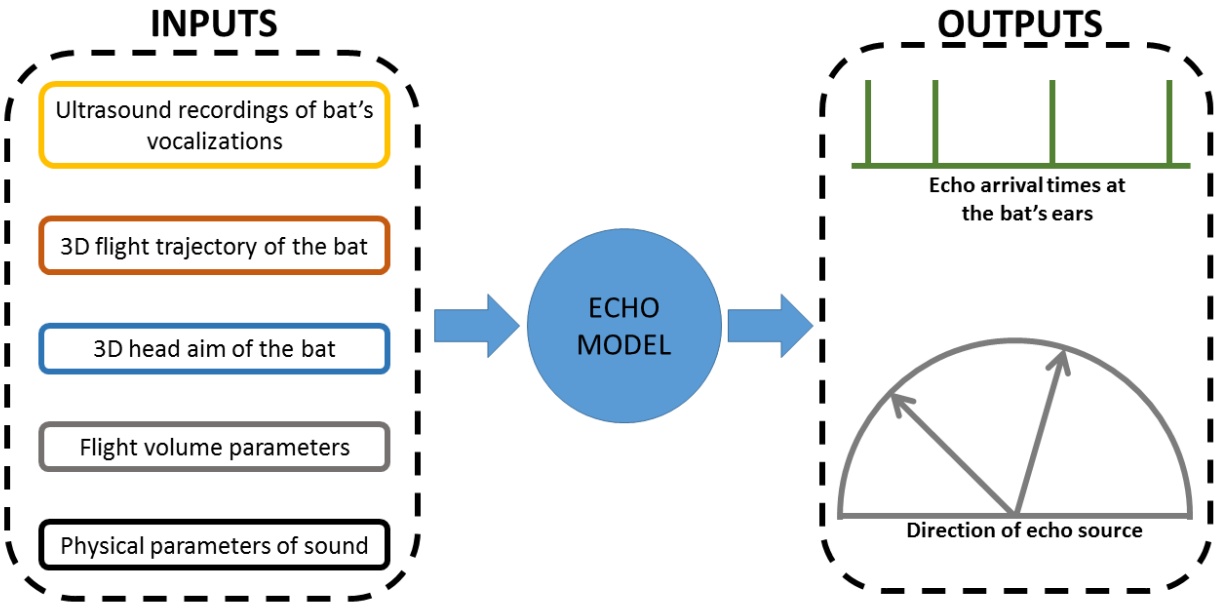

Figure 4.1. A flow diagram schematic of the echo model

4.2.1 Reconstruction of 3D flight trajectory, head aim and egocentric axes

Figure. 4.1A shows an outline of a bat with the neural telemetry headstage (TBSI). The headstage is shown as a grey box with a 16-channel Omnetics connector (male and female) at the bottom. Three reflective markers (4 mm diameter), P, Q and R (black), which are tracked by the infrared motion tracking cameras (Vicon) are also shown. A top view (cartoon) of the bat and telemetry headstage, with markers is shown in Figure. 4.1B.

The bats flight trajectory was reconstructed by computing the centroid (geometric center) of the 3 markers on the head stage. In case of missing points, only the points visible to the motion tracking system were used. The 3 points (P, Q, R) on the head stage were arranged as a triangle, with two of the points (Q and R) at the trailing edge of the headstage (Figure. 4.1B), and marker P at the front of the headstage. The 3D head aim of the bat was computed by first calculating the midpoint (P') of $\overline{QR}$ and then constructing $\overrightarrow{PP'}$ along the mid line of the head (Figure. 4.1B, head aim vector is shown as a dashed red arrow).

$$\widehat{p_x} = \frac{\overrightarrow{PP'}}{\left|\overrightarrow{PP'}\right|} \ (head\ aim\ unit\ vector) \qquad (1)$$

The z-direction of the egocentric axes was computed as the cross product of $\overrightarrow{PQ}$ and $\overrightarrow{PR}$.

$$\widehat{p_z} = \frac{\overrightarrow{PQ}\ X\ \overrightarrow{PR}}{\left|\overrightarrow{PQ}\right|\ X\ \left|\overrightarrow{PR}\right|} \qquad (2)$$

Further, the y-direction of the egocentric axes was computed as the cross product of p_x and p_z.

$$\widehat{p_y} = \widehat{p_z}\ X\ \widehat{p_x} \qquad (3)$$

Where X denotes cross product between vectors.

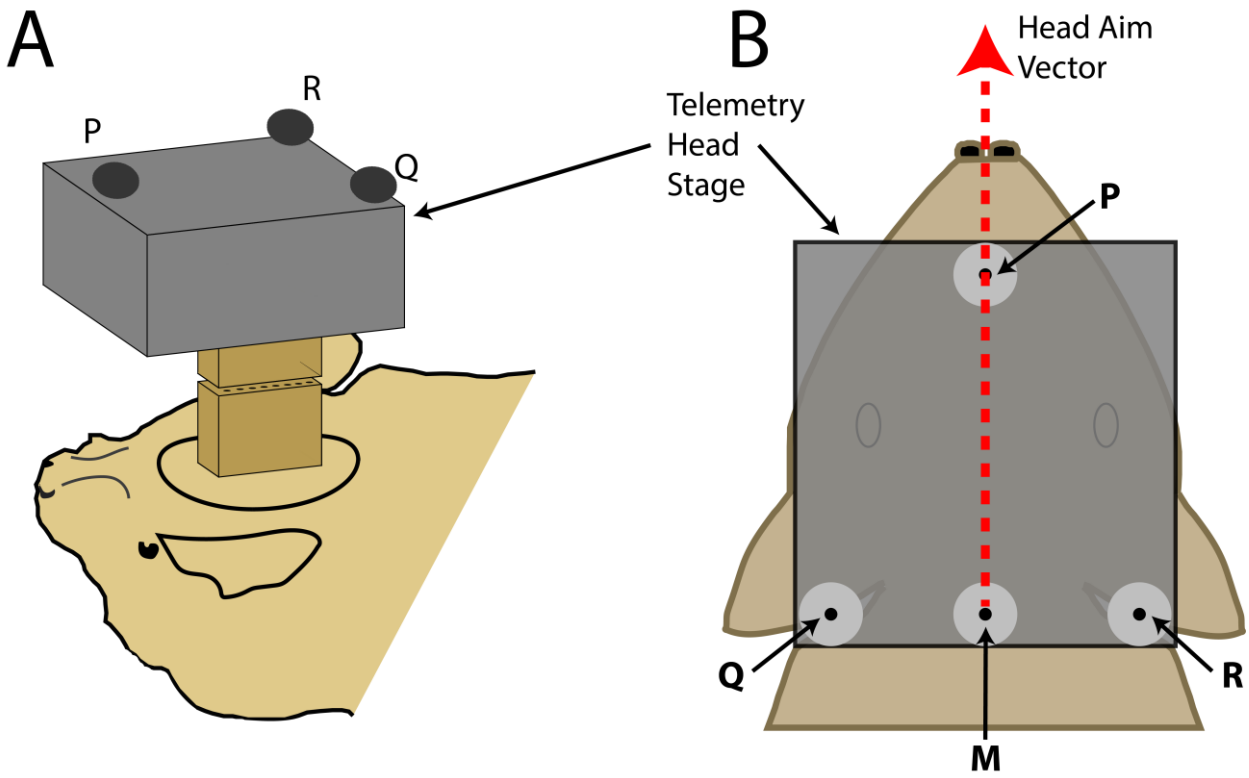

Figure 4.2. **<u>Head aim reconstruction.</u>** A. Cartoon of the bat with the TBSI telemetry head-stage (grey box), and the Omnetics connectors (brown boxes) which connect the head-stage with the plug on the bat's head. **B.** Top view of the bat's head with the telemetry head-stage (grey rectangle) and head markers, P,Q and R. Grey circles around the markers indicate the maximum error in reconstruction. M is the midpoint of Q and R. The reconstructed head-aim is indicated by the red arrow.

We refer to the above instantaneous egocentric coordinate system (p_x, p_y, p_z) as the 'local' coordinate system and the coordinate system from the frame of reference of the motion capture cameras as the 'world' coordinate system (P_X, P_Y, P_Z). An example of a reconstructed flight trajectory is shown in Figure. 4.3C. This trajectory is in the 'world' coordinates shown as the X, Y, Z axes (red, green and blue colors respectively) at the left corner of Figure. 4.3C. The bats head aim during vocalizations (solid yellow circles on the flight trajectory) is indicated by black lines.

Figure. 4.3C also shows two example points, P(x_1, y_1, z_1) and Q(x_2, y_2, z_2), in the bats flight trajectory when the bat produces sonar calls. [p_x, p_y, p_z] and [q_x, q_y, q_z] (red, green, blue respectively) are the axes which form the 'local' instantaneous egocentric coordinate system (computed as per equations 1, 2 and 3) with respect to the bat's current position in space and head aim.

To compute the instantaneous microphone, object and room boundary coordinates from the 'world' coordinate system to the 'local' instantaneous egocentric coordinate system, translation and transformation of points are performed using quaternion rotations (Altmann, 2005).

For example, if A(X_a, Y_a, Z_a) are the coordinates of an object in the global coordinate system (P_X, P_Y, P_Z). Then the new coordinates A(x_a,y_a,z_a) of the same object with respect to the instantaneous egocentric coordinate system (p_x, p_y, p_z) are computed as below (4).

$$A(x_a, y_a, z_a) = ROT(P_X, P_Y, P_Z)(p_x, p_y, p_z)(X_a, Y_a, Z_a) \qquad (4)$$

4.2.2 Steps to compute direction and time of arrival of echoes at the bats ears.

Once the Euclidian object coordinates are transformed into the instantaneous Euclidian coordinate system $A(x_a, y_a, z_a)$, unit vectors of object directions are computed (5) and the direction angles of echo source locations can be computed by transforming from the Euclidian coordinates to spherical coordinate $A(\theta, \varphi, R)$ (azimuth, elevation, range) as given in (6).

$$\hat{a} = \frac{\overrightarrow{A(x_a, y_a, z_a)}}{\left|\overrightarrow{A(x_a, y_a, z_a)}\right|} \ (unit\ vector) \tag{5}$$

The range of the object is simply the distance between the bat's instantaneous location and the object.

$$\boldsymbol{\theta} = \sin^{-1}(\hat{a}.\widehat{p_x}) \ and \ \boldsymbol{\varphi} = \sin^{-1}(\hat{a}.\widehat{p_y}), \boldsymbol{Range}\ (\boldsymbol{R}) = \left|\overrightarrow{A(x_a, y_a, z_a)}\right| \tag{6}$$

Time of arrival of echoes at the bat's ear is computed as given in (7).

$$T_{arr} = 2 * \frac{R}{c_{air}}, where\ c_{air}\ is\ the\ speed\ of\ sound\ in\ air \tag{7}$$

Figure. 4.3D shows how the instantaneous solid angle of the bat's head aim vector to each object changes as the bat flies through the room. The data here refers to the flight trajectory shown in Figure. 4.3C. Figure. 4.3E shows the echo arrival times at the bat's ears as computed by the echo model. Figure. 4.3F and 3G show the room, objects and microphones from the bat's egocentric point of 'view' as computed using the echo model. These figures correspond to the highlighted points, P and Q, in Figure. 4.3C. The egocentric y and z axes are marked in green and blue respectively. The head aim vector (x-axis) is going into the plane of the paper and is denoted by a red circle.

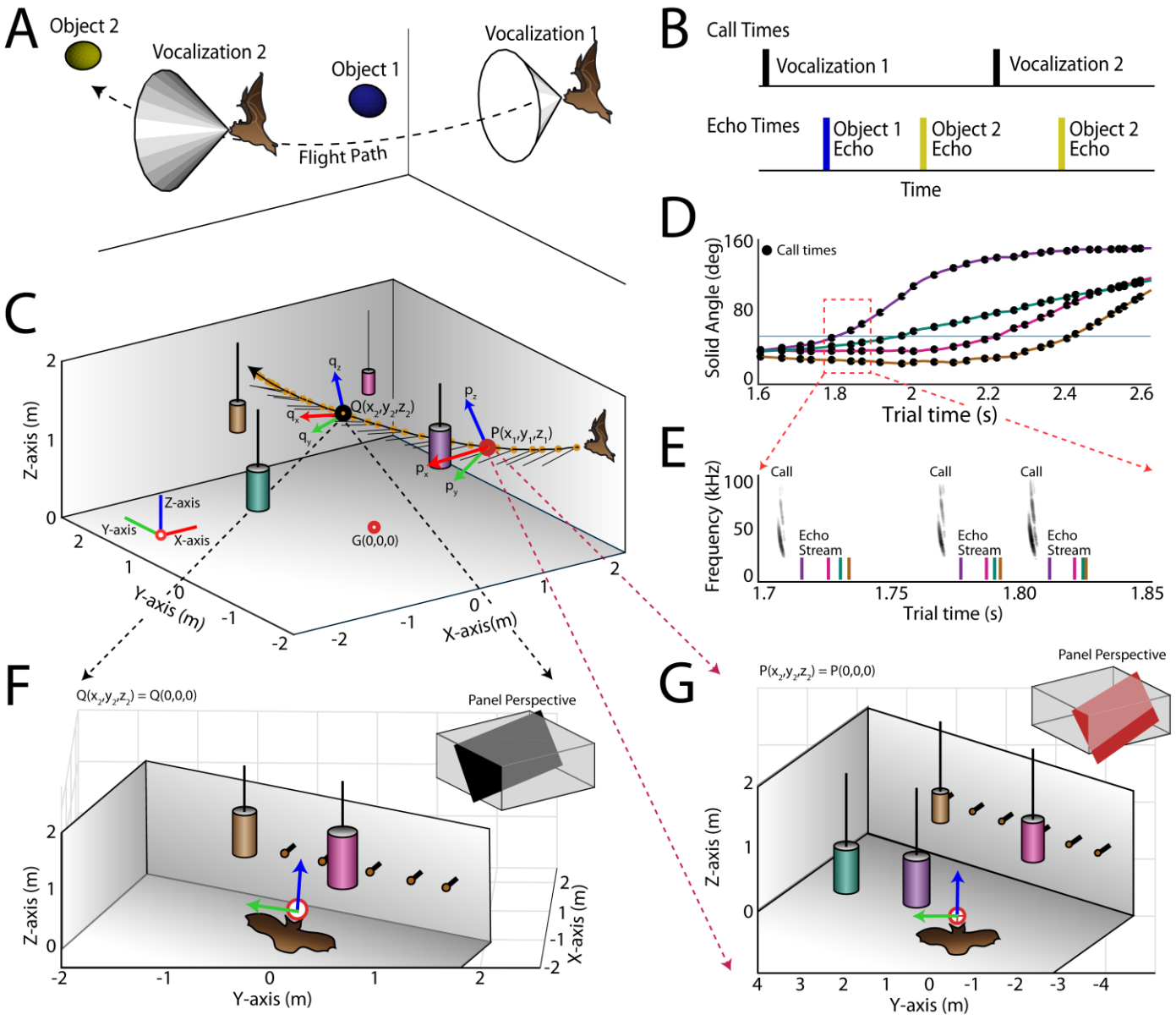
A
Object 2
Vocalization 2
Object 1
Vocalization 1
Flight Path
B
Call Times
Vocalization 1
Vocalization 2
Echo Times
Object 1 Echo
Object 2 Echo
Object 2 Echo
Time
C
Z-axis (m)
Y-axis (m)
X-axis(m)
Z-axis
Y-axis
X-axis
G(0,0,0)
D
Solid Angle (deg)
Call times
Trial time (s)
E
Frequency (kHz)
Call
Echo Stream
Trial time (s)
F
Panel Perspective
Z-axis (m)
Y-axis (m)
X-axis (m)
G
Panel Perspective
Z-axis (m)
Y-axis (m)

Figure 4.3. Use of the echo model to determine the bat's ongoing sensory experiences. A. Cartoon of a bat flying through space encountering 2 obstacles. The bat's flight trajectory moves from right to left, and is indicated by the black dotted line. Two sonar vocalizations while flying are indicated by the gray cones. **B.** Reconstruction of sonar vocal times (top), and returning echo times (bottom) for the cartoon bat in panel a. Note that two echoes (blue and yellow) return to the bat following the first sonar vocalization, while only one echo (yellow) returns after the second vocalization, because the relative positions of the bat and objects change over time. **C.** One experimental trial of the bat flying and navigating around obstacles (large circular objects). The bat's flight path (long black line) starts at the right and the bat flies to the left. Each vocalization is indicated with a yellow circle, and the direction of the vocalization is shown with a short black line. **D.** Trial time versus solid angle to each obstacle for flight shown in A. Individual vocalizations are indicated with black circles, and the color of each line corresponds to the objects shown in A. **E.** Time expanded spectrogram of highlighted region in B. Shown are three sonar vocalizations, and the colored lines indicate the time of arrival of each object's echo as determined by the echo model (colors as in A). **F.** Snapshot of highlighted region in panel C showing the position of objects when the bat vocalized at that moment. **G.** Snapshot of highlighted region in panel C showing the position of objects when the bat vocalized at that moment.

4.2.3 Error analysis of the 3D head-aim reconstruction

As the dimensions of the headstage were known and remain fixed over the period of the experiment. Tracking errors due to the motion tracking system is simplified. For example, the distance between the P and Q head markers was 21 millimeters (see Figure. 4.1B). We allowed a maximum error of 1 millimeter. Tracked points which exceeded this threshold were excluded from the analysis. In reality, the error in distance between markers is actually a distributed error in the position of the two markers (P and Q in this case). We show this error as grey spheres/discs around each marker in Figure. 4.1B. The head-aim is reconstructed as the vector $\overrightarrow{PM}$. To compute the maximum and average error in the estimation of the head-aim vector, it is important to estimate the error in computing the midpoint of $\overline{QR}$. We compute this error by first estimating the errors in the coordinates of M.

For simplicity, let us consider a 2D case and let M be the origin as shown in Figure 4A. Hence, the coordinates of Q and R can be written as (-L, 0) and (L, 0), respectively. Where, 2L is the length of $\overline{QR}$. Let us consider points $Q'(x_{Q'}, y_{Q'})$ and $R'(x_{R'}, y_{R'})$ which belong to the circles of radius 'r' centered at Q and R, respectively and point $M'(x_{M'}, y_{M'})$ which is the midpoint of $\overline{Q'R'}$. Here 'r' is the maximum allowed error in distance estimation of $\overline{QR}$ (See Figure 4A). Equations of circles can be written as below (8)

$$(x_{Q'} + L)^2 + {y_{Q'}}^2 \leq r^2 \; and \; (x_{R'} - L)^2 + {y_{R'}}^2 \leq r^2 \qquad (8)$$

Adding these equations and rearranging the terms we can rewrite the final equation as

$$\left(\frac{(x_{Q'} + x_{R'})}{2}\right)^2 + \left(\frac{(y_{Q'} + y_{R'})}{2}\right)^2 \leq ({x_{M'}}^2 + {y_{M'}}^2) \leq \frac{r^2}{2} - \frac{L^2}{2} + \frac{\left|\overrightarrow{MQ'}\right|\left|\overrightarrow{MR'}\right| \cos\alpha}{2} \qquad (9)$$

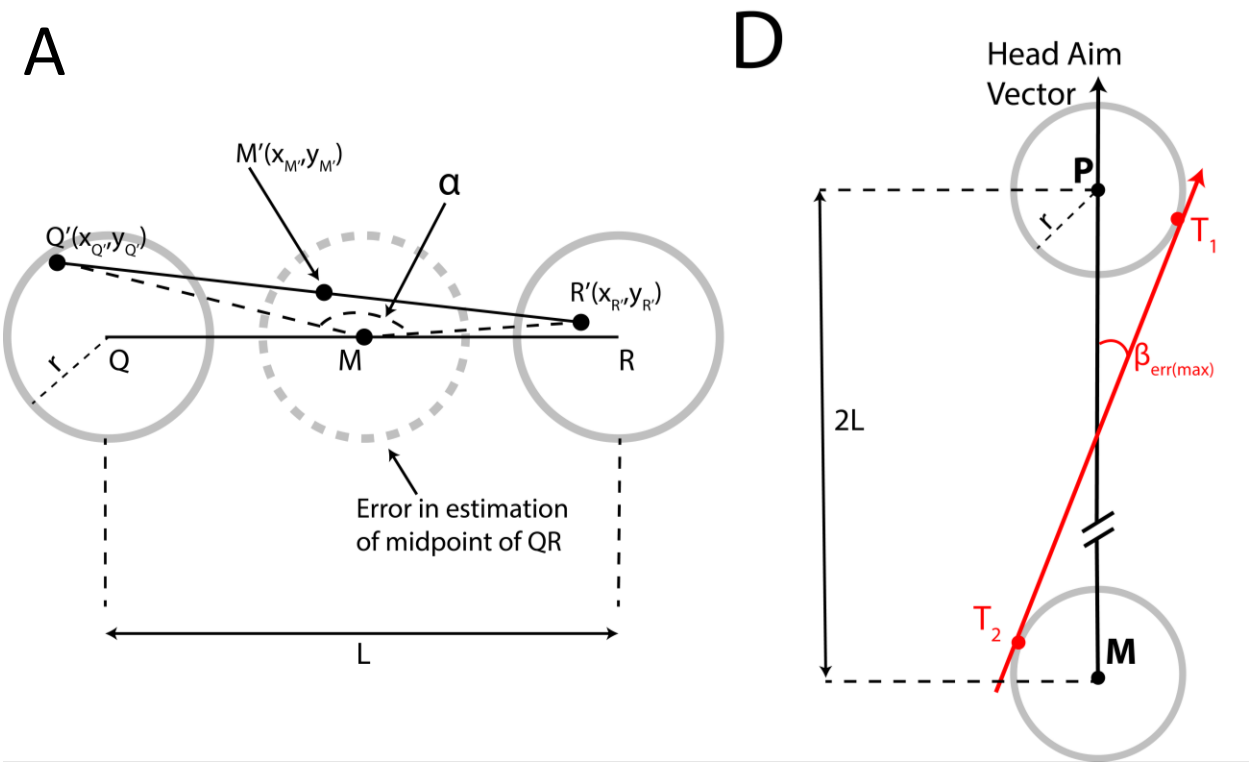

Figure 4.4. Error analysis of head aim reconstruction. A. Estimation of the maximum error in reconstruction of the midpoint of QR (see Methods for details). **B.** Estimation of the maximum error in the measurement of the head-aim vector (see Methods for details).

Where α is the angle between the vectors $\overrightarrow{MQ'}$ and $\overrightarrow{MR'}$ as shown in Figure 4A. Solving the equation for the extreme cases when α is 0 or 180 degrees shows that equation (9) reduces to (10) proving that the error in the estimation of the midpoint M' is also a sphere/circle of radius 'r'.

$$x_{M'}{}^2 + y_{M'}{}^2 \leq r^2 \tag{10}$$

Figure 4B shows the head-aim vector as $\overrightarrow{PM}$ and the grey circles around each point as the error in the position of each marker. In the 2D case, as shown in Figure 4B it is easy to prove that the maximum angular error in the estimation of the head-aim vector is the angle between $\overrightarrow{PM}$ and $\overrightarrow{T_1T_2}$, where $\overrightarrow{T_1T_2}$ is the line tangent to both maximum error circles (indicated in grey) and is can be computed as given in (11).

$$\beta_{err(max)} = \sin^{-1}\frac{r}{L} = 5.45^{\circ} \tag{11}$$

4.2.4 Error analysis of the point object approximation

When estimating echo arrival times and echo source locations, all objects are assumed to be point objects and sources. Figure. 4.5A shows the cross-section of a cylindrical object which was used as an obstacle in the bat's flight path. The error in the estimation of echo arrival time depends on the position of the bat with respect to the object. Figure. 4.5B shows how the error in estimation of echo arrival changes as a function of the angle (θ) between the bats position and the objects horizontal axis as shown in Figure. 4.5A. Figure. 4.5C shows a computation of the accuracy of the echo model as a function of the position of the bat as it moves around the object in a sphere of 2 meters. To summarize, the minimum and maximum errors in time of arrival of

the echo at the bat‘s ears, due to the point object approximation are 0.35 milliseconds and 0.68 milliseconds.

4.2.5 Echo model validation

The echo model was verified using 2 different approaches.

1) Playing sounds from a speaker and recording echoes reflected back from objects using a microphone (shown in Figure. 4.5D). Here, the distance of the object from the microphone/speaker is ‘d’ while ‘L’ is the distance used by the echo model due to the point object approximation. This introduces a systematic error of ‘L-d’ in the time of arrival of the echo. In this setup the reflecting object was placed at different distances from the speaker and microphone and recorded echo arrival times were compared with the arrival times computed by the echo model. Figure. 4.5E shows spectrograms of microphone recordings when the object was placed 0.7, 1.2 and 1.8 meters away from the recording microphone. The results matched the theoretical error bounds (as discussed above and shown in Figure. 4.5A, 5B and 5C) within an error less than 0.1 milliseconds (Figure. 4.5F).

2) A 14-channel microphone array was placed on the wall opposite to the flight direction of the bat. As the bat navigated around objects in its flight path, the microphone array recorded echoes reflected off of objects. Using Time of Arrival of Difference (TOAD) algorithms (Madsen and Wahlberg, 2007), the 3D locations of the echo sources were computed and matched with the locations computed by the *echo model* (see supplementary video SV1 and SV2).

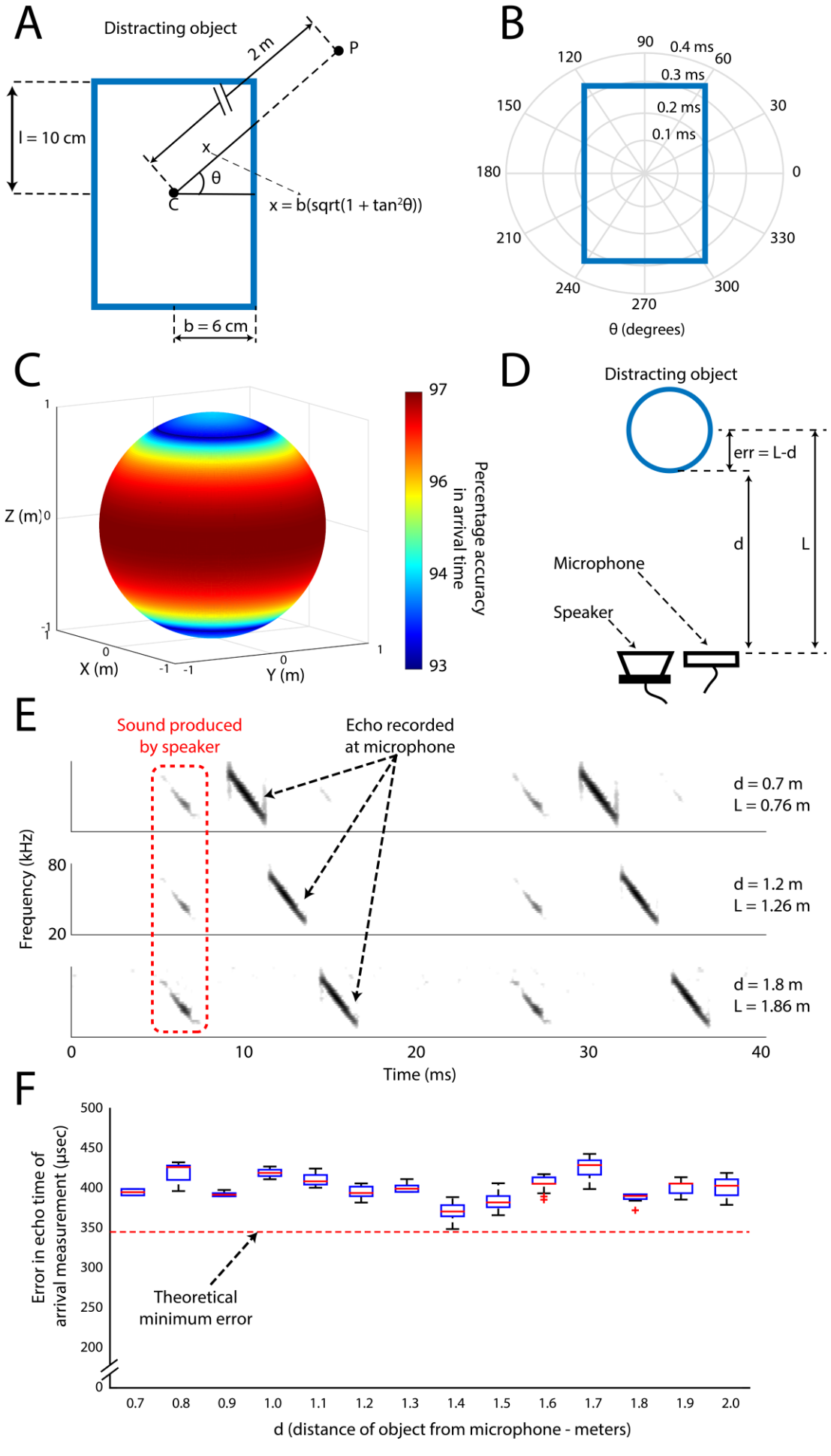
A
Distracting object
2 m
P
l = 10 cm
x
θ
C
x = b(sqrt(1 + tan²θ))
b = 6 cm
B
90
0.4 ms
120
60
0.3 ms
150
0.2 ms
30
0.1 ms
180
0
210
330
240
300
270
θ (degrees)
C
Z (m)
X (m)
Y (m)
97
96
94
93
Percentage accuracy in arrival time
D
Distracting object
err = L-d
d
L
Microphone
Speaker
E
Sound produced by speaker
Echo recorded at microphone
d = 0.7 m
L = 0.76 m
d = 1.2 m
L = 1.26 m
d = 1.8 m
L = 1.86 m
Frequency (kHz)
80
20
0
10
20
30
40
Time (ms)
F
Error in echo time of arrival measurement (μsec)
500
450
400
350
300
250
200
0
Theoretical minimum error
0.7
0.8
0.9
1.0
1.1
1.2
1.3
1.4
1.5
1.6
1.7
1.8
1.9
2.0
d (distance of object from microphone - meters)

Figure 4.5. Error analysis and validation of the echo-model. A. Cross-section of the cylindrical object placed along the flight path of the object. The height and radius of the object are 10 cm and 6 cm respectively. P is an example point in the trajectory of the bat at a distance of 2m from the center of the object. **B.** Polar plot demonstrating how the error in the measurement of the echo arrival changes a function of the angular position of the bat with respect to the angle between the bat and the horizontal direction. **C.** Accuracy in the estimation of the echo arrival time as a function of the 3D position, along a sphere of 2m radius, of the bat with respect to the center of the object. **D.** Arrangement used to validate the echo model. Here, the distance of the object from the microphone/speaker is 'd' while 'L' is the distance used by the echo model due to the point object approximation. This introduces a systematic error of 'L-d' in the time of arrival of the echo. The distance of the object from the speaker/microphone was varied and measurements of echo arrival time were made and verified with the echo model **E.** Spectrograms of microphone recordings when the object was placed 0.7, 1.2 and 1.8 meters away from the recording microphone. **F.** Box plots (n=20 for each distance) showing the error in the time estimated by the echo model, computed as 2*(d-L). The echo model estimate of target distance matched the theoretical error bounds (see Methods and Fig. S4A, S4B and S4C) within an error less than 0.1 milliseconds.

4.3 Chapter Summary

In this chapter, I have described the importance of estimating and reconstructing the echo stimuli, both in timing of arrival at the ears and the direction, that a bat experiences as it flies in a complex environment. The reconstruction of the echo scape is essential for further constructing 3D spatial receptive fields of neurons and understanding how the brain encodes egocentric auditory space. This part will be described in Chapter 5. Further, it is important to highlight that the *echo model* opens the door for further investigations using free flying echolocating bats.

> “Can an instantaneous cube exist?' 'Don't follow you,' said Filby. 'Can a cube that does not last for any time at all, have a real existence?' Filby became pensive. 'Clearly,' the Time Traveller proceeded, 'any real body must have extension in four directions: it must have Length, Breadth, Thickness, and—Duration. But through a natural infirmity of the flesh, which I will explain to you in a moment, we incline to overlook this fact. There are really four dimensions, three which we call the three planes of Space, and a fourth, Time.”
>
> — H.G. Wells,
> The Time Machine

5

Dynamic representation of 3D auditory space in the midbrain of the free-flying echolocating bat

5.1 INTRODUCTION

As humans and other animals move in a 3D world, they rely on dynamic sensory information to guide their actions, seek food, track targets and steer around obstacles. Such natural behaviors invoke feedback between sensory space representation, attention and action-selection (Lewicki et al., 2014). Current knowledge of the brain’s representation of sensory space comes largely from decades of research on neural activity in restrained animals, generally studied with 2D stimuli (Van Horn et al., 2013); however, far less is known about 3D sensory representation, particularly in freely moving animals that must process changing stimulus information to localize objects and guide motor decisions as they navigate the physical world.

Animals that rely on active sensing provide a powerful system to investigate the neural underpinnings of sensory-guided behaviors, as they produce the very signals that inform motor actions. Echolocating bats, for example, transmit sonar signals and process auditory information carried by returning echoes to guide behavioral decisions for spatial orientation (Griffin, 1958). Work over the past decade has revealed that echolocating bats produce clusters of sonar calls, termed sonar sound groups (SSGs), to inspect objects in their surroundings or to negotiate complex environments (Kothari et al., 2014; Moss et al., 2006; Petrites et al., 2009; Sändig et al., 2014). We hypothesize that the bat's sonar inspection behavior sharpens spatio-temporal echo information processed by the auditory system in a manner analogous to the active control of eye movements to increase visual resolution through sequences of foveal fixations (Hayhoe and Ballard, 2005; Moss and Surlykke, 2010; Tatler et al., 2011). Importantly, the bat's acoustic behaviors provide a quantitative metric of spatial gaze, and can thus be analyzed together with neural recordings to investigate the dynamic representation of sensory space.

Echolocating bats compute the direction of echo sources using a standard mammalian auditory system (Wohlgemuth et al., 2016). The dimension of target distance is computed from the time delay between sonar emissions and echoes (Simmons, 1973). Neurophysiological investigations of echo processing in bats reveal that a class of neurons shows facilitated and delay-tuned responses to **simulated** pulse-echo pairs. It has been hypothesized that echo delay-tuned neurons carry information about the distance to objects (Feng et al., 1978; O'Neill and Suga, 1982; Suga and O'Neill, 1979; Valentine and Moss, 1997); however, the neural representation of target distance in bats listening to self-generated echoes from physical objects has never previously been empirically established.

The midbrain superior colliculus (SC) has been implicated in sensory-guided spatial orienting behaviors, such as visual and auditory gaze control in primates, cats and barn owls (Knudsen, 1982; du Lac and Knudsen, 1990; Middlebrooks and Knudsen, 1984; Munoz et al., 1991; Stein et al., 1989), prey-capture behavior in frog and pit viper (Grobstein, 1988; Hartline et al., 1978; Newman and Hartline, 1981), and echolocation in bats (Valentine and Moss, 1997; Valentine et al., 2002). Previous work has also demonstrated that the SC is an integral part of the *egocentric* spatial attention network, specifically for target selection and goal-directed action (Krauzlis et al., 2013; Lovejoy and Krauzlis, 2010; McPeek and Keller, 2004; Mysore and Knudsen, 2011; Zénon and Krauzlis, 2012). Work in freely behaving rodents has also demonstrated a more general role of the SC in sensory-guided orienting behaviors (Duan et al., 2015; Felsen and Mainen, 2008). Additionally, measures of the local field potential (LFP) in the midbrain optic tectum (avian homologue of the SC) have shown that increases in the gamma band (~40-140 Hz) correlate with attended sensory stimuli (Sridharan and Knudsen, 2015). The research reported here is the first to investigate the behavioral modulation of depth-tuned single unit responses and gamma band oscillations in the SC of a mammal inspecting objects in its physical environment.

Prior work on sensorimotor representation in the mammalian SC has been largely carried out in restrained animals performing 2D tasks, leaving gaps in our knowledge about the influence of action and attention on sensory responses in animals moving freely in a 3D physical environment. To bridge this gap, we conducted wireless chronic neural recordings of both single unit activity and LFPs in the SC of free-flying bats that used echolocation to localize and inspect obstacles along their flight path. Central to this research, we developed a novel echo model to

reconstruct the bat's instantaneous egocentric stimulus space, which we then used to analyze echo-evoked neural activity patterns. Our data provide the first demonstration that neurons in the midbrain SC of a ***freely moving animal represent the 3D egocentric location of physical objects in the environment and that active sonar inspection sharpens and shifts the depth tuning of 3D neurons***.

5.2 RESULTS

We trained big brown bats, *Eptesicus fuscus*, to fly in a large experimental test room and navigate around obstacles for a reward (Figure 5.1A, wall landing; Figure 5.1B, platform landing). Each bat showed natural adjustments in flight and sonar behaviors in response to echoes arriving at its ears. The positions of objects were varied across recording sessions, and the bats were released from different points in the room within recording sessions, to limit their use of spatial memory for navigation and instead invoke their use of echo feedback. While the bats performed natural sensory-guided behaviors, sonar calls were recorded using a wide-band ultrasound microphone array (Figure 5.1A, B – grey circles are microphones; see Figure 5.1B, raw oscillogram in middle panel and spectrograms in bottom panel and inset). The bat's 3D flight trajectory and head aim were measured using high-speed Vicon motion capture cameras (Figure 5.1A, B, frame-rate 300 Hz). Extracellular neural activity was recorded with a 16-channel silicon probe, affixed to a microdrive, and implanted in the bat SC. Neural activity was transmitted wirelessly via radio telemetry (Triangle BioSystems International; Figure 5.1A – green box). Figure 5.1C shows histology of SC recording sites, and Figure 5.1D shows simultaneous neural recordings from 2 channels (see also Methods). Figure 5.1 - figure supplement 1, demonstrates single cell neural

recordings across multiple trials. In flight, bats displayed natural adaptations in sonar behavior (Griffin, 1958; Simmons et al., 1979). Specifically, they increased echolocation pulse rate (PR) and decreased pulse duration (PD) as they approached objects or their landing points (Figure 5.1E), and they also produced sonar sound groups (SSGs), or clusters of vocalizations, to inspect objects in space (Falk et al., 2014; Moss et al., 2006; Petrites et al., 2009; Sändig et al., 2014; Wheeler et al., 2016).

5.2.1 Echo model - Reconstructing the instantaneous acoustic stimulus space at the ears of the bat

To measure auditory spatial receptive fields in the bat SC, we first determined the azimuth, elevation and distance of objects, referenced to the bat's head direction and location in the environment (Figure 5.2 - figure supplement 1A shows a cartoon of a bat with a telemetry recording device and markers to estimate the bat's head direction, Figure 5.2 – figure supplement 1B shows a top view of the bat's head with the telemetry device and head tracking markers, also see Methods). In order to determine the 3D direction and arrival time of sonar echoes returning to the bat, we relied on the physics of sound to develop an echo model of the bat's instantaneous sensory space. The echo model takes into account an estimate of the beam width of the bat's sonar calls, its 3D flight trajectory, its head direction, as well as physical parameters of sound (Figure 5.2 – figure supplement 1A and 1B – schematic, see Methods) to compute a precise estimate of the time of arrival of echoes at the bat's ears, as well as the 3D location of

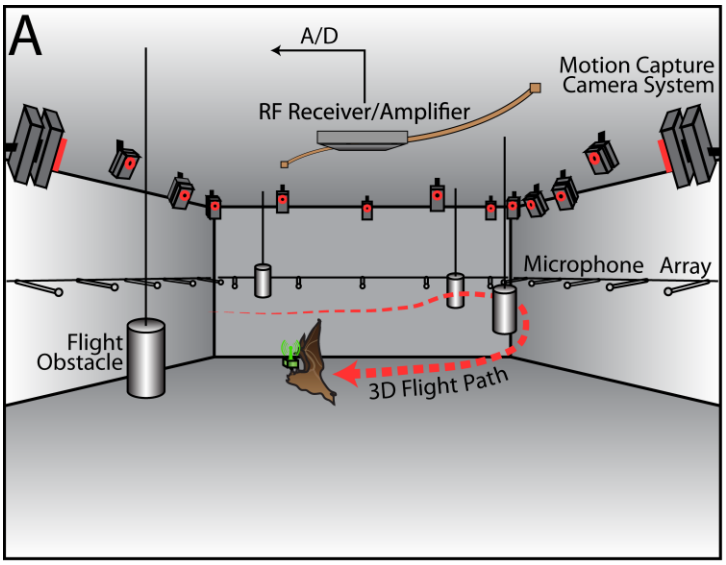
A
A/D
RF Receiver/Amplifier
Motion Capture
Camera System
Microphone Array
Flight
Obstacle
3D Flight Path

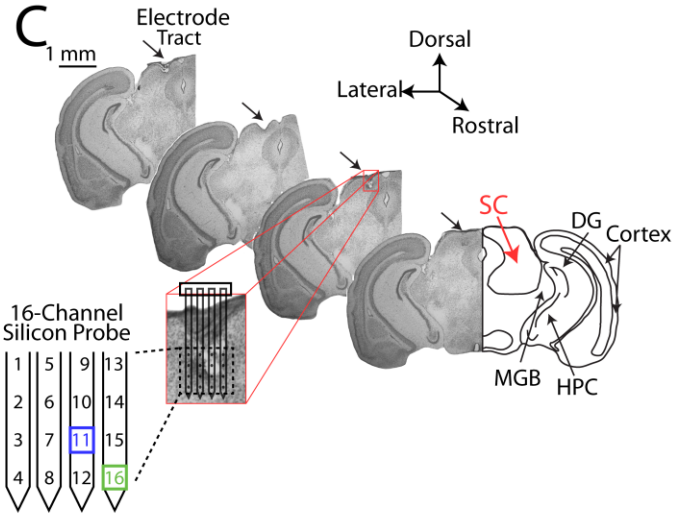
C
1 mm
Electrode
Tract
Dorsal
Lateral
Rostral
SC
DG
Cortex
16-Channel
Silicon Probe
1 2 3 4
5 6 7 8
9 10 11 12
13 14 15 16
MGB
HPC

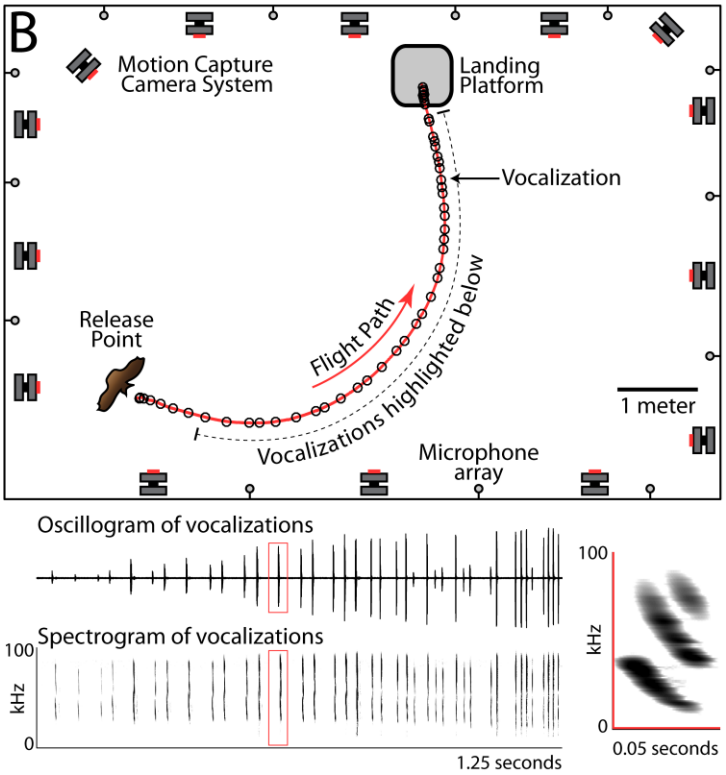
B
Motion Capture
Camera System
Landing
Platform
Vocalization
Release
Point
Flight Path
Vocalizations highlighted below
1 meter
Microphone
array

Oscillogram of vocalizations
Spectrogram of vocalizations
100
kHz
0
1.25 seconds
100
kHz
0
0.05 seconds

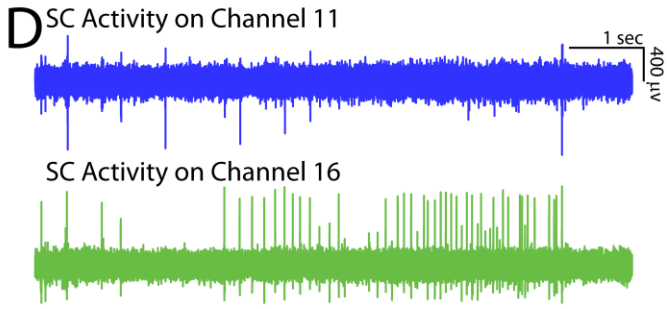
D
SC Activity on Channel 11
1 sec
400 µv
SC Activity on Channel 16

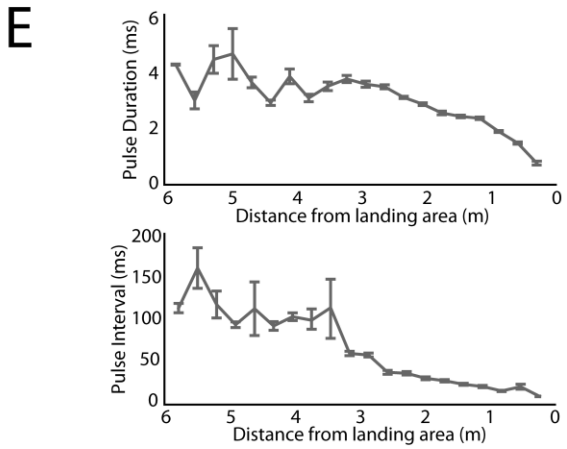
E
Pulse Duration (ms)
0
2
4
6
6 5 4 3 2 1 0
Distance from landing area (m)
Pulse Interval (ms)
0
50
100
150
200
6 5 4 3 2 1 0
Distance from landing area (m)

Figure 5-1. Experimental setup and methodology. A. Configuration of the experimental flight room for wireless, chronic neural recordings from freely flying echolocating bats. Shown is the bat (in brown) with the neural telemetry device mounted on the head (in green). The telemetry device emits an RF signal received by an RF receiver connected to an amplifier and an analog-to-digital recording system. The bat's flight path (in red) is reconstructed by 16 motion capture cameras (not all are shown) tracking 3 reflective markers mounted on the dorsal surface of the telemetry device (3 mm round hemispheres). While the bat flies, it encounters four different, cylindrical flight obstacles (in grey), and the sonar vocalizations are recorded with a wide-band microphone array mounted on the walls. **B.** Overhead view of the room in the platform-landing task. The bat flew across the room (red line) using echolocation to navigate (black circles are sonar vocalizations) while recordings were made wirelessly from the SC (as shown in pane A). Vocalizations produced on this trial are shown in greater detail in bottom panels (filtered audio trace and corresponding spectrogram). The inset, on the right, shows a zoomed in view of the spectrogram of one call, indicated by the red box. **C.** Histological reconstruction of the silicon probe tract through the superior colliculus (SC) of one bat in the study. Shown are four serial coronal sections, approximately 2.5 mm from bregma, at the location of the SC. Lesions from the silicon probe are indicated with black arrows. Also marked in the most rostral section are the locations of the SC, medial geniculate body (MGB), hippocampus (HPC), cortex, and dentate gyrus (DG). **D.** Simultaneous neural recordings from SC from the recording sites identified with a blue square and green square in the silicon probe layout panel in Figure 5.1C. (layout of the 16-channel silicon probe used for SC recordings). **F.** Top, change in sonar pulse duration as a function of object distance. Bottom, change in pulse interval as a function of object distance.

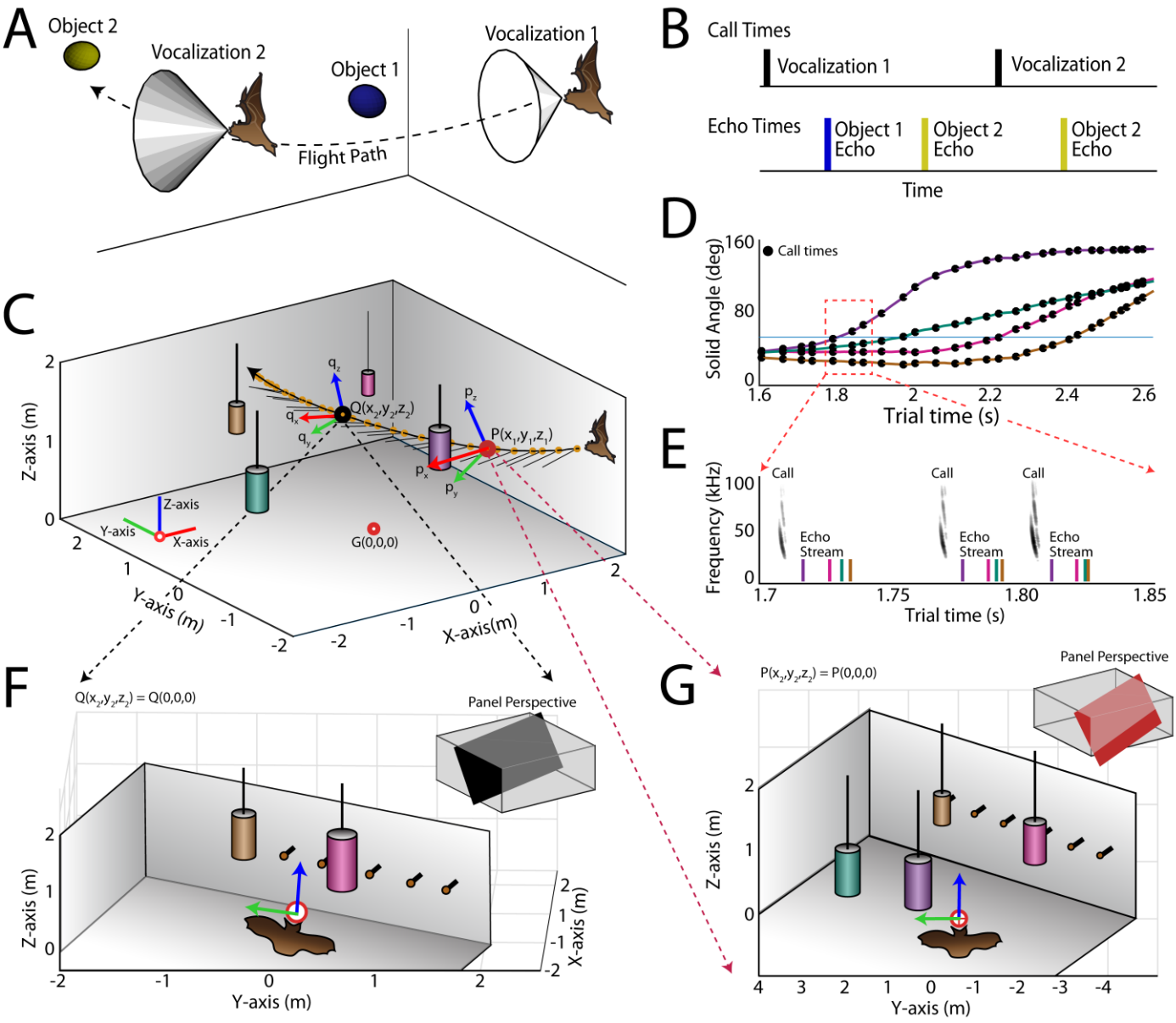
A
Object 2
Vocalization 2
Object 1
Vocalization 1
Flight Path
B
Call Times
Vocalization 1
Vocalization 2
Echo Times
Object 1 Echo
Object 2 Echo
Object 2 Echo
Time
C
Z-axis (m)
Y-axis (m)
X-axis(m)
Z-axis
Y-axis
X-axis
G(0,0,0)
D
Solid Angle (deg)
Call times
Trial time (s)
E
Frequency (kHz)
Call
Echo Stream
Trial time (s)
F
Panel Perspective
Z-axis (m)
Y-axis (m)
X-axis (m)
G
Panel Perspective
Z-axis (m)
Y-axis (m)

Figure 5-2. Use of the echo model to determine the bat's ongoing sensory experiences. A. Cartoon of a bat flying through space encountering 2 obstacles. The bat's flight trajectory moves from right to left, and is indicated by the black dotted line. Two sonar vocalizations while flying are indicated by the gray cones. **B.** Reconstruction of sonar vocal times (top), and returning echo times (bottom) for the cartoon bat in panel a. Note that two echoes (blue and yellow) return to the bat following the first sonar vocalization, while only one echo (yellow) returns after the second vocalization, because the relative positions of the bat and objects change over time. **C.** One experimental trial of the bat flying and navigating around obstacles (large circular objects). The bat's flight path (long black line) starts at the right and the bat flies to the left. Each vocalization is indicated with a yellow circle, and the direction of the vocalization is shown with a short black line. **D.** Trial time versus solid angle to each obstacle for flight shown in A. Individual vocalizations are indicated with black circles, and the color of each line corresponds to the objects shown in A. **E.** Time expanded spectrogram of highlighted region in B. Shown are three sonar vocalizations, and the colored lines indicate the time of arrival of each object's echo as determined by the echo model (colors as in A). **F.** Snapshot of highlighted region in panel C showing the position of objects when the bat vocalized at that moment. **G.** Snapshot of highlighted region in panel C showing the position of objects when the bat vocalized at that moment.

Please note, Figure 5.2 has been reused here, from Chapter 4, to maintain continuity of the text.

the echo sources (Figure 5.2A – cartoon explains the echo model, with cones showing the sonar beam pattern, Figure 5.2B – the time series of call and echoes from the cartoon in Figure 5.2A; Figure 5.2C – actual bat flight trajectory with sonar vocalizations, orange circles, and 3D head aim vectors, black lines; Figure 5.2D and 2E – the instantaneous solid angles of the head aim with

respect to objects and echo arrival times of sonar returns from different objects along the trajectory in 2C; also see Methods).

In broad strokes, we first determined the onset of each vocalization produced by the bat, then the 3D position of the bat at the time of each sonar vocalization, and the 3D relative positions of flight obstacles. Past work has demonstrated that the big brown bat's sonar beam axis is aligned with its head (Ghose and Moss, 2003, 2006), and the direction of the sonar beam was inferred in our study from the head-mounted markers showing the head aim of the bat. We then referenced the 50 deg -6 dB width of the sonar beam at 30 kHz (Hartley and Suthers, 1989), and the time at which the sonar beam reflected echoes from flight obstacles in the animal's path. From this calculation, we computed the direction and time of arrival of all echoes returning to the bat's ears each time the animal emitted a sonar call. The echo model, therefore, was used to construct the instantaneous acoustic sensory space of the bat each time it vocalized and received echoes from physical objects in its flight path. The development of the echo model was a critical step in computing 3D spatial tuning of SC neurons recorded while the animal was in flight.

Although it is possible to use a wireless, head-mounted microphone to record the returning echo stream, there are significant limitations to this methodology. First, a single head-mounted microphone has a higher noise floor than the bat's auditory receiver. Moreover, a microphone would add weight to the devices carried by the bat in flight and could only provide information regarding echo arrival time. A head-mounted microphone is therefore insufficient to compute the 3D locations of echo sources, thus highlighting the importance of the echo model in our study to compute the bat's instantaneous 3D sensory space. We also computed errors in

the measurements of head-aim as well as in the estimation of echo arrival times at the bat's ears (Figure 5.2 - figure supplement 2). Our measurements indicate that the maximum error in the reconstruction of the bat head-aim does not exceed 5.5 degrees, and the error in echo arrival time measurement is between 0.35 and 0.65 ms (see Figure 5.2 - figure supplement 2C and D – estimation of errors in head-aim reconstruction, Figure 5.2 - figure supplement 2 – errors in echo arrival time; see Methods). To confirm that the echo model accurately calculated the 3D positions of sonar objects, we used echo playbacks from a speaker and microphone pair (see Methods, Figure 5.2 - figure supplement 2), with additional validation by using a microphone array placed behind the bat's flight direction. The microphone array recorded the echoes reflected off objects as the bat flew and produced sonar vocalizations, which were analyzed with time of arrival difference (TOAD) algorithms to compare the measured echo sources with the calculated echo sources based on our echo model (see Methods).

5.2.2 3D spatial tuning of single neurons in the SC of free flying bats

The spatial acoustic information (echo arrival times and 3D locations of echo sources) obtained from the echo model was converted into 3D egocentric coordinates to compute the acoustic stimulus space from the point of view of the flying bat as it navigated the room (Figure 5.1 - figure supplement 1F and G, see Methods). Bats were released from different locations in order to cover the calibrated volume of the flight room (Figure 5.3 - figure supplement 1A), and they continuously produced echolocation calls, which resulted in series of echoes from objects during each recording session (Figure 5.3-figure supplement 1A, B and C). We also released the bats from multiple locations in the room so that they to took a variety of flight paths through the

room, and interacted with the flight obstacles from a broad range of directions and distances, which is necessary for computing spatial receptive fields. These data therefore yielded measurements of echoes returning to the animal from objects at many different directions and distances in egocentric space (Figure 5.3 - figure supplement 1D - range coverage, E - azimuth coverage, and F - elevation coverage).

The output of the echo model was used to analyze audio/video-synchronized neural recordings from single units (see Figure 5.1E, Figure 5.1, supplement 1 and Methods) taken in the midbrain SC using a 16-channel wireless telemetry system. We recorded a total of 182 single neurons. We then classified neurons as sensory (n=67), sensorimotor (45), vocal premotor (n=26), or unclassified (n=44), as described in the Methods section. Here we focus on sensory neurons in the SC of free-flying bats. For all sensory neurons we first calculated the distance, or echo-delay tuning (Figure 5.3A and 3B). An example reconstruction of a neuron's spatial tuning along the distance axis is displayed in Figure 5.3B, showing neural activity aligned to sonar vocalization times (red arrows), and responses to echoes returning at ~10 ms delay. Arrival time of the first echo at the bat's ears is indicated with a green arrow, and a second returning echo (from another, more distant object) is indicated with a blue arrow. Note that this example neuron does not spike in response to the second echo, nor to echoes arriving very early (Figure 5.3C, top panel), or late (Figure 5.3C, bottom panel). Figure 5.3D shows the computed distance (echo-delay) tuning profile of this same example neuron.

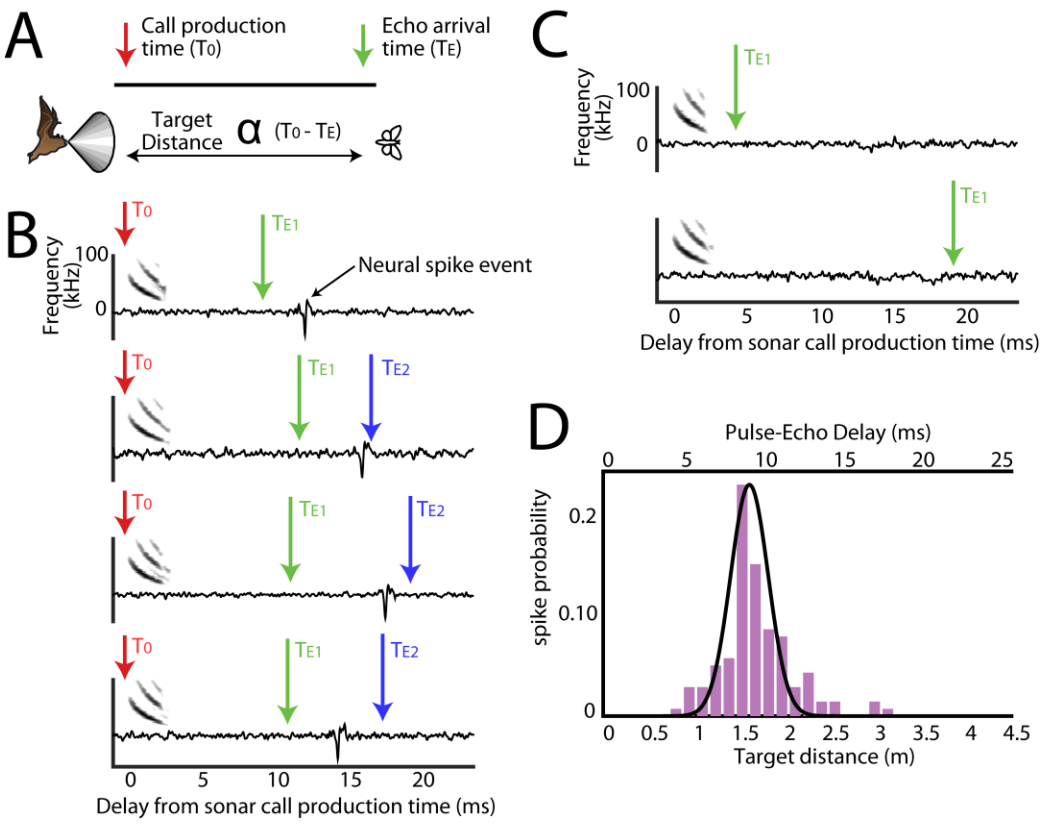

Figure 5-3. Range tuning of midbrain neurons. A. A cartoon representation showing the encoding of target range in echolocating bats. The time difference between the call production time (T0, red arrow) and the echo arrival time (TE, green arrow) is a function of target distance. **B.** Sensory responses to echo returning at a specific delay with respect to sonar vocal onset from actual trial data. The arrival time of the first echo (TE_1) is indicated with a green arrow, the second echo (TE_2 – from a more distant object) is indicated with a blue arrow. Note that this neuron responds to the echo arriving at ~10 milliseconds. **C.** When the echo returns at a shorter delay, the neuron does not respond; and the neuron similarly does not respond to longer pulse-echo delays. **D.** Histogram showing target distance tuning (i.e. pulse-echo delay tuning) for the neuron in panel B and C. Note the narrow tuning curve.

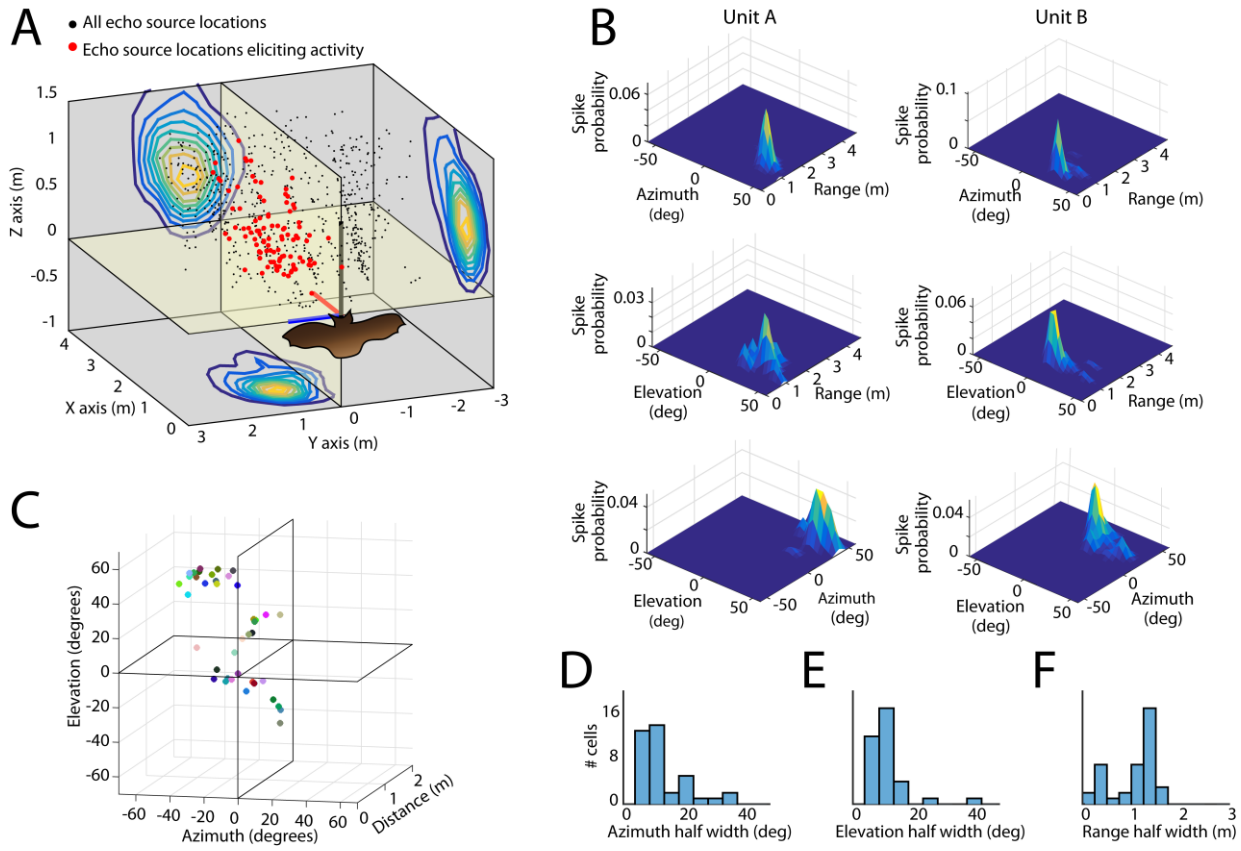

Figure 5-4. Spatial tuning of neurons recorded in the SC. A. Egocentric locations of echo sources eliciting activity from a single SC neuron. Red dots indicate echo source locations eliciting spikes, black dots indicate echo source locations where a spike is not elicited. Contour plots show the XY, YZ, and ZX projections of the spatial tuning of the neuron. **B.** 2D spatial tuning plots for two separate neurons (left column and right column). Shown are surface heat plots, where the size of the peak indicates the spike probability for a neuron for each 2D coordinate frame. **C.** Centers of 3D spatial tuning for 46 different neurons recorded in the SC. Different neurons are indicated by different colors. **D, E and F.** Left to right: azimuth, elevation, and range half width tuning properties for 46 different neurons recorded in the SC

Using the echo model, we also calculated the tuning profiles of each neuron in azimuth and elevation (Figure 5.3 - figure supplement 2A – azimuth and B – elevation). Once we calculated the azimuth, elevation, and distance tuning of neurons (Figure 5.4A), we constructed three-dimensional spatial response profiles for each neuron. Figure 5.4B shows surface plots of the three-dimensional tuning for two other example neurons. Of the 67 single sensory neurons (Bat A – 28 and Bat B – 39) recorded in the SC of two big brown bats, 46 neurons (Bat A -19 and Bat B – 27) in the data set showed selectivity to stimulus locations in 3D egocentric space (Figure 5.4C, see Methods for details about spatial selectivity analysis), and these spatial tuning profiles were stable within recording sessions (Figure 5.4 - figure supplement 1). Additionally, the selectivity of the neurons, in the distance dimension, did not vary as a function of dorsal-ventral location in the SC (Figure 5.4 – figure supplement 2). Further, 3 neurons were tuned to both azimuth and range, 2 to both range and elevation, and 5, 3 and 3 neurons tuned exclusively to range, azimuth and elevation, respectively (see Figure 5.4 - figure supplement 3). Best echo delays spanned values of 4 to 12 ms, corresponding to the distances of objects encountered by the bat (~70-200 cm) in our flight room (Figures 4D, 4E and 4F show histograms of standard deviations of normal fits to spatial receptive fields, also see Methods).

5.2.3 Adaptive sonar behavior modulates 3D spatial receptive fields

Guided by growing evidence that an animal's adaptive behaviors and/or attentional state can modulate sensory responses of neurons in the central nervous system (e.g. Bezdudnaya and Castro-Alamancos, 2014; Fanselow and Nicolelis, 1999; McAdams and Maunsell, 1999; Reynolds and Chelazzi, 2004; Spitzer et al., 1988; Winkowski and Knudsen, 2006; Womelsdorf et al., 2006), we investigated whether the bat's active sonar inspection in space alters the 3D sensory tuning

of SC neurons. We compared the spatial receptive fields of single SC neurons when the bat produced isolated sonar vocalizations (non-SSGs) to times when it adaptively increased sonar resolution by producing SSGs (Figure 5.5A – an example trial; non-SSGs, blue circles; SSGs, red circles; Figure 5.5B – spectrograms from the data in 6A, with SSGs again highlighted in red; Figure 5.5C – a plot where SSGs can be quantitatively identified, see Methods). We find that distance tuning is sharper to echo returns from the bat's production of SSGs, as compared to responses to echoes returning from single (non-SSG) calls (Figure 5.5D shows an example neuron). Figure 5.5E shows summary data comparing the sharpness of the distance tuning for SSG and non-SSG calls (n=56, all neurons which showed tuning in the distance dimension, see Methods), Supplementary File 1A – gives details of sharpness of distance tuning comparisons for SSG and non-SSG tuning, using the Brown-Forsyth test, for each of the neurons in Figure 5.5E. We also find that a neuron's best delay (target distance) is shifted to shorter delays (closer objects) when the bat is engaged in the production of SSGs, suggesting that distance tuning is dynamically remapped when the bat actively inspects objects in its environment (Figure 5.5D example). Figure 5.5F shows summary data, comparing the mapping of the distance tuning for SSG and non-SSG calls (n=56, all neurons which showed tuning in the distance dimension, see Methods). Supplementary File 1B – gives details of mean distance tuning comparisons for SSG and non-SSG tuning, using the Brown-Forsyth test. For each of the neurons in Figures 5E and 5F; blue points indicate cells with a significant sharpening as well as a decrease in peak distance tuning. Red points (Figure 5.5E) indicate cells which only show a significant sharpening of distance tuning, while green points (Figure 5.5F) indicate cells which only show a significant shifting of distance tuning. We also examined the responses to echoes returning from the first sonar vocalization of

an SSG versus the last vocalizations of an SSG. We find that there is no difference in spatial tuning profiles computed separately for the first and last echoes of SSGs, but there is a significant increase in spike probability in response to echoes from the last vocalization of an SSG (Figure 5.5 - figure supplement 1).

5.2.4 Gamma power increases during epochs of sonar sound group production

Similar to foveation, which is a behavioral indicator of visual attention to resolve spatial details (Reynolds and Chelazzi, 2004), measurements of adaptive sonar behavior have been used as a metric for the bat's acoustic gaze to closely inspect objects (Moss and Surlykke, 2010). Previous behavioral research shows that bats increase the production of sonar sound groups (SSGs) under conditions that demand high spatial resolution, e.g. in dense acoustic clutter and when tracking erratically moving targets (Kothari et al., 2014; Moss et al., 2006; Petrites et al., 2009; Sändig et al., 2014). SSG's are clusters of echolocation calls, often produced at stable rate (Figure 5.6A, see Methods), which are hypothesized to sharpen acoustic images of objects in the environment (Moss and Surlykke, 2010), and are distinct from the overall increase in sonar call rate of a bat approaching a target. Previous work in other systems has shown that the gamma frequency band (40-140 Hz -Sridharan and Knudsen, 2015) of the LFP in the SC increases in power when an animal is attending in space (Gregoriou et al., 2009; Gunduz et al., 2011; Sridharan and Knudsen, 2015), and we investigated whether this conserved indicator of spatial attention also appears during SSG production. Shown in Figure 5.6B is a comparison of gamma band activity during the bat's production of SSGs over non-SSGs, demonstrating an increase around the time of SSG production. Displayed is the call triggered average (+/- s.e.m.) of the gamma band across recording sites, for SSG (red, n = 539) and non-SSG (blue, n = 602)

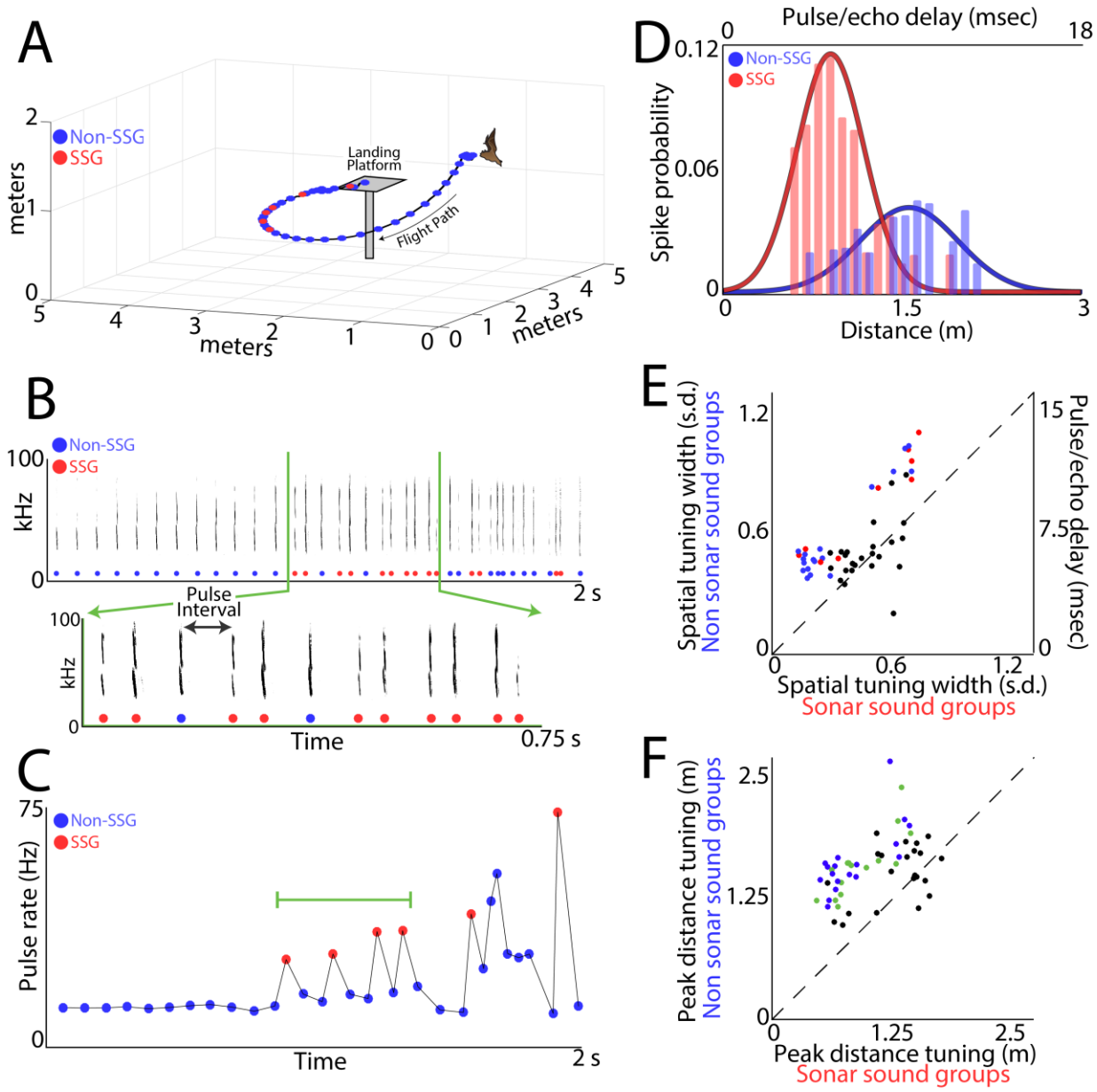
A
Non-SSG
SSG
meters
Landing Platform
Flight Path
B
kHz
Pulse Interval
Time
0.75 s
2 s
C
Pulse rate (Hz)
Time
2 s
D
Pulse/echo delay (msec)
Spike probability
Distance (m)
E
Spatial tuning width (s.d.)
Non sonar sound groups
Sonar sound groups
Pulse/echo delay (msec)
F
Peak distance tuning (m)
Non sonar sound groups
Sonar sound groups

Figure 5-5. Adaptive vocal behavior drives changes in spatial tuning of SC neurons. A. Three-dimensional view of one flight path (in black) through the experimental room. Individual sonar vocalizations that are not included in a sonar sound group (non-SSG) are shown as blue circles, with sonar vocalizations within a sonar sound group (SSG) are shown in red. **B.** Top, spectrogram of sonar vocalizations emitted by the bat in panel A. Bottom, expanded region of top panel to indicate SSGs and the definition of pulse interval. **C.** Change in pulse rate during the flight shown in panel A, and for the vocalizations shown in panel B. Note the increase in pulse rate indicative of SSG production. **D.** Change in spatial tuning of example neuron when the bat is producing SSGs (red) as opposed to non-SSGs (blue). Note that the distance tuning decreases, as well as the width of the tuning curve, when the bat is producing SSGs. E. Summary plot of change in spatial tuning width when the bat is producing SSGs (n = 56 neurons). Many single neurons show a significant sharpening (n=28) in spatial tuning width along the distance axis when the bat is producing SSGs and listening to echoes as compared to times when the bat is receiving echoes from non-SSG vocalizations. **F.** Summary plot of change in mean peak spatial tuning when the bat is producing SSGs. Many neurons also show a significant decrease in the mean of the peak distance tuning during the times of SSG production as compared to when the bat is producing single sonar vocalizations (non-SSGs). In E. and F, blue dots indicate neurons that show significant difference between SSG and non-SSG for both the spatial tuning width and peak range tuning. Green dots indicate neurons that show significant difference in distance tuning width between SSG and non-SSG. Red dots indicate neurons that show significant difference in peak distance tuning between SSG and non-SSG spatial tuning. Black dots indicate neurons that show no difference in spatial tuning width or peak range tuning for SSG's and non-SSG's.

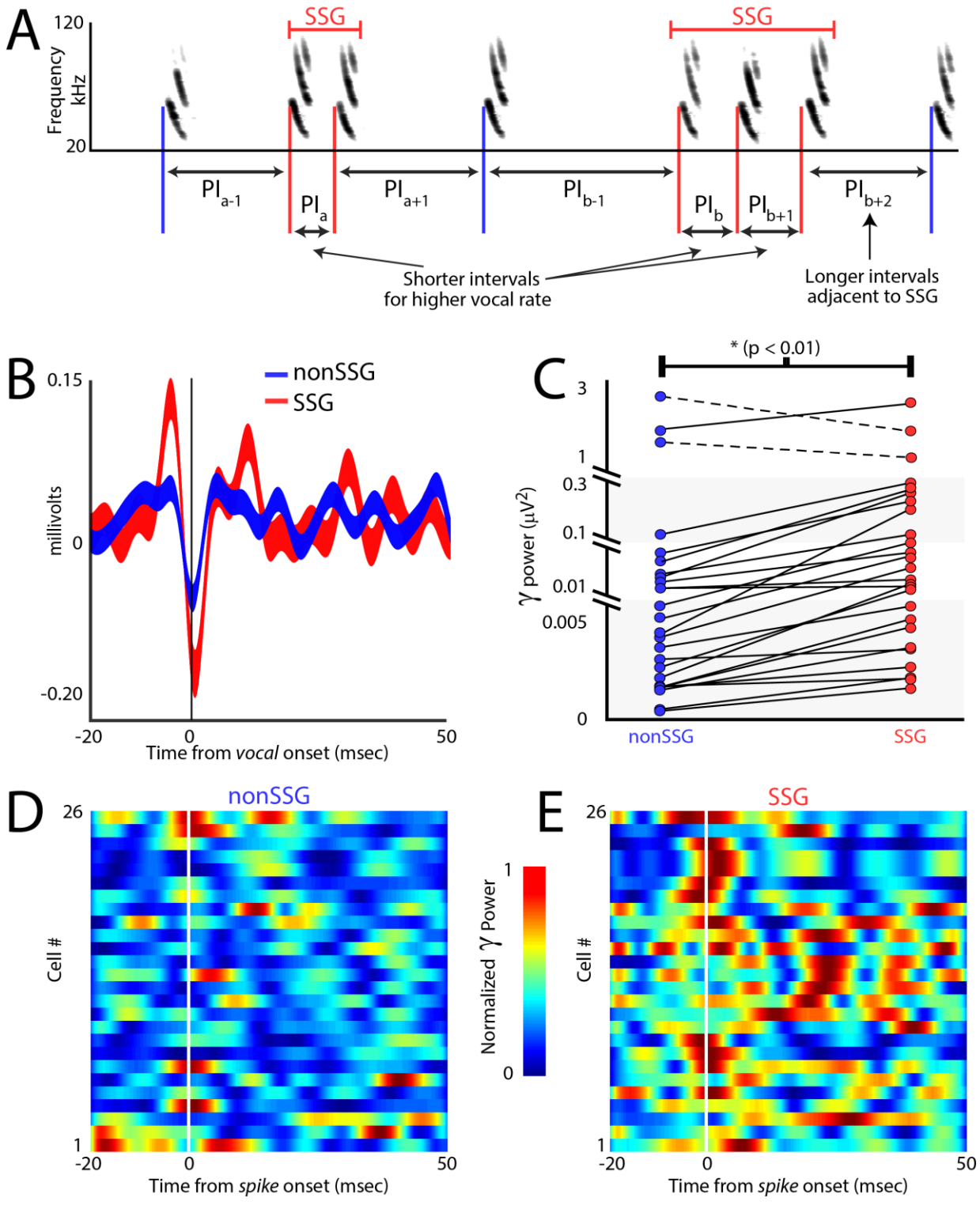
A
120
Frequency
kHz
20
SSG
SSG
PI a-1
PI a
PI a+1
PI b-1
PI b
PI b+1
PI b+2
Shorter intervals
for higher vocal rate
Longer intervals
adjacent to SSG
B
0.15
nonSSG
SSG
millivolts
0
-0.20
-20
0
50
Time from vocal onset (msec)
C
* (p < 0.01)
3
1
0.3
0.1
0.01
0.005
0
γ power (μV²)
nonSSG
SSG
D
nonSSG
26
Cell #
1
-20
0
50
Time from spike onset (msec)
E
SSG
26
Cell #
1
-20
0
50
Time from spike onset (msec)
Normalized γ Power
1
0

Figure 5-6. Increases in gamma power correlate with adaptive vocalizations for spatial attention. **A.** Schematic of sonar sound group (SSG) determination. SSG's are identified by brief epochs of higher vocal rate (i.e. shorter interval in red) surrounded by vocalizations at a lower rate (i.e. longer interval in blue). **B.** Average gamma waveform at the onset of single sonar vocalizations, or non-SSG's (blue, n = 26), compared to the average gamma waveform at the onset of vocalizations contained within an SSG (red, n = 26). Plotted is the mean +/- s.e.m. **C.** Pair-wise comparison of power in the gamma band during the production of non-SSG vocalizations (blue) and SSG vocalization (red). There is a significant increase in gamma power during SSG production across neurons (n = 26, Wilcoxon sign-rank rest, $p < 0.01$). **D.** Normalized increase in gamma power at the time of auditory spike onset for each neuron during the production of non-SSG vocalizations. **E.** Normalized increase in gamma power at the time of auditory spike onset for each neuron during the production of SSG vocalizations. Note the higher gamma power during SSG production, and the temporal coincidence of the increase in gamma with spike time (white line).

production. Figure 5.6C illustrates the significant increase in power of the gamma band during the production of SSGs (red) as compared to non-SSGs (blue) on a neuron-by-neuron basis (n = 26), and this finding was consistent across recording depths (Figure 5.6 - figure supplement 1). Only sites on which neural recordings were unaffected by motion artifact were used in this analysis (Figure 5.6, figure supplement 2, Also see Methods). In agreement with past work in other systems and brain areas (Gregoriou et al., 2009; Gunduz et al., 2011; Sridharan and Knudsen, 2015), there is a significant increase in gamma power when the bat produces SSGs,

providing further evidence that SSGs indicate times of sonar inspection and spatial attention (Figure 5.6C, $p < 0.005$, Wilcoxon sign-rank test).

Additionally, we analyzed the timing of gamma power increase with respect to echo-evoked neural activity. Because sensing through echolocation temporally separates vocal production time from echo arrival time, we can accurately measure the amplitude of gamma activity with respect to motor production and/or sound reception. The data show that the increase in gamma power occurs specifically around the time of the echo-evoked spike events in SC sensory neurons (Figure 5.6D – SSGs and 6E – non-SSGs, white line indicates onset of sensory evoked spikes), and that the increase in gamma band power is temporally precise, with the peak in gamma power occurring within 10 milliseconds of spike time.

5.3 DISCUSSION

Spatially-guided behaviors, such as obstacle avoidance, target tracking and reaching, all depend on egocentric sensory representations of the 3D positions of objects in the environment. An animal must not only compute the direction and distance to targets and obstacles, but also update this information as it moves through space. How does the nervous system of a freely moving animal encode 3D information about the location of objects in the physical world? And does active inspection of objects in the environment shape 3D sensory tuning? Our neural recordings from the midbrain of a freely moving animal engaged in natural, spatially-guided behaviors offer answers to these fundamental questions in systems neuroscience.

Here we present the first characterization of 3D sensory responses of single neurons in the midbrain SC of an animal actively interacting with its physical environment. We also show

that echo-evoked spatial tuning of SC neurons sharpens along the range axis and shifts to closer distances when the bat inspects objects in its acoustic scene, as indexed by the production of sonar sound groups (SSGs) (Falk et al., 2014; Kothari et al., 2014; Moss et al., 2006; Petrites et al., 2009; Sändig et al., 2014). It has been hypothesized that the bat produces SSGs to enhance spatial resolution, in a manner similar to foveal fixation to increase visual resolution (Moss and Surlykke, 2010; Surlykke et al., 2016). Our data provide the first empirical evidence of sharpened 3D spatial resolution of single neurons in the bat's auditory system with natural and dynamic adaptations in the animal's active orienting behaviors.

5.3.1 Role of SC in orienting in 3D space

The superior colliculus (SC), a midbrain sensorimotor structure, is implicated in species-specific sensory-guided orienting behaviors, target selection and 2D spatial attention (Duan et al., 2015; Knudsen, 2011; Krauzlis et al., 2013; Lovejoy and Krauzlis, 2010; McPeek and Keller, 2004; Mysore and Knudsen, 2011; Mysore et al., 2011; Zénon and Krauzlis, 2012). Past research has led to conflicting views as to whether the SC plays a role in orienting in 3D space (Chaturvedi and Gisbergen, 1998; Chaturvedi and van Gisbergen, 1999; Chaturvedi and Van Gisbergen, 2000; Hepp et al., 1993; Van Horn et al., 2013; Leigh and Zee, 1983; Walton and Mays, 2003), but limited evidence from sensory mapping in primates shows response selectivity to binocular disparity (Berman et al., 1975; Dias et al., 1991), and vergence eye movements (Chaturvedi and Gisbergen, 1998; Chaturvedi and van Gisbergen, 1999; Chaturvedi and Van Gisbergen, 2000; Van Horn et al., 2013). Here, we present the first direct evidence of 3D egocentric sensory responses to physical

stimuli in the midbrain of an animal freely moving through its environment. Our results therefore provide a critical bridge to understanding the brain's representation of the 3D physical world.

5.3.2 Behavioral and neural correlates of spatial attention

Psychophysical studies have reported that human and non-human primates show increased visual detection and discrimination performance when stimuli are presented at attended locations (Bichot et al., 2005; Carrasco, 2011; Posner, 1980; Wurtz and Mohler, 1976; Yeshurun and Carrasco, 1999). Neural recording experiments have corroborated these results by showing that spatial attention modulates firing rates of cortical neurons representing the attended locations (McAdams and Maunsell, 1999; Reynolds and Chelazzi, 2004; Reynolds et al., 1999; Spitzer et al., 1988; Womelsdorf et al., 2006). Other studies report an increase in the gain of tuning curves at an attended location or a selected stimulus feature, while a decrease in neural response occurs for unattended locations or features (McAdams and Maunsell, 1999; Treue and Trujillo, 1999; Verghese, 2001). The SC has been specifically implicated in an attention network through past studies of SC inactivation that produced behavioral deficits (Lovejoy and Krauzlis, 2017; McPeek and Keller, 2004), but these studies did not measure spatial selectivity of single SC neurons under conditions in which animals freely inspected objects in the physical environment. Evidence for sharpening of tuning curves and/or remapping spatial receptive fields with attention has been limited to a few studies showing shifts in 2D cortical tuning to artificial visual stimuli in restrained animals (Spitzer et al., 1988; Womelsdorf et al., 2006). In the auditory system, behavioral discrimination of acoustic stimuli has been shown to influence the response profiles of cortical neurons in restrained ferrets (Fritz et al., 2003, 2007). Here we report for the first time

dynamic shifts in 3D sensory tuning with sonar-guided attention in animals engaged in natural orienting behaviors.

Our study not only reveals changes in single neuron 3D spatial selectivity with dynamic sonar inspection of objects in the physical scene, but also a corresponding increase in the gamma band of the local field potential (LFP). Past work in humans, non-human primates, other mammals, and birds have reported stimulus driven gamma band modulation by attention when stimuli are presented at attended locations (Fries et al., 2001; Goddard et al., 2012a; Gregoriou et al., 2009; Sridharan and Knudsen, 2015; Sridharan et al., 2011). Moreover, changes in the gamma band of the LFP have been shown to occur for stimulus selection and discrimination mediated by touch, vision, and hearing, suggesting that gamma oscillations may reflect multi-modal network activity related to attention (Bauer et al., 2006; Canolty et al., 2006; Gruber et al., 1999; Senkowski et al., 2005). Our findings that gamma power increases during epochs of SSG production and echo reception support the hypothesis that the bat's adaptive sonar behaviors serve as indicators of spatial attention (Moss and Surlykke, 2010).

5.3.3 3D allocentric versus 3D egocentric representations in the brain

It is important to emphasize the distinction between our report here on 3D ***egocentric sensory responses*** in the midbrain SC of the echolocating big brown bat, and 3D ***allocentric memory-based representation*** of space in the hippocampus of the Egyptian fruit bat (Yartsev and Ulanovsky, 2013). These two distinct frames of reference are used for different suites of natural behaviors. ***Egocentric sensory representation*** of space contributes to overt and covert orienting to salient stimuli; whereas, 3D allocentric (Geva-Sagiv et al., 2015; Yartsev and

Ulanovsky, 2013) and vectorial representations (Sarel and Finkelstein, 2017) in the bat hippocampus support spatial memory and navigation. In other words, past work on the bat hippocampus shows 3D spatial memory representation, whereas our work presented here reveals important new discoveries of dynamic midbrain sensory representation of 3D object location for orienting behaviors.

5.3.4 Depth tuning of single neurons in the bat auditory system

Finally, and importantly, our results fill a long-standing gap in the literature on the neural representation of target distance in the bat auditory system, which has almost exclusively been studied in passively listening animals (Dear and Suga, 1995; Feng et al., 1978; O'Neill and Suga, 1979; Valentine and Moss, 1997), but see Kawasaki et al., 1988 and Metzner, 1989. Echolocating bats estimate target distance from the time delay between sonar call emission and echo reception, and show behavioral range discrimination performance of less than 1 cm, which corresponds to an echo delay difference of about 60 µsec (Moss and Schnitzler, 1995; Simmons, 1973). The bat's sonar signal production is therefore integral to target ranging, and yet, for over nearly four decades of research, scientists have simulated the dimension of target distance in neural recording experiments by presenting pairs of synthetic sound stimuli (P/E pairs – pulse/echo pairs), one mimicking the echolocation call, and a second, delayed and attenuated signal, mimicking the echo. Here, we report the first delay-tuned neural responses to echoes from physical objects in the auditory system of free-flying bats, thus providing a critical test of a long-standing hypothesis that neurons in actively echolocating bats respond selectively to echoes from objects in 3D space.

Beetz et al. (2016a) report that distance tuning of neurons in the auditory cortex of passively listening, anesthetized bats (*Carollia perspicillata)* is more precise when neurons are stimulated with natural sonar sequences, such as those produced by echolocating bats in the research reported here. Another study of auditory cortical responses in anesthetized bats (*Phyllostomus discolor*) reports that delay-tuned neurons shift their receptive fields under stimulus conditions that simulate echo flow. (Bartenstein et al., 2014). In a related study, Beetz et al. (2016b) show a higher probability of neural firing in cortical neurons of the bat species *Carollia perspicillata* to the first echo in a sequence, which leads them to hypothesize that global cortical inhibition contributes to the representation of the closest object, without active attention. It is possible that global cortical inhibition is an intrinsic feature, which enables an animal to represent the most salient (in the above case, closest) stimulus. Our data also show that sensory neurons respond primarily to the first echo arriving in a neuron's receptive field, as compared to later echoes, and may depend on a similar mechanism. A mechanism of global inhibition for selective attention has been demonstrated in the barn owl optic tectum (Mysore et al., 2010). Additionally, our data demonstrate a higher probability of auditory responses in the midbrain SC to echoes returning from the last echo of a SSG, a finding, which can only be demonstrated in a behaving echolocating bat, as it involves feedback between sensing and action. And while studies of auditory cortical processing in anesthetized, passively listening animals can shed light on sensory processing mechanisms, ultimately this information must be relayed to sensorimotor structures, such as the midbrain superior colliculus, which serve to orchestrate appropriate motor commands for spatial navigation and goal-directed orientation.

Our study reveals the novel finding that auditory neurons in awake and behaving echolocating bats show shifts in receptive field with echolocation call dynamics in animals orienting to objects in space. Crucially, because bats in our study were engaged in a natural spatial navigation task, we could directly investigate the effects of sonar-guided attention on the 3D spatial tuning of single auditory neurons. Our results demonstrate the dynamic nature of 3D spatial selectivity of single neurons in the SC of echolocating bats and show that active behavioral inspection of objects not only remaps range response areas, but also sharpens depth tuning. Furthermore, our data reveal echo-delay tuning of single SC neurons in response to echoes from actively echolocating bats is sharper than previously reported from recordings in passively listening bats (Dear and Suga, 1995; Menne et al., 1989; Moss and Schnitzler, 1989; Simmons et al., 1979, 1990; Valentine and Moss, 1997) and bear relevance to a long-standing controversy on the neural basis of fine echo ranging acuity of bats (Menne et al., 1989; Moss and Schnitzler, 1989; Simmons, 1979; Simmons et al., 1990).

In summary, our study generated new discoveries in the field of systems neuroscience by integrating chronic neural recordings, multimedia tracking of dynamic animal behaviors in the 3D physical environment and modeling. We report here the first empirical demonstration that auditory neurons in a freely moving animal encode the 3D egocentric location of objects in the real world and dynamically shift spatial selectivity with sonar-guided attention. Specifically, we show that single neurons in the actively echolocating, free-flying bat respond selectively to the location of objects over a restricted distance (echo delay), azimuth and elevation. Importantly, we discovered that the sensory response profiles of SC neurons become sharper along the range

axis and shift to shorter distances (echo delays) when the bat actively inspects physical objects in its environment, as indicated by temporal adjustments in its echolocation behavior. Our findings not only reveal dynamic 3D sensory representations in freely behaving animals, but also call for comparative studies in other species, which can collectively contribute to a more complete understanding of nervous system function in the context of natural behaviors.

5.4 METHODS

5.4.1 Bats

Two adult big brown bats, Eptesicus fuscus, served as subjects in this study. Bats were wild caught in the state of Maryland under a permit issued by the Department of Natural Resources and housed in an animal vivarium at the University of Maryland or Johns Hopkins University. Both the University of Maryland's, and Johns Hopkins University's Institutional Animal Care and Use Committee approved all of the procedures utilized for the current study.

5.4.2 Experimental design

The two big brown bats were trained on related tasks, carried out in a 6 x 6 x 2.5 m room, illuminated with IR and equipped with 16 high-speed cameras and an ultrasound microphone array (Figure 5.1, see below). The first bat was trained to navigate around objects in a large flight room and land on a platform. In order to ease the task for the second bat, we trained it to fly around the room, navigate around objects, and land on any wall. Both bats were fed mealworms at the end of each trial to keep them motivated, but they were not rewarded for flight. The flight

room was illuminated with infrared lighting (~850 nm) to preclude the bat's use of vision, ERG data show that Eptesicus does not see wavelengths longer than 600 nanometers (Hope and Bhatnagar, 1979). The room was also equipped with high-speed cameras and an ultrasound microphone array to track the bat's flight path and record the bat's echolocation behavior. Bats navigated around obstacles in the room (explained in detail below), and were released at different locations in the room for each trial, which required them to use sonar echoes to steer around obstacles rather than a consistent or memorized flight path around objects in the room (see Figure 5.3 - figure supplement 1A). As such, the bats determined the duration and flight path of each trial. The obstacles were four plastic cylinders (hard plastic as to be acoustically reflective), approximately 13 cm in diameter and 30 cm in length.

Once the bat flew freely throughout the room and in the case of Bat A, learned to land on a platform, a surgery was performed to implant in the midbrain superior colliculus (SC) a 16-channel chronic recording silicon probe (Neuronexus) mounted on a custom microdrive. The bats' weights were between 18 and 21 grams, and the weight of the implant, microdrive and transmitter device was 3.8 grams. The bat was given several days to rest and acclimate to the implanted device, after which they were able to fly and navigate around objects in the flight room. Data collection began after the animal was able to perform ~30 flight trials per session, which took place twice a day (morning and afternoon) in the experimental test room. Bat A flew for 12 sessions, and Bat B flew for 15 sessions. For each recording session, the positions of the 4 flight obstacles were varied. Further, across trials the bat was released from different locations in the room. The obstacle configurations and flight start locations were varied to ensure that the bat's flight trajectories covered the entire room, and the stimulus space sampled by the bat

changed from trial to trial. This approach prevented the bats from relying on spatial memory and/or stereotyped flight paths. Figure 5.3 - figure supplement 1A shows the bat's flight trajectories in a single session and illustrates room coverage. Coverage was restricted in elevation, due to the height of the flight room, with a floor to ceiling dimension of approximately 250 cm. Although the landing behavior of the bats differed slightly (i.e. landing on a platform vs. a wall), neural analysis was focused on the times when the animals were in flight and the data from the two bats are comparable. Additionally, both bats performed natural echolocation and flight behaviors as neural recordings were taken.

5.4.3 Video recording

The flight trajectory of the bat was reconstructed using a motion tracking system with 16 high-speed cameras (Vicon). The motion tracking system was calibrated with a moving wand-based calibration method (Theriault et al., 2014), resulting in sub-millimeter accuracy and 3D spatial location information of the bat at a frame rate of 300 Hz. Once the motion tracking system is calibrated, it tracks the bat in a 3D coordinate frame of reference, which we refer to as 'world coordinates.' Affixed on the dorsal side of the transmitter board were three IR reflective markers (3 mm round) that were then tracked with the high-speed motion tracking system (Vicon). By tracking the 3D position of these three markers, we were able to determine the 3D position and head aim of the bat during the experiment. Around the perimeter of the room, at a distance from the walls of about 0.5 meters, the motion capture cameras did not provide adequate coverage, and data from the bat at these locations was not used for analysis.

5.4.4 Audio recordings

In addition to recording the position of the bat, we also recorded the sonar calls of the bat using an array of ultrasonic microphones (Pettersson Elektronik, Ultrasound Advice, see Figure 5.1A). The microphone recordings were hardware bandpass filtered between 10 KHz and 100 KHz (Alligator Technologies and Stanford Research Systems) and were digitized using data acquisition systems (National Instruments + custom built hardware).

5.4.5 Synchronization of systems

All three hardware systems (i.e. neural recording, video-based 3D positioning, and microphone array) were synchronized using the rising edge of a square pulse generated using a custom circuit. The square pulse was manually triggered at the end of each trial (i.e. at the end of each individual flight) when the bat landed on the platform/wall. At the generation of the TTL pulse, each system (video and audio) saved 8 seconds of pre-buffered data into the hard disk of the local computer.

5.4.6 Surgical Procedure, neural recordings and spike sorting

Once the bats were trained on the task, a surgery was performed to implant a 16-channel silicon probe (Neuronexus). The probe consisted of four shanks spaced 100 □m micrometers apart, with four recording sites also spaced 100 □m apart on each shank, resulting in a 300 x 300 square □m grid of recording sites. The silicon probe was connected by a ribbon cable to an electrical connector (Omnetics), and this assembly was then mounted on a custom-made, manual microdrive so that it could be moved through the dorsal/ventral axis (i.e. across layers) of the

superior colliculus during the experiment. The silicon probe and microdrive assembly was then mounted on the head of the bat over a craniotomy performed above the superior colliculus (SC). The SC sits on the dorsal surface of the brain of the big brown bat (Valentine and Moss, 1997; Valentine et al., 2002), allowing for skull surface landmarks to be used in determining the implant location. Once the recording implant was positioned, a cap was made with cyanoacrylate (Loctite 4013) to protect and secure the implant to the skull surface. The bat was allowed several days to recover, and then we started running the neural recording experiment.

In order to study neural activity in the superior colliculus during a real-world navigation task, a wireless neural-telemetry system (Triangle BioSystems International) was used in conjunction with a multi-channel neural acquisition platform (Plexon). This allowed for chronic neural recordings to be collected from the superior colliculus (SC) while the echolocating bat was navigating around obstacles in flight. During the experiment, a wireless RF telemetry board (Triangle BioSystems International) was connected to the plug of the silicon probe mounted on top of the bat's head. Bat A flew for 12 sessions while recordings were made in the SC, and Bat B flew for 15 sessions. Each session typically lasted 30-45 minutes, and the microdrive was advanced at the end of each session to collect activity from a new set of neurons in the following recording session.

Neural data were sorted offline after filtering between 800 and 6000 Hz using a 2nd order elliptic filter. Filtered neural traces were then sorted using a wavelet based algorithm and clustering technique (Quiroga et al., 2004). This algorithm also separated movement artifact out of the raw neural traces. If any spike events occurred simultaneously with movement artifact, however, they were not recoverable. Movement artifact rarely occurred across all channels during flight,

and was mostly confined to times when the bat was landing. We only used data from the bats in flight for analysis. Of all sorted single units (n = 182), 67 units (sensory neurons) were selected for analysis, as described below. The isolated single units were stable throughout the session (see Figure 5.1 - figure supplement 1).

5.4.7 Analysis of audio recordings

Audio recordings were analyzed using custom Matlab software to extract the relevant sound features, i.e. pulse timing, duration, and interval. Combining the pulse timing (time when sound reached a stationary microphone) with the 3D flight trajectory data allowed compensating for the sound-propagation delays and calculating the actual call production times at the source (i.e. the veridical time when the bat produced the sonar sound).

5.4.8 Identification of sonar sound groups

Sonar sound groups (SSGs) are defined as clusters of two or more vocalizations which occur at a near constant PI (within 5% error with respect to the mean PI of the sound group), and are flanked by calls with a larger PI at both ends (at least 1.2 times larger) (Kothari et al., 2014; Moss and Surlykke, 2001; Moss et al., 2006). SSGs of two vocalizations are also produced by the bat, and our criteria for these SSGs is that surrounding PI's must be at least 1.2 times larger than the PI between the 2 vocalizations contained within the SSG. Here, we use the same definitions and thresholds as used in prior work (see Figure 5.6A for a visual explanation). As we use pulse rate in the main text, it is important to note that Pulse Interval = 1/Pulse Rate.

5.4.9 Echo model

The details of the echo model have already been discussed in the previous chapter, Chapter 4.

4.3.1 Classification of neurons into sensory, sensorimotor and vocal-premotor cells

In order to classify neurons, we developed an algorithm based on variability in the firing latency distributions of spike times with respect to echo arrival time, previous call production time, and next call production time. In simple terms, this algorithm measures the variability in spike latencies to echo time and call time (previous and next) as a way of classifying neurons as sensory, vocal premotor or sensorimotor. This determination was based on the assumption that a neuron's activity is most temporally coupled with its functionally relevant event. If a neuron's spike latency distribution was sharpest with respect to echo arrival time, it was classified as sensory; if spike latencies were sharpest with respect to pulse time, the neuron was classified as vocal premotor, and if spike latencies showed clustering around pulse time and echo arrival times, it was classified as sensorimotor. It is important to mention that for sensory neurons we further solved the problem of echo assignment by only considering neurons that fire for the first arriving echo and do not exhibit activity for subsequent echo events (see Figure 5.3). This also solves the problem of wall/camera/microphone echoes, as they were the last to arrive. More than 90% of the sensory neurons analyzed in this study responded only to the first echo. For the remaining neurons that responded to a cascade of echoes (about 10% of those sampled), it was not possible to reliably assign their activity to specific echo arrival times and we therefore

excluded them from the data reported in this paper. Using this algorithm, the 182 recorded neurons were classified as sensory (n-67), vocal premotor (n=26) and sensorimotor (n=45). Classification into sensory, sensorimotor and premotor categories is common for SC neurons (Mays and Sparks, 1980; Schiller and Koerner, 1971). The remaining 44 neurons were unclassified. 3D spatial tuning profiles were only constructed for the sensory neurons (n = 67).

4.3.2 Construction of 3D spatial response profiles

Once a neuron was identified as sensory (see above criterion), direction information from the echo model was converted into egocentric coordinates of the bat's instantaneous position and the X, Y and Z information was converted into azimuth, elevation and range coordinates. Further, we test spatial selectivity based on an ANOVA ($p < 0.05$) performed along each dimension (azimuth, elevation and range). Only cells which pass the ANOVA for each dimension are used for further analysis. Neural responses of cells that pass the spatial selectivity test were normalized based on the amount of coverage in each of these dimensions, as explained below.

The spatial response profiles (for neurons which pass the spatial selectivity test (see above) were then normalized using the stimulus space, i.e. the time spent by the animal, in each dimension (see Figure 5.3-figure supplement 1D – range, E – azimuth and F – elevation): that is, the spike-count spatial response profile was divided by the time-spent spatial profile, to yield a spiking probability per bin in each dimension (distance, azimuth, and elevation). Regions of the stimulus space with echo events per bin less than 1 standard deviation from the mean were excluded from the computations (indicated by open bins in Figure 5.3-figure supplement 1D, E and F). Finally, normalized spatial response profiles in each dimension were then fit to a Gaussian function using

the fit function in Matlab. Spatial response profile means, half widths and standard deviations are then taken from the Gaussian fit.

Out of the 67 sensory neurons (see criterion above), overlapping populations of neurons showed either 3D, 2D or 1D spatial selectivity. 46 neurons (Bat A -19 and Bat B – 27) showed spatial selectivity in 3D (azimuth, elevation and depth). Further, 56, 52 and 51 neurons showed 1D spatial selectivity, for depth, azimuth and elevation, respectively. Figure 5.4 - figure supplement 2 describes the complete distribution of 3D, 2D and 1D neurons.

4.3.2.1 Stability of 3D spatial receptive fields:

Further, we determined the stability of receptive fields for individual 3D tuned neurons (n=46) by comparing the spatial tuning for the first and second half of recording sessions. 37 neurons showed significant 3D spatial selectivity for both the first and second half (see above methods for details). Firing is sparse in the auditory system of echolocating bats, we believe that because of this sparse firing, 9 neurons (out of 46) did not show significant spatial tuning (in either the first or second half of the recording session) as a result of limited amount of data in either the first or second half of the recording session. On comparing the selectivity for the first and second half of the recording session, 33 neurons did not show any change in peak tuning along any dimension. Only 4 neurons showed a significant change in tuning across the session (2 in the distance dimension and 1 each in the azimuth and elevation dimension), thus demonstrating that a majority of the neurons have stable receptive fields across the recording session. Figure 5.4, figure supplement 1, shows the stability of spatial tuning for the depth dimension. Red dots

indicate neurons that show a significant change in depth tuning across the first and second half of the recording session.

Neural selectivity was analyzed only with respect to spatial selectivity along the X, Y, and Z dimensions. The bat's echolocation calls are wide-band frequency modulated sounds, which are well suited to evoke activity from SC neurons that respond well to broadband acoustic stimuli. Since variations in the bat's own calls evoked echoes that stimulated SC neurons, we could not systematically analyze responses to other stimulus dimensions, such as sound frequency or intensity. Stimulus selectivity of SC neurons in the bat to non-spatial acoustic parameters will be the topic of a future study.

4.3.3 SSG and non-SSG analysis.

Separate range tuning profiles are computed for each cell for SSG and non-SSG vocalizations. Variance (sharpening) of SSG and non-SSG tuning profiles was tested using the non-parametric Brown-Forsythe test of variance at the α level of 0.05. The test results for each cell are described in detail in table ST1 (also see Figure 5.5E). Also, SSG and non-SSG distance tuning curves were tested using the Wilcoxon rank-sum test. Test statistic details for each cell is given in table ST2 (also see Figure 5.5F).

4.3.4 Local field potential.

The local field potential (<300 Hz) was extracted from each channel recording using 2nd order elliptical filters. Further, we analyzed the gamma band (50-140 Hz) (Goddard et al., 2012;

Sridharan and Knudsen, 2015) to investigate whether the epochs when the bat produced sonar sound groups (SSGs) were correlated with gamma band activity. We first identified channels without distortions in the LFP as a result of movement artifact (Figure 5.6 – figure supplement 2). We then extracted 100 ms spike triggered LFP windows from corresponding recording sites. We separated these into SSG and non-SSG events and averaged these separately to estimate the root mean squared (RMS) gamma band power (Jaramillo and Zador, 2011) (Figure 5.6A and 6B) when the bat produced SSG and non-SSGs. Further, to investigate the timing of the gamma signal (Figure 5.6C and 6D), the averaged gamma band amplitude envelope was normalized across SSG and non-SSG trials across each neuron. A Gaussian was fit to each time waveform to estimate the peak. The average of the peaks across all units was taken as the average latency of the LFP following the spike event.

We also examined whether movement artifact from the bat's wing beats could have corrupted the LFP analysis. The bat's wingbeat is approximately 12 Hz, whereas the frequency range for the Gamma band we analyzed was 50-140 Hz. The 3rd harmonic of the wingbeat, which would be in the frequency range of the Gamma band, was significantly attenuated. To further ensure that movement artifact did not corrupt the analysis of the LFP, we chose channels where the power ratio between the low frequency band (10-20 Hz) and the gamma band was less than 6 dB. We identified 21 such, low noise, channels (see Figure 5.6, figure supplement 2), which were then used for further analysis.

Figure supplements (Titles and legends), Tables and Movies

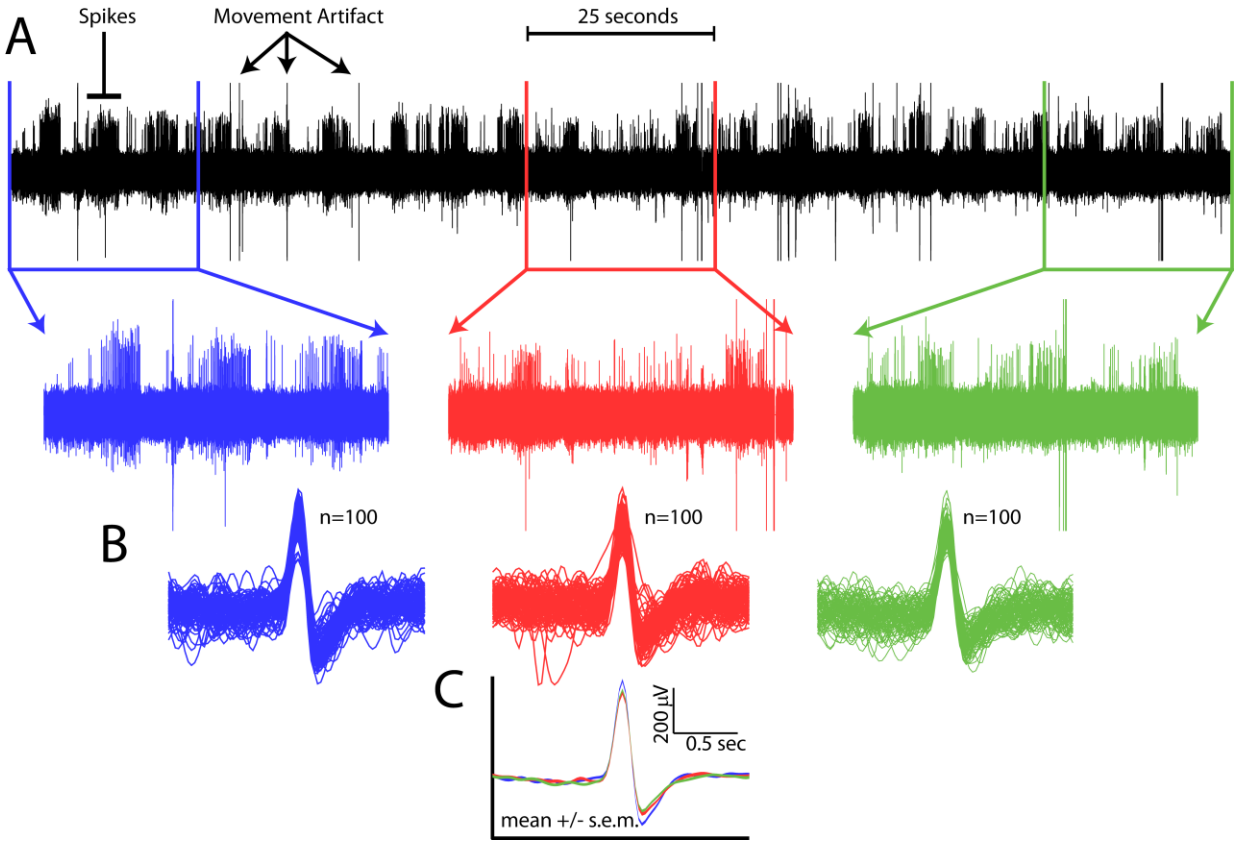

Figure 5.1-figure supplement 1. Spike waveform consistency throughout a single recording session. A. Top, all data from a single channel from a single recording session. Spikes and movement artifact are indicated. Bottom, time expanded portions of the beginning (blue), middle (red), and end (green) of the recording session. **B.** 100 randomly selected spikes from the beginning (blue), middle (red), and end (green) of the recording session. **C.** Mean +/- s.e.m. of spike waveforms for the beginning (blue), middle (red), and end (green) of the recording session.

Figure 5.2-figure supplement 1. Head aim reconstruction.

Please refer to Figure 4.2 (Chapter 4)

Figure 5.2-figure supplement 2. Error analysis and validation of the echo-model. A.

Please refer to Figure 4.5 (Chapter 4)

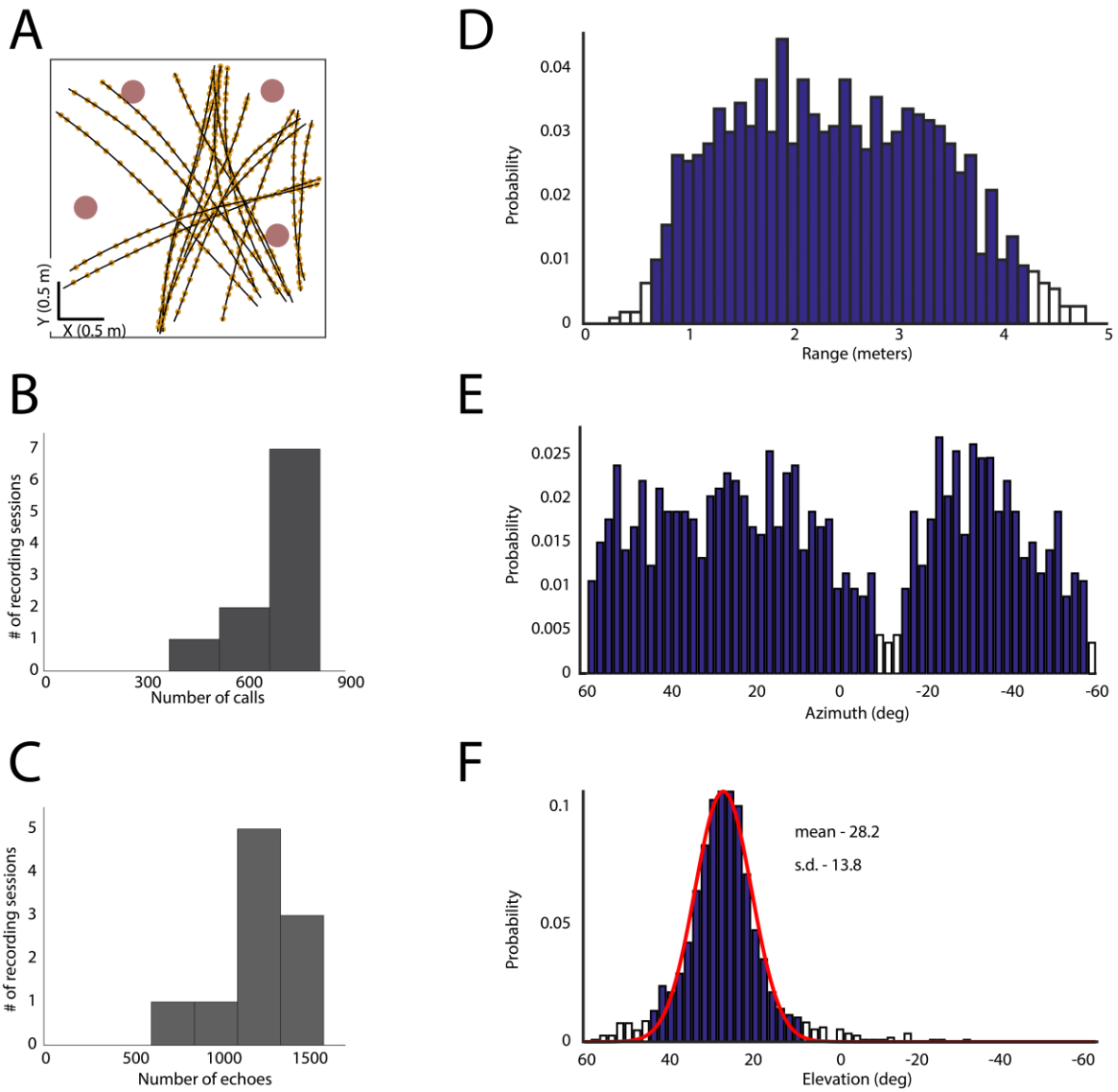

Figure 5.3-figure supplement 1. Spatial coverage during the experiment. A. Flight paths (black lines), vocalizations (yellow dots) and obstacles (pink circles) for one recording session. **B.** Histogram of calls per recording session. **C.** Histogram of number of echoes per recording session. **D.** All egocentric azimuthal angles for obstacles encountered in flight. **E.** All egocentric ranges for obstacles encountered in flight. **F.** All egocentric elevation angles for obstacles encountered in flight.

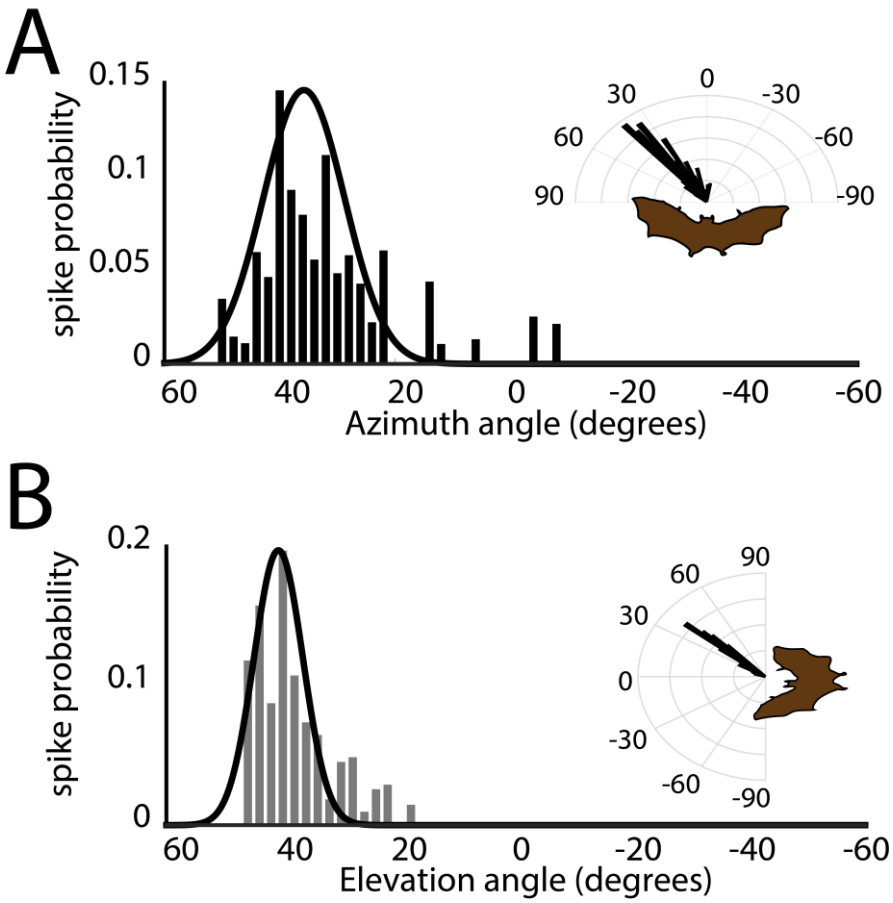

Figure 5.3-figure supplement 2. Spatial tuning in azimuth and elevation. A. Histogram of azimuthal tuning for the neuron in **Figure 5.3B**. Inset is a polar-plot representation of azimuthal tuning. **B.** Histogram of elevation tuning for the neuron in panel Figure 5.3B. Inset is a polar-plot representation of elevation tuning. Note the narrow tuning curves.

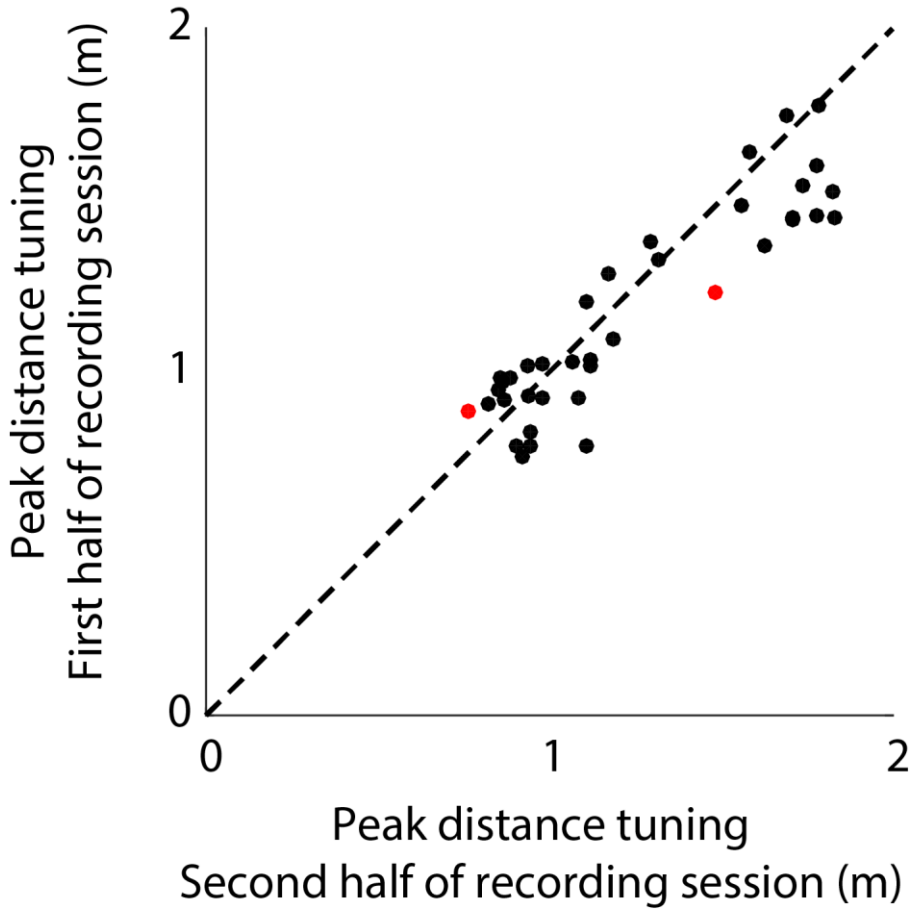

Figure 5.4-figure supplement 1. Stability of distance tuning across the first and last half of each recording session. Shows the comparison of peak distance tuning of neurons (n=37) for the first and second half of each recording session. Dots in red indicate neurons, which show significant change in distance tuning across the session. Black dots indicate, which have stable distance tuning. See Methods for details.

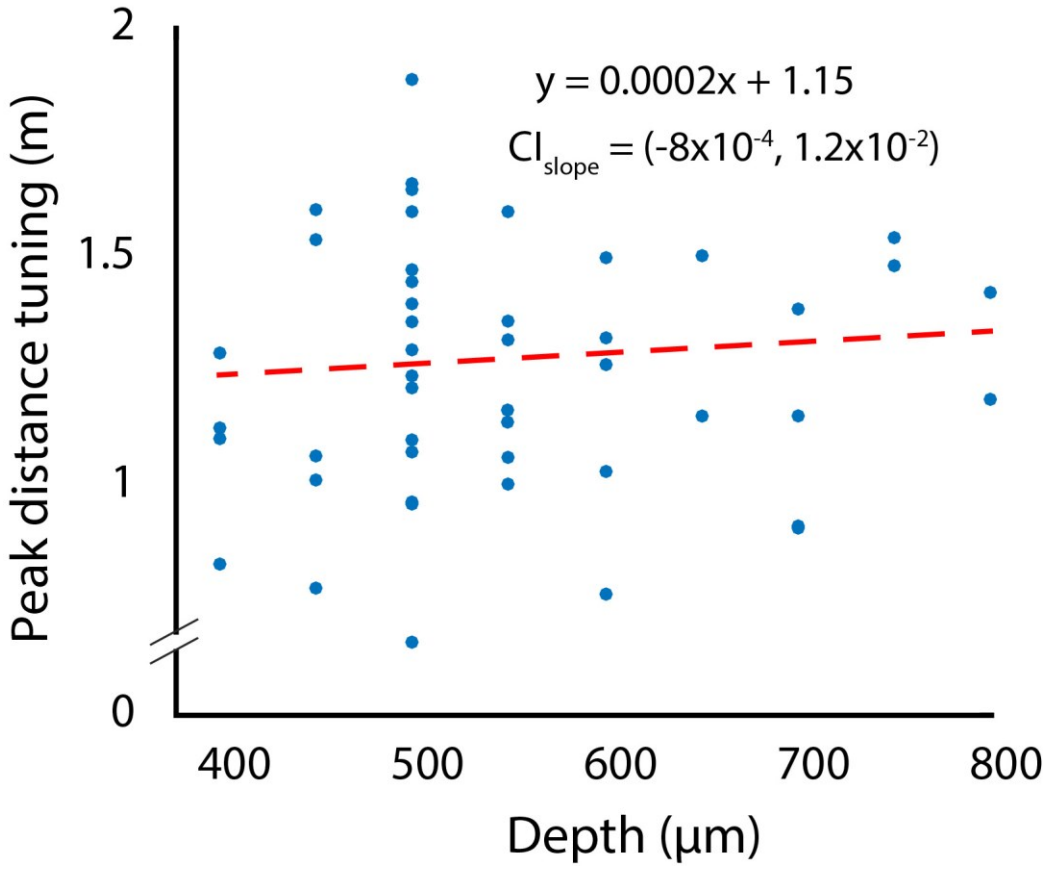

Figure 5.4-figure supplement 2. Changes in depth tuning as a function of recording depth. CI_{slope} indicates the 95% confidence interval of the slope fitted using bootstrapping.

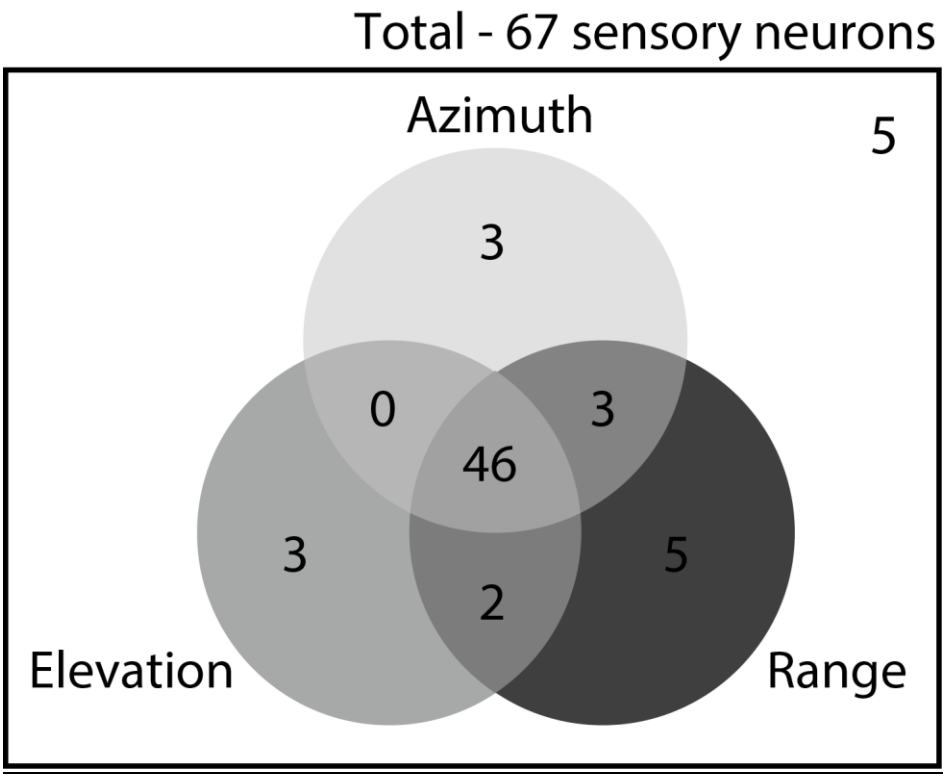

Figure 5.4-figure supplement 3. Distribution of cells showing 3D, 2D and 1D spatial tuning. Out of the 67 sensory neurons (see criterion above), overlapping populations of neurons showed either 3D, 2D or 1D spatial selectivity. 46 neurons showed spatial selectivity in 3D (azimuth, elevation and depth). Further, 56, 52 and 51 neurons showed 1D spatial selectivity, for depth, azimuth and elevation, respectively. Figure 5.4 - figure supplement 2 describes the complete distribution of 3D, 2D and 1D neurons.

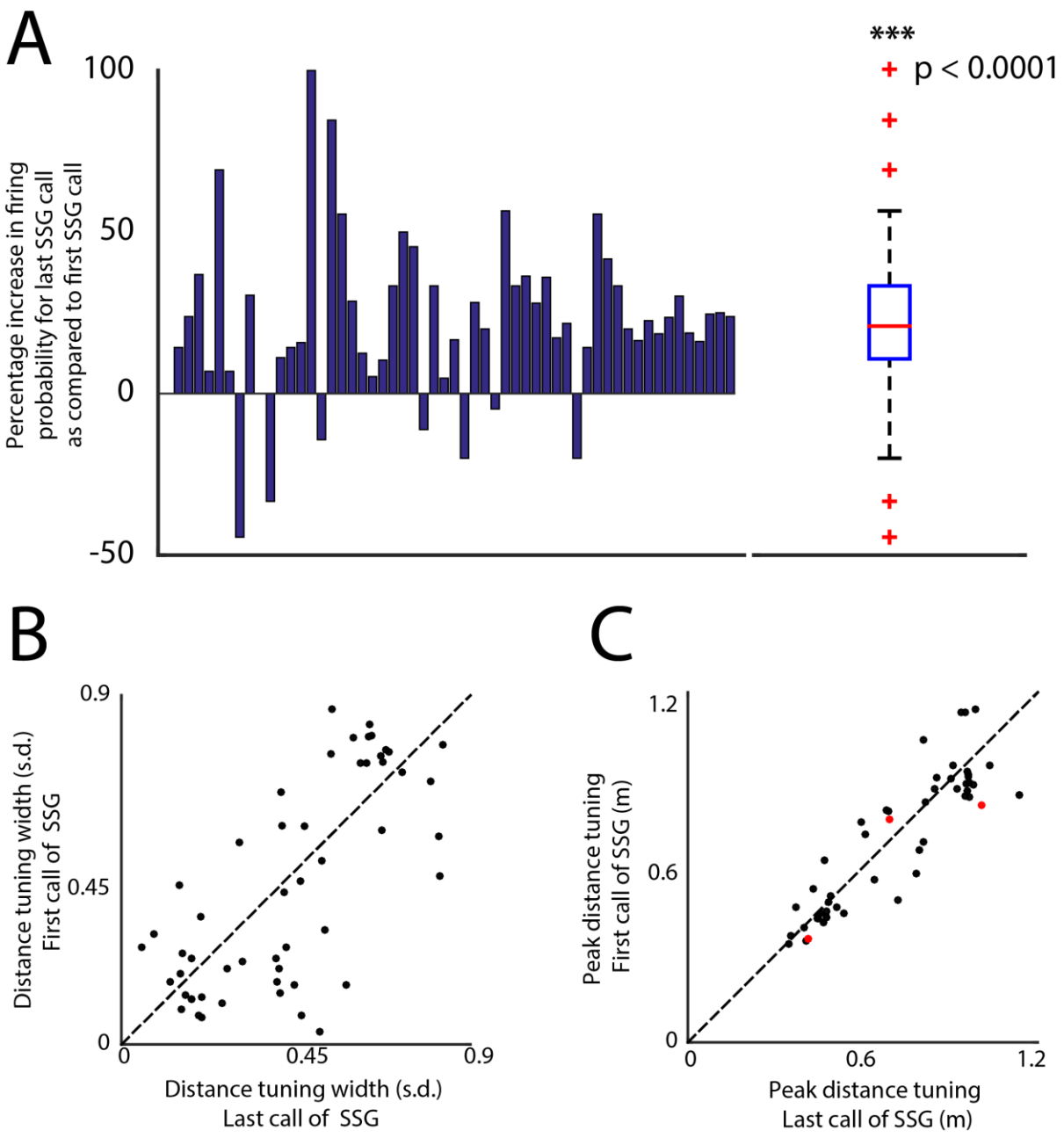

<u>Figure 5.5-figure supplement 1.</u> Changes in firing probability and spatial receptive fields for the first and last call of SSGs. A. Shows the percentage increase in firing probability (y-axis) for every 3D tuned neuron (x-axis, n = 46). Panel on the right shows the summary box plot of the distribution of the same data in the left panel. There is a significant increase in the mean firing probability for last call of SSGs compared to the first call (T-test, $p<0.0001$). **B.** Shows a unity plot comparing the sharpening of distance tuning for the

first call of SSGs and last call of SSGs. Black dots indicate no significant change in distance tuning. C**.** Shows a unity plot comparing the shifting of distance tuning for the first call of SSGs and last call of SSGs. Black dots indicate no significant change in distance tuning. Red dots indicate significant change in the peak distance tuning.

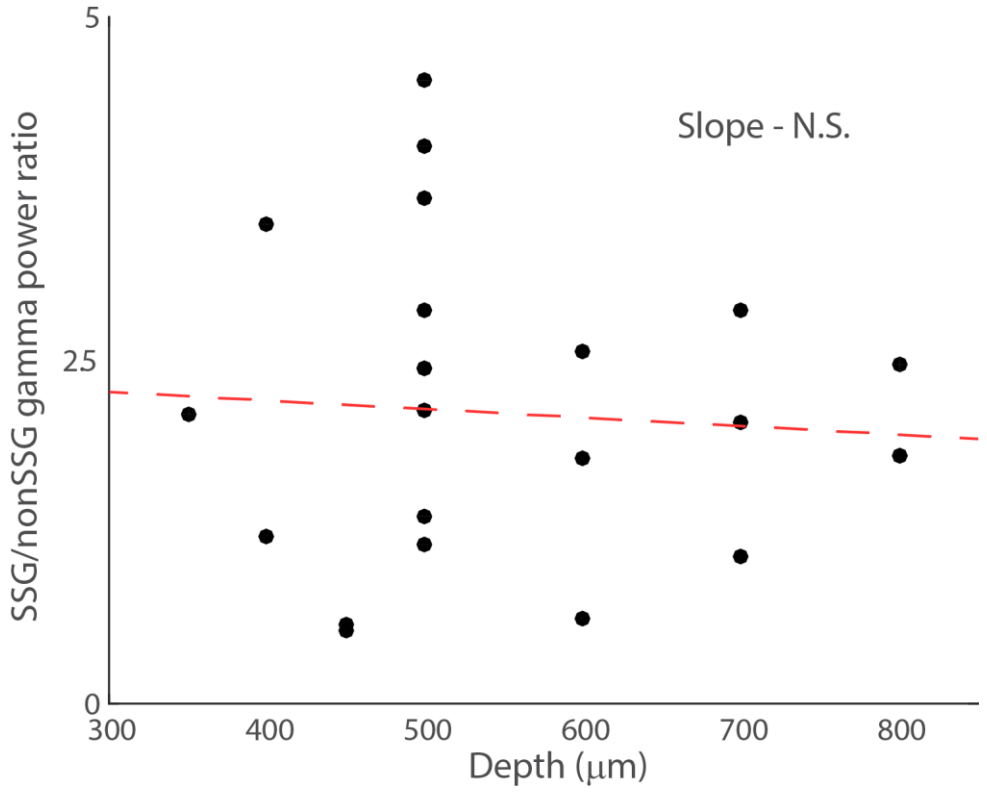

<u>Figure 5.6-figure supplement 1.</u> Changes in gamma band power ratio for SSG and non-SSGs with recording depth.

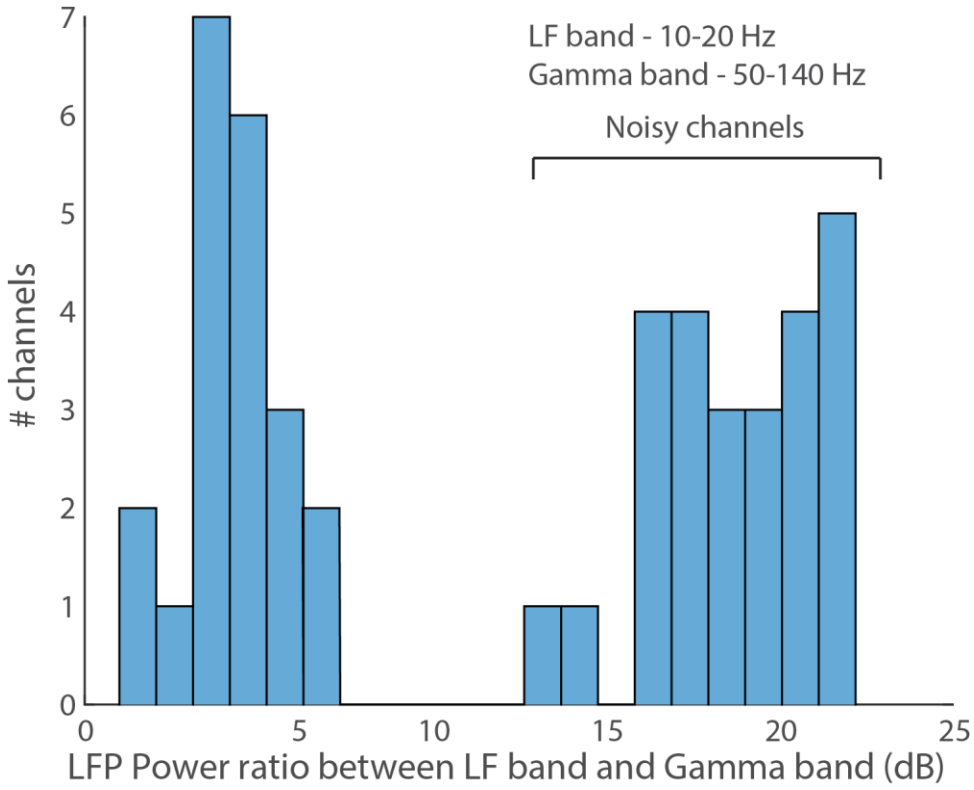

Figure 5.6-figure supplement 2. Wing beat motion artifact in LFP. The x-axis is the ratio of power in the low frequency (10-20 Hz) LFP band to the gamma LFP band in dB.

Table S1. Comparison of the variance of SSG and non-SSG distance tuning distributions for each cell in Figure 4d. The SSG and non-SSG distance tuning distributions were compared using the non-parametric Brown-Forsythe Test at the level α of 0.05. Cells in red show a significant sharpening in the distance tuning distribution when the bat emitted SSGs as compared to the variance of the distance tuning distribution when the bat produced single calls (non-SSGs). Cells in gray did not show a significant effect. Cells in blue showed a significant effect but in the opposite direction.

Cell	Statistic	df	p-value
U161	0.133	70	>0.05
U162	9.098	48	<0.05
U164	0.000	41	>0.05
U009	15.96	58	< 0.001
U006	19.71	62	< 0.0001
U011	72.28	153	<0.0001
U248	6.821	84	<0.01
U253	8.893	115	<0.005
U259	4.618	128	<0.05
U012	17.41	87	=0.0001
U016	71.203	158	<0.0001
U017	9.988	47	< 0.005

U019	29.92	60	<0.0001
U025	7.407	124	< 0.01
U036	10.30	45	< 0.01
U247	0.923	40	>0.05
U250	4.094	68	<0.05
U252	5.392	77	<0.05

Table S2. Comparison of the SSG and non-SSG distance tuning distributions for each cell in Figure. 4f. The SSG and non-SSG distance tuning distributions were compared using the non-parametric Wilcoxon Rank Sum Test at an α of 0.05. Cells marked with red ink show a significant shortening in distance tuning for SSGs as compared to the condition when the bat produces single calls (non-SSGs). Cells marked with gray ink did not show a significant effect.

Unit No	Wilcoxon rank-sum test p-value at α = 0.05
U161	<0.01
U162	<0.01
U164	<0.01
U009	< 0.01
U006	>0.05
U011	<0.0001
U248	>0.05
U253	<0.05
U259	<0.05
U012	<0.001
U016	<0.0001
U017	<0.01
U019	<0.001

U025	<0.001
U036	>0.05
U247	>0.05
U250	<0.05
U252	<0.01

5.4.10 Supplementary Movies

Movie S1. Experimental setup for validating the echo model. This is a two part movie. The first part shows the layout of the primary microphone array which is used to capture the sonar vocalizations of the bat as it flies and navigates around objects in its path. For simplicity only two objects are shown here. The second part of the movie shows the construction of the 14 channel echo microphone array which captures the returning echoes as the bats flies in the forward direction. Note that the echo microphone array is placed behind the bat on the wall opposite to its flight direction.

Movie S2. Validation of echo model using TDOA algorithms. This is a two part movie. The first part consists of 3 panels. The top panel shows an example trajectory as the bat navigates across objects (white and green). The red line is the reconstructed trajectory and green circles along the trajectory are positions when the bat vocalized. The center and bottom panels are time series when the bat vocalizes and when echoes arrive at the bat's ears respectively. The echoes arrival times have been computed using the echo model. The second part of the movie demonstrates the localizations of echo sources using TDOA algorithms. This movie has 4 panels. The top left panel shows the spectrogram representation of the recording of the bat's vocalizations. The left center and bottom panels show spectrograms of 2 channels of the echo microphone array. The right panel shows the reconstructed flight trajectory of the bat. Echoes received on 4 or more channels, of the echo microphone array, are then used to localize the 3D spatial location of the

echo sources. These are then compared with the computations of the echo model and lines are drawn from the microphones to the echo source if the locations are validated.

"Reality is infinitely diverse, compared with even the subtlest conclusions of abstract thought, and does not allow of clear-cut and sweeping distinctions. Reality resists classification."

— Fyodor Dostoyevsky
The House of the Dead

6

Characterizing sensorimotor neural activity in the SC of free flying echolocating bats

6.1 Introduction

In the natural environment, animals exhibit complex behaviors like foraging for food, interacting with conspecifics and navigating through space. Understanding the neural correlates of such complex behaviors is a central goal of neuroscience. For decades, researchers have recorded neural activity from the brain of animals that are anesthetized or restrained. However, understanding how the brain represents sensory stimuli and encodes motor actions in a freely moving animal, by definition, requires an experimental preparation, which allows the observation and classification of neural activity under completely unrestrained conditions. There are many instances where recording in unrestrained and freely moving animals has been crucial for the understanding complex behaviors. For example, the encoding of an animal's spatial

location with reference to objects in the external world (place cells), or the encoding of an animal's head direction (head direction cells) would have never been found if neural activity in the hippocampus and subiculum, respectively, would not have been recorded in freely moving animals (O'Keefe and Dostrovsky, 1971; Taube et al., 1990). Similarly, an experimental paradigm where monkeys were free to make eye and head movements was required to understand the role of the SC in attention and orienting movements (Goldberg and Wurtz, 1972b; Jay and Sparks, 1984).

The midbrain superior colliculus has been widely studied for its role in species-specific orienting movements and as a hub for sensorimotor integration (Hartline et al., 1978; Henkel and Edwards, 1978; McIlwain, 1988; Masino and Knudsen, 1993; Stein and Meredith, 1993; Valentine et al., 2002). Although, many studies in the SC, especially studies involving primates, have used awake, behaving animals (Goldberg and Wurtz, 1972b; Kustov and Robinson, 1996; Ignashchenkova et al., 2004; Krauzlis et al., 2004; Zénon and Krauzlis, 2012), however, in all previous studies in the SC, animals have been restrained and not engaged in freely moving natural behavior or naturalistic tasks.

Characterizing and classifying neural activity as sensory or motor in a freely moving animal engaged in natural behavior is difficult, mainly because of two issues, 1) identifying sensory and motor events. For example, when an animal that relies on vision is moving, stimuli received at the eyes could be affected by the dynamic properties of the stimuli itself but also could be influenced by active movements of the animal's eyes, head and body. Differentiating and identifying these events is difficult. It involves recording different aspects of the animal's behavior as well as algorithms to detect and identify different events. 2) The problem of assigning

neural activity to different behavioral (sensory or motor) events. For example, determining whether a neural spike has a relationship with a previous sensory stimuli or whether it was a premotor spike for initiating a motor movement. In previous studies of the SC, animals perform artificial tasks in highly controlled environments, which allow the experimenter to separate sensory and motor events in time. For example, in a typical task, animals are trained to fixate on a central spot, after which a visual stimulus is flashed (sensory event), but, the subsequent saccade (motor event) to the location is only performed once the fixation spot is turned off, thus, separating sensory events and motor events in time (Wurtz and Goldberg, 1972; Basso and Wurtz, 1998). Complex natural behavior, however, consists of a cascade of sensory and motor events, occurring in close tandem.

The active sensing system of echolocating bats provides a powerful model to investigate the neural underpinnings of sensory-guided behaviors, as they produce the sensory signals that inform motor actions. Echolocating bats transmit ultrasonic signals and process auditory information carried by echoes to guide behavioral decisions for orienting in space. Bats compute the direction of objects from differences in echo intensity, spectrum and timing at the two ears, while an object's distance is determined by the time delay between sonar emission and echo return (Simmons, 1973b; Lawrence and Simmons, 1982; Wohlgemuth et al., 2016b). Together, this acoustic information gives rise to a 3D representation of the world through sound (Wohlgemuth et al., 2016b). In the lab, measurements of sonar calls and echoes provide discrete and unambiguous measures of the cues available to the bat for orienting in space. Further, the bat adapts its echolocation behavior in response to 3D spatial information computed from echo returns, and therefore, the directional aim and temporal patterning of the bat's calls provide a

window to the animal's attention to objects in the environment (Moss and Surlykke, 2010). Thus, the bat's sonar vocalization, head and ear movement behaviors, together with a measurement or estimation of echo stimuli arriving at the bat's ears, provide discrete time points of sensory and motor events which can be combined with neural recordings to characterize sensory and motor neural activity in freely flying echolocating bats.

In this chapter, I first provide details of an algorithm to characterize neural activity as sensory (S), sensorimotor (SM) or vocal premotor (VPM) and then present the first description of sensorimotor cells which have 3D spatial sensory receptive fields. Our results not only give strength to previous results where neural activity in the SC of restrained animals has been classified as sensory, sensorimotor and premotor but also extend the results by demonstrating that the SC plays a role in orienting in 3D space.

Here, I use data previously presented in Chapters 4 and 5. Briefly, we recorded neural activity in the SC of freely flying echolocating bats performing a naturalistic spatial navigation task. We combined the neural data with simultaneously recorded measurements of echolocation and flight behavior and a computational model, to estimate the instantaneous echo stimuli arriving at the bat's ears, to characterize sensory and vocal premotor neural activity in the SC. Chapter 4 gave a detailed description of the echo model and chapter 5 presented a detailed description of sensory activity in the SC.

6.2 Results

We used two big brown bats (*Eptesicus fuscus*) in this experiment where each bat flew in an experimental flight room (6x7x2.5 meters) and navigated obstacles and either landed on a platform or on the far wall of the room, where they were fed (Figure. 5.6.1). Once the bats were well acquainted with the task, a chronic 16 recording site, silicon microelectrode was surgically implanted in the SC (see Methods, Chapter 5, for details). On recording days, high speed infrared video data (Vicon systems) for computing the beam aim of the bat, ultrasonic microphone recordings using a 32 channel microphone array to record the sonar vocalization behavior of the bat were computed with synchronized neural activity from the SC using a wireless telemetry

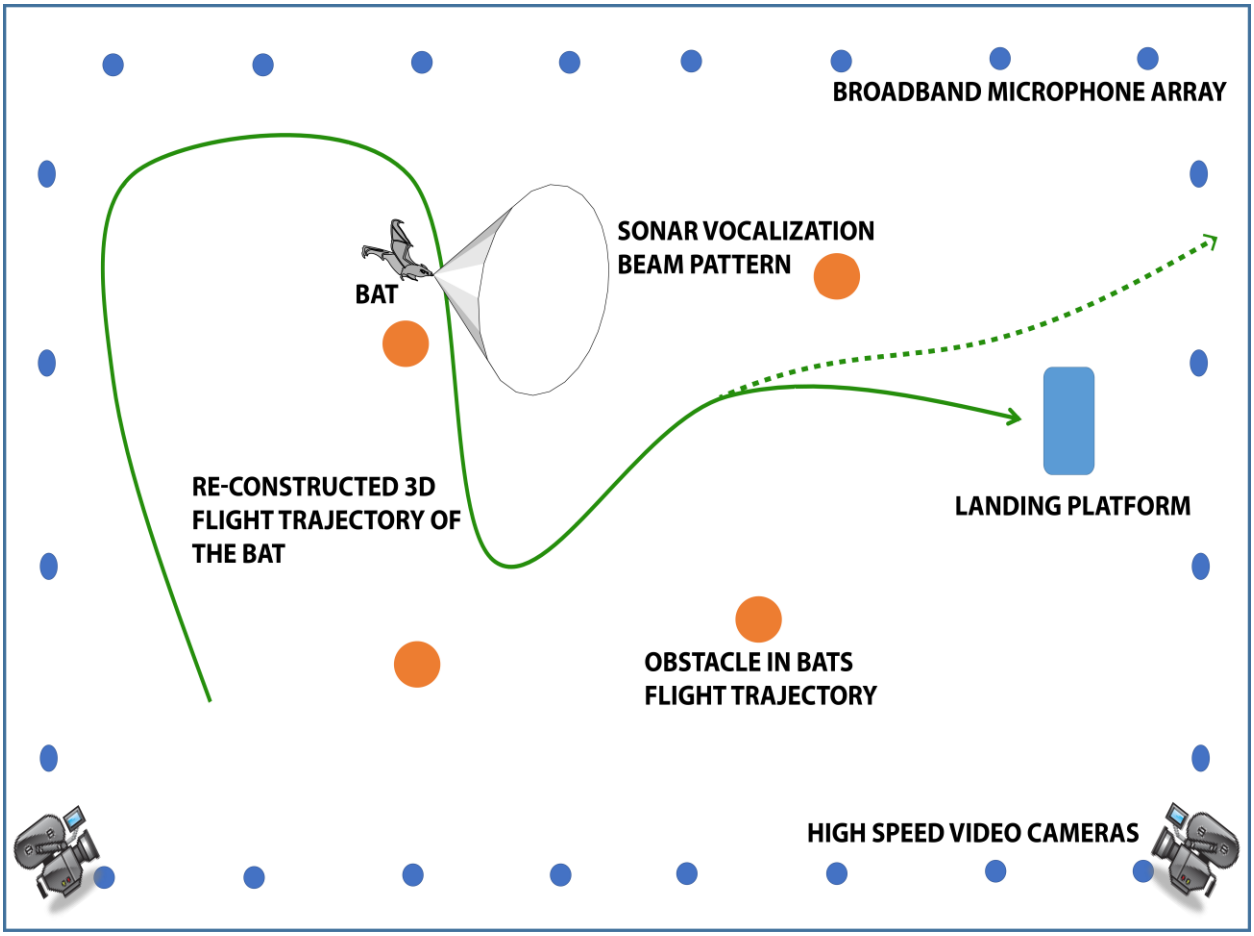

Figure 6.1. Experimental design

system (TBSI systems). After data collection, using a physics based model, referred to in chapter 4 as the *echo model*, we computed the instantaneous directions and arrival times of echoes at the bat's ears (See chapter 4 for details of the *echo model*). Combining the results from the echo model, we were then able to further characterize neural activity in the SC. Below, I present details of the algorithm I used to classify neural activity into sensory (S), sensorimotor (SM) and vocal premotor (VPM), Following this, I present further characterization of sensorimotor and vocal premotor cells.

6.2.1 Characterizing S, SM and VPM neural activity

An important aspect of neurophysiological studies in the brain, involving neural recordings, is to determine the causal relationship between neural activity and sensory stimuli or motor movements. Experimental paradigms that involve restrained animals and passive presentation of stimuli have complete over stimulus presentation and thus can unambiguously establish a relationship between stimulus presentation and neural activity. The problem of assigning neural activity to sensory stimuli or motor movements, is greatly complicated in animals which are freely behaving and moving. In such experimental paradigms, the animal is completely in control of its movements and thus the stimuli it receives. Here the experimenter has to, first, determine the stimuli the animal receives and second, associate the stimuli with neural activity. In this experiment, we computed the instantaneous echo stimuli that is received at the bat's ears using a physics based model that we call *echo model*. The *echo model* has been previously described in detail, in chapter 4. Below, I describe an algorithm to solve the problem of assigning spikes to echoes and/or motor activity.

For sensory guided behaviors, information about the external world, received at end receptors, needs to be quickly interpreted and transformed into motor actions. For example, in the case of a free flying echolocating bat performing a spatial navigating task, information (from returning echoes) regarding the spatial locations and distances of objects from the bat, needs to be computed before echoes from the next sonar vocalization arrive. Similarly, a vocal premotor neuron, which initiates sonar vocalizations, needs to fire early enough to account for the latency in neural transmission to the motor neurons. Thus, when a sensory neuron is presented with stimuli in its receptive field, it will have an orderly and sharp distribution of latencies with respect to stimulus presentations. Similarly, a premotor neuron, which communicates with motor nuclei for issuing motor commands will have an orderly and sharp distribution with respect to motor movements. Further, in sensorimotor integration areas like the SC, a neuron can fire for both sensory and premotor events.

In the case of an echolocating bat, as the bat produces sonar vocalizations it receives echoes, thus the experimenter needs to solve the problem of assigning neural activity to a preceding sensory event (echo) or a succeeding motor event (Call – sonar vocalization). Figure. 6.2A illustrates this as a cartoon. In such a scenario, the basic premise for characterizing neural activity as sensory, sensorimotor or vocal premotor is the assumption that the latency of sensory neural activity would exhibit a tight distribution around specific sensory events, while the lead time of premotor activity would exhibit a tight distribution around vocal premotor events. Similarly, sensorimotor neural activity would have tight distributions around both, sensory and vocal motor events. This is explained in a cartoon form in Figure. 6.2B. It must be noted, however, such an algorithm would not be able to identify neural activity which is being planned over a

sequence of sensory and motor events. Further, in order to quantitatively classify neurons as S, SM or VPM, I used the tightness of a neuron's latency distribution with respect to the echo event as compared to the tightness of its latency distribution for the subsequent vocalization. Thus, clustering neural activity based on these distributions should allow us to classify S, SM and VPM activity (as shown in Figure. 6C, S – red, SM – green, VPM – blue and unclassified neurons – black).

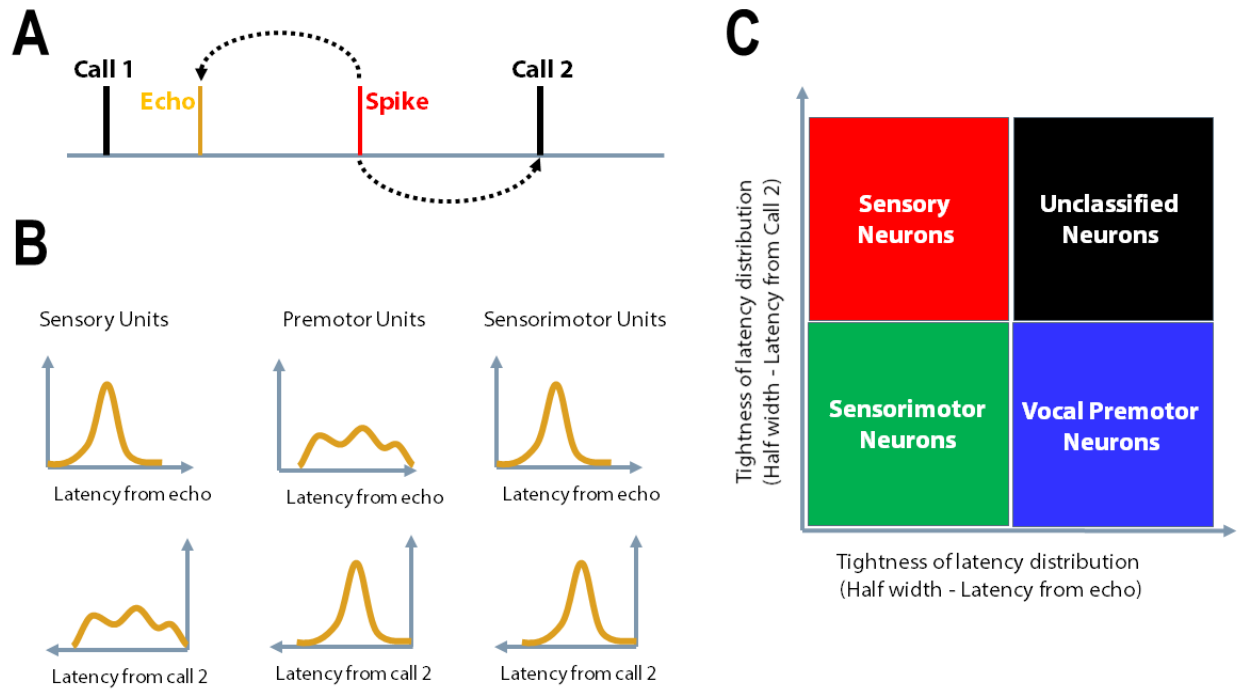

Figure 6.2. Cartoon depicting the outline of the classification algorithm.

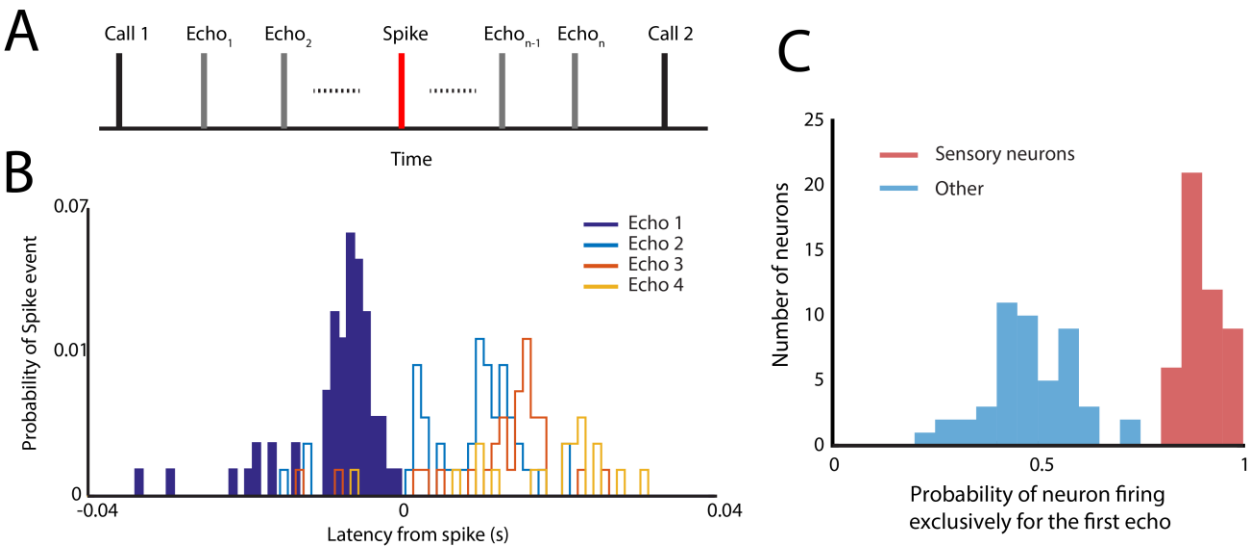

Figure 6.3. The Echo-to-spike assignment problem.

In their natural environment, especially when flying or foraging in presence of clutter, bats receive a series of echoes for different objects. In the present experiment, as the bat navigates and makes echolocation calls, it receives a series of echoes from the different objects in its flight path (including echoes from walls and cameras). While the earlier figure (Figure. 6.2A) showed a more simplified situation, where there is only a single echo arriving at the bats ears, Figure. 6 .3A shows a more naturalistic situation where the bat receives a number of echoes following a call (Call 1) and before it makes the next call. In the situation where a bat receives a stream of echoes between successive calls, we need to solve the problem of echo-to-spike assignment. In other words, the problem of determining the stimulus for which a neural spiking event occurred. To solve the echo-to-spike assignment problem, we opted for a very simple solution; only neurons which fire maximally in response to the first echo of a cascade, are considered as sensory. Figure. 6.3B shows an example of once such neuron, which only fires in response to the first echo. In this figure, the x-axis represents the time delay (latency) between

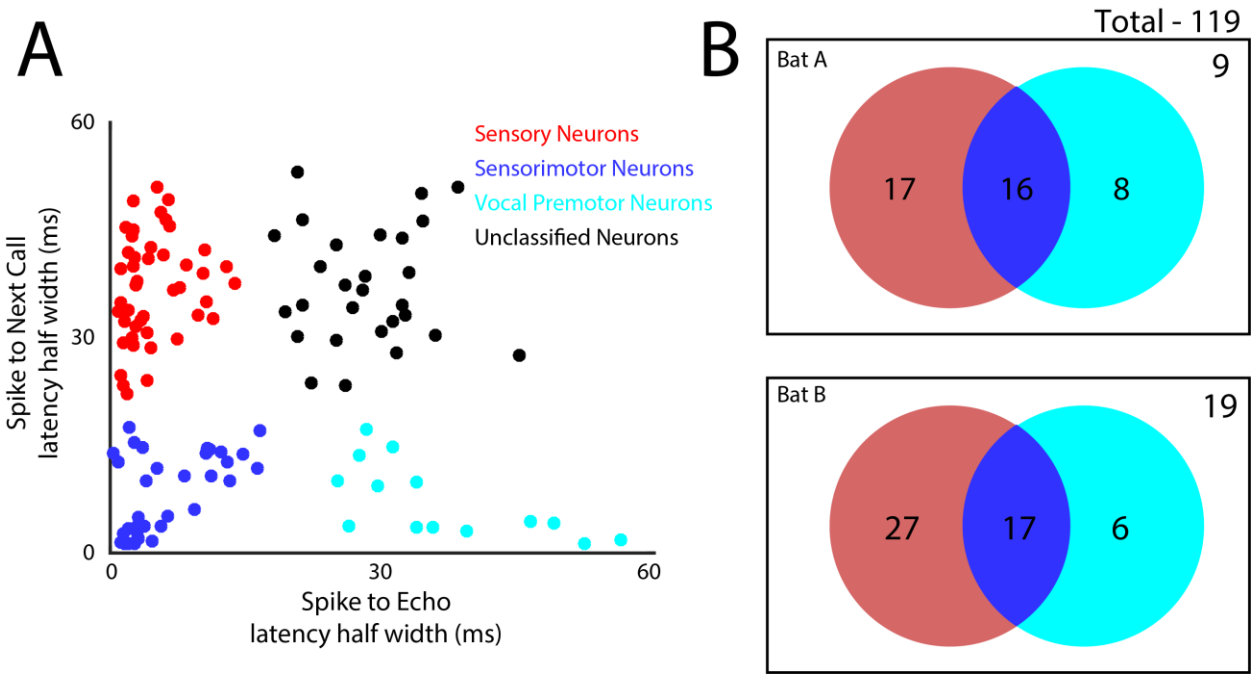

Figure 6.4. Classification of neural activity into sensory, sensorimotor and vocal premotor. **A.** Shows the classification of all 119 cells into 44 sensory, 33 sensorimotor and 14 vocal premotor cells. **B.** Displays the bat wise break-up of the classified cells.

echoes and spikes. Zero represents spike time. Thus, for echoes which occur before the spiking event have a negative latency, while echoes arriving after the spiking event have positive latencies. This unambiguously solves the spike-to-echo assignment problem. However, it also restricts that number of sensory neurons in the data, whose echo-delay tuning response can be characterized. Further, it must be noted that auditory evoked spiking activity in the bat auditory system is very sparse (Valentine and Moss, 1997), which further simplifies the echo-to-spike assignment problem. Figure. 6.3C show a histogram of all 119 neurons, where the x-axis is the spiking probability of a neuron to the first echo. The histogram in red shows a group of neurons, which predominantly (80%) have spikes associated with the first echo and can be classified as sensory (see Methods for more details).

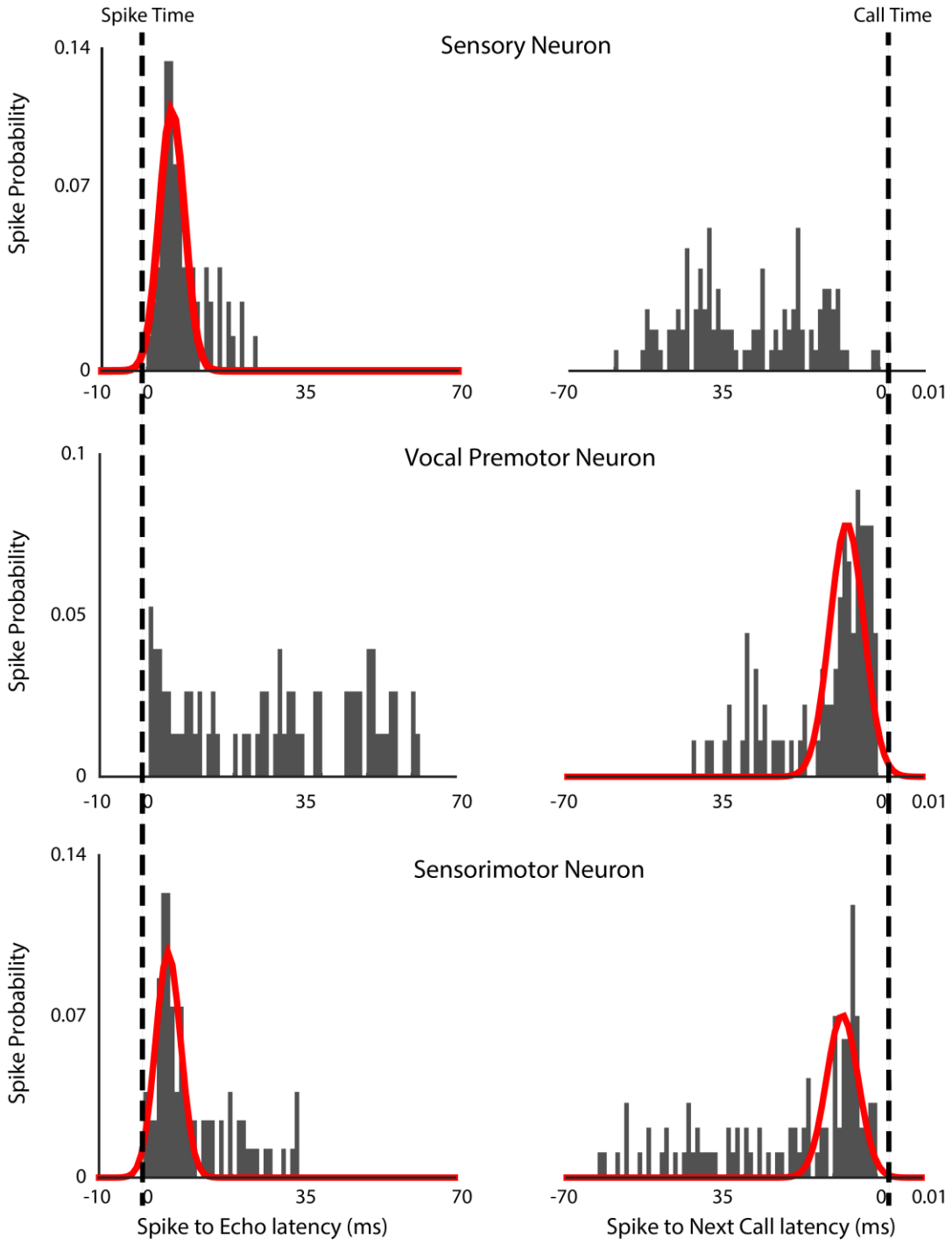
Spike Time
Call Time
Sensory Neuron
Vocal Premotor Neuron
Sensorimotor Neuron
Spike Probability
0.14
0.07
0
0.1
0.05
-10
0
35
70
-70
0.01
Spike to Echo latency (ms)
Spike to Next Call latency (ms)

Figure 6.5. Examples of sensory, vocal premotor and sensorimotor neurons. The panels on the left are spike to first echo latency histograms. Zero on the x-axis (for the left panels) represents time of arrival of the first echo. The panels on the right are spike to next call latency histograms. Zero on the x-axis (for the right panels) represents call production time. The y-axis for each plot is the spiking probability. Each row is an example of a sensory, vocal premotor and sensorimotor neuron, from top to bottom, respectively. The normal fits to the latency distribution are shown in red. Only the fits which have an R^2 greater than 0.5 are shown (see Methods for more details).

Figure. 6.4 shows the classification of neurons based on the algorithm illustrated in Figure. 6.2C (for further details of identifying the half widths of latency histograms, see the Methods section). Figure. 6.5 gives examples of 3 representative neurons, one each of the sensory, vocal premotor and sensorimotor class. Figure. 6.6A shows the histogram of mean spike to first echo latency for all sensory cells (44 cells). The mean latency of all cells was 6.5 ± 2.3 (ms) (See methods for more details). Figure. 6.6B shows the histogram of mean spike to next call latency for all vocal premotor cells (14 cells). The mean latency of all cells was -12 ± 6.4 (ms). The negative sign indicates that the spike occurred before the call production time (See methods for more details).

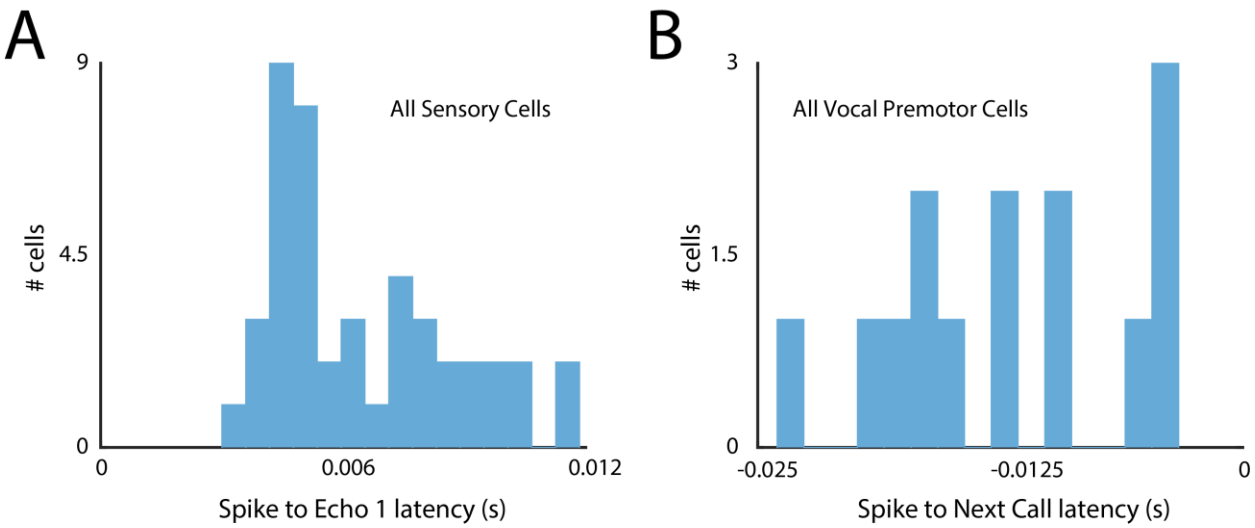

Figure 6.6. Mean spike latencies. **A.** Shows the histogram of mean spike to first echo latency for all sensory cells (44 cells). The mean latency of all cells was 6.5 ± 2.3 ms. B**.** Shows the histogram of mean spike to next call latency for all vocal premotor cells (14 cells). The mean latency of all cells was -12 ± 6.4 ms. See text and Methods for more details.

6.2.2 Further characterization of sensorimotor activity

By definition, a sensorimotor cell fires both when it receives sensory stimuli in its receptive field, and when it precedes a motor command. In studies of sensorimotor cells in the SC of animals trained to saccade to visual stimuli, sensory events can be clearly separated from motor events (Mays and Sparks, 1980; Ignashchenkova et al., 2004). In the present experiment, this separation was not possible, as the animal controlled the timing of sonar vocalizations, which in turn, influenced the reception of echoes. Figure. 6.6A shows an example sensorimotor neuron where the x and y axes represent the lead-time and latency of a spike from the next and previous call, respectively (Also, see Figure. 6.2A for a cartoon of the time series of Call 1, Spike and Call 2). Thus, the sum of the x and y intercepts of each point is the PI. The figure demonstrates the separation between premotor activity which occurs close to x-axis (i.e. the latency of the spike to the next call is small) and sensory activity which occurs close to the y-axis (i.e. the latency of the spike the echo evoked activity is closer to the previous call). In Figure. 6.7A, the spikes identified as sensory in red and spikes identified as vocal premotor in cyan (see Methods for more details). Figure. 6.7B displays latency histograms of spikes classified as sensory (red) and premotor (cyan) of the neuron shown in Figure. 6.7A. The top panel is a histogram of latency between spike and previous call while the bottom panel is the latency between spike and next call. Figures 6.7C and 6.7D are summary plots comparing the means of the classified sensory and premotor spiking activity latency distributions for each SM neuron (Figure. 6.7C – distribution of spike to previous call latencies and Figure. 6.7D is the distribution of spike to next call latencies). Closed circles represent neurons in which sensory latency and premotor lead-time distributions were significantly different (see Methods for further details). Figure. 6.7C demonstrates that all

SM activity classified as sensory occurs closer to the previous call, while Figure. 6.7D demonstrates that all SM activity classified as premotor occurs closer to the next call.

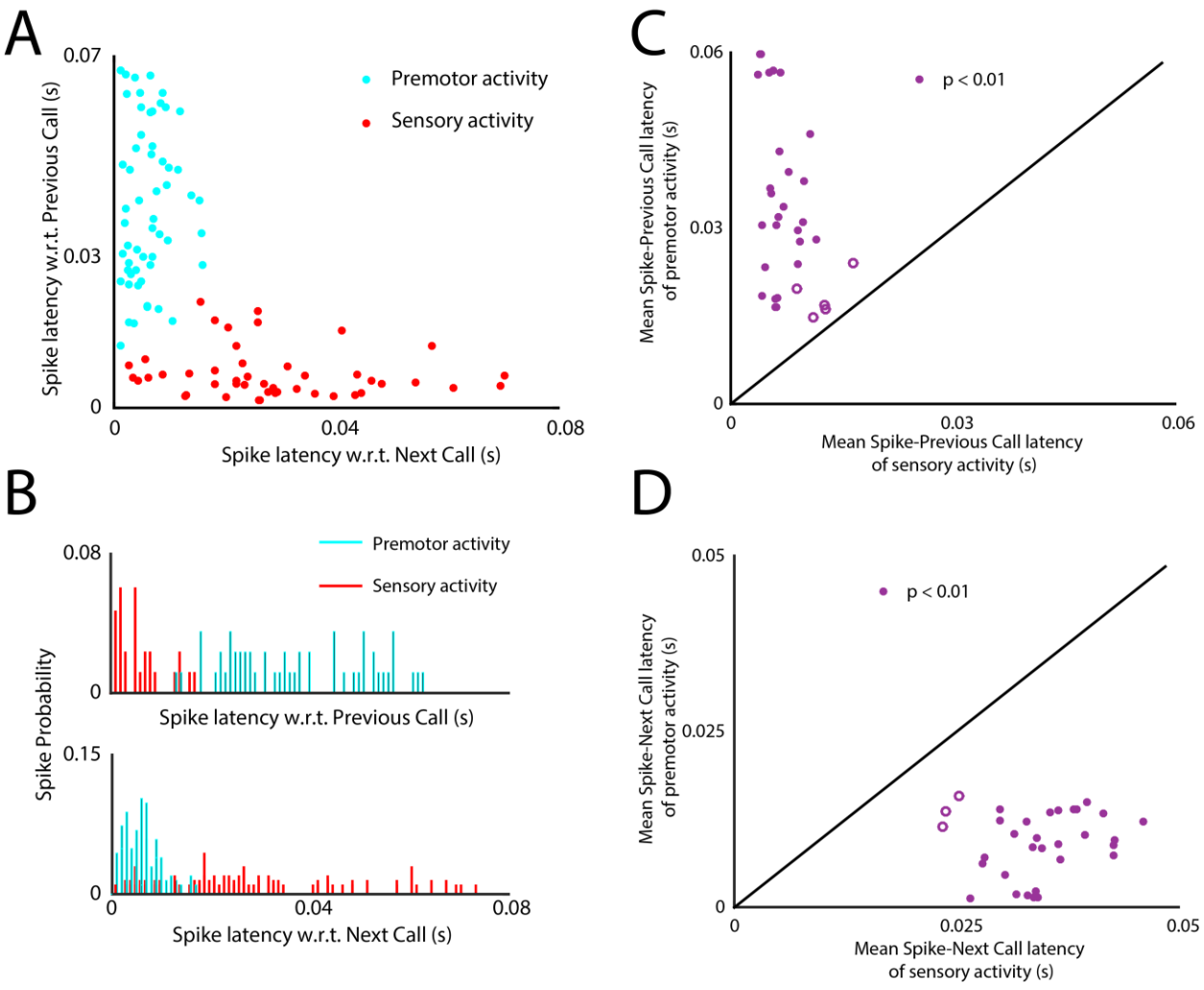

Figure 6.7. Separation of sensory and premotor spikes in the sensorimotor neuron. **A.** Shows a scatter plot of an example sensorimotor neuron where each point represents a spike and the x and y intercept are the latency of the spike from the next and previous calls, respectively (sensory activity in red and vocal premotor activity is shown in cyan – see text and Methods for more details on how the activity was classified). **B**. Displays latency histograms of spikes classified as sensory (red) and premotor (cyan) of the same neuron as in Figure 6.7A. The top panel is a histogram of latency between spike and previous call while the top panel is the latency between spike and next call. **C and D**. Provides further quantification of the classification of sensory and premotor activity of SM neurons. In **C**, the means of the distributions of sensory and premotor activity latency w.r.t. previous call are compared. In **D**, the means of the distributions of sensory and premotor activity latency w.r.t. next call are compared. Filled circles, in **C** and **D**, represent cells with significant difference between mean of the two distributions (two tailed test, $\alpha = 0.01$ – see Methods for further details)

After separating sensory and motor activity of SM cells, we combined the neural spiking information to construct 3D spatial receptive (azimuth, elevation and range) fields of individual neurons (see Methods for more details). Figure. 6.8A shows the 3D receptive field of an example as projections on the azimuth-range (AR), azimuth-elevation (AE), and elevation-range (ER) planes. The z-axis represents the spiking probability per bin. Figure. 6.8B shows a summary plot of the peak tuning along each A, E and R dimension as a 3D Cartesian plot. Figures 6.8C, 6.8D and 6.8E show the distribution of tuning half widths (see Methods for more details) along the A, E and R dimensions, respectively.

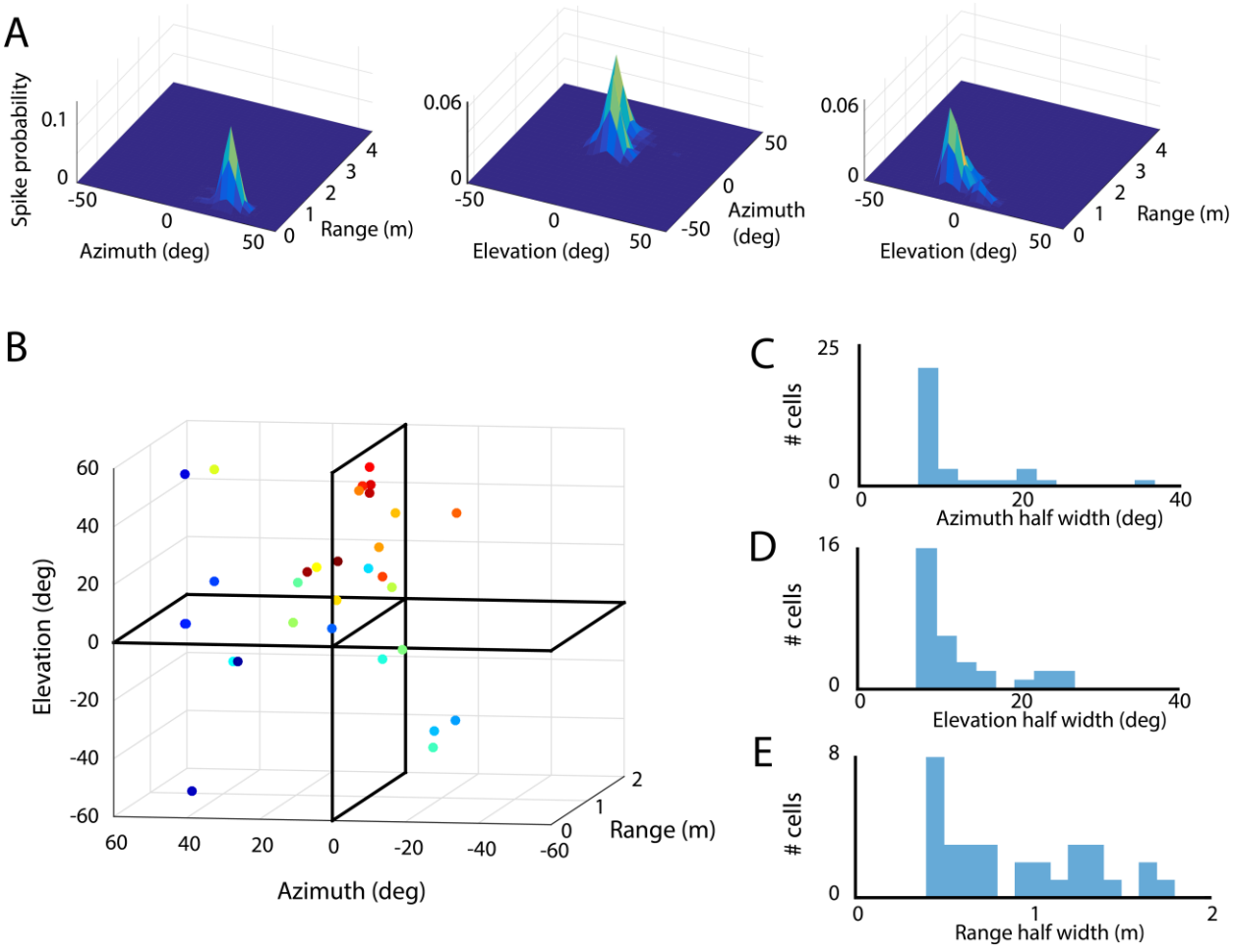

Figure 6.8. 3D spatial receptive fields of the sensory activity of SM cells. **A.** Shows the projections of the 3D receptive field of an example cell. The projections are along the AR, EA and ER planes. **B.** Summary plot of the peak tuning of each SM cell along the A, E and R dimensions. The plot is a Cartesian plot of A-E-R space. Colors have been chosen randomly. **C, D and E.** show histograms of the half tuning widths along each dimension, A, E and R, respectively (see Methods for more details).

6.3 Discussion

Complex natural behavior consists of the dynamic interplay between sensation and action. Linking sensation and action to brain activity is an important goal of neuroscience. Here, I present analysis methods to classify and characterize sensory, sensorimotor and premotor neural activity in the completely freely moving animal engaged in a naturalistic task. I developed a simplified approach to classify neural activity into sensory, sensorimotor and premotor categories based on the firing patterns of neurons and the alignment of neural activity with discrete sensory (echo evoked) and motor (sonar vocalizations) events. Further, I used this analysis method to characterize the 3D spatial selectivity of sensorimotor neurons. The results not only give strength to previous reports of sensory, sensorimotor and premotor activity in the mammalian SC (Wurtz and Albano, 1980; Sparks, 1986; Edelman and Keller, 1996) but also extends previous research to show that the SC also plays a role in orienting in 3D space.

6.3.1 Classification of sensory, sensorimotor and premotor activity in the SC of a freely moving animal

Several studies have recorded sensory activity in moving but head fixed animals (Ferezou et al., 2006; Sawinski et al., 2009; Niell and Stryker, 2010; Deschênes et al., 2012; Keller et al., 2012; Saleem et al., 2013; Schneider et al., 2014). Visual orientation tuning responses have also been recorded in freely moving mice, where the visual stimulus on the eyes been estimated using head movements (Sawinski et al., 2009). Recently, several studies have recorded reward related neural activity in the SC of freely moving mice (Felsen and Mainen, 2008; Duan et al., 2015).

However, to the best of our knowledge, no study to date has recorded and characterized sensory, sensorimotor and premotor activity in a freely moving animal in the SC.

To solve the problem of classifying a neuron as sensory or motor, I assumed that a sensory neuron will have a narrow latency distribution with respect to the echo reception time. Similarly, a vocal premotor neuron will have a narrow lead-time distribution with respect to vocalizations. The algorithm is illustrated in Figure. 6.2 as a cartoon (Also see Methods for details of the algorithm).

Further, as the bat navigates around obstacles while producing sonar sounds, it receives a series of echoes for every vocalization. In such a situation, to determine the sensory component of a neuron, there is further ambiguity regarding the assignment of individual echo events to spikes (echo-to-spike assignment problem – Figure. 6.3A). Here we make a simplifying assumption of considering a neuron as sensory only if it fires maximally (Figure. 6.3C) for the first echo. Using this approach, we were able to classify 44 sensory, 33 sensorimotor and 14 premotor neurons out of the 119 neurons recorded from the two bats (Figure. 6.4 and Figure. 6.5).

6.3.1.1 Limitations of classification algorithm:

1) Neurons with large variance in spiking. The classification algorithm requires a neurons to have a tight distribution of latencies with respect to either a sensory or motor event, to be classified as sensory or premotor, respectively. Such an approach will be unable to classify neurons, which have a very large variance with respect to the time of occurrence of a relevant sensory or motor event. We, however, argue that such neurons, if they exist in the SC of an echolocating bat, would be unable to transmit useful information regarding

the occurrence of a sensory event or issue a motor command for the successful and timely execution of motor behaviors.

2) Cells firing for specific pulse intervals: Consider a cell, which only fires when the bat produces echolocation calls at a specific pulse interval. Such a cell will exhibit a tight echo to spike latency distribution, as well as a tight spike to next call lead-time distribution. A hypothetical neuron, which fires only for a particular range of PIs will exhibit a tight cluster when its spikes are plotted similar to Figure. 6.7A. Each SM neuron was individually examined, and not a single neuron, out of the 33 classified SM neurons, exhibited PI based firing.

6.3.2 3D spatial receptive fields of sensorimotor neurons

The superior colliculus (SC), has been implicated in species-specific sensory-guided orienting behaviors in 2D space, target selection and 2D spatial attention (McPeek and Keller, 2004; Lovejoy and Krauzlis, 2010; Knudsen, 2011; Mysore and Knudsen, 2011; Mysore et al., 2011; Zénon and Krauzlis, 2012; Krauzlis et al., 2013; Duan et al., 2015). Past research has led to conflicting views as to whether the SC plays a role in orienting in 3D space (Leigh and Zee, 1983; Hepp et al., 1993; Chaturvedi and Gisbergen, 1998; Chaturvedi and van Gisbergen, 1999; Chaturvedi and Van Gisbergen, 2000b; Walton and Mays, 2003; Van Horn et al., 2013). Limited evidence, however, from sensory mapping in primates shows response selectivity to binocular disparity (Berman et al., 1975; Dias et al., 1991), and vergence eye movements (Chaturvedi and Gisbergen, 1998; Chaturvedi and van Gisbergen, 1999; Chaturvedi and Van Gisbergen, 2000a; Van Horn et al., 2013). In Chapter 5, we presented the first direct evidence of 3D egocentric

sensory responses to natural stimuli in a freely behaving animal. In the present work, we were able to segregate neural activity of SM neurons into sensory and vocal premotor parts (Figure. 6.6). We combined this separated sensory activity with echo direction information from the echo model to construct, for the first time, 3D spatial receptive fields of SM neurons in the SC (Figure. 6.7).

6.4 Methods

6.4.1 Methods in brief

Chapter 5 contains detailed discussion of methods regarding the animals, behavioral training, surgical procedures and neural recordings, experimental setup and audio, video recordings. In brief, two wild caught big brown bats, *Eptesicus fuscus*, were trained to navigate around objects and either land on a platform or a wall. Prior to data collection, a 16-channel silicon probe (Neuronexus) was chronically implanted into the right superior colliculus. A wireless telemetry system (Triangle Biosystems) linked to a data acquisition platform (Plexon) were used to wirelessly record neural data while the bat was in flight. All procedures and experimental protocols were approved by, the University of Maryland's and Johns Hopkins University's, Institutional Animal Care and Use Committee and complied with US Public Health Service policy on the humane care and use of laboratory animals. During the experiment motion capture cameras (Vicon) were used to capture the bat's flight trajectory and head direction, and ultrasonic microphones were used to capture the sonar calls. Neural data was sorted to identify single units (Quiroga et al., 2004).

6.4.2 Analysis of audio recordings

Audio recordings were analyzed using custom Matlab software to extract the relevant sound features, i.e. pulse timing, duration, and interval. Combining the pulse timing (time when sound reached a stationary microphone) with the 3D flight trajectory data allowed compensating for the sound-propagation delays and calculating the actual call production times at the source (i.e. the veridical time when the bat produced the sonar sound).

6.4.3 Echo model

The details of the echo model are presented in Chapter 4.

6.4.4 Constructing latency and lead-time histograms

The latency of spike-to-echo was computed for each spike of every sorted neuron. Here, for each spike, the nearest (in time) preceding sonar vocalization was identified. For the spike in the cartoon of Figure. 6.2A, Call 1, is the preceding call (we name this vocalization as the *previous call* - PC). Similarly, the earliest call produced after the spike will be Call 2 (we name this as the *next call* - NC). Once the PC is identified, the echoes generated by this call are computed and the latency of the spike to the first echo is calculated. Similarly, the lead-time of the spike from the NC is computed. Once the latencies and lead-times for all spikes of the neuron are recorded, histograms for each distribution is computed (this is shown in cartoon format in Figure. 6.2C and for real data in Figure. 6.4)

6.4.5 Echo-to-spike assignment problem

Similar to the construction of latency histogram for the first echo, latency histograms for every spike of a neuron for every echo after the PC are computed. Figure. 6.3B shows latency histograms for an example neuron for every neuron (dark blue, light blue, red and yellow are the latency histograms for the neuron from echo 1, 2, 3 and 4 respectively). This example neuron, almost exclusively, fires only for the first echo. After computing the latencies for every spike form each echo, the ratio of spikes which occur after the first echo but before the second echo is computed. Figure. 6.3C shows a histogram of this ratio, for all 119 neurons. Here the x-axis is the probability that a neuron fires exclusively to the first echo. This distribution of ratios was then clustered into two groups. Neurons that fire exclusively to the first echo, with more than 80% probability, shown in red, are considered as predominantly sensory neurons. Group 2 (blue) consists of the rest of the neurons, which consists of both SM and VPM neurons.

6.4.6 Classification of neurons into S, SM and VPM categories

The spike-to-first-echo latency histogram and the spike-to-next-call lead time latency histograms are fit to normal curves. The fit is considered good if the R^2 is equal to or above 0.5. The half widths of the latency and lead-time distributions are computed as follows.

1) $R^2 \geq 0.5$ (good fit): Half width (HW) = σ (of the normal fit)
2) $R^2 < 0.5$: Half width (HW) = width of distribution between the 16^{th} and 86^{th} percentile of the distribution.

The half widths of each of the 119 neurons is plotted as a scatter plot in Figure. 6.4A, where the x-axis is the half-width for the spike-to-first-echo latency distribution and the y-axis is the half

width of the spike-to-next-call lead time distribution. The data are then clustered into four groups using k-means algorithm (Figure. 6.4A).

6.4.7 Separating sensory and vocal premotor activity of SM neurons

Similar to construction of spike to echo latency histograms, spike-to-previous-call histograms and spike-to-next-call lead time histograms were constructed. Based on this spikes which were closer to the PC were considered as sensory and spikes closer to the NC were considered VPM. This is demonstrated for an example neuron in Figure. 6.6A. The sensory spikes are identified in red and VPM spikes in cyan. To further check whether the identified distributions are different, further checks were performed. For each distribution, sensory and VPM, two means were computed (that is total four means). The mean spike-to-previous-call latency of the S and VPM parts as well as the mean spike-to-next-call lead time of the S and VPM parts of each sensorimotor neuron. These means were compared using the Wilcoxon Signed Rank test. These comparisons are shown in Figures 6.6C and Figure. 6.6D for the spike-to-previous-call means and spike-to-next-call means, respectively. Cells which did not show a significant difference in both comparisons (Figure. 6.6C and 6.6D) were not considered for further analysis of construction of 3D spatial receptive fields.

6.4.8 Construction of 3D spatial response profiles

The 119 single neurons were further classified according to sensory (which have echo-evoked responses), sensorimotor (which respond to echoes and also fire before production of sonar vocalizations) and vocal-premotor neurons. Classification into sensory, sensorimotor and premotor categories is common for SC neurons (Mays and Sparks, 1980; Schiller and Koerner,

1971). Only sensory neurons were used for the construction of 3D spatial response profiles. Output of the echo model, in the form of azimuth, elevation and range coordinates of echo sound sources as well as arrival times of echoes at the bat's ears are combined with spike times of single neurons. The spatial response profiles are then normalized using the stimulus space, i.e. the time spent by the animal, in each dimension (see Chapter 5 - Figure S2D – range, S2E – azimuth and S2F – elevation): that is, the spike-count spatial response profile was divided by the time-spent spatial profile, to yield a spiking probability per bin in each dimension (distance, azimuth, and elevation). Regions of the stimulus space with echo events per bin less than 1 standard deviation from the mean were excluded from the computations (indicated by open bins in Chapter 5 - Figure S2D, S2E and S2F). Spatial response profiles in each dimension are then fit to a Gaussian function using the *fit* function in Matlab. Spatial response profile means, half widths and standard deviations are then taken from the Gaussian fit.

Sometimes questions are more important than answers.

— Nancy Willard

7

CONCLUSION AND FUTURE DIRECTIONS

The main theme of my thesis has been the representation of 3D space in the brain, and, how adaptive behaviors, shape these spatial representations. We first investigated the production of sonar sound groups (SSGs), an adaptive vocal-motor behavior which has been extensively studied in both the field and the laboratory, and our results, using behaving bats resting on a platform and tracking an approaching target, support the hypothesis that bats increase the production of SSGs to enhance the spatio-temporal resolution of sonar targets (Chapters 2 and 3). Further, using electrophysiological recordings in free flying bats performing a spatial navigation task, we demonstrated that neurons in the midbrain superior colliculus (SC) have 3D spatial receptive fields. Our results also revealed that the spatial tuning of SC neurons sharpens and shifts when bats produce SSGs, thus, providing direct neurophysiological support for the hypothesis that SSGs help enhance the spatio-temporal resolution of sonar targets.

The results in this thesis advance our knowledge regarding the representation of egocentric 3D sensory space in the mammalian brain and that these representations are dynamic and are modulated with an animal's adaptive natural behavior.

As with any scientific endeavor, answering questions always opens the door to more and more interesting questions. Below, I briefly describe avenues to extend the results and experiments presented in this thesis.

7.1 Neural recordings in the rostral SC of echolocating bats

A number of previous studies have recorded neural activity in the superior colliculus of passively listening awake/anesthetized echolocating bats (Jen et al., 1984; Poussin and Schlegel, 1984; Wong, 1984; Thiele et al., 1996; Valentine and Moss, 1997; Hoffmann et al., 2016). Except for a couple of studies, which were performed in bats which use vision extensively (*Rousettus aegyptiacus* and *Phyllostomus discolor*) (Thiele et al., 1996; Hoffmann et al., 2016), none have recorded in the rostral pole of the SC of an echolocating bat. Also, it must be noted that no study, to the best of our knowledge (including the results presented in Chapters 5 and 6; however, see Appendix A*), has recorded sensory or motor responses in the rostral pole of the SC of *Eptesicus fuscus*. Figure 7.1 shows electrode penetration locations from previous studies in the SC of *Eptesicus fuscus* (Jen et al., 1984; Wong, 1984; Valentine and Moss, 1997).

As previously discussed in Chapter 1, the rostral pole of the SC encodes frontal sensory space of an animal. Further, it is known that bats direct their head and sonar beam directly at sonar targets of interest (Ghose and Moss, 2003, 2006). The lack of neural recording data from the rostral SC of echolocating bats leaves gaps in our knowledge regarding the representation of 3D sensory space as well as the classification of sensory, sensorimotor and premotor cells in the

* See Appendix A for a pilot experiment demonstrating the feasibility of recording in the rostral SC of *Eptesicus Fuscus in a passive listening paradigm*

rSC. Thus, to fully understand the role of the SC in 3D orienting behaviors it is important to answer the following open questions.

Open questions:

1) Are there sensory, sensorimotor and premotor neuron classes in the rostral SC of echolocating bats?

   Are neurons in the rostral SC of echolocating bats tuned in 3D space?

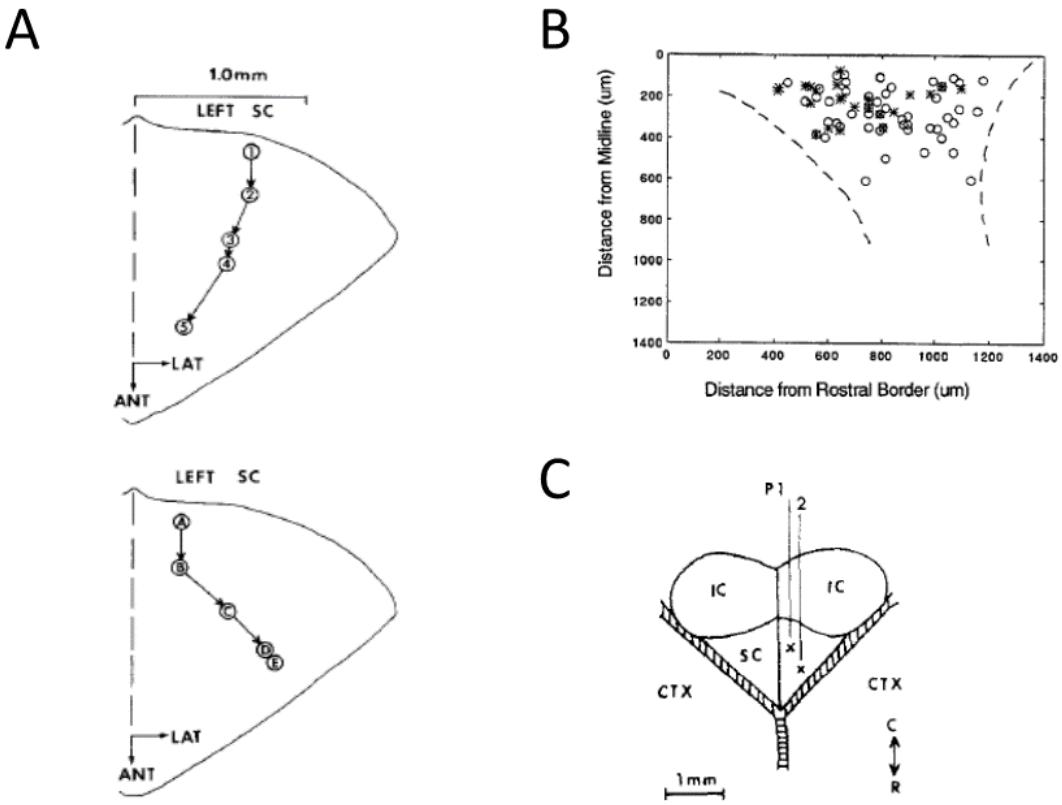

Figure 7-1. Previous literature of neural recordings in the SC of Eptesicus fuscus. A) *adapted from* (Jen et al., 1984)***. B)*** *Adapted from* (Valentine and Moss, 1997)***. C)*** *Adapted from* (Wong, 1984)

Hypothesis:

Neurons in the rSC of echolocating bats can be classified as sensory, sensorimotor and premotor neurons, and, sensory neurons in the rSC are tuned to locations in 3D space.

Experimental design:

Briefly, a direct way to answer the above questions would be to perform extracellular neural recordings in the rostral SC of echolocating bats as shown in Figure 2.2F. Detailed methodology has been recently published in Wohlgemuth et al. (2017), where bats track approaching targets while seated on a platform. Further, neural activity can be classified based on the algorithm described in Chapter 6 and finally, sensory 3D spatial tuning can be computed as described in Chapter 5.

7.2 Does active echolocation shape spatial response profiles of neurons in the SC?

Research in diverse species demonstrates modulation in neural activity with behavioral state (Posner and Petersen, 1989; Reynolds and Chelazzi, 2004; Petersen and Posner, 2012). A most dramatic effect is observed when neural responses are compared in anesthetized and awake animals (Niell and Stryker, 2008, 2010). Recent work in monkeys, rodents and even flies has demonstrated that the animal's behavioral state, and more specifically action, can significantly modulate neural responses to sensory stimuli (Niell and Stryker, 2010; Maimon, 2011; Keller et al., 2012; Fu et al., 2014). The bat's adaptive and self-generated sonar

vocalizations are an essential element of their natural behavior for completing the loop between sensing and action. All studies of echo delay-tuned neurons have measured responses in bats passively listening to simulated pulse-echo pairs (P/E pairs) (O'Neill and Suga, 1982; Wong et al., 1992; Dear et al., 1993; Tanaka and Wong, 1993; Chittajallu et al., 1995; Dear and Suga, 1995; Yan and Suga, 1996; Valentine and Moss, 1997; Bartenstein et al., 2014), but see (Kawasaki et al., 1988). The results presented in Chapter's 5 and 6 are the first empirical demonstration of range tuned neurons in the auditory system of echolocating bats engaged in a naturalistic spatial navigation task.

This, however, still calls into question whether neurons in the auditory system of the echolocating bat respond to P/E delay in the passive listening behavioral state in the same way as neurons respond to echoes from objects at different distances/delays when bats actively echolocate and engage in a goal oriented task. This question attempts to bridge the gap in our knowledge by investigating whether neurons in the SC show the same range-tuning to an artificial P/E pair stimulus as compared to a more natural condition in which bats listen to target echoes from self-generated vocalizations.

Open questions:

1) Do P/E delay tuned neurons in the SC of a passively listening bat also show range tuning when the bat is actively echolocating and tracking a moving target?
2) How does the range tuning of SC neurons, in passively listening and active echolocating bats, compare?

Hypothesis:

Range tuned neurons in the bat rSC show sharper spatial selectivity in animals actively engaged in echolocation, as compared to passive listening animals.

Experimental design:

Passive listening experiments. Head-restrained bats passively listen to P/E auditory stimuli (Figure 7.2) while neural signals from the SC are recorded (Plexon Omniplex data acquisition system). Custom made ultrasound loudspeakers broadcast the Pulse-Echo Delay (P/E Delay) auditory stimuli to the bat (Figure 7.2A). Broadcasting computer generated P/E pairs

Active echolocation experiments. This is the same experimental design as presented in Section 7.1.

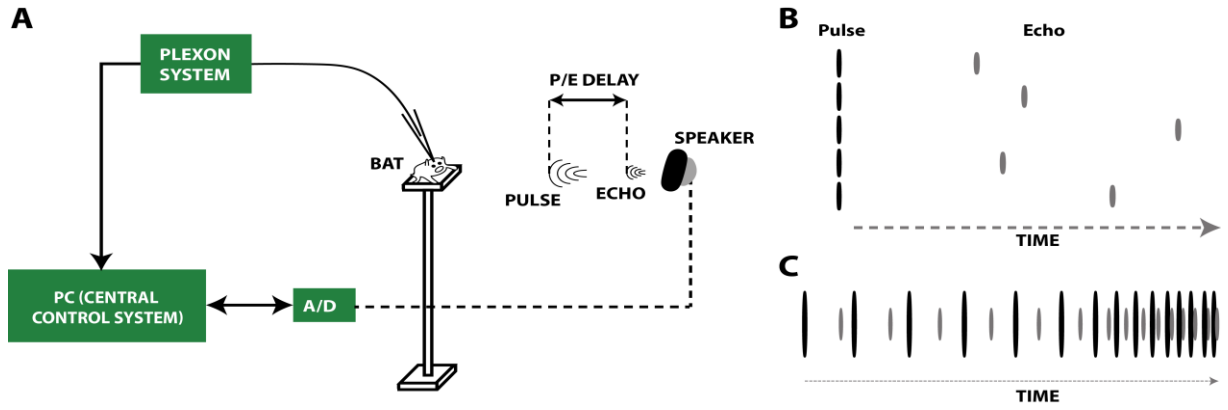

Figure 7-2 Passive listening experiment*. (A) Schematic of experimental set-up showing head-restrained bat resting on a platform, with ultra-sound speakers in front of the bat for playing sound stimuli. (B) An example sequence of randomly generated P/E delays. (C) Sequences of P/E delay simulating an approaching target are also presented.*

After recording neural activity in passively listening bats, as presented above, the active echolocation experiment is performed, while recording the same neurons as in the passively listening experiment. This will allow direct comparison of P/E delay tuning across the two behavioral states.

7.3 Extending the *echo model*

The current *echo model*, as presented in Chapter 4, only computes the direction of (azimuth, elevation and range) and the time of arrival of the echo at the bats ears. It does not take into account the following parameters.

1) **Frequency:** Spectral content of echolocation calls and the call-to-call variations in the beam pattern.
2) **Intensity:** The intensity at source for each echolocation call. In other words, how loud is each echolocation call at the point when the sound leaves the bats mouth (emitter)?
3) **The reflectivity pattern of echo objects.** When sound impinges on an echoic object, depending on the material of the reflecting object, it undergoes frequency dependent absorption. Additionally, the intensity of the reflected echo depends on the surface pattern and orientation of the object.

7.3.1 Possible solutions

Some of the recent experiments in the lab have already demonstrated the capability of estimating both the frequency and intensity, at an individual call level (Lee et al., 2016). These experiments, however, were performed in a small volume of space in order to maximize the

reception of the bats sonar calls on ultrasonic microphones. One possible solution to this would be to perform such experiments where bats are trained to rest on a platform and track and approaching food reward (see Figure 7.1).

Further, solving the problem of reflectivity pattern of echoic objects can be addressed by computing the directionality and reflectivity patterns of objects used in each experiment. Using objects with simple shapes (say spheres or cylinders) will greatly simplify the data collection as well as reduce errors in estimation of echo patterns.

7.4 Conclusion

Bats have evolved echolocation to navigate and forage in 3D space (Griffin, 1958). Bats actively modulate sonar call parameters, such as pulse duration, interval, intensity, bandwidth, sonar beam aim and temporal pattern to influence the information content carried by reflected echoes (Moss and Schnitzler, 1995; Moss and Surlykke, 2001; Ghose and Moss, 2006; Aytekin et al., 2010; Kothari et al., 2014). We can record bat echolocation calls and orienting behaviors using ultrasonic microphones and motion tracking systems to obtain direct measurements of the signals used to guide actions. Furthermore, the discrete nature of bat echolocation signals, combined with simultaneous recordings of coordinated behaviors and neural signals can enable the classification of sensory and motor neural activity. This makes bats ideal animal models for answering questions for informing the general principles of sensorimotor integration, 3D space representation and goal-directed movement in the central nervous system using experimental paradigms involving freely moving animals performing naturalistic behaviors.

I hope, the experiments and results presented as a part of this thesis prompt further research in other mammalian models to investigate the role of the SC in encoding 3D orienting behaviors. I also, hope that our results showing the dynamic nature of 3D spatial receptive fields motivates other researchers to use naturalistic experimental paradigms for investigating the neural correlates of behavior.

A

Neural recordings in the rostral SC of passively listening bats

In the Chapter 4, 5 and 6 it was shown that neurons in the SC of free flying echolocating bats respond to returning echoes and these neurons are tuned to locations in 3D egocentric space. Further, our data demonstrated that neurons in the SC of behaving echolocating bats are tuned to targets at specific distances. In Chapter 7 (Future directions), I had mentioned how to take the previous work forward by recording neurons responses in the rostral pole of the SC, of behaving bats engaged in a target tracking task. Neurons responses to auditory in the rostral SC in the *Eptesicus fuscus* have not been recorded before. Below, I present preliminary data from neural recordings in the rostral SC of passively listening bats. The neural data that I collected from the rSC of bats actively tracking a target has not been presented in this thesis.

A.1 Experimental design

The experimental design is shown in Figure A.1. In brief, bats which had undergone surgery, with a craniotomy, were head restrained in a custom made frame, inside an acoustic booth. Detailed methods can be found in (Wohlgemuth and Moss, 2016).

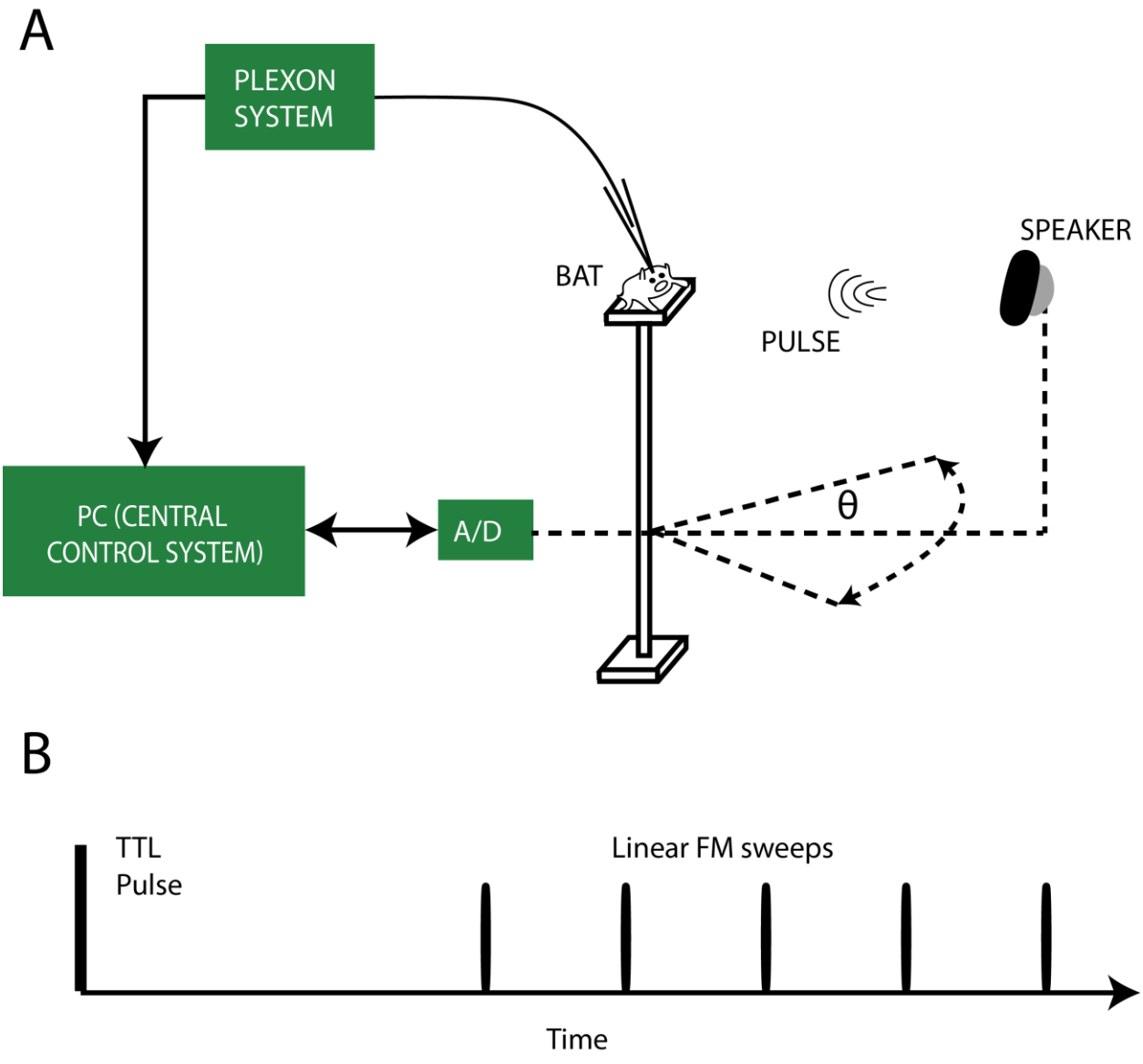

Figure A.1 Experimental design for neural recordings in the rSC of passively listening bats

A.2 Locating the rostral SC

Figure A.2A shows a skull of a euthanized bat with the surficial part of the SC outlined in white. Figure A.2B shows the same outline with recording sites (sites A, B and C) indicated by green, blue and purple color. The preliminary data was recorded from a single bat and 11 neurons single neurons were isolated in 3 different penetrations. The insect in Figure A.2B shows the rough location of a section from the bat atlas indicating that the rostral pole of the SC dips 500 µm under the surface.

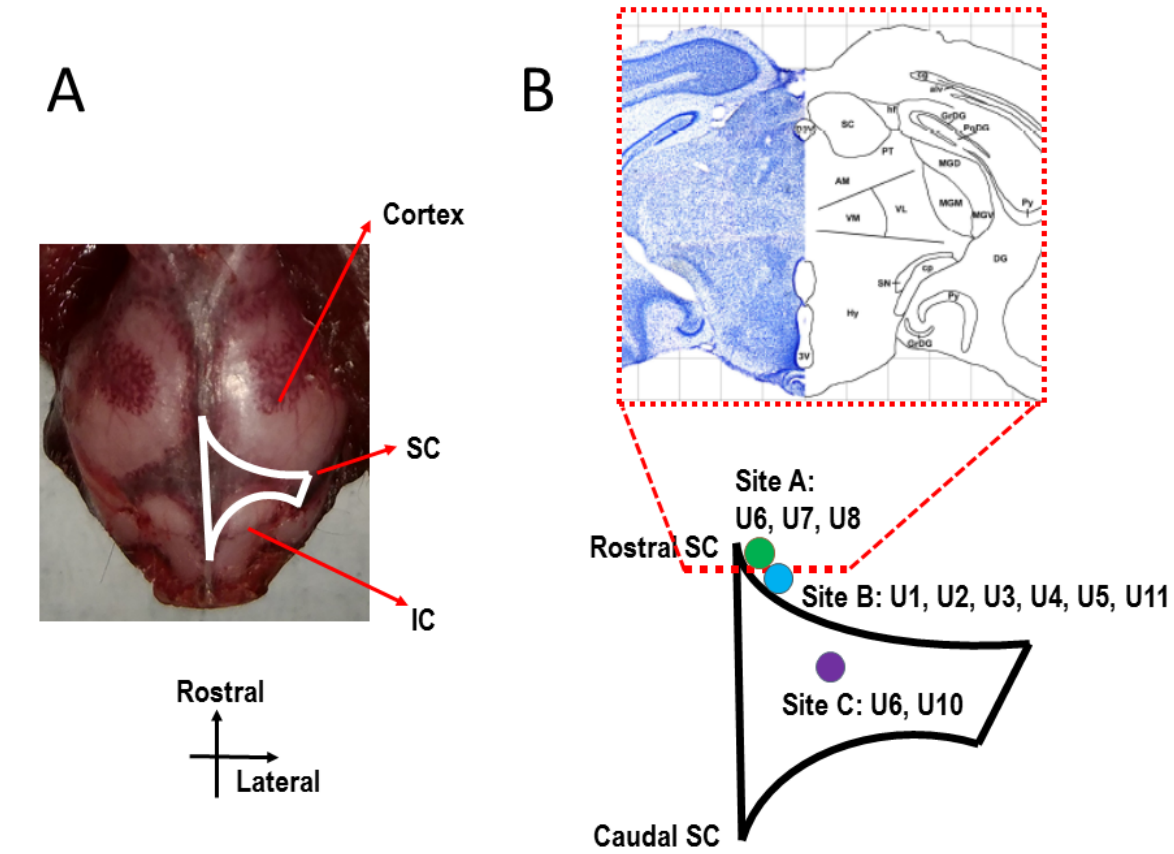

Figure A.2. ***Recording site locations.***

A.3 Neural recordings

Figure A.3A shows the raw trace of the auditory stimuli (top panel) and a time synchronized raw bandpassed neural trace (bottom panel). Figure A.3B shows a zoom in of a 35 ms window (indicated in red in Figure A.3A) with two isolated neurons highlighted. Figure A.3C shows 3 will isolated neurons from this recording site.

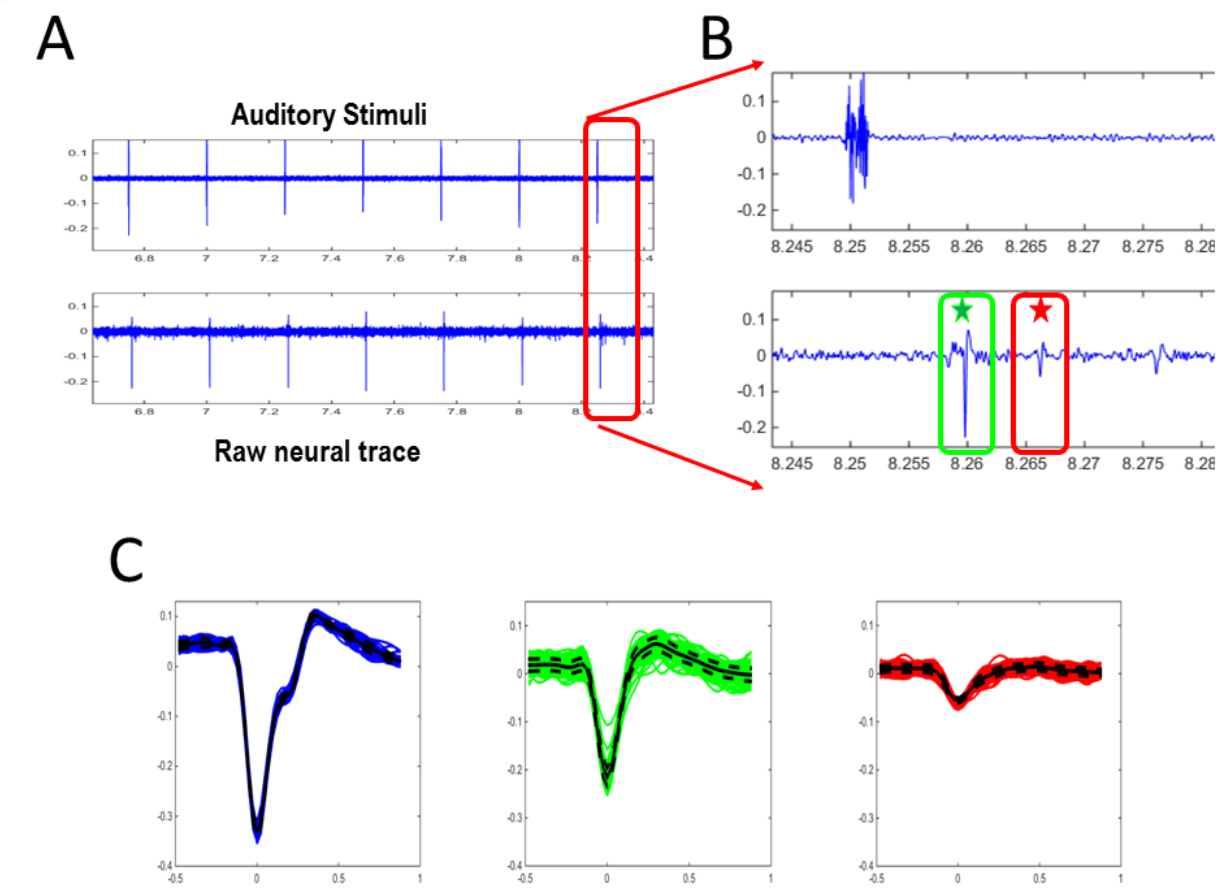

Figure A.3. Raw data and spike sorting.

A.4 Tuning of rSC neurons in azimuth

Figre A.4 shows the roughly mapped tuning (at 15 degree steps) of an example neuron.

Figure A.5A is a summary histogram of the peak azimuthal tuning of all the neurons recorded from the bat. Figure A.5B demonstrates the change in peak azimuthal tuning along the rostro-caudal axis of the SC. This result matches with previous results in several species where rostral region of the SC encodes more frontal azimuthal space, while more caudal locations encode peripheral azimuthal space (Knudsen, 1982; Middlebrooks and Knudsen, 1984b).

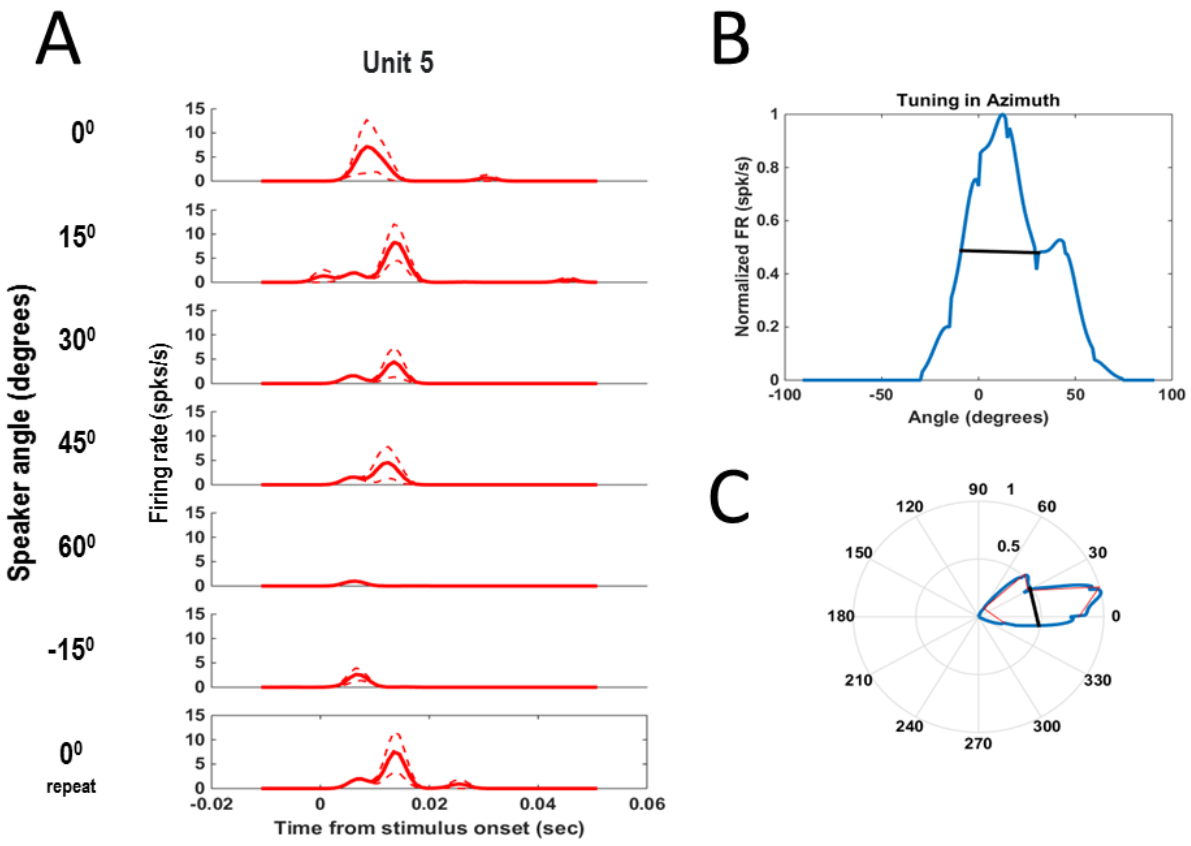

Figure A.4. Tuning to stimulus azimuth of an example cell in the rSC.

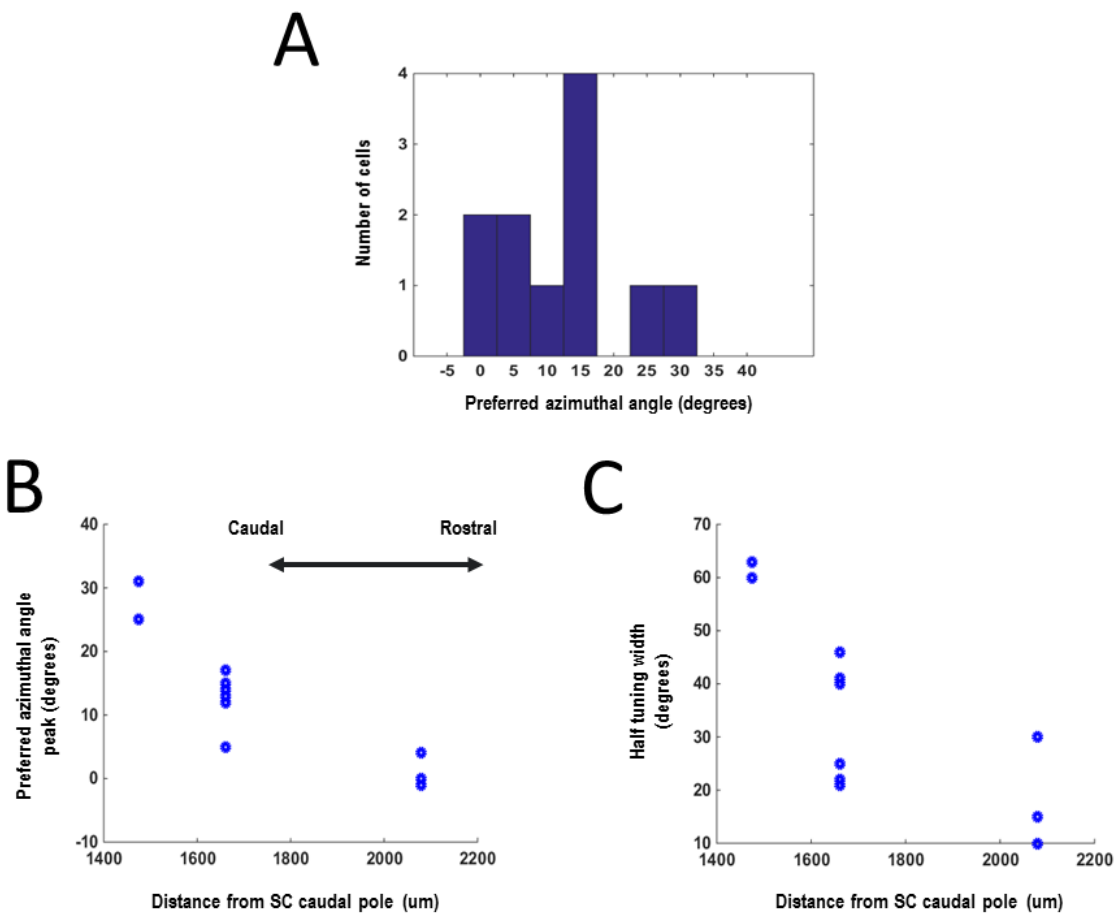

Figure A.5. Change in preferred azimuthal angle and tuning half width with distance from caudal pole of SC.

A.5 Conclusion

The neural recordings described here were performed to demonstrate the feasibility of recording in the rSC in the rSC of the *E. fuscus*. Following this we further performed chronic recordings in the rSC of two big brown bats while they performed a target tracking task. The results of these studies are not described here.

B

Epilogue

When I first started my PhD, little did I know, that I would end up writing a thesis that involved bats, let alone 'flying bats.' I had never trained an animal before in my life, but I did grow up having Diane Fossey, Jane Goodall and Ian Hamilton as my childhood heroes, if that counts at all. I am glad that I made the decision to switch to Cindy's lab as that made me realize my passion for working with animals and observing their behavior. When I first started training bats, I was blown away by the mere emotion of working in such close proximity of a completely different animal. I started observing their behavior, and noticed, with my naïve 'eye' (ears and by watching spectrograms) the clustering of their sonar calls (SSGs). I went up to Cindy and narrated my remarkable discovery, when I learnt, to my dismay, that I had just not read her paper published in 2001 (Moss and Surlykke, 2001). Little did I know that most of my thesis would be exploring this adaptive sonar behavior, which remains quite unexplained.

I also, remember, in one of my first visits to the batlab in UMD, while looking at the platform tracking setup (see Figure 7.1), I had remarked to Ben, "why can't we just record the bat's vocalizations using a mic array, record where it is looking, get the physical locations of the objects in room and just build an estimate of what the bat 'hears' at its ears?" Little did I know that I would be doing the exact same thing, but, in flying bats.

I am glad that I left my corporate job and took the chance of exploring science. Now, I won't have to look back, when I am old, and say 'Ninad, you should have tried that'. Ofcourse, I cannot discount the fact that I could not have done it without an amazing family (both mine and my wifes) and amazing mentors.

I would like to end, with this (slightly lengthy) quote from ‘The Hitchhikers guide to the Galaxy’. This is just a thought, just like the number ‘42’.

****

“O Deep Thought computer," he said, "the task we have designed you to perform is this. We want you to tell us...." he paused, "The Answer."

"The Answer?" said Deep Thought. "The Answer to what?"

"Life!" urged Fook.

"The Universe!" said Lunkwill.

"Everything!" they said in chorus.

Deep Thought paused for a moment's reflection.

"Tricky," he said finally.

"But can you do it?"

Again, a significant pause.

"Yes," said Deep Thought, "I can do it."

"There is an answer?" said Fook with breathless excitement.

"Yes," said Deep Thought. "Life, the Universe, and Everything. There is an answer. But, I'll have to think about it."

...

Fook glanced impatiently at his watch.

“How long?” he said.

“Seven and a half million years,” said Deep Thought.

Lunkwill and Fook blinked at each other.

“Seven and a half million years...!” they cried in chorus.

“Yes,” declaimed Deep Thought, “I said I’d have to think about it, didn’t I?"

[Seven and a half million years later.... Fook and Lunkwill are long gone, but their descendents continue what they started]

"We are the ones who will hear," said Phouchg, "the answer to the great question of Life....!"

"The Universe...!" said Loonquawl.

"And Everything...!"

"Shhh," said Loonquawl with a slight gesture. "I think Deep Thought is preparing to speak!"

There was a moment's expectant pause while panels slowly came to life on the front of the console. Lights flashed on and off experimentally and settled down into a businesslike pattern. A soft low hum came from the communication channel.

"Good Morning," said Deep Thought at last.

"Er..good morning, O Deep Thought" said Loonquawl nervously, "do you have...er, that is..."

"An Answer for you?" interrupted Deep Thought majestically. "Yes, I have."

The two men shivered with expectancy. Their waiting had not been in vain.

"There really is one?" breathed Phouchg.

"There really is one," confirmed Deep Thought.

"To Everything? To the great Question of Life, the Universe and everything?"

"Yes."

Both of the men had been trained for this moment, their lives had been a preparation for it, they had been selected at birth as those who would witness the answer, but even so they found themselves gasping and squirming like excited children.

"And you're ready to give it to us?" urged Loonsuawl.

"I am."

"Now?"

"Now," said Deep Thought.

They both licked their dry lips.

"Though I don't think," added Deep Thought. "that you're going to like it."

"Doesn't matter!" said Phouchg. "We must know it! Now!"

"Now?" inquired Deep Thought.

"Yes! Now..."

"All right," said the computer, and settled into silence again. The two men fidgeted. The tension was unbearable.

"You're really not going to like it," observed Deep Thought.

"Tell us!"

"All right," said Deep Thought. "The Answer to the Great Question..."

"Yes..!"

"Of Life, the Universe and Everything..." said Deep Thought.

"Yes...!"

"Is..." said Deep Thought, and paused.

"Yes...!"

"Is..."

"Yes...!!!...?"

"Forty-two," said Deep Thought, with infinite majesty and calm."

— **Douglas Adams**

The Hitchhiker's Guide to the Galaxy

Bibliography

Agosta SJ (2002) Habitat use, diet and roost selection by the Big Brown Bat (Eptesicus fuscus) in North America: a case for conserving an abundant species. Mamm Rev 32:179–198.

Altmann S (2005) Rotations, quaternions, and double groups. Mineola, N.Y.: Courier Corporation.

Appell PP, Behan M (1990) Sources of subcortical GABAergic projections to the superior colliculus in the cat. J Comp Neurol 302:143–158.

Aytekin M, Mao B, Moss CF (2010) Spatial perception and adaptive sonar behavior. J Acoust Soc Am 128:3788–3798.

Bacon BA, Villemagne J, Bergeron A, Lepore F, Guillemot J-P (1998) Spatial disparity coding in the superior colliculus of the cat. Exp Brain Res 119:333–344.

Badea TC, Cahill H, Ecker J, Hattar S, Nathans J (2009) Distinct roles of transcription factors brn3a and brn3b in controlling the development, morphology, and function of retinal ganglion cells. Neuron 61:852–864.

Baizer JS, Whitney JF, Bender DB (1991) Bilateral projections from the parabigeminal nucleus to the superior colliculus in monkey. Exp Brain Res:467–470.

Banks MS (1980) The development of visual accommodation during early infancy. Child Dev 51:646–666.

Barris RW, Ingram WR, Ranson SW (1935) Optic connections of the diencephalon and midbrain of the cat. J Comp Neurol 62:117–153.

Bartenstein SK, Gerstenberg N, Vanderelst D, Peremans H, Firzlaff U (2014) Echo-acoustic flow dynamically modifies the cortical map of target range in bats. Nat Commun 5:4668.

Basso MA, Wurtz RH (1998) Modulation of neuronal activity in superior colliculus by changes in target probability. J Neurosci 18:7519–7534.

Bauer M, Oostenveld R, Peeters M, Fries P (2006) Tactile Spatial Attention Enhances Gamma-Band Activity in Somatosensory Cortex and Reduces Low-Frequency Activity in Parieto-Occipital Areas. J Neurosci 26.

Beetz MJ, Hechavarría JC, Kössl M (2016) Temporal tuning in the bat auditory cortex is sharper when studied with natural echolocation sequences. Sci Rep 6:29102.

Beninato M, Spencer RF (1986) A Cholinergic Projection to the Rat Superior Colliculus Demonstrated by Retrograde Transport of Horseradish-Peroxidase and Choline-Acetyltransferase Immunohistochemistry. J Comp Neurol 253:525–538.

Berman N, Blakemore C, Cynader M (1975) Binocular interaction in the cat's superior colliculus. J Physiol 246:595–615.

Bezdudnaya T, Castro-Alamancos MA (2014) Neuromodulation of whisking related neural activity in superior colliculus. J Neurosci 34:7683–7695.

Bichot NP, Rossi AF, Desimone R (2005) Parallel and Serial Neural Mechanisms for Visual Search in Macaque Area V4. Science (80-) 308.

Brigham RM, Fenton MB (1986) The influence of roost closure on the roosting and foraging behaviour of Eptesicus fuscus (Chiroptera: Vespertilionidae). Can J Zool 64:1128–1133.

Brinkløv S, Kalko EK V., Surlykke A (2010) Dynamic adjustment of biosonar intensity to habitat clutter in the bat Macrophyllum macrophyllum (Phyllostomidae). Behav Ecol Sociobiol 64:1867–1874.

Bruce CJ, Friedman HR, Kraus MS, Stanton GB (2004) The Primate Frontal Eye Fields. In: The Visual

Neurosciences (Chalupa LM, Werner JS, eds). MIT Press.

Bunt a H, Hendrickson a E, Lund JS, Lund RD, Fuchs a F (1975) Monkey retinal ganglion cells: morphometric analysis and tracing of axonal projections, with a consideration of the peroxidase technique. J Comp Neurol 164:265–285.

Byun H, Kwon S, Ahn HJ, Liu H, Forrest D, Demb JB, Kim IJ (2016) Molecular features distinguish ten neuronal types in the mouse superficial superior colliculus. J Comp Neurol 524:2300–2321.

Canolty RT, Edwards E, Dalal SS, Soltani M, Nagarajan SS, Kirsch HE, Berger MS, Barbaro NM, Knight RT (2006) High Gamma Power Is Phase-Locked to Theta Oscillations in Human Neocortex. Science (80-) 313.

Carandini M, Churchland AK (2013) Probing perceptual decisions in rodents. Nat Neurosci 16:824–831.

Carello CD, Krauzlis RJ (2004) Manipulating intent: evidence for a causal role of the superior colliculus in target selection. Neuron 43:575–583.

Carrasco M (2011) Visual attention: The past 25 years. Vision Res 51:1484–1525.

Casseday JH, Kobler JB, Isbey SF, Covey E (1989) Central acoustic tract in an echolocating bat: An extralemniscal auditory pathway to the thalamus. J Comp Neurol 287:247–259.

Chalupa LM, Rhoades RW (1977) Responses of visual, somatosensory, and auditory neurones in the golden hamster's superior colliculus. J Physiol 270:595–626.

Charlton SG, Starkey NJ (2011) Driving without awareness: The effects of practice and automaticity on attention and driving. Transp Res Part F Traffic Psychol Behav 14:456–471.

Chaturvedi V, Gisbergen J a (1998) Shared target selection for combined version-vergence eye

movements. J Neurophysiol 80:849–862.

Chaturvedi V, van Gisbergen J a (1999) Perturbation of combined saccade-vergence movements by microstimulation in monkey superior colliculus. J Neurophysiol 81:2279–2296.

Chaturvedi V, Van Gisbergen J a (2000a) Stimulation in the rostral pole of monkey superior colliculus: effects on vergence eye movements. Exp Brain Res 132:72–78.

Chaturvedi V, Van Gisbergen JAM (2000b) Stimulation in the rostral pole of monkey superior colliculus: effects on vergence eye movements. Exp Brain Res 132:72–78.

Chittajallu SK, Palakal MJ, Wong D (1995) Analysis and classification of delay-sensitive cortical neurons based on response to temporal parameters in echolocation signals. Hear Res 84:157–166.

Chiu C, Xian W, Moss CF (2009) Adaptive echolocation behavior in bats for the analysis of auditory scenes. J Exp Biol 212:1392–1404.

Cohen YE, Knudsen EI (1999) Maps versus clusters: different representations of auditory space in the midbrain and forebrain. Trends Neurosci 22:128–135.

Collewijn H, Erkelens CJ, Steinman RM (1995) Voluntary binocular gaze-shifts in the plane of regard: dynamics of version and vergence. Vision Res 35:3335–3358.

Corcoran AJ, Barber JR, Conner WE (2009) Tiger moth jams bat sonar. Science 325:325–327.

Cornilleau-Pérès V, Gielen CCAM (1996) Interactions between self-motion and depth perception in the processing of optic flow. Trends Neurosci 19:196–202.

Cotter JR (1981) Retinofugal projections of an echolocating megachiropteran. Dev Dyn 160:159–174.

Cotter JR (1985) Retinofugal projections of the big brown bat, Eptesicus fuscus and the

neotropical fruit bat, Artibeus jamaicensis. Am J Anat 172:105–124.

Cotter JR, Pierson Pentney RJ (1979) Retinofugal projections of nonecholocating (Pteropus giganteus) and echolocating (Myotis lucifugus) bats. J Comp Neurol 184:381–399.

Covey E, Casseday JH (1995) The Lower Brainstem Auditory Pathways. In: Hearing by Bats, pp 235–295.

Covey E, Hall WC, Kobler JB (1987) Subcortical connections of the superior colliculus in the mustache bat, Pteronotus parnellii. J Comp Neurol 263:179–197.

Cowie RJ, Robinson DL (1994) Subcortical contributions to head movements in macaques. I. Contrasting effects of electrical stimulation of a medial pontomedullary region and the superior colliculus. J Neurophysiol 72:2648–2664.

Crosby EC, Henderson JW (1948) The mammalian midbrain and isthmus regions. Part II. Fiber connections of the superior colliculus. B. Pathways concerned in automatic eye movements. J Comp Neurol 88:53–91.

Cullen KE, Van Horn MR (2011) The neural control of fast vs. slow vergence eye movements. Eur J Neurosci 33:2147–2154.

Cumming BG, DeAngelis GC (2001) The Psyiology of Steriopsis. Annu Rev Neurosci:203–238.

Cynader M, Berman N (1972) Receptive-field organization of monkey superior colliculus. J Neurophysiol 35:187–201.

Davies MNO, Green PR (1994) Multiple Sources of Depth Information: An Ecological Approach. In: Perception and Motor Control in Birds, pp 339–356. Berlin, Heidelberg: Springer Berlin Heidelberg.

Dean P, Redgrave P, Sahibzada N, Tsuji K (1986) Head and body movements produced by

electrical stimulation of superior colliculus in rats: Effects of interruption of crossed tectoreticulospinal pathway. Neuroscience 19:367–380.

DeAngelis GC (2000) Seeing in three dimensions: the neurophysiology of stereopsis. Trends Cogn Sci 4:80–90.

Dear SP, Fritz J, Haresign T, Ferragamo M, Simmons J a (1993a) Tonotopic and functional organization in the auditory cortex of the big brown bat, Eptesicus fuscus. J Neurophysiol 70:1988–2009.

Dear SP, Simmons J a, Fritz J (1993b) A possible neuronal basis for representation of acoustic scenes in auditory cortex of the big brown bat. Nature 364:620–623.

Dear SP, Suga N (1995) Delay-tuned neurons in the midbrain of the big brown bat. J Neurophysiol 73:1084–1100.

Deschênes M, Moore J, Kleinfeld D (2012) Sniffing and whisking in rodents. Curr Opin Neurobiol 22:243–250.

Desimone R, Duncan J (1995) Neural mechanisms of selective visual attention. Annu Rev Neurosci 18:193–222.

Dias EC, Rocha-Miranda CE, Bernardes RF, Schmidt SL (1991) Disparity selective units in the superior colliculus of the opossum. Exp Brain Res 87.

Domesick VB (1969) Projections from the cingulate cortex in the rat. Brain Res 12:296–320.

Drager UC, Hubel DH (1975) Physiology of visual cells in mouse superior colliculus and correlation with somatosensory and auditory input. Nature 253:203–204.

Drager UC, Hubel DH (1976) Topography of visual and somatosensory projections to mouse superior colliculus. J Neurophysiol 39:91–101.

Dräger UC, Hubel DH (1975) Responses to visual stimulation and relationship between visual, auditory, and somatosensory inputs in mouse superior colliculus. J Neurophysiol 38:690–713.

Dragoi V, Sharma J, Miller EK, Sur M (2002) Dynamics of neuronal sensitivity in visual cortex and local feature discrimination. Nat Neurosci 5:883–891.

du Lac S, Knudsen EI (1990) Neural maps of head movement vector and speed in the optic tectum of the barn owl. J Neurophysiol 63:131–146.

Duan CA, Erlich JC, Brody CD (2015) Requirement of Prefrontal and Midbrain Regions for Rapid Executive Control of Behavior in the Rat. Neuron 86:1491–1503.

Edelman JA, Keller EL (1996) Activity of visuomotor burst neurons in the superior colliculus accompanying express saccades. J Neurophysiol 76:908–926.

Edwards MA, Schneider GE, Caviness VS (1986) Development of the crossed retinocollicular projection in the mouse. J Comp Neurol 248:410–421.

Edwards SB, Ginsburgh CL, Henkel CK, Stein BE (1979a) Sources of subcortical projections to the superior colliculus in the cat. J Comp Neurol 184:309–329.

Edwards SB, Ginsburgh CL, Henkel CK, Stein BE (1979b) Sources of subcortical projections to the superior colliculus in the cat. J Comp Neurol 184:309–329.

Ehrlich D, Casseday JH, Covey E (1997) Neural tuning to sound duration in the inferior colliculus of the big brown bat, Eptesicus fuscus. J Neurophysiol 77:2360–2372.

Engel SA, Glover GH, Wandell BA (1997) Retinotopic organization in human visual cortex and the spatial precision of functional MRI. Cereb Cortex 7:181–192.

Erlich JC, Bialek M, Brody CD (2011) A cortical substrate for memory-guided orienting in the rat.

Neuron 72:330–343.

Falk B, Jakobsen L, Surlykke A, Moss CF (2014) Bats coordinate sonar and flight behavior as they forage in open and cluttered environments. J Exp Biol 217:4356–4364.

Falk B, Kasnadi J, Moss CF (2015) Tight coordination of aerial flight maneuvers and sonar call production in insectivorous bats. J Exp Biol 218:3678–3688.

Fanselow EE, Nicolelis MA (1999) Behavioral modulation of tactile responses in the rat somatosensory system. J Neurosci 19:7603–7616.

Fecteau JH, Munoz DP (2006) Salience, relevance, and firing: a priority map for target selection. Trends Cogn Sci 10:382–390.

Feig S, Harting JK (1994) Ultrastuctural studies of the primate lateral geniculate nucleus: Morphology and spatial relationships of axon terminals arising from the retina, visual cortex (area 17), superior colliculus, parabigminal nucleus, and pretectum of Galago crassicaudatus. J Comp Neurol 343:17–34.

Felsen G, Mainen ZF (2008) Neural substrates of sensory-guided locomotor decisions in the rat superior colliculus. Neuron 60:137–148.

Feng A, Simmons J, Kick S (1978) Echo detection and target-ranging neurons in the auditory system of the bat Eptesicus fuscus. Science (80-) 202:645–648.

Fenton MB, Simmons NB (2015) A world of Science and mystery: BATS.

Ferezou I, Bolea S, Petersen CCH (2006) Visualizing the Cortical Representation of Whisker Touch: Voltage-Sensitive Dye Imaging in Freely Moving Mice. Neuron 50:617–629.

Finlayson NJ, Zhang X, Golomb JD (2015) The representation and perception of 3D space: Interactions between 2D location and depth. Vis cogn 6285:1–5.

Freedman EG, Sparks DL (1997) Activity of Cells in the Deeper Layers of the Superior Colliculus of the Rhesus Monkey: Evidence for a Gaze Displacement Command. J Neurophysiol 78:1669–1690.

Freedman EG, Stanford TR, Sparks DL (1996) Combined eye-head gaze shifts produced by electrical stimulation of the superior colliculus in rhesus monkeys. J Neurophysiol 76:927–952.

Fries P, Reynolds JH, Rorie AE, Desimone R (2001) Modulation of Oscillatory Neuronal Synchronization by Selective Visual Attention. Science (80-) 291.

Fries W (1984) Cortical projections to the superior colliculus in the macaque monkey: a retrograde study using horseradish peroxidase. J Comp Neurol 230:55–76.

Fries W (1985) Inputs from motor and premotor cortex to the superior colliculus of the macaque monkey. Behav Brain Res 18:95–105.

Fritz J, Shamma S, Elhilali M, Klein D (2003) Rapid task-related plasticity of spectrotemporal receptive fields in primary auditory cortex. Nat Neurosci 6:1216–1223.

Fritz JB, Elhilali M, David S V., Shamma SA (2007) Auditory attention - focusing the searchlight on sound. Curr Opin Neurobiol 17:437–455.

Frost BJ, Wylie DR (2000) A common frame of reference for the analysis of optic flow and vestibular information. Int Rev Neurobiol 44:121–140.

Fu Y, Tucciarone JM, Espinosa JS, Sheng N, Darcy DP, Nicoll RA, Huang ZJ, Stryker MP (2014) A cortical circuit for gain control by behavioral state. Cell 156:1139–1152.

Fuzessery ZM, Wenstrup JJ, Pollak GD (1990) Determinants of horizontal sound location selectivity of binaurally excited neurons in an isofrequency region of the mustache bat

inferior colliculus. J Neurophysiol 63:1128–1147.

Gaither NS, Stein BE (1979) Reptiles and mammals use similar sensory organizations in the midbrain. Science 205:595–597.

Gamlin PD, Yoon K (2000) An area for vergence eye movement in primate frontal cortex. Nature 407:1003–1007.

Gandhi NJN, Katnani H a H (2011) Motor Functions of the Superior Colliculus. Annu Rev Neurosci.

Gawryszewski L de G, Riggio L, Rizzolatti G, Umiltá C (1987) Movements of attention in the three spatial dimensions and the meaning of “neutral” cues. Neuropsychologia 25:19–29.

Geva-Sagiv M, Las L, Yovel Y, Ulanovsky N (2015) Spatial cognition in bats and rats: from sensory acquisition to multiscale maps and navigation. Nat Rev Neurosci 16:94–108.

Ghitani N, Bayguinov PO, Vokoun CR, McMahon S, Jackson MB, Basso M a (2014) Excitatory synaptic feedback from the motor layer to the sensory layers of the superior colliculus. J Neurosci 34:6822–6833.

Ghose K, Moss CF (2003) The sonar beam pattern of a flying bat as it tracks tethered insects. J Acoust Soc Am 114:1120.

Ghose K, Moss CF (2006) Steering by hearing: a bat’s acoustic gaze is linked to its flight motor output by a delayed, adaptive linear law. J Neurosci 26:1704–1710.

Ghose K, Triblehorn JD, Bohn K, Yager DD, Moss CF (2009) Behavioral responses of big brown bats to dives by praying mantises. J Exp Biol 212:693–703.

Gnadt JW, Mays LE (1995) Neurons in monkey parietal area LIP are tuned for eye-movement parameters in three-dimensional space. J Neurophysiol 73:280–297.

Goddard CA et al. (2012a) Gamma oscillations are generated locally in an attention-related

midbrain network. Neuron 73:567–580.

Goddard CA, Mysore SP, Bryant AS, Huguenard JR, Knudsen EI (2014) Spatially reciprocal inhibition of inhibition within a stimulus selection network in the avian midbrain. PLoS One 9.

Goddard CA, Sridharan D, Huguenard J, Knudsen E (2012b) Gamma oscillations are generated locally in an attention-related midbrain network. Neuron 73:567–580.

Goldberg ME, Wurtz RH (1972a) Activity of superior colliculus in behaving monkey. I. Visual receptive fields of single neurons. J Neurophysiol 35:542–559.

Goldberg MEM, Wurtz RH (1972b) Activity of superior colliculus in behaving monkey. II. Effect of attention on neuronal responses. J Neurophysiol 35:560–574.

Golomb JD, Kanwisher N (2012) Higher level visual cortex represents retinotopic, not spatiotopic, object location. Cereb Cortex 22:2794–2810.

Gottlieb JP, Kusunoki M, Goldberg ME (1998) The representation of visual salience in monkey parietal cortex. Nature 391:481–484.

Graybiel AM (1975) Anatomical organization of retinotectal afferents in the cat: An autodiographic study. Brain Res 96:1–23.

Graybiel AM (1978) A satellite system of the superior colliculus: the parabigeminal nucleus and its projections to the superficial collicular layers. Brain Res 145:365–374.

Green DG, Powers MK, Banks MS (1980) Depth of focus, eye size and visual acuity. Vision Res 20:827–835.

Gregoriou GG, Gotts SJ, Zhou H, Desimone R (2009) High-Frequency, Long-Range Coupling Between Prefrontal and Visual Cortex During Attention. Science (80-) 324.

Griffin DR (1958) Listening in the Dark: The acoustic orientation of bats and men. Yale University Press, New Haven.

Griffin DR, Webster FA, Michael CR (1960) The echolocation of flying insects by bats. Anim Behav 8:141–154.

Grobstein P (1988) Between the retinotectal projection and directed movement: topography of a sensorimotor interface. Brain Behav Evol 31:34–48.

Grothe B (2003) New roles for synaptic inhibition in sound localization. Nat Rev Neurosci 4:540–550.

Grothe B, Pecka M, McAlpine D (2010) Mechanisms of sound localization in mammals. Physiol Rev 90:983–1012.

Gruber T, Müller MM, Keil A, Elbert T (1999) Selective visual-spatial attention alters induced gamma band responses in the human EEG. Clin Neurophysiol 110:2074–2085.

Guitton D, Roucoux A, Crommelinck M (1980) Stimulation of the superior colliculus in the alert cat I. Eye Movements and Neck EMG Activity Evoked when the Head is Restrained. Exp Brain Res 39:63–73.

Gunduz A, Brunner P, Daitch A, Leuthardt EC, Ritaccio AL, Pesaran B, Schalk G (2011) Neural Correlates of Visual?Spatial Attention in Electrocorticographic Signals in Humans. Front Hum Neurosci 5:89.

Gutnisky DA, Dragoi V (2008) Adaptive coding of visual information in neural populations. Nature 452:220–224.

Hagemann C, Esser K-H, Kössl M (2010) Chronotopically organized target-distance map in the auditory cortex of the short-tailed fruit bat. J Neurophysiol 103:322–333.

Harting JK, Casagrande VA, Weber JT (1978) The projection of the primate superior colliculus upon the dorsal lateral geniculate nucleus: autoradiographic demonstration of interlaminar distribution of tectogeniculate axons. Brain Res 150:593–599.

Harting JK, Diamond IT, Hall WC (1973) Anterograde degeneration study of the cortical projections of the lateral geniculate and pulvinar nuclei in the tree shrew (Tupaia glis). J Comp Neurol 150:393–439.

Harting JK, Huerta MF, Frankfurter AJ, Strominger NL, Royce GJ (1980) Ascending Pathways From the Monkey Superior Colliculus: An Autoradiographic Analysis. J Comp Neurol 882.

Harting JK, Huerta MF, Hashikawa T, van Lieshout DP (1991a) Projection of the mammalian superior colliculus upon the dorsal lateral geniculate nucleus: Organization of tectogeniculate pathways in nineteen species. J Comp Neurol 304:275–306.

Harting JK, Van Lieshout DP, Hashikawa T, Weber JT (1991b) The parabigeminogeniculate projection: Connectional studies in eight mammals. J Comp Neurol 305:559–581.

Hartline PH, Kass L, Loop MS (1978) Merging of modalities in the optic tectum: infrared and visual integration in rattlesnakes. Science 199:1225–1229.

Hartridge H (1945) Acoustic control in the flight of bats. Nature 156:692.

Harvey AR, Worthington DR (1990) The projection from different visual cortical areas to the rat superior colliculus. J Comp Neurol 298:281–292.

Hayhoe M, Ballard D (2005) Eye movements in natural behavior. Trends Cogn Sci 9:188–194.

Haynes H, White BL, Held R (1965) Visual Accommodation in Human Infants. Science 148:528–530.

Hayward B, Davis R (1964) Flight speeds in western bats. J Mammal 45:236–242.

Hechavarría JC, Macías S, Vater M, Voss C, Mora EC, Kössl M (2013) Blurry topography for precise target-distance computations in the auditory cortex of echolocating bats. Nat Commun 4:1–11.

Helms MC, Ozen G, Hall WC (2004) Organization of the intermediate gray layer of the superior colliculus. I. Intrinsic vertical connections. J Neurophysiol 91:1706–1715.

Henkel CK, Edwards SB (1978) The superior colliculus control of pinna movements in the cat: possible anatomical connections. J Comp Neurol 182:763–776.

Hepp K, Van Opstal AJ, Straumann D, Hess BJ, Henn V (1993) Monkey superior colliculus represents rapid eye movements in a two-dimensional motor map. J Neurophysiol 69.

Hiryu S, Bates ME, Simmons J a, Riquimaroux H (2010) FM echolocating bats shift frequencies to avoid broadcast-echo ambiguity in clutter. Proc Natl Acad Sci U S A 107:7048–7053.

Hofbauer A, Dräger UC (1985) Depth segregation of retinal ganglion cells projecting to mouse superior colliculus. J Comp Neurol 234:465–474.

Hoffmann S, Vega-Zuniga T, Greiter W, Krabichler Q, Bley A, Matthes M, Zimmer C, Firzlaff U, Luksch H (2016) Congruent representation of visual and acoustic space in the superior colliculus of the echolocating bat Phyllostomus discolor. Eur J Neurosci.

Hong YK, Kim IJ, Sanes JR (2011) Stereotyped axonal arbors of retinal ganglion cell subsets in the mouse superior colliculus. J Comp Neurol 519:1691–1711.

Hope GM, Bhatnagar KP (1979) Electrical response of bat retina to spectral stimulation: comparison of four microhiropteran species. Experientia 35:1189–1191.

Horton JC, Hoyt WF (1991) The Representation of the Visual Field in Human Striate Cortex. Arch Opthalmology 109:816–824.

Horwitz G, Newsome W (1999) Separate signals for target selection and movement specification in the superior colliculus. Science (80-) 2735.

Hubel DH, LeVay S, Wiesel TN (1975) Mode of termination of retinotectal fibers in macaque monkey: an autoradiographic study. Brain Res 96:25–40.

Huerta MF, Harting JK (1983) Sublamination within the superficial gray layer of the squirrel monkey: an analysis of the tectopulvinar projection using anterograde and retrograde transport methods. Brain Res 261:119–126.

Huerta MF, Harting JK (1984a) Connectional organization of the superior colliculus. Trends Neurosci 7:286–289.

Huerta MF, Harting JK (1984b) The mammalian superior colliculus: Studies of its morphology and connections. In: The Comparative Neurology of the Optic Tectum. (Vanegas H, ed), pp 687–773. New York: Plenum Press.

Hyde P, Knudsen E (2000) Topographic projection from the optic tectum to the auditory space map in the inferior colliculus of the barn owl. J Comp Neurol 160:146–160.

Ignashchenkova A, Dicke PW, Haarmeier T, Thier P (2004) Neuron-specific contribution of the superior colliculus to overt and covert shifts of attention. Nat Neurosci 7:56–64.

Itti L, Koch C (2001) Computational modelling of visual attention. Nat Rev Neurosci 2:194–203.

Jakobsen L, Brinkløv S, Surlykke A (2013a) Intensity and directionality of bat echolocation signals. Front Physiol 4:89.

Jakobsen L, Ratcliffe JM, Surlykke A (2013b) Convergent acoustic field of view in echolocating bats. Nature 493:93–96.

Jaramillo S, Zador AM (2011) The auditory cortex mediates the perceptual effects of acoustic

temporal expectation. Nat Neurosci 14:246–251.

Jay MF, Sparks DL (1984) Auditory receptive fields in primate superior colliculus shift with changes in eye position. Nature 309:345–347.

Jay MF, Sparks DL (1987) Sensorimotor integration in the primate superior colliculus. I. Motor convergence. J Neurophysiol 57:22–34.

Jen P, Sun X, Kamada T (1984) Auditory response properties and spatial response areas of superior collicular neurons of the FM bat, Eptesicus fuscus. J Comp …:407–413.

Jen PH-S, McCarty JK (1978) Bats avoid moving objects more successfully than stationary ones. Nature 275:743–744.

Jones G, Holderied MW (2007) Bat echolocation calls: adaptation and convergent evolution. Proc Biol Sci 274:905–912.

Kalko EKV (1995) Insect pursuit, prey capture and echolocation in pipestirelle bats (Microchiroptera). Anim Behav 50:861–880.

Kalko EV, Schnitzler H-U (1993) Plasticity in echolocation signals of European pipistrelle bats in search flight: implications for habitat use and prey detection. Behav Ecol Sociobiol 33:415–428.

Kalko EK V., Schnitzler H-U (1989) The echolocation and hunting behavior of Daubenton's bat, Myotis daubentoni. Behav Ecol Sociobiol 24:225–238.

Kanaseki T, Sprague JM (1974) Anatomical organization of pretectal nuclei and tectal laminae in the cat. J Comp Neurol 158:319–337.

Kawamura S, Sprague JM, Niimi K (1974) Corticofugal projections from the visual cortices to the thalamus, pretectum and superior colliculus in the cat. J Comp Neurol 158:339–362.

Kawasaki M, Margoliash D, Suga N (1988) Delay-tuned combination-sensitive neurons in the auditory cortex of the vocalizing mustached bat. J Neurophysiol 59:623–635.

Keller GB, Bonhoeffer T, Hübener M (2012) Sensorimotor Mismatch Signals in Primary Visual Cortex of the Behaving Mouse. Neuron 74:809–815.

Kick SA, Simmons JA (1984) Automatic gain control in the bat's sonar receiver and the neuroethology of echolocation. J Neurosci 4:2725–2737.

King AJ, Palmer AR (1983) Cells responsive to free-field auditory stimuli in guinea-pig superior colliculus: distribution and response properties. J Physiol 342:361–381.

Kirschfeld K (1976) The Resolution of Lens and Compound Eyes. In, pp 354–370. Springer, Berlin, Heidelberg.

Knudsen EI (1982) Auditory and visual maps of space in the optic tectum of the owl. J Neurosci 2:1177–1194.

Knudsen EI (2007a) Fundamental components of attention. Annu Rev Neurosci 30:57–78.

Knudsen EI (2007b) Fundamental components of attention. Annu Rev Neurosci 30:57–78.

Knudsen EI (2011) Control from below: the role of a midbrain network in spatial attention. Eur J Neurosci 33:1961–1972.

Knudsen EI, Brainard MS (1991) Visual instruction of the neural map of auditory space in the developing optic tectum. Science 253:85–87.

Knudsen EI, Brainard MS (1995) Creating a unified representation of visual and auditory space in the brain. Annu Rev Neurosci 18:19–43.

Knudsen EI, Cohen YE (1995) Characterization of a Forebrain the Barn Owl : Microstimulation Gaze Field in the Archistriatum and Anatomical Connections. 15:5139–5151.

Knudsen EI, Cohen YE, Masino T (1995) Characterization of a forebrain gaze field in the archistriatum of the barn owl: microstimulation and anatomical connections. J Neurosci 15:5139–5151.

Knudsen EI, Konishi M (1978) A neural map of auditory space in the owl. Science 200:795–797.

Kober R, Schnitzler H (1990) Information in sonar echoes of fluttering insects available for echolocating bats. J Acoust Soc Am 87:882–896.

Kobler JB, Isbey SF, Casseday JH (1987) Auditory pathways to the frontal cortex of the mustache bat, Pteronotus parnellii. Science 236:824–826.

Koblitz JC, Stilz P, Schnitzler H-U (2010) Source levels of echolocation signals vary in correlation with wingbeat cycle in landing big brown bats (Eptesicus fuscus). J Exp Biol 213:3263–3268.

Köck A, Jakobs A-K, Kral K (1993) Visual prey discrimination in monocular and binocular praying mantis Tenodera sinensis during postembryonic development. J Insect Physiol 39:485–491.

Kothari NB, Wohlgemuth MJ, Hulgard K, Surlykke A, Moss CF (2014) Timing matters: Sonar call groups facilitate target localization in bats. Front Physiol 5 MAY.

Kral K (2003) Behavioural-analytical studies of the role of head movements in depth perception in insects, birds and mammals. Behav Processes 64:1–12.

Krauzlis RJ, Liston D, Carello CD (2004) Target selection and the superior colliculus: goals, choices and hypotheses. Vision Res 44:1445–1451.

Krauzlis RJ, Lovejoy LP, Zénon A (2013) Superior colliculus and visual spatial attention. Annu Rev Neurosci 36:165–182.

Künzle H, Akert K, Wurtz RH (1976) Projection of area 8 (frontal eye field) to superior colliculus in the monkey. An autoradiographic study. Brain Res 117:487–492.

Kustov a a, Robinson DL (1996) Shared neural control of attentional shifts and eye movements. Nature 384:74–77.

Land MF (1999) Motion and vision: why animals move their eyes. J Comp Physiol A 185:341–352.

Land MF, Collett TS (1974) Chasing behaviour of houseflies (Fannia canicularis). J Comp Physiol 89:331–357.

Langer TP, Lund RD (1974) The upper layers of the superior colliculus of the rat: a Golgi study. J Comp Neurol 158:418–435.

Lawrence BD, Simmons J a (1982) Echolocation in bats: the external ear and perception of the vertical positions of targets. Science 218:481–483.

Lee W-J, Falk B, Chiu C, Krishnan A, Moss CF (2016) Asymmetric multi-frequency biosonar beam pattern of tongue-clicking bat, *Rousettus aegyptiacus*. J Acoust Soc Am 139:2115–2115.

Leigh J, Zee DS (1983) The neurology of eye movements. Oxford University Press.

Lewicki MS, Olshausen B a., Surlykke A, Moss CF (2014) Scene analysis in the natural environment. Front Psychol 5:1–21.

Linden R, Perry VH (1983) Massive retinotectal projection in rats. Brain Res 272:145–149.

Livingston CA, Mustari MJ (2000) The anatomical organization of the macaque pregeniculate complex. Brain Res 876:166–179.

Lovejoy LP, Krauzlis RJ (2010) Inactivation of primate superior colliculus impairs covert selection of signals for perceptual judgments. Nat Neurosci 13:261–266.

Lui F, Gregory KM, Blanks RHI, Giolli RA (1995) Projections from Visual Areas of the Cerebral-Cortex to Pretectal Nuclear-Complex, Terminal Accessory Optic Nuclei, and Superior Colliculus in Macaque Monkey. J Comp Neurol 363:439–460.

Lund RD (1965) Uncrossed Visual Pathways of Hooded and Albino Rats. Science (80-) 149:1506–1507.

Lund RD (1972) Anatomic studies on the superior colliculus. Invest Ophthalmol 11:434–441.

Lund RD (1975) Variations in the laterality of the central projections of retinal ganglion cells. Exp Eye Res 21:193–203.

Lund RD, Land PW, Boles J (1980) Normal and abnormal uncrossed retinotectal pathways in rats: An HRP study in adults. J Comp Neurol 189:711–720.

Madsen PT, Wahlberg M (2007) Recording and quantification of ultrasonic echolocation clicks from free-ranging toothed whales.

Maimon G (2011) Modulation of visual physiology by behavioral state in monkeys, mice, and flies. Curr Opin Neurobiol 21:559–564.

Maltby A, Jones KE, Jones G (2009) Understanding the evolutionary origin and diversification of bat echolocation calls. In: Handbook of Behavioral Neuroscience, pp 37–47.

Mantani S, Hiryu S, Fujioka E, Matsuta N, Riquimaroux H, Watanabe Y (2012) Echolocation behavior of the Japanese horseshoe bat in pursuit of fluttering prey. J Comp Physiol A Neuroethol Sens Neural Behav Physiol 198:741–751.

Mao B, Aytekin M, Wilkinson GS, Moss CF (2016) Big brown bats (Eptesicus fuscus) reveal diverse strategies for sonar target tracking in cluttera). J Acoust Soc Am 140:1839–1849.

Masino T, Knudsen EI (1990) Horizontal and vertical components of head movement are controlled by distinct neural circuits in the barn owl. Nature 345:434–437.

Masino T, Knudsen EI (1993) Orienting head movements resulting from electrical microstimulation of the brainstem tegmentum in the barn owl. J Neurosci 13:351–370.

May PJ (2006) The mammalian superior colliculus: laminar structure and connections. Prog Brain Res 151:321–378.

Mays LE, Sparks DL (1980) Dissociation of visual and saccade-related responses in superior colliculus neurons. J Neurophysiol 43:207–232.

McAdams CJ, Maunsell JHR (1999) Effects of Attention on Orientation-Tuning Functions of Single Neurons in Macaque Cortical Area V4. J Neurosci 19.

McHaffie JG, Stein BE (1982) Eye movements evoked by electrical stimulation in the superior colliculus of rats and hamsters. Brain Res 247:243–253.

McIlwain JT (1986) Effects of eye position on saccades evoked electrically from superior colliculus of alert cats. J Neurophysiol 55:97–112.

McIlwain JT (1988) Saccadic eye movements evoked by electrical stimulation of the cat's visual cortex. Vis Neurosci 1:135–143.

McIlwain JT (1990) Topography of eye-position sensitivity of saccades evoked electrically from the cat's superior colliculus. Vis Neurosci 4:289–298.

McPeek RM, Keller EL (2004) Deficits in saccade target selection after inactivation of superior colliculus. Nat Neurosci 7:757–763.

Menne D, Kaipf I, Wagner I, Ostwald J, Schnitzler HU (1989) Range estimation by echolocation in the bat Eptesicus fuscus: trading of phase versus time cues. J Acoust Soc Am 85:2642–2650.

Meredith M a, Stein BE (1996) Spatial determinants of multisensory integration in cat superior colliculus neurons. J Neurophysiol 75:1843–1857.

Meredith M, Wallace M, Stein B (1992) Visual, auditory and somatosensory convergence in output neurons of the cat superior colliculus: multisensory properties of the tecto-reticulo-

spinal projection. Exp brain Res:181–186.

Metzner W (1989) A possible neuronal basis for Doppler-shift compensation in echo-locating horseshoe bats. Nature 341:529–532.

Middlebrooks J, Knudsen E (1984a) A neural code for auditory space in the cat's superior colliculus. J Neurosci 4.

Middlebrooks JC, Knudsen EI (1984b) A neural code for auditory space in the cat's superior colliculus. J Neurosci 4:2621–2634.

Miller EK, Cohen JD (2001) An integrative theory of prefrontal cortex function. Annu Rev Neurosci 24:167–202.

Mimeault D, Paquet V, Molotchnikoff S, Lepore F, Guillemot J-P (2004) Disparity sensitivity in the superior colliculus of the cat. Brain Res 1010:87–94.

Mize RR, Butler GD (1996) Postembedding immunocytochemistry demonstrates directly that both retinal and cortical terminals in the cat superior colliculus are glutamate immunoreactive. J Comp Neurol 371:633–648.

Mooney RD, Fish SE, Rhoades RW (1984) Anatomical and functional organization of pathway from superior colliculus to lateral posterior nucleus in hamster. J Neurophysiol 51:407–431.

Morin LP, Blanchard JH, Provencio I (2003) Retinal ganglion cell projections to the hamster suprachiasmatic nucleus, intergeniculate leaflet, and visual midbrain: Bifurcation and melanopsin immunoreactivity. J Comp Neurol 465:401–416.

Moss CF, Bohn K, Gilkenson H, Surlykke A (2006) Active listening for spatial orientation in a complex auditory scene. PLoS Biol 4:e79.

Moss CF, Schnitzler H-U (1995) Behavioral Studies of Auditory Information Processing. In: Hearing

by Bats (Popper, ArthurN. and Fay R, ed), pp 87–145. Springer New York.

Moss CF, Schnitzler HU (1989) Accuracy of target ranging in echolocating bats: acoustic information processing. J Comp Physiol A 165:383–393.

Moss CF, Surlykke A (2001) Auditory scene analysis by echolocation in bats. J Acoust Soc Am 110:2207.

Moss CF, Surlykke A (2010) Probing the natural scene by echolocation in bats. Front Behav Neurosci 4:1–16.

Moss CF, Zagaeski M (1994) Acoustic information available to bats using frequency-modulated sounds for the perception of insect prey. J Acoust Soc Am 95:2745–2756.

Müller JR, Philiastides MG, Newsome WT (2005) Microstimulation of the superior colliculus focuses attention without moving the eyes. Proc Natl Acad Sci U S A 102:524–529.

Munoz DP, Guitton D (1991) Control of orienting gaze shifts by the tectoreticulospinal system in the head-free cat. II. Sustained discharges during motor preparation and fixation. J Neurophysiol 66:1624–1641.

Munoz DP, Guitton D, Pélisson D (1991) Control of orienting gaze shifts by the tectoreticulospinal system in the head-free cat. III. Spatiotemporal characteristics of phasic motor discharges. J Neurophysiol 66:1642–1666.

Mysore SP, Asadollahi A, Knudsen EI (2010) Global inhibition and stimulus competition in the owl optic tectum. J Neurosci 30:1727–1738.

Mysore SP, Asadollahi A, Knudsen EI (2011) Signaling of the strongest stimulus in the owl optic tectum. J Neurosci 31:5186–5196.

Mysore SP, Knudsen EI (2011) The role of a midbrain network in competitive stimulus selection.

Curr Opin Neurobiol 21:653–660.

Mysore SP, Knudsen EI (2012) Reciprocal inhibition of inhibition: a circuit motif for flexible categorization in stimulus selection. Neuron 73:193–205.

Mysore SPP, Knudsen EII (2014) Descending control of neural bias and selectivity in a spatial attention network: rules and mechanisms. Neuron 84:214–226.

Nagata T, Magalhães-Castro HH, Saraiva PES, Magalhães-Castro B (1980) Absence of tectotectal pathway in the rabbit: An anatomical and electrophysiological study. Neurosci Lett 17:125–130.

Neafsey EJ, Hurley-Gius KM, Arvanitis D (1986) The topographical organization of neurons in the rat medial frontal, insular and olfactory cortex projecting to the solitary nucleus, olfactory bulb, periaqueductal gray and superior colliculus. Brain Res 377:261–270.

Necker R (2007) Head-bobbing of walking birds. J Comp Physiol A Neuroethol Sensory, Neural, Behav Physiol 193:1177–1183.

Neuweiler G (1990) Auditory adaptations for prey capture in echolocating bats. Physiol Rev 70:615–641.

Newman E, Hartline P (1981) Integration of visual and infrared information in bimodal neurons in the rattlesnake optic tectum. Science (80-) 213:789–791.

Niell CM, Stryker MP (2008) Highly selective receptive fields in mouse visual cortex. J Neurosci 28:7520–7536.

Niell CM, Stryker MP (2010) Modulation of Visual Responses by Behavioral State in Mouse Visual Cortex. Neuron 65:472–479.

Nordström K, O'Carroll DC (2009) Feature detection and the hypercomplex property in insects.

Trends Neurosci 32:383–391.

O'Keefe J, Dostrovsky J (1971) The hippocampus as a spatial map. Preliminary evidence from unit activity in the freely-moving rat. Brain Res 34:171–175.

O'Neill WE, Suga N (1979) Target range-sensitive neurons in the auditory cortex of the moustache bat. Science (80-) 203:69–72.

O'Neill WE, Suga N (1982) Encoding of target range and its representation in the auditory cortex of the mustached bat. J Neurosci 2:17–31.

Olivier E, Corvisier J, Pauluis Q, Hardy O (2000) Evidence for glutamatergic tectotectal neurons in the cat superior colliculus: a comparison with GABAergic tectotectal neurons. Eur J Neurosci 12:2354–2366.

Olivier E, Porter JD, May PJ (1998) Comparison of the distribution and somatodendritic morphology of tectotectal neurons in the cat and monkey. Vis Neurosci 15:903–922.

Olsen JF, Suga N (1991) Combination-sensitive neurons in the medial geniculate body of the mustached bat: encoding of target range information. J Neurophysiol 65.

Pare M, Crommelinck M, Guitton D (1994) Gaze shifts evoked by stimulation of the superior colliculus in the head-free cat conform to the motor map but also depend on stimulus strength and fixation activity. Exp Brain Res 101.

Perry VH (1980) A tectocortical visual pathway in the rat. Neuroscience 5:915–927.

Petersen SE, Posner MI (2012) The attention system of the human brain: 20 years after. Annu Rev Neurosci 35:73–89.

Petrites AE, Eng OS, Mowlds DS, Simmons J a, DeLong CM (2009) Interpulse interval modulation by echolocating big brown bats (Eptesicus fuscus) in different densities of obstacle clutter. J

Comp Physiol A Neuroethol Sens Neural Behav Physiol 195:603–617.

Pettigrew JD (1986) Flying primates? Megabats have the advanced pathway from eye to midbrain. Science 231:1304–1306.

Pettigrew JD, Maseko BC, Manger PR (2008) Primate-like retinotectal decussation in an echolocating megabat, Rousettus aegyptiacus. Neuroscience 153:226–231.

Pollack G (2000) Who, what, where? recognition and localization of acoustic signals by insects. Curr Opin Neurobiol 10:763–767.

Pollack JG, Hickey TL (1979) The distribution of retino-collicular axon terminals in rhesus monkey. J Comp Neurol 185:587–602.

Pollak GD, Burger RM, Klug A (2003) Dissecting the circuitry of the auditory system. Trends Neurosci 26:33–39.

Pöppel E (1973) Comment on “Visual system’s view of acoustic space.” Nature 243:231.

Popper a. N (1994) The Mammalian Auditory Pathway: Neurophysiology (Richard R Fay ANP, ed).

Popper AN, Fay RR (1995) Hearing by bats. Springer Handb Audit Res.

Portfors C V, Wenstrup JJ (1999) Delay-tuned neurons in the inferior colliculus of the mustached bat: implications for analyses of target distance. J Neurophysiol 82:1326–1338.

Posner MI (1980) Orienting of attention. Q J Exp Psychol 32:3–25.

Posner MI, Petersen SE (1989) The Attention System of the Human Brain.

Poussin C, Schlegel P (1984a) Directional sensitivity of auditory neurons in the superior colliculus of the bat,Eptesicus fuscus, using free field sound stimulation. J Comp Physiol A 154:253–261.

Poussin C, Schlegel P (1984b) Directional sensitivity of auditory neurons in the superior colliculus

of the bat, Eptesicus fuscus, using free field stimulation. J Comp Physiol A 154:253–261.

Quiroga RQ, Nadasdy Z, Ben-Shaul Y (2004) Unsupervised Spike Detection and Sorting with Wavelets and Superparamagnetic Clustering. Neural Comput 16:1661–1687.

Rashbass C, Westheimer G (1961) Independence of conjugate and disjunctive eye movements. J Physiol 159:361–364.

Ratcliffe JM, Elemans CPH, Jakobsen L, Surlykke A (2013) How the bat got its buzz. Biol Lett 9:20121031.

Reynolds JH, Chelazzi L (2004) Attentional modulation of visual processing. Annu Rev Neurosci 27:611–647.

Robinson DA (1972) Eye movements evoked by collicular stimulation in the alert monkey. Vision Res 12:1795–1808.

Robinson DL, Petersen SE (1992) The pulvinar and visual salience. Trends Neurosci 15:127–132.

Roeder KD (1962) The behaviour of free flying moths in the presence of artificial ultrasonic pulses. Anim Behav 10:300–304.

Roeder KD (1967) Turning tendency of moths exposed to ultrasound while in stationary flight. J Insect Physiol 13:873–888.

Rosa MGP, Schmid LM (1994) Topography and extent of visual-field representation in the superior colliculus of the megachiropteran Pteropus. Vis Neurosci 11:1037–1057.

Roucoux a., Guitton D, Crommelinck M (1980a) Stimulation of the superior colliculus in the alert cat - II. Eye and head movements evoked when the head is unrestrained. Exp Brain Res 39:75–85.

Roucoux A, Guitton D, Crommelinck M (1980b) Stimulation of the superior colliculus in the alert

cat. Exp Brain Res 39.

Saleem AB, Ayaz A, Jeffery KJ, Harris KD, Carandini M (2013) Integration of visual motion and locomotion in mouse visual cortex. Nat Neurosci 16:1864–1869.

Salinas-Navarro M, Mayor-Torroglosa S, Jiménez-López M, Avilés-Trigueros M, Holmes TM, Lund RD, Villegas-Pérez MP, Vidal-Sanz M (2009) A computerized analysis of the entire retinal ganglion cell population and its spatial distribution in adult rats. Vision Res 49:115–126.

Sändig S, Schnitzler H-UH-U, Denzinger A (2014) Echolocation behaviour of the big brown bat (Eptesicus fuscus) in an obstacle avoidance task of increasing difficulty. J Exp Biol 217:2876–2884.

Sarel A, Finkelstein A (2017) Vectorial representation of spatial goals in the hippocampus of bats. Science (80-) 180:176–180.

Sawa M, Ohtsuka K (1994) Lens accommodation evoked by microstimulation of the superior colliculus in the cat. Vision Res 34:975–981.

Sawinski J, Wallace DJ, Greenberg DS, Grossmann S, Denk W, Kerr JN (2009) Visually evoked activity in cortical cells imaged in freely moving animals. ProcNatlAcadSciUSA 106:19557–19562.

Schiller PH, Koerner F (1971) Discharge characteristics of single units in superior colliculus of the alert rhesus monkey. J Neurophysiol 34:920–936.

Schiller PH, Stryker M (1972) Single-unit recording and stimulation in superior colliculus of the alert rhesus monkey. J Neurophysiol 35:915–924.

Schiller PH, Stryker M, Cynader M, Berman N (1974) Response characteristics of single cells in the monkey superior colliculus following ablation or cooling of visual cortex. J Neurophysiol

37:181–194.

Schneider DM, Nelson A, Mooney R (2014) A synaptic and circuit basis for corollary discharge in the auditory cortex. Nature 513:189–194.

Schnitzler H-U, Kalko E, Miller L, Surlykke A (1987) The echolocation and hunting behavior of the bat,Pipistrellus kuhli. J Comp Physiol A 161:267–274.

Schnitzler H-U, Kalko EK V. (2001) Echolocation by Insect-Eating Bats. Bioscience 51:557.

Schnupp JWH, Carr CE (2009) On hearing with more than one ear: lessons from evolution. Nat Neurosci 12:692–697.

Scholl B, Burge J, Priebe NJ (2013) Binocular integration and disparity selectivity in mouse primary visual cortex. J Neurophysiol 109:3013–3024.

Schuller G, O'Neill W, Radtke-Schuller S (1991) Facilitation and Delay Sensitivity of Auditory Cortex Neurons in CF - FM Bats, Rhinolophus rouxi and Pteronotus p.parnellii. Eur J Assoc 3:1165–1181.

Schuller G, Radtke-Schuller S (1990) Neural control of vocalization in bats: mapping of brainstem areas with electrical microstimulation eliciting species-specific echolocation calls in the rufous horseshoe bat. Exp Brain Res 79:192–206.

Senkowski D, Talsma D, Herrmann CS, Woldorff MG (2005) Multisensory processing and oscillatory gamma responses: effects of spatial selective attention. Exp Brain Res 166:411–426.

Sereno MI, Huang RS (2014) Multisensory maps in parietal cortex. Curr Opin Neurobiol 24:39–46.

Shimozawa T, Suga N, Hendler P, Schuetze S (1974) Directional sensitivity of echolocation system in bats producing frequency-modulated signals. J Exp Biol 60:53–69.

Simmons JA (1973a) The resolution of target range by echolocating bats. J Acoust Soc Am 54:157.

Simmons J a (1971) Echolocation in bats: signal processing of echoes for target range. Science 171:925–928.

Simmons J a (1973b) The resolution of target range by echolocating bats. J Acoust Soc Am 54:157–173.

Simmons J a (1979) Perception of echo phase information in bat sonar. Science 204:1336–1338.

Simmons J a., Eastman KM, Horowitz SS, O'Farrell MJ, Lee DN (2001) Versatility of biosonar in the big brown bat, Eptesicus fuscus. Acoust Res Lett Online 2:43.

Simmons J a, Ferragamo M, Moss CF, Stevenson SB, Altes R a (1990a) Discrimination of jittered sonar echoes by the echolocating bat, Eptesicus fuscus: the shape of target images in echolocation. J Comp Physiol A 167:589–616.

Simmons JA, Fenton MB, O'Farrell MJ (1979) Echolocation and pursuit of prey by bats. Science 203:16–21.

Simmons J, Ferragamo M, Moss C, Stevenson S, Altes R (1990b) Discrimination of jittered sonar echoes by the echolocating bat, Eptesicus fuscus: The shape of target images in echolocation. J Comp Physiol A 167.

Sinha SR, Moss CF (2007) Vocal premotor activity in the superior colliculus. J Neurosci 27:98–110.

Slee SJ, Young ED (2010) Sound localization cues in the marmoset monkey. Hear Res 260:96–108.

Sommer MA, Wurtz RH (2000) Composition and topographic organization of signals sent from the frontal eye field to the superior colliculus. J Neurophysiol 83:1979–2001.

Sparks DL (1986) Translation of sensory signals into commands for control of saccadic eye movements: role of primate superior colliculus. Physiol Rev 66:118–171.

Sparks DL (1988) Neural cartography: sensory and motor maps in the superior colliculus. Brain Behav Evol 31:49–56.

Sparks DL, Hartwich-Young R (1989) The deep layers of the superior colliculus. Rev Oculomot Res 3:213–255.

Sparks DL, Mays LE (1990) Signal transformations required for the generation of saccadic eye movements. Annu Rev Neurosci 13:309–336.

Sparks L, Jay MF, Sparks DL (1987) Sensorimotor integration in the primate superior colliculus. II. Coordinates of auditory signals. J Neurophysiol 57:35–55.

Speakman JR, Anderson ME, Racey PA (1989) The energy cost of echolocation in pipistrelle bats (Pipistrettus pipistrellus). J Comp Physiol A 165:679–685.

Speakman JR, Racey PA (1991) No cost of echolocation for bats in flight. Nature 350:421–423.

Spitzer H, Desimone R, Moran J (1988) Increased attention enhances both behavioral and neuronal performance. Science 240:338–340.

Sridharan D, Boahen K, Knudsen EI (2011) Space coding by gamma oscillations in the barn owl optic tectum. J Neurophysiol 105.

Sridharan D, Knudsen EI (2015) Gamma oscillations in the midbrain spatial attention network: Linking circuits to function. Curr Opin Neurobiol 31:189–198.

Srinivasan M V., Poteser M, Kral K (1999) Motion detection in insect orientation and navigation. Vision Res 39:2749–2766.

Srinivasan M V., Zhang S (2004) Visual Motor Computations in Insects. Annu Rev Neurosci 27:679–696.

Srinivasan M V, Zhang S, Altwein M, Tautz J (2000) Honeybee navigation: nature and calibration

of the “odometer”. Science 287:851–853.

Stein BE, Clamann HP (1981) Control of pinna movements and sensorimotor register in cat superior colliculus. Brain Behav Evol 19:180–192.

Stein BE, Gaither NS (1981) Sensory representation in reptilian optic tectum: Some comparisons with mammals. J Comp Neurol 202:69–87.

Stein BE, Magalhães-Castro B, Kruger L (1976) Relationship between visual and tactile representations in cat superior colliculus. J Neurophysiol 39:401–419.

Stein BE, Meredith MA (1993) The merging of the senses. MIT Press.

Stein BE, Meredith M a, Huneycutt WS, McDade L (1989) Behavioral Indices of Multisensory Integration: Orientation to Visual Cues is Affected by Auditory Stimuli. J Cogn Neurosci 1:12–24.

Steinman RM, Kowler E, Collewijn H (1990) New directions for oculomotor research. Vision Res 30:1845–1864.

Sterling P, Wickelgren BG (1969) Visual receptive fields in the superior colliculus of the cat. J Neurophysiol 32:1–15.

Sterratt DC, Lyngholm D, Willshaw DJ, Thompson ID (2013) Standard Anatomical and Visual Space for the Mouse Retina: Computational Reconstruction and Transformation of Flattened Retinae with the Retistruct Package. PLoS Comput Biol 9.

Stryker M, Blakemore C (1972) Saccadic and disjunctive eye movements in cats. Vision Res 12:2005–2013.

Stuesse SL, Newman DB (1990) Projections from the medial agranular cortex to brain stem visuomotor centers in rats. Exp Brain Res 80:532–544.

Stuphorn V, Bauswein E, Hoffmann KP (2000) Neurons in the primate superior colliculus coding for arm movements in gaze-related coordinates. J Neurophysiol 83:1283–1299.

Suga N, Horikawa J (1986) Multiple time axes for representation of echo delays in the auditory cortex of the mustached bat. J Neurophysiol 55:776–805.

Suga N, O'Neill WE (1979a) Neural axis representing target range in the auditory cortex of the mustache bat. Science 206:351–353.

Suga N, O'Neill WE (1979b) Neural axis representing target range in the auditory cortex of the mustache bat. Science 206:351–353.

Surlykke A, Boel Pedersen S, Jakobsen L (2009a) Echolocating bats emit a highly directional sonar sound beam in the field. Proc Biol Sci 276:853–860.

Surlykke A, Ghose K, Moss CF (2009b) Acoustic scanning of natural scenes by echolocation in the big brown bat, Eptesicus fuscus. J Exp Biol 212:1011–1020.

Surlykke A, Kalko EK V (2008) Echolocating bats cry out loud to detect their prey. PLoS One 3:e2036.

Surlykke A, Moss CF (2000) Echolocation behavior of big brown bats, Eptesicus fuscus, in the field and the laboratory. J Acoust Soc Am 108:2419.

Suthers RA, Thomas SP, Suthers BJ (1972) Respiration, Wing-Beat and Ultrasonic Pulse Emission in an Echo-Locating Bat. J Exp Biol 56:37–48.

Syka J, Radil-Weiss T (1971) Electrical stimulation of the tectum in freely moving cats. Brain Res 28:567–572.

Takahashi M, Sugiuchi Y, Shinoda Y (2010) Topographic organization of excitatory and inhibitory commissural connections in the superior colliculi and their functional roles in saccade

generation. J Neurophysiol 104:3146–3167.

Tanaka H, Wong D (1993) The influence of temporal pattern of stimulation on delay tuning of neurons in the auditory cortex of the FM bat, Myotis lucifugus. Hear Res 66:58–66.

Tatler BW, Hayhoe MM, Land MF, Ballard DH, H. R, G. S, R. D, M. B, W. HG (2011) Eye guidance in natural vision: Reinterpreting salience. J Vis 11:5–5.

Taube JS, Muller RU, Ranck JB (1990) Head-direction cells recorded from the postsubiculum in freely moving rats. I. Description and quantitative analysis. J Neurosci 10:420–435.

Taylor AM, Jeffery G, Lieberman AR (1986) Subcortical afferent and efferent connections of the superior colliculus in the rat and comparisons between albino and pigmented strains. Exp Brain Res 62:131–142.

Thiele a, Vogelsang M, Hoffmann KP (1991) Pattern of retinotectal projection in the megachiropteran bat Rousettus aegyptiacus. J Comp Neurol 314:671–683.

Thiele A, Rübsamen R, Hoffmann KP (1996) Anatomical and physiological investigation of auditory input to the superior colliculus of the echolocating megachiropteran bat Rousettus aegyptiacus. Exp brain Res 112:223–236.

Thomas JA, Moss C, Vater M (2004) Echolocation in bats and dolphins. University of Chicago Press.

Thompson KG, Bichot NP (2004) A visual salience map in the primate frontal eye field. Prog Brain Res 147:251–262.

Tigges J, Nakagawa S, Tigges M (1979) Efferents of area 4 in a South American monkey (Saimiri). I. Terminations in the spinal cord. Brain Res 171:1–10.

Tigges J, Tigges M (1981) Distribution of retinofugal and corticofugal axon terminals in the

superior colliculus of squirrel monkey. Investig Ophthalmol Vis Sci 20:149–158.

Treue S, Trujillo JCM (1999) Feature-based attention influences motion processing gain in macaque visual cortex. Nature 399:575–579.

Triblehorn JD, Ghose K, Bohn K, Moss CF, Yager DD (2008) Free-flight encounters between praying mantids (Parasphendale agrionina) and bats (Eptesicus fuscus). J Exp Biol 211:555–562.

Triblehorn JD, Yager DD (2005) Timing of praying mantis evasive responses during simulated bat attack sequences. J Exp Biol 208:1867–1876.

Troje NF, Frost BJ (2000) Head-bobbing in pigeons: how stable is the hold phase? J Exp Biol 203:935–940.

Ulanovsky N, Moss CF (2008) What the bat's voice tells the bat's brain. Proc Natl Acad Sci U S A 105:8491–8498.

Valentine DE, Moss CF (1997) Spatially selective auditory responses in the superior colliculus of the echolocating bat. J Neurosci 17:1720–1733.

Valentine DE, Sinha SR, Moss CF (2002) Orienting responses and vocalizations produced by microstimulation in the superior colliculus of the echolocating bat, Eptesicus fuscus. J Comp Physiol A Neuroethol Sens Neural Behav Physiol 188:89–108.

Van Horn MR, Waitzman DM, Cullen KE (2013) Vergence Neurons Identified in the Rostral Superior Colliculus Code Smooth Eye Movements in 3D Space. J Neurosci 33:7274–7284.

Verghese P (2001) Visual Search and Attention. Neuron 31:523–535.

Vertes RP, Fortin WJ, Crane AM (1999) Projections of the median raphe nucleus in the rat. J Comp Neurol 407:555–582.

Wallace MMT, Meredith MA, Stein BE (1998) Multisensory Integration in the Superior Colliculus of the Alert Cat. J Neurophysiol 80:1006–1010.

Wallace MT, Perrault TJ, Hairston WD, Stein BE (2004) Visual experience is necessary for the development of multisensory integration. J Neurosci 24:9580–9584.

Walton MMG, Mays LE (2003) Discharge of saccade-related superior colliculus neurons during saccades accompanied by vergence. J Neurophysiol 90:1124–1139.

Wardak C, Ibos G, Duhamel J-R, Olivier E (2006) Contribution of the monkey frontal eye field to covert visual attention. J Neurosci 26:4228–4235.

Wessberg J, Stambaugh CR, Kralik JD, Beck PD, Laubach M, Chapin JK, Kim J, Biggs SJ, Srinivasan M a, Nicolelis M a (2000) Real-time prediction of hand trajectory by ensembles of cortical neurons in primates. Nature 408:361–365.

Westheimer G (1954) Mechanism of Saccadic Eye Movements. Arch Ophthalmol 52:710–724.

Wheeler AR, Fulton KA, Gaudette JE, Simmons RA, Matsuo I, Simmons JA (2016) Echolocating Big Brown Bats, Eptesicus fuscus, Modulate Pulse Intervals to Overcome Range Ambiguity in Cluttered Surroundings. Front Behav Neurosci 10:1–13.

Wilson, W.W., and Moss CF (2004) Sensory-motor behavior of free-flying FM bats during target capture. In: Advances in the study of echolocation in bats and dolphins (J. Thomas CFM and MV, ed), pp 22–27. University of Chicago Press, Chicago.

Wilson JR, Hendrickson AE, Sherk H (1995) Sources of Subcortical Afferents to the Macaque ' s Dorsal Lateral Geniculate Nucleus. 574.

Wilson ME, Toyne MJ (1970) Retino-tectal and cortico-tectal projections inMacaca mulatta. Brain Res 24:395–406.

Wilson SA (1921) Original Papers: SOME PROBLEMS IN NEUROLOGY. J Neurol Psychopathol 2:1–25.

Wilson D. E., Reeder D. M. eds. (2005) Mammal species of the world: a taxonomic and geographic reference, 3rd ed. Baltimore: Smithsonian Institution Press, Washington, D.C.

Winkowski DE, Knudsen EI (2006) Top-down gain control of the auditory space map by gaze control circuitry in the barn owl. Nature 439:336–339.

Wohlgemuth MJ, Kothari NB, Moss CF (2016a) Action enhances 3-D auditory localization. PLoS Biol.

Wohlgemuth MJ, Moss CF (2016) Midbrain auditory selectivity to natural sounds. Proc Natl Acad Sci 113:2508–2513.

Wohlgemuth MJMJ, Luo J, Moss CFCF (2016b) Three-dimensional auditory localization in the echolocating bat. Curr Opin Neurobiol 41:78–86.

Wolfe JM (1994) Guided Search 2 . 0 A revised model of visual search. Psychnomic Bull Rev 1:202–238.

Womelsdorf T, Anton-Erxleben K, Pieper F, Treue S (2006) Dynamic shifts of visual receptive fields in cortical area MT by spatial attention. Nat Neurosci 9:1156–1160.

Wong D (1984) Spatial tuning of auditory neurons in the superior colliculus of the echolocating bat, Myotis lucifugus. Hear Res 16:261–270.

Wong D, Maekawa M, Tanaka H (1992) The effect of pulse repetition rate on the delay sensitivity of neurons in the auditory cortex of the FM bat, Myotis lucifugus. J Comp Physiol A 170:393–402.

Wong JG, Waters D a (2001) The synchronisation of signal emission with wingbeat during the

approach phase in soprano pipistrelles (Pipistrellus pygmaeus). J Exp Biol 204:575–583.

Wurtz RH, Albano JE (1980) Visual-motor function of the primate superior colliculus. Annu Rev Neurosci 3:189–226.

Wurtz RH, Goldberg ME (1972) Activity of superior colliculus in behaving monkey. III. Cells discharging before eye movements. J Neurophysiol 35:575–586.

Wurtz RH, Mohler CW (1976) Organization of monkey superior colliculus: enhanced visual response of superficial layer cells. J Neurophysiol 39:745–765.

Wylie DR, Bischof WF, Frost BJ (1998) Common reference frame for neural coding of translational and rotational optic flow. Nature 392:278–282.

Xiao Q, Frost BJ (2013) Motion parallax processing in pigeon (Columba livia) pretectal neurons. Eur J Neurosci 37:1103–1111.

Yamasaki DS, Krauthamer G, Rhoades RW (1984) Organization of the intercollicular pathway in rat. Brain Res 300:368–371.

Yan J, Suga N (1996) The midbrain creates and the thalamus sharpens echo-delay tuning for the cortical representation of target-distance information in the mustached bat. Hear Res 93:102–110.

Yarbus AL (1967) Eye Movements and Vision. Boston, MA: Springer US.

Yartsev MM, Ulanovsky N (2013) Representation of three-dimensional space in the hippocampus of flying bats. Science 340:367–372.

Yeshurun Y, Carrasco M (1999) Spatial attention improves performance in spatial resolution tasks. Vision Res 39:293–306.

Zagha E, Casale AE, Sachdev RNS, McGinley MJ, McCormick DA (2013) Motor cortex feedback

influences sensory processing by modulating network state. Neuron 79:567–578.

Zénon A, Krauzlis RJ (2012) Attention deficits without cortical neuronal deficits. Nature 489:434–437.

Zhang S, Sun X, H.-S. Jen P (1987) Anatomical study of neural projections to the superior colliculus of the big brown bat,Eptesicus fuscus. Brain Res 416:375–380.

Zhou H, Schafer RJ, Desimone R (2016) Pulvinar-Cortex Interactions in Vision and Attention. Neuron 89:209–220.

Zuidam I, Collewijn H (1979) Vergence eye movements of the rabbit in visuomotor behavior. Vision Res 19:185–194.

Ninad B. Kothari

Johns Hopkins University, Baltimore
Department of Psychology and Brain Sciences
3400 N Charles Street, #124 Ames Hall, Baltimore, MD 21218 USA
email: ninadbkothari@jhu.edu

Education

2014-2017	**Johns Hopkins University, Baltimore** PhD in Psychology and Brain Sciences
2011-2014	**University of Maryland, College Park** (transferred to JHU) PhD in Neuroscience and Cognitive Science
2004-2006	**Birla Institute of Technology and Science, Pilani (BITS, Pilani)** Master of Engineering in Microelectronics (M.E.)
2000-2004	**Visvesvaraya Technological University (VTU - Karnataka)** Bachelor of Engineering in Electronics and Communication (B.E.)

Previous work experience

2007-2011	**Intel Research (Intel Labs, Bangalore)** Senior Researcher* *more details about my work at Intel can be provided on request

Honors and awards

2017	The G. Stanley Hall Scholar's Award (for Graduate Thesis)
2016	Collaborative Research Award, Psychology and Brain Sciences, JHU
2014	Heiligenberg Travel Award for the 11th International Congress for Neuroethology. Sapporo, Japan
2013	Jacob K. Goldhaber Travel Grant for travel to Society for Neuroscience
2013	Neuroscience and Cognitive Science Travel Award for presenting at the Gordon Research Conference on Neuroethology
2010	Intel Accendo Award for Innovation
2004-2006	BITS, Pilani Scholarship for Teaching Assistants
2005-2006	First runners up position at the Intel India Student Research Contest (IISRC-2006) for Zigbee chip design
2005	High Performance Computing Conference Travel Scholarship

Publications

Published and in review

Kothari, N. B., Wohlgemuth, M. J., Hulgard, K., Surlykke, A. & Moss, C. F. Timing matters: Sonar call groups facilitate target localization in bats. *Frontiers in Physiology* (2014)

Wohlgemuth, M. J., **Kothari, N. B.** & Moss, C. F. Functional organization and dynamic activity in the superior colliculus of the echolocating bat, *Eptesicus fuscus*. *Journal of Neuroscience*. (2017)

Wohlgemuth, M. J., **Kothari, N. B.** & Moss, C. F. Action enhances 3-D auditory localization. *PLoS Biology*. (2016)

Kothari, N. B., Wohlgemuth, M. J. & Moss, C. F. Spatial Attention sharpens 3D tuning of auditory neurons in free-flying bats. (in review – eLife)

J. Luo, **Kothari, N. B.** & Moss, C. F. Audio vocal integration on a rapid scale (2017) PNAS

Kothari, N. B., Sudarshan, T. S. B., Gurunarayanan, S. & Chandrasekar, S. SOC design of a Low Power Wireless Sensor network node for Zigbee Systems. in *International Conference on Advanced Computing and Communications* 462–466 (IEEE, 2006)

Kothari, N. B., T.S.B. Sudarshan, Shipra Bhal, Tejesh.E.C & S. Gururnarayanan. Design of an Efficient Low Power AES Engine for Zigbee Systems in *10th VLSI Design and Test Symposium* (VDAT, 2006)

In preparation

Kothari, N. B., Wohlgemuth, M. J. & Moss, C. F. Control over sonar call timing supports target tracking in echolocating bats (to be submitted to Journal of Experimental Biology)

Patents

Sasikanth Avancha, **Kothari N. B.**, Banginwar Rajesh, Kgil Taeho (2014) Delivering data from a range of input devices over a secure path to trusted services in a secure element (US20140310799)

Sasikanth Avancha, **Kothari N. B.**, Banginwar Rajesh, Kgil Taeho (2013) Delivering data from a secure execution environment to a display controller (US20130111219)

Invited talks (* indicates presenter)

Kothari N. B.* & Moss CF. Dynamic representation of 3D auditory space in the midbrain of the free-flying echolocating bat (2017). Acoustical Society of America, New Orleans

Kothari N. B.* & Moss CF. 3D receptive fields in the midbrain are modulated by spatial attention in free-flying bats (2016). Biology-Psychology Colloquium, JHU

Kothari N. B.* & Moss CF. Orienting in 3D space: Neural recordings in freely flying bats. (2015) Talk at Johns Hopkins Medical School, JHU

Kothari N. B.*, Moss CF. Timing matters: From behavioral studies to neural recordings in freely flying bats. (2015) Psychology and Brain Sciences Colloquium, JHU

Kothari N. B.*, Moss CF. Neural recordings in freely flying bats. (2014) Psychology and Brain Sciences Colloquium, JHU

Kothari N. B.*, Moss C.F. Temporal control of sonar call production supports target tracking by bats. (2013). Talk to Neuroscience Minors Undergraduate students. University of Maryland, College Park

Kothari N. B.* Introduction to the retina (2013). Talk to students enrolled in the Perception course. University of Maryland, College Park

Abstracts in scientific meetings

Kothari N.B., Wohlgemuth MJ, Moss CF. Representing space in 3D: Response profiles of midbrain neurons in the free-flying bat. Annual Meeting of the Society for Neuroscience, San Diego (2016 – Dynamic Poster)

Kothari N.B., Wohlgemuth MJ, Moss CF. Neural activity in the SC of a flying echolocating bat Annual Meeting of the Society for Neuroscience, Chicago (2015).
The poster was also selected for a presentation at the SfN Press Conference "Tools, Technologies and Big Data"

Kothari N.B., Wohlgemuth MJ, Moss CF. Sensorimotor neural activity in the Superior Colliculus of freely flying bats. Annual Meeting of the Society for Neuroscience, Washington D.C. (2014 – Dynamic poster)

Kothari N.B., Wohlgemuth MJ, Moss CF. Temporal control of sonar call production supports target tracking Abstract for poster presentation, Gordon Research Conference on Neuroethology, Mt. Snow, VT, USA (2013)

Professional memberships

Society for Neuroscience

International Congress of Neuroethology

Acoustical Society of America

References

Dr. Cynthia Moss (PhD mentor)
Professor, Department of Psychological and Brain Sciences
Johns Hopkins University, Baltimore

Dr. Shreesh Mysore
Assistant Professor, Department of Psychological and Brain Science

Johns Hopkins University, Baltimore

Dr. Catherine Carr
Professor, Department of Biology
University of Maryland, College Park